NEW FRONTIERS IN ENGINEERING

Editors:
Assoc. Prof.Bayram AKDEMİR
Assist Prof. Umut ÖZKAYA

DUVAR

NEW FRONTIERS IN ENGINEERING

Editors:
Assoc. Prof.Bayram AKDEMİR
Assist Prof. Umut ÖZKAYA

TABLE OF CONTENTS

Chapter 1

Innovative Designs and Design Rules for Additive Manufacturing

Ahmet DAYANÇ[1], Feridun KARAKOÇ[2]

[1] *Arş. Gör.; Kütahya Dumlupınar Üniversitesi Mühendislik Fakültesi Makine Mühendisliği Bölümü. ahmet.dayanc@dpu.edu.tr ORCID No: 0000-0002-5214-9021*

[2] *Dr. Öğr. Üyesi; Kütahya Dumlupınar Üniversitesi Mühendislik Fakültesi Makine Mühendisliği Bölümü. feridun.karakoc@dpu.edu.tr ORCID No: 0000-0002-6210-4070*

ABSTRACT

Innovation means the improvement of a product, service, or process and creates a competitive advantage for various sectors today. Innovation is important not just for large companies, but also for individuals, small businesses, and governments. Design is one of the most important pathways for innovation as it has a direct impact on how a product looks, how it functions, and how it is manufactured. Innovative design enables products to make a difference in the market, improves user experience, and reduces production costs. Nowadays, artificial intelligence also plays an active role in this area. Additive manufacturing allows for the production of complex and lightweight designs. New design methods and tools, especially with the involvement of artificial intelligence, increase the potential for innovation.

When designing for additive manufacturing (DFAM), certain principles need to be taken into account. These principles aim to minimize production cost, time loss, and quality issues. For example, the orientation in which a part will be 3D printed can affect its mechanical properties and surface quality. In addition, algorithm-based approaches such as generative design and topology optimization can be used in the design process to develop more effective and functional products. Topology optimization, in particular, helps to determine how material can be used most minimally and effectively under specified volume and load conditions. While topology optimization focuses on optimizing structural performance, generative design can perform broader optimizations.

In conclusion, innovation and design are inseparable in the context of modern production and market dynamics. Technologies like artificial intelligence, new design methods, and additive manufacturing are radically changing design and production processes and making innovation more accessible. However, for these technologies to be effectively used, careful planning and optimization are required at every stage of the design process. In this context, innovative design and additive manufacturing are of critical importance to improve the performance of current and future products, reduce costs, and produce sustainable solutions.

Keywords: Additive Manufacturing, Design Rules, Innovative Design, Lightweighting, topology

INTRODUCTION

The definition and scope of innovation are quite broad, not only in the ISO 56000:2020 standard and the ISO TC 279 technical committee focused on 'Standardization of terminology, tools, methods and interactions between relevant parties to enable innovation', but also in various domains in the literature (ISO, 2023). Innovation is generally the systematic application of a new or improved product, service, idea, or business model. Naturally, there is a distinction between innovation and invention. In today's competitive lifestyle, innovation is not only necessary for large-scale companies but also has the potential to bring sustainability and success. Therefore, innovation is also required in individuals' lives, governments, small businesses, and start-ups (McKinsey, 2023).

Design is one of the prominent fields where innovation can occur. Design is no longer merely an application of human thought; today, we see examples of innovative designs belonging to non-biological structures like artificial intelligence. The collaboration between humans, machines, computers, and artificial intelligence is increasing day by day. Artificial intelligence can be trained based on past data and knowledge and can present its own designs. It also has the potential to increase creativity by providing new inputs to designers. Artificial intelligence can analyze large amounts of data quickly and offer design suggestions, enabling faster and more cost-effective design. It can also analyze data to predict future design trends. According to IBM CEO Ginni Rometty, artificial intelligence today serves as an 'augmented intelligence' for workers rather than posing a short-term risk of replacing designers (Toptal, 2023).

As a result of the development of tools and equipment used in design and the production of designed products, the diversity of methods used in creating innovative designs is also increasing over time. Innovative designs continue to be created through existing sculpting software or CAD modeling software that uses the 'Boundary Representation' method. With AI-Driven design, like in the example of artificial intelligence, designs can be personalized, optimized, and innovative results can be achieved (Fireart, 2023). In an example of algorithmic design, a packaging production system capable of creating tens of different patterns and colors and personalized labels for the Nutella Unica project produced 7 million different Nutella labels (Dezeen, 2023).

Thanks to advancing manufacturing methods, the increased manufacturability of complex product designs is also expanding the possibilities for innovation in design. For instance, additive manufacturing allows for the production of lightweight, hollow, and complex internal structure designs. It also provides rapid prototyping, allowing for quick testing of design iterations. In the design process to take advantage of the benefits of additive manufacturing, a 'lattice structure'

can be created within the part. Using innovative methods like implicit modeling technology with Field-Driven design and Data-Driven Design techniques for the easy creation and spatial modification of lattice structures made up of numerous unit cells provides significant advantages and conveniences to the designer (nTopology, 2023-b).

INNOVATIVE DESIGNS

The first example of innovative designs is shown in Figure 1 below. As a result of a project where engineers came together to redesign hydraulic pipe clamps for F-16 planes and make them suitable for additive manufacturing, it has been reported that the new design is twice as strong as the old design, easier to assemble, and can be produced in high volumes on demand. The project met the full flight qualification criteria set by the U.S. Air Force's 'Rapid Sustainment Office' within 30 days. Additionally, a reusable method for qualifying new components has been developed as a result of this project. The project team won a $100,000 prize in a competition organized by the U.S. Air Force (nTopology, 2023-a).

Figure 1: F-16 Aircraft Hydraulic Tube Clamps

In Figure 2a below, the body design of the robot arm is customized by a team of engineers from Penn State University, Flow 3D, and Humtown, and has used the SIMP algorithm-based topology optimization method. Advanced casting techniques have also been used for the production of the part, and as a result, the part has been lightened by 40%, and common casting errors have been prevented (nTop, 2023-b). In Figure 2b below, a 3D printed wooden guitar is seen. Designed by Olaf Diegel, an experienced professor at Auckland University in New Zealand, who also manages ODD Guitars, the guitar was produced using binder jetting technology and designed using wood chips and bio-epoxy materials. This

work may show that 3D printed high-quality wooden products have a sustainable future (Diegel, 2023).

Figure 2: a) Robot Arm b) 3D-Printed Guitar

In Figure 3 below, an assembly view of a part belonging to the Lion team is given. This part, a suspension connection point developed for a Formula Student race car, has been designed by Jan-Rickmer Luth, Jannes Briese, and the Lions Racing Team e.V., and they won a competition in 2021. The SIMP algorithm has been used to keep the mass minimal while maximizing durability. The new geometry formed as a result of the algorithm completing iterations according to certain conditions is 40% lighter compared to the previous design (nTop, 2023-c).
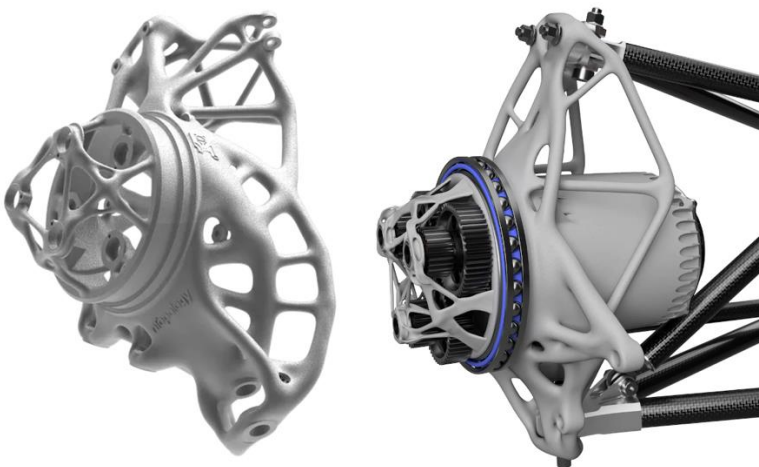
Figure 3: Lightweight Automotive Upright Bracket

In Figure 4a below, the VAEN bicycle saddle has an ergonomic design and features a cage structure inspired by giraffe patterns from nature, making it a

high-performance product. This innovative design has utilized all the advantages of 3D printing and Voronoi lattice structures (Vaen, 2023). Seen in Figure 4b below, the compact cooling plate with an improved heat transfer coefficient has been designed by the Temisth team. This design has been produced and tested under real conditions. The results show that the cooling plate can effectively cool electronic components even under heavy loads (Temisth, 2023).
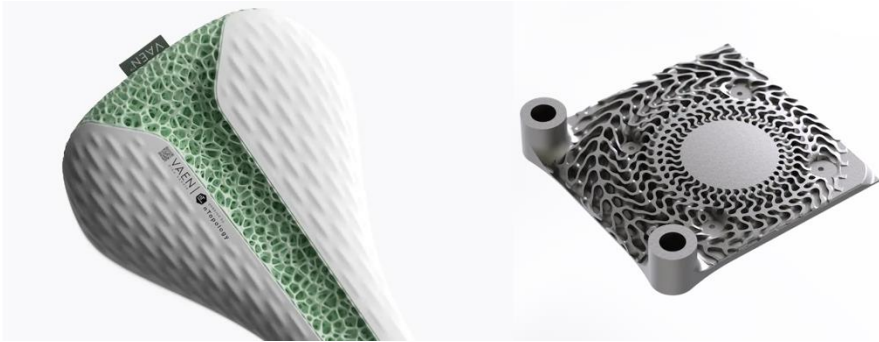
Figure 4: a) Voronoi Bike Saddle b) The Cold Plate for GPU

As seen in Figure 5a below, SI-BONE, a leader in minimally invasive joint surgery, has designed implantable orthopedic devices with a cage structure that promotes osseointegration, under the commercial name iFuse TORQ (SI-BONE, 2023). In Figure 5b, the Puntozero company has redesigned the heat management system related to the power electronics of Dynamis PRC's electric race car for production through additive manufacturing. As a result, the new design is a liquid-cooled heat sink system that is 25% lighter. A design has been achieved that has flow guides inspired by biological structures and increases the heat transfer surface area by 300% (AM Media, 2023).
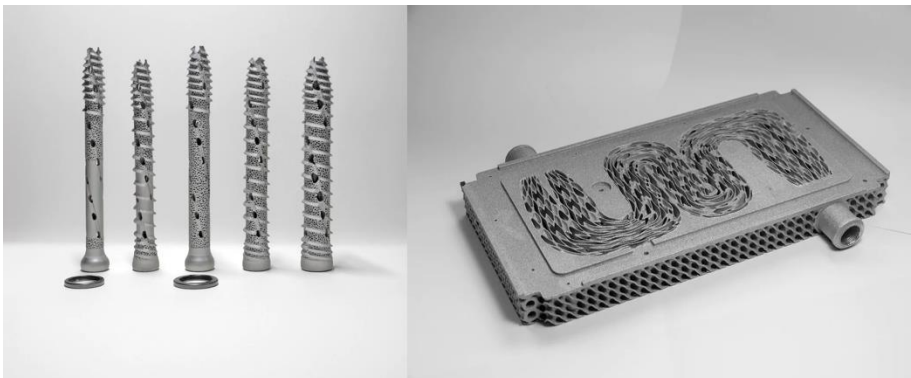
Figure 5: a) SI-BONE iFuse TORQ b) Biomimicry Heat Exchanger

The air duct seen in Figure 6a below was developed in collaboration between nTop and EOS. This air duct designed using structural beams, topology optimization, and lattice structures, has been manufactured as a single piece instead of an assembly consisting of 44 parts. This has saved labor that would have been spent on determining how to assemble the parts. Therefore, engineers designing for additive manufacturing can use this saved labor to optimize flow control (nTop, 2023-a). In Figure 6b, Impressio engineers have leveraged the advantages of design for additive manufacturing and innovative materials developed in the liners of impact-absorbing helmets used in the NFL. They can complete the entire process from design to production with a quick workflow (Impressio, 2023).
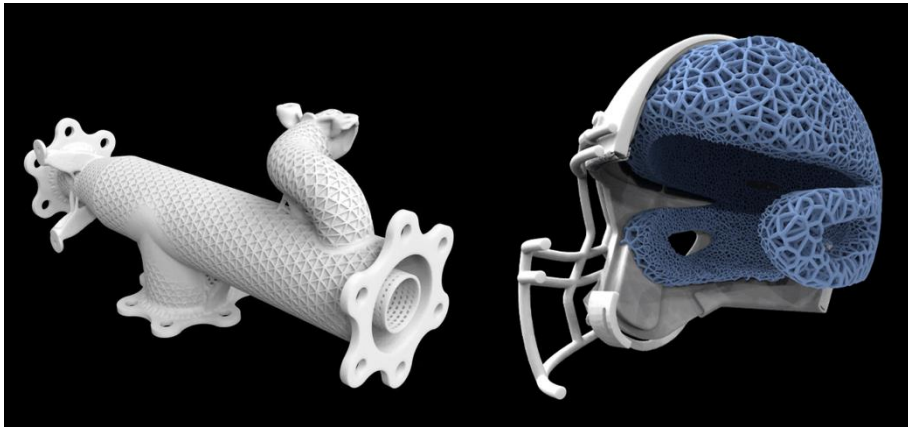
Figure 6: a) Air Duct b) NFL Helmet

In Figure 7 below, the development of additive manufacturing technologies in a zero-gravity environment could be one of the biggest breakthroughs that will make humanity's future activities in space a reality. One of the most fundamental elements required to achieve this goal is to conduct studies for additive manufacturing in a zero-gravity environment. More than 200 parts have been manufactured in the International Space Station since 2016 using the commercial-space 3D printer jointly produced by Lowe's Innovation Labs and MadeInSpace and used by NASA (3DPrint, 2023). Academically, work is ongoing worldwide at universities like Cranfield, Nottingham, and Clausthal on additive manufacturing in a zero-gravity environment.
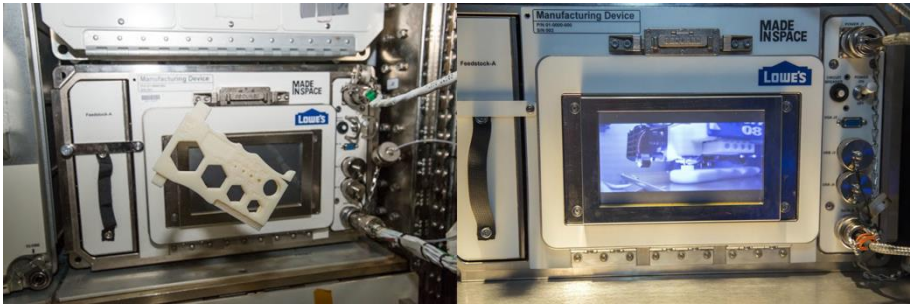
Figure 7: 3D Printing in Space

For innovative designs, topology optimization, lattice structures, and finite element analysis can be used together to achieve a high degree of weight reduction. Commercially developed software like nTopology plays a significant role in this regard. Many companies use this software to maintain the structural strength of their existing products while innovatively implementing design optimizations. The diversity of innovative designs and the differences in materials and technologies used in additive manufacturing are giving rise to 'design principles for additive manufacturing' and sometimes require specific approaches depending on the situation.

DESIGN RULES FOR ADDITIVE MANUFACTURING(DFAM)

Understanding the fundamental principles is essential when applying DFAM, and these principles can vary depending on the additive manufacturing technology being used. These principles should be considered at the very beginning of the design process and adhered to throughout. A good understanding of DFAM principles and designing in accordance with them enables the effective use of all the advantages of additive manufacturing. However, violating these principles can have negative consequences, some of which may include:

- High production costs,
- Time loss,
- Quality issues,
- Loss of functionality,
- Material waste,
- Process inefficiency,
- Post-processing difficulties,
- Customer dissatisfaction,

To avoid these pitfalls, it's crucial to be well-aware of the advantages and disadvantages offered by the additive manufacturing technology to be used in the

production of the design. Being conscious of these advantages and disadvantages at the design stage can help engineers and designers make more informed decisions and maximize the potential of additive manufacturing.

The principles to be adhered to during the design process can vary depending on the technology being used. For instance, one of the basic rules for design for additive manufacturing points to principles related to the orientation of the part. This rule indicates that the direction in which a part is printed during additive manufacturing can have a significant impact on the part's performance, surface quality, and the efficiency of the production process. Since additive manufacturing is a layer-by-layer building process, and these layers vary based on the part's orientation, it can have significant effects on a variety of factors for the final part.

The first factor to consider is that the mechanical properties of a part related to 3D printing can change depending on its orientation. A part printed vertically may have different durability and strength properties than a part printed horizontally. This means that the print direction can affect strength, leading to anisotropic or orthotropic differences in various directions, which can lower the final part's performance. Anisotropic materials have physical or mechanical properties that vary depending on the direction in which the material is examined. For example, some crystals may conduct electricity and heat better in a particular direction. Wood is also anisotropic because its properties differ along its fibrous structure (generally along the direction of tree growth). Orthotropic material is a type of anisotropic material that has different properties in three perpendicular directions.

Especially in a 3D printing technique called Fused Deposition Modeling (FDM), it's observed that layers have different properties horizontally (x-y plane) compared to vertically (z-axis), and thus FDM prints usually have anisotropic properties. These properties can also vary depending on the material choice. Popular 3D printing materials like PLA (Polylactic Acid), ABS (Acrylonitrile Butadiene Styrene), and PETG (Polyethylene Terephthalate Glycol) can have different mechanical properties based on print parameters and especially the print direction.

However, some additive manufacturing technologies can help minimize the direction-dependency of material properties. For instance, powder-based technologies like Selective Laser Sintering (SLS) or Direct Metal Laser Sintering (DMLS) generally produce parts with more isotropic properties. Additionally, post-processing applications can also reduce the anisotropic properties of the material.

As a second factor, surface quality can be significantly affected by part orientation. Certain print directions provide smoother surfaces, while other directions can create a stair-step effect that increases microscale roughness on sloped or curved surfaces.

As a third factor, support structures are needed to prevent the part from collapsing during the 3D printing process, and these structures are often dependent on part orientation. Overuse of support structures increases both the time and cost of the print and extends the time required for post-processing, such as support structure removal.

As the final and fourth factor, part orientation can affect the amount of material used and the ultimate production time for manufacturing the part. Choosing the correct print direction can enable faster printing and reduce the extra material usage in support structures.

The most important aspect of this rule is to consider the print direction from the very beginning of the design process and to design accordingly. The designer must understand and balance these factors to achieve the best results. If maximum strength is required, the direction providing the best mechanical properties will be the most important. If surface quality is more crucial, the direction that provides the best surface quality will be the most important. Therefore, the print direction should always be considered during the design process, and designs should be optimized accordingly.

Another important rule for designing for additive manufacturing is to optimize the design and eliminate elements that are non-functional or not fit for purpose. A detailed functional analysis should be done to ensure the design meets requirements. Simplifying the design optimizes material use and energy consumption, thereby reducing cost and production time. Innovative approaches like topology optimization may be needed to simplify the design.

Topology Optimization is a mathematical method, usually based on the 'Solid Isotropic Material with Penalization' algorithm, that optimizes the minimum amount of material required and its distribution within a pre-defined design volume while considering predicted loads, boundary conditions, and some constraints. The goal is to maximize part performance around desired objectives. This method removes unnecessary material and strengthens high-stress areas, usually based on desired preconditions like maximum stiffness and minimum weight.

In one study, the weight-reduction-focused structural optimization of a race car's brake calipers is examined. The topology optimization method applied in the research managed to reduce the total weight of the supercar's calipers by approximately 668 g, which corresponds to 41.6% of the weight of ISR calipers.

Additionally, the maximum displacements in the y-direction for the front and rear calipers were reduced by 50% and 17.5%, respectively. Even though the produced calipers have not yet been tested, they theoretically surpass their commercial counterparts (Tyflopoulos et al., 2021). Future studies based on this research may involve surface finishing of 3D-printed and topology-optimized calipers, assembly of calipers, and mechanical testing of calipers. Furthermore, to collect significant data regarding the behavior of the braking system under high temperatures and to observe real disc wear, temperature sensors could be placed in the brake hydraulic system, and the calipers could be tested.

Unlike topology optimization, generative design uses algorithms and machine learning techniques more extensively to create design solutions that meet set goals and constraints, not limited to just optimizing material layout and meeting structural performance. Additionally, depending on the sophistication level of the algorithms, it can also include functionality, aesthetics, production methods, and different material properties as parameters. Using evolutionary algorithms and other artificial intelligence techniques that are often inspired by nature and mimic evolutionary processes, it has a very broad spectrum for design solutions.

The fundamental difference between the two is that topology optimization is a subset of generative design. Topology optimization primarily concerns itself with structural performance and looks at how material can be used most minimally and effectively within a certain volume. Generative design, on the other hand, incorporates a much broader set of variables in the final design process, including not just structural performance but also production constraints, cost, aesthetics, and other similar parameters.

Let's give an example for designing a chair. With generative design, we can specify that the chair needs to support a certain weight, fit within a certain space, be made from a particular material, be aesthetically pleasing, and be producible through a certain method and process. The algorithm can generate different designs that meet these criteria simultaneously. Furthermore, if we proportionally weight these various, distinct design objectives, the algorithm can also generate new and alternative designs based on these new, proportionally differentiated balances. Topology optimization could be an intermediate step in this process and could optimize the chair's structure for carrying the required load, but the SIMP algorithm won't address other aspects like aesthetics or producibility.

To prevent the most fundamental drawbacks that can be encountered in design for additive manufacturing, some general principles should be considered as preventative measures. To prevent high production costs, excessive material use and incorrect material selection should be avoided. Otherwise, production costs can increase. For example, designing walls that are unnecessarily thick can lead

to the use of excessive material and consequently to high costs. Also, incorrect material selection can increase not just the cost of the material but also the costs of post-processing. To avoid time loss, adequate design knowledge and preparation are required. Overly complex designs and incorrect technology selection can extend the production time. Designs that are not suitable for additive manufacturing in particular require major revisions and redesign, which negatively affects the project timeline. To prevent loss of functionality and quality issues, the additive manufacturing technology must be correctly chosen, and errors that could lead to incorrect tolerances, incorrect layer thickness, and incorrect resolution should be avoided. This can lead to quality issues and ultimately customer dissatisfaction. Additionally, design errors like not paying attention to overhang angles can lead to incorrect support structures. When support structures are unnecessarily or incorrectly placed, this leads to the use of extra material and waste. Moreover, design errors in inaccessible areas and incorrect support structures can make post-processing difficult, leading to additional time and cost. Alongside these, other factors like incorrect expectation management, poor communication, and inadequate quality control can also lead to customer dissatisfaction.

Avoiding these and similar mistakes in additive manufacturing projects can both improve the efficiency of the process and enhance customer satisfaction. Furthermore, correct design and technology choices can improve the quality and performance of the final product, which can positively affect customer satisfaction.

CONCLUSION

This study provides information in various fields such as innovation, design, additive manufacturing, topology optimization, and generative design. Concepts like DFAM (Design Rules for Additive Manufacturing), topology optimization, and generative design are of great importance in engineering design and production processes.

Advancements in modern production technologies like additive manufacturing allow for the creation of geometries with complex internal structures and functional forms. However, to effectively utilize all the advantages of these technologies, the design process must also be arranged in a manner that accommodates these new possibilities. For this purpose, DFAM principles address a range of factors.

Topology optimization and generative design offer mathematical and algorithmic methods for creating complex and functional designs. Through these,

material usage is minimized while maximizing the mechanical and functional performance of the design.

These technologies and methods are gaining increasing importance particularly in fields like mechanical engineering, automotive, aviation, and aerospace. For example, the weight of a car's brake caliper can be reduced through topology optimization. This can enhance fuel efficiency and thereby result in a more sustainable product.

Lastly, the contribution of artificial intelligence and machine learning to the design process is also increasing. Artificial intelligence can quickly analyze large data sets and offer design suggestions, thereby accelerating the design process and reducing costs.

REFERENCES

3DPrint. (2023). Lowe's and Made In Space will Launch First Commercial 3D Printer into Space and First In-Store VR Design Tool. Retrieved September 20, 2023, from https://3dprint.com/102841/lowes-made-in-space-3d-printer/

AM Media. (2023). 3D Printed Cold Plate for an Electric Race Car: The Cool Parts Show #51. Retrieved September 18, 2023, from https://www.additivemanufacturing.media/articles/3d-printed-cold-plate-for-an-electric-race-car-the-cool-parts-show-51

Dezeen. (2023). Algorithm designs seven million different jars of Nutella. Retrieved September 18, 2023, from https://www.dezeen.com/2017/06/01/algorithm-seven-million-different-jars-nutella-packaging-design/

Diegel, O. (2023). Oddguitars. Retrieved September 18, 2023, from https://www.oddguitars.com/index.html

Fireart. (2023). AI-Driven Design: How Artificial Intelligence Is Shaping UI/UX Design. Retrieved September 18, 2023, from https://fireart.studio/blog/ai-driven-design-how-artificial-intelligence-is-shaping-ui-ux-design/

Impressio. (2023). NFL Helmet — Impressio.Tech. Retrieved September 20, 2023, from https://www.impressio.tech/human-protection

ISO. (2023). ISO/TC 279 - Innovation management. Retrieved September 17, 2023, from https://www.iso.org/committee/4587737.html

McKinsey. (2023). What is innovation? Retrieved September 17, 2023, from https://www.mckinsey.com/featured-insights/mckinsey-explainers/what-is-innovation

nTop. (2023-a). Air duct assembly consolidation. Retrieved September 20, 2023, from https://www.ntop.com/innovation/air-duct-assembly-consolidation/

nTop. (2023-b). Design brief: 3D printed casting of 3-foot long robot arm. Retrieved September 18, 2023, from https://www.ntop.com/resources/blog/design-brief-3d-printed-casting-of-3-foot-long-robot-arm/

nTop. (2023-c). The 2021 nTop Ed Challenge winners announced. Retrieved September 18, 2023, from https://www.ntop.com/resources/blog/the-2021-ntoped-challenge-winners-announced/

nTopology. (2023-a). F-16 aircraft part qualification in 30 days with AM. Retrieved September 18, 2023, from

https://www.ntop.com/resources/case-studies/aerospace-f-16-aircraft-qualification-for-additive-manufacturing/

nTopology. (2023-b). Next-Gen Engineering Design Software: nTop (formerly nTopology). Retrieved September 18, 2023, from https://www.ntop.com/

SI-BONE. (2023). iFuse-TORQ ™ Implant System. Retrieved September 18, 2023, from www.SI-BONE.com

Temisth. (2023). » The cold plate for GPU card is printed. Retrieved September 18, 2023, from http://temisth.com/the-cold-plate-for-gpu-card-is-printed/

Toptal. (2023). The Present and Future of AI in Design (with infographic). Retrieved September 18, 2023, from https://www.toptal.com/designers/product-design/infographic-ai-in-design

Tyflopoulos, E., Lien, M., & Steinert, M. (2021). Optimization of Brake Calipers Using Topology Optimization for Additive Manufacturing. *Applied Sciences 2021, Vol. 11, Page 1437*, *11*(4), 1437. https://doi.org/10.3390/APP11041437

Vaen. (2023). VORONOI BIKE SADDLE. Retrieved September 18, 2023, from https://vaen.es/vaen-saddle

Chapter 2

Elucidating the Categories of Additive Manufacturing Processes According to ASTM F2792 Standard

Ahmet DAYANÇ[1], Feridun KARAKOÇ[2]

[1] *Arş. Gör.; Kütahya Dumlupınar Üniversitesi Mühendislik Fakültesi Makine Mühendisliği Bölümü. ahmet.dayanc@dpu.edu.tr ORCID No: 0000-0002-5214-9021*

[2] *Dr. Öğr. Üyesi; Kütahya Dumlupınar Üniversitesi Mühendislik Fakültesi Makine Mühendisliği Bölümü. feridun.karakoc@dpu.edu.tr ORCID No: 0000-0002-6210-4070*

ABSTRACT

Additive manufacturing is a technology capable of layer-by-layer production, particularly excelling in the fabrication of complex structures, hollow designs, and innovative products. This technology is invaluable across various sectors such as aerospace, medical, automotive, and space, providing new opportunities for design.

Various methods of additive manufacturing have been standardized by organizations like ASTM and ISO. These classifications include distinct categories such as Binder Jetting, Directed Energy Deposition, Material Extrusion, Material Jetting, Powder Bed Fusion, Sheet Lamination, and Vat Photopolymerization.

Each additive manufacturing method comes with its own set of advantages and limitations. For instance, Material Jetting is renowned for its fine detailing and high resolution, whereas Powder Bed Fusion is well-suited for complex geometries and high mechanical properties. The diversity in additive manufacturing methods has a profound impact on product design and design engineering.

This subject matter is crucial for numerous sectors and applications, requiring careful selection of the most suitable additive manufacturing method based on its distinct advantages and limitations.

Consequently, the diversity and flexibility offered by additive manufacturing create new opportunities and paradigms in product design and design engineering, while the advantages and limitations of various methods should be meticulously considered.

Keywords: Additive Manufacturing, Directed Energy Deposition, Material Extrusion, Powder Bed Fusion, Vat Photopolymerization

INTRODUCTION

Additive Manufacturing is an innovative fabrication method distinguished from traditional manufacturing techniques by its ability to construct a product layer by layer. This enables the production of designs with hollow and complex internal structures, a process often unattainable through traditional manufacturing methods such as subtractive manufacturing, casting, and injection molding. For instance, a component with intricate air channels or specialized lattice structures can be directly fabricated using additive manufacturing. This is particularly valuable in sectors such as aerospace, space, medical, and automotive, offering advantages like new functional integrations, design enhancements, and material-saving light-weighting (Additive Manufacturing, 2023-a).

To thoroughly understand additive manufacturing technologies and their differences, classification is essential. To meet this need, a classification has been made according to the standards of ASTM (American Society for Testing and Materials) International. According to ASTM F2792 standards, additive manufacturing technologies are categorized as follows (ASTM International, 2012). There is also ISO TC 261 standard available (ISO, 2023). Although ISO (International Organization for Standardization) has made a similar classification, ASTM's categorization is more commonly used. Both organizations play significant roles in setting and updating the standards for additive manufacturing. The following list enumerates various categories related to additive manufacturing technologies:

- Binder Jetting
- Directed Energy Deposition
- Material Extrusion
- Material Jetting
- Powder Bed Fusion
- Sheet Lamination
- Vat Photopolymerization

The technology of 'Binder Jetting' was developed by the Massachusetts Institute of Technology (MIT) in the early 1990s (WhiteClouds, 2023). Generally, in this process, a layer of powder evenly spread on the build area is selectively bound by jets of a binding agent from a nozzle-equipped apparatus and then cured. The metal box containing the produced part is removed from the machine and placed in an oven for sintering. Parts exiting the oven are cleaned of residual powder and are then returned to an oven to allow a filler metal to wick into the pores via capillary action. Variations in this process exist

depending on the binder and material used, and some steps may be unnecessary depending on specific requirements (3DTechValley, 2023).

The technology of 'Binder Jetting' offers high speed, multi-color printing, material flexibility, and high-volume production capacity. Therefore, compared to other additive manufacturing technologies, this technology has certain advantages. Additionally, the binding agent is sprayed onto the powder layers, similar to the ink in traditional inkjet printers used in paper printing (ExOne, 2023). This feature positively impacts the speed of the process. Materials such as silica sand, molding sand, stainless steel, Inconel 625 and 718 alloys, chromite, cobalt chrome, zircon, tungsten, and tungsten carbide can be used in this technology (AMFG, 2023). The production process is illustrated in Figure 1 below.
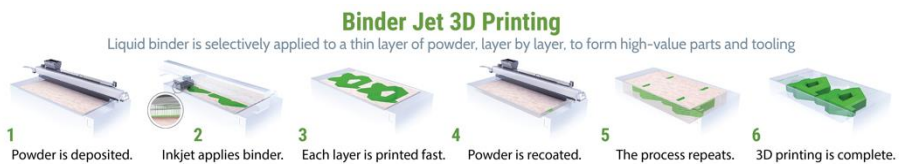
Figure 1: Binder Jetting

'Directed Energy Deposition' technology was developed by Sandia National Laboratories in 1995 but has subcategories depending on the energy source used. The first subcategory uses laser energy and is called Laser Engineered Net Shaping. The one using electron beam is known as Electron Beam Additive Manufacturing. The other two methods are Plasma Transferred Arc Deposition and Wire Arc Additive Manufacturing. In this technology, a coaxial nozzle is used for both the energy source and material feed. The process takes place in a hermetically sealed chamber filled with inert gas or a vacuum created for EBAM systems. This chamber environment is specially designed to prevent metal oxidation, particularly with reactive materials like titanium. The nozzle is mounted on a mechanism like a gantry system, a multi-axis CNC head, or a robotic arm. The build platform can also move in multiple axes to create complex shapes and can be used for repairing or modifying existing parts by adding material. It generally offers a rapid production process, and the resulting parts exhibit superior mechanical properties. Compared to other systems, the capital cost is high, and due to the nature of the process, no support structures are formed, preventing overhangs (EPD, 2023-a). This method is illustrated in Figure 2 below.
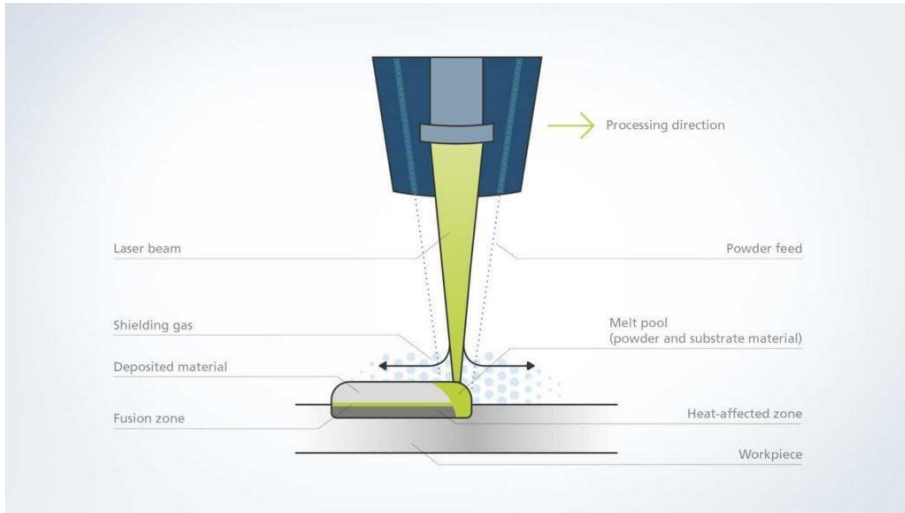
Figure 2: Directed Energy Deposition

'Material Extrusion' technology was developed in the 1980s and operates by using a heated nozzle to lay down layers of thermoplastic polymer material in a continuous flow, resulting in part production (Siemens, 2023-a). This method is known as Fused Deposition Modeling. The names of the subcategories vary depending on the material used. Direct Ink Writing or Robotic Deposition methods use nozzles without heating features and work with more fluid materials. Another method under this category is 3D Bioprinting, which can extrude biologically relevant hydrogel materials with varying rheological properties (Fernández et al., 2023). This technology is generally slower and less geometrically accurate compared to other manufacturing methods. Thermoplastic materials are more common and affordable, and hobby-level devices have low setup and operational costs. Although industrial-scale devices are more expensive, they can be cost-effective for rapid prototyping. Multiple design iterations and improvements on non-functional prototypes can lead to design optimization in the final product. Some materials used in this method may be toxic (TWI Global, 2023). An example application of this method is illustrated in Figure 3 below.
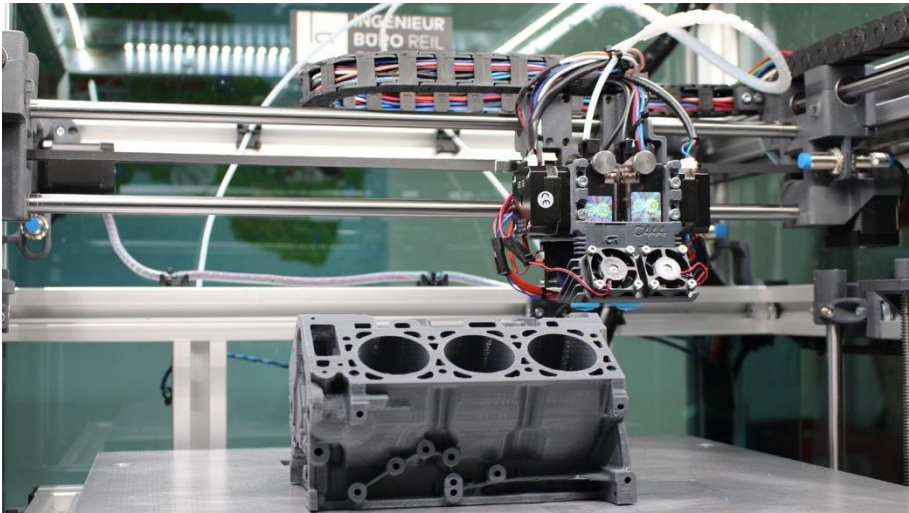
Figure 3: Material Extrusion

The 'Material Jetting' technology dates back to the mid-1990s and is a technology where the material is atomized. Examples of this technology include the PolyJet method, where photopolymeric resins are jetted and cured with UV light, and the Wax Jetting method, where wax-based materials are jetted for casting applications. Furthermore, the NanoParticle Jetting method involves jetting metallic or ceramic nanoparticles within a binding matrix to create objects (AM Media, 2023-b). This technology can achieve high-quality surfaces. Although the process is high-resolution and can easily create geometric details with thin layers, support material is required for overhanging geometries. Material variety is limited, resulting in thermal and mechanical constraints on the final product. Unlike Material Extrusion technologies, other bioprinting methods that jet bio-inks in droplet form can be included in Material Jetting technology. However, as the polymer concentration and molecular weight increase in the non-Newtonian bio-inks, droplet formation becomes difficult, and droplet speed decreases. Time-Independent Non-Newtonian Fluids, such as dilatant or pseudoplastic, and Time-Dependent Non-Newtonian Fluids, displaying rheological, thixotropic, or rheopectic characteristics exist depending on the material (Elkaseer et al., 2022). A printer using this method is shown in Figure 4 below.
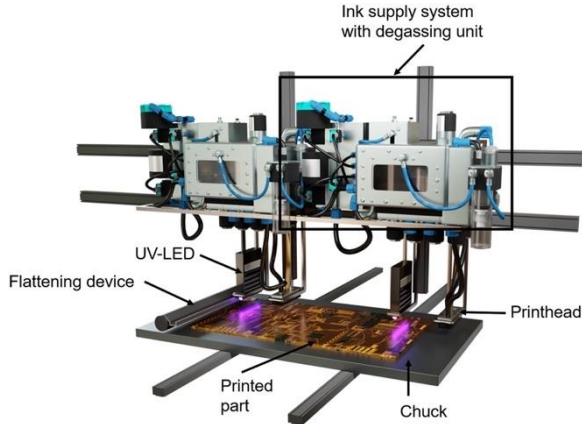
Figure 4: Material Jetting

The initial method where 'Powder Bed Fusion' technology was developed is Selective Laser Sintering, originating from the University of Texas in the late 1980s. In this method, powder layers are sintered to form solid layers using metals, ceramics, and polymers. Selective Laser Melting, on the other hand, fully melts the powder and is generally used for metals, while Direct Metal Laser Sintering is generally used for alloys. Electron Beam Melting uses a high-energy electron beam instead of a laser and can be used for metals like titanium alloys. In Multi Jet Fusion technology, powder layers are heated and sintered using jetting technology instead of high-energy beams (Dassault, 2023). Highly detailed parts with complex geometries and excellent mechanical properties can be produced. Since only the required amount of powder is melted, some of the remaining powder can be reused. The method is shown in Figure 5 below.
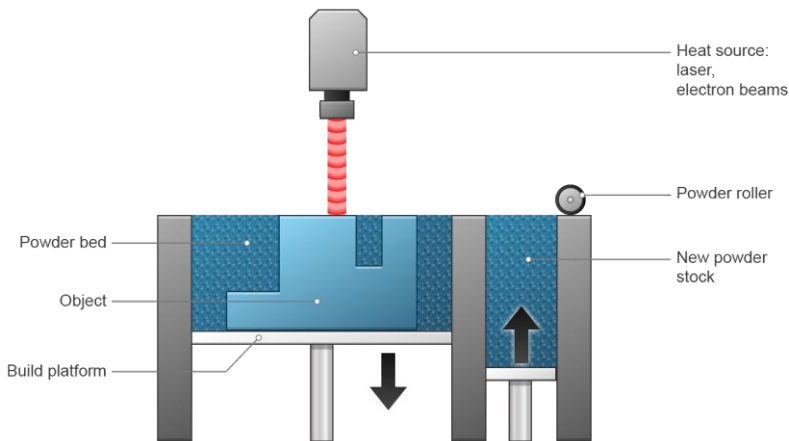
Figure 5: Powder Bed Fusion

'Sheet Lamination' technology involves combining thin layers of metal, paper, or polymer through continuous material feed rollers and external force (Siemens, 2023-b). For example, in the Laminated Object Manufacturing method, which dates back to the late 1980s, paper sheets are used with adhesives and can be dimensioned using precision-cutting blades. In Ultrasonic Additive Manufacturing, metal sheets are welded together using ultrasonic welding. Although large parts can be produced relatively easily, quickly, and cost-effectively, creating internal cavities and complex structures can be challenging. Moreover, the mechanical properties may be limited in these methods that use adhesive or ultrasonic energy. Nowadays, Sheet Lamination technology can be categorized into seven different sub-methods (EPD, 2023-b). This technology is shown in Figure 6 below.
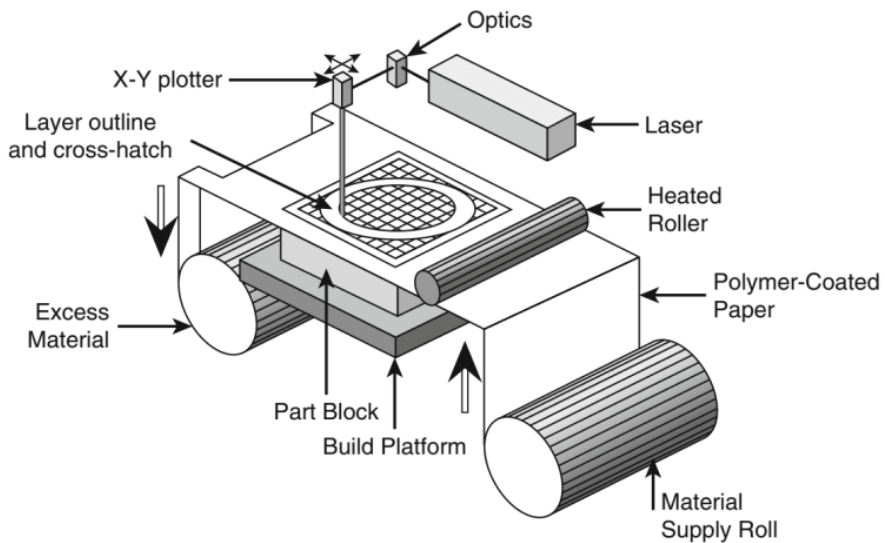
Figure 6: Sheet Lamination

The origin of the 'Vat Photopolymerization' technology dates back to 1986, and the first and most well-known method is Stereolithography. Suitable for relatively small models, this method is a fast and highly accurate process that uses special photopolymer resins activated by ultraviolet light. However, one disadvantage of using photopolymer material is the potential for structural weakness and degradation over time. This technology includes sub-methods like Direct Light Processing, Solid Ground Curing, and Continuous Liquid Interface Production (Siemens, 2023-c). In Figure 7 below, the SLA method is

shown on the left, and the CLIP method is shown on the right (EngineersGarage, 2023).
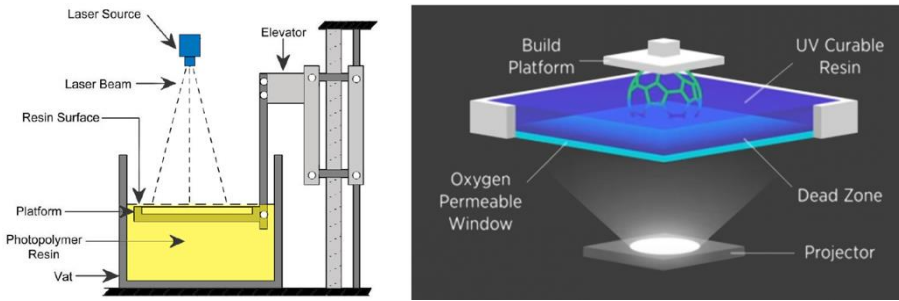
Figure 7: Vat Photopolymerization a) SLA, b) CLIP

These classifications are highly useful for understanding the various technologies of additive manufacturing and selecting the method most suitable for the design purpose of the part to be produced.

In conclusion, the capabilities of additive manufacturing significantly impact processes related to product design and design engineering, creating new design paradigms. Consequently, design principles for additive manufacturing are emerging, which take into account the advantages and limitations of methods that vary according to the diversity of additive manufacturing technologies.

CONCLUSION

Additive manufacturing distinguishes itself from traditional manufacturing methods through its ability to construct products layer by layer, making it ideal for complex geometries, hollow structures, and innovative designs. Industries such as aerospace, automotive, medical, and space significantly benefit from the advantages offered by this technology.

Additive manufacturing technologies have been classified by standard organizations like ASTM and ISO. These classifications include various methods such as Binder Jetting, Directed Energy Deposition, Material Extrusion, Material Jetting, Powder Bed Fusion, Sheet Lamination, and Vat Photopolymerization.

Each method possesses its own set of advantages and limitations. For instance, Material Jetting excels in high resolution and fine detailing, while Powder Bed Fusion is advantageous for complex geometries and high mechanical properties. Sheet Lamination is suitable for the production of large parts, and Vat Photopolymerization is adept at fast and precise manufacturing.

In conclusion, the diversity and flexibility provided by additive manufacturing have a significant impact on product design and design engineering. The selection of the most appropriate additive manufacturing method varies depending on the design purpose and needs of different sectors and applications. Therefore, a comprehensive understanding and consideration of the advantages and limitations of various additive manufacturing methods are essential.

REFERENCES

3DTechValley. (2023). *Binder Jetting 3D Printing Technology & Process.* Retrieved September 11, 2023, from https://www.3dtechvalley.com/binder-jetting-3d-printing/

Additive Manufacturing. (2023-a). *What Is Additive Manufacturing?* Retrieved September 11, 2023, from https://www.additivemanufacturing.media/kc/what-is-additive-manufacturing

AM Media. (2023-b). *What Is Material Jetting 3D Printing?* Retrieved September 11, 2023, from https://www.additivemanufacturing.media/articles/material-jetting---its-like-printing-just-in-3d

AMFG. (2023). *A Short Guide to 3D Printing with Binder Jetting.* Retrieved September 11, 2023, from https://amfg.ai/2018/03/13/3d-printing-binder-jetting-short-guide/

ASTM International. (2012). Designation: F2792 − 12a. *Standard Terminology for Additive Manufacturing Technologies.* https://doi.org/10.1520/F2792-12A

WhiteClouds. (2023). *Binder Jetting in 3D Printing.* Retrieved September 11, 2023, from https://www.whiteclouds.com/3dpedia/binder-jetting/

Dassault. (2023). *Powder bed fusion - DMLS, SLS, SLM, MJF, EBM.* Retrieved September 11, 2023, from https://make.3dexperience.3ds.com/processes/powder-bed-fusion

Elkaseer, A., Chen, K. J., Janhsen, J. C., Refle, O., Hagenmeyer, V., & Scholz, S. G. (2022). Material jetting for advanced applications: A state-of-the-art review, gaps and future directions. *Additive Manufacturing* (Vol. 60). Elsevier B.V. https://doi.org/10.1016/j.addma.2022.103270

EngineersGarage. (2023). *3D Printing Processes - Vat Photo polymerisation (Part 3/8).* Retrieved September 12, 2023, from https://www.engineersgarage.com/3d-printing-processes-vat-photo-polymerisation-part-3-8/

EPD. (2023-a). *What is Direct energy deposition, its types and pros and cons.* Retrieved September 11, 2023, from? https://engineeringproductdesign.com/knowledge-base/direct-energy-deposition/

EPD. (2023-b). *What is Sheet Lamination, its types and application.* Retrieved September 12, 2023, from https://engineeringproductdesign.com/knowledge-base/sheet-lamination/

ExOne. (2023). *Binder Jetting Technology.* Retrieved September 11, 2023, from https://www.exone.com/en-US/Resources/case-studies/what-is-binder-jetting

Fernández, H. ;, Aguilar, M. A. ;, Herrada-Manchón, H., Fernández, M. A., & Aguilar, E. (2023). Essential Guide to Hydrogel Rheology in Extrusion 3D Printing: How to Measure It and Why It Matters? *Gels,* Vol. 9, Page 517, 9(7), 517. https://doi.org/10.3390/GELS9070517

ISO. (2023). *ISO/TC 261 - Additive manufacturing.* Retrieved September 11, 2023, from https://www.iso.org/committee/629086.html

Siemens. (2023-a). *Material Extrusion.* Retrieved September 11, 2023, from https://www.plm.automation.siemens.com/global/en/our-story/glossary/material-extrusion/53981

Siemens. (2023-b). *Sheet Lamination.* Retrieved September 12, 2023, from https://www.plm.automation.siemens.com/global/en/our-story/glossary/sheet-lamination/55512

Siemens. (2023-c). *Vat Photopolymerization.* Retrieved September 12, 2023, from https://www.plm.automation.siemens.com/global/en/our-story/glossary/vat-photopolymerization/53338

TWI Global. (2023). *What is Material Extrusion? (A Complete Guide).* Retrieved September 11, 2023, from https://www.twi-global.com/technical-knowledge/faqs/what-is-material-extrusion#Advantages

Chapter 3

Security Violations and Threats in The Applications of IoT

Bora ASLAN[1], Füsun YAVUZER ASLAN[2]

[1]Asist.Prof.Dr.; Kırklareli University Faculty of Engineering Department of Software Engineering. bora.aslan@klu.edu.tr ORCID No: 0000-0002-8069-8204

[2]Asist.Prof.Dr.; Kırklareli University Faculty of Engineering Department of Software Engineering. fusun.yavuzer@klu.edu.tr ORCID No: 0000-0001-7096-3425

INTRODUCTION

In a presentation for Procter & Gamble in 1999, Kevin Ashton discussed the IoT (Internet of Things) for the first time. In fact, in his presentation, Ashton highlighted the company's desired benefits of using RFID technology. However, Ashton may have inspired the IoT concept, which is gaining traction today, and many products in this regard by introducing the connectivity of all devices to one other.

In the internet world, the number of devices connected to the internet and internet traffic are increasing daily. According to Cisco's research, traffic in 2017 was 100 EB (Exabyte), 212 EB in 2020 and predicted to be 333 EB in 2022. The number of devices linked to the network is expected to increase from 18.4 billion in 2018 to 29.3 billion in 2023, as the ratio of devices employed in IoT applications to all devices approaches 50% (Cisco, 2018).

Devices produced for IoT applications provide many advantages and many disadvantages following their nature. Attackers are particularly interested in these disadvantages. Some of the reasons why attackers choose IoT devices as targets are discussed in this article.

Many devices in the IoT realm grabs attackers' attention in a major way. As stated at the outset of the study, the number of IoT devices used much outnumbers the number of laptops or desktop PCs. Attackers are interested in this large attack surface area. Because the more devices there are, the more access points there are for an attacker to capture.

The devices utilized in the IoT environment are only designed to require the minimum number of resources necessary to complete their functions. As a result, different security measures, such as firewall and antivirus software, used on PCs cannot be deployed to such devices. Due to this predicament, attackers anticipate that these devices will be easy to target.

Regrettably, manufacturers prioritize operability over security, which is a major issue in the informatics sector. Companies producing devices within the scope of IoT primarily aim to operate the system healthily. When security issues develop, these companies frequently try to come up with new products. The first products manufactured are typically released to the market with poor security measures in order to become the first and most widely utilized product.

Users are concerned about the security of their personal information greatly. IoT products, particularly for end-users, collect and preserve a lot of personal information. For example, healthcare applications and home automation products can be examples of this category. Understandably, retaining people's confidential information in a system catches attackers' interest, leading to a surge in attacks on this subject.

Only when there is an issue or a high-end innovation does a manufacturer offer an update. Nonetheless, delays in cases like not applying these updates to every system or not applying them at all and instead urging customers to buy new items cause concerns, particularly regarding security.

To interfere in devices remotely, manufacturers utilize various access techniques known only to them, referred to as back doors. If attackers discover this technique, all devices may become vulnerable.

Most devices are delivered with the default username and password issued at the factory during the initial setup to log in to the admin interface. The devices used without modifying the default settings can be captured in this manner.

SEVERAL ATTACKS EXPERIENCED ON IOT DEVICES

IoT devices are considered easy targets for attackers for the reasons stated above, and they are vulnerable to various attacks. It is impossible to keep track of every security vulnerability that occurs in the IoT world. Most manufacturers conceal security flaws or are unable to detect them at all. Below are some security breaches related to IoT historically are represented.

Vitek Boden, an Australian citizen, carried out a remote cyberattack on the state sewage treatment plant in 2000 after his job application was rejected. Due to the attack, 800,000 liters of liquid waste flowed into local parks, waterways, and the garden of a luxury hotel (Abrams & Weiss, 2008).

A virus called "Sobig" that infected the computers of the CSX railway business in North America caused significant delays in train service by disabling the railway's signaling systems (Niland, 2003).

In the United States in 2008, a series of Internet worms shut down Daimler Chrysler's 13 vehicle manufacturing plants for about an hour, disrupting over 50,000 assembly lines (Roberts, 2008).

In 2008, a 14-year-old kid in Lodz, Poland, used a homemade transmitter system to attack the city's tram system, taking control of certain trains and caused the injury of 12 people (Baker, 2008).

More than 15 Iranian power stations were targeted by the Stuxnet internet worm in 2010, destroying 984 uranium enrichment centrifuges. Experts estimated that this major attack caused a 30% reduction in uranium enrichment efficiency. A worker USB drive is thought to have started the attack. Stuxnet is reported to be designed to attack PLC (Programmable Logic Controller) devices in nuclear power plants in order to sabotage them. This attack is seen as a milestone moment in the history of cyberwarfare (Farwell & Rohozinski, 2011).

In 2011, a Russian internet service provider attacked the SCADA systems of a water distribution company in the USA. Attackers have been found to gain

unauthorized access to a company's database and steal usernames and passwords for SCADA systems, including those used by water districts. (Keszthelyi, 2014).

According to the findings, attacks on the US electrical distribution corporation in 2012 resulted in millions of dollars in losses (Cárdenas, Amin, & Sastry, 2008).

In 2015, attackers used malware to break into a major air conditioning company and steal personal information from more than 70 million consumers, including credit and debit card information for more than 40 million (Krebs, 2014).

A well-known automobile manufacturer recalled 1.4 million vehicles in 2015. It was mentioned in the statement that there was a detected vulnerability in the automatic control software of the vehicles, and they demonstrated that someone else could take over the control via remote connection in a test scenario (Greenberg, 2015).

Security specialists from the Sucuri firm announced in June 2016 that they had uncovered a botnet of more than 25,000 CCTV equipment that could be used to launch DDoS assaults. Sucuri discovered that the malicious botnet's IP addresses are registered in 105 different countries (Bawany, Shamsi, & Salah, 2017).

NyaDrop, a malicious malware that hijacked IoT devices with default username and password, was discovered in September 2016. NyaDrop analysis revealed that the attack originated from Russian IP addresses. When the software infects a device, it allows it to connect to a remote network and guarantees that other control software is loaded. NyaDrop only targeted devices such as DVRs, CCTV cameras, routers, and other embedded systems. It's thought that the goal here is enabling devices to join a botnet. (Beltov, 2016)

On September 22, 2016, the site "Krebs on Security," which distributed security information, was attacked by a DDoS attack and became inoperable. According to reports, attackers used a data transmission rate of almost 620 Gbps per second. A similar DDoS attack was launched against the French internet provider OVH on the same day. The attack, which used 1 Tbps of data transmission per second, is thought to be the world's largest DDoS attack. It is known that attackers used more than 150,000 CCTV devices and digital video recorders in the attacks. These and other incidents demonstrate how hazardous compromised IoT devices may be (Krebs, 2016).

On October 21, 2016, DDoS attacks were active worldwide, making access to several web platforms such as PayPal, Amazon, Twitter, GitHub, and Reddit difficult or impossible. The Mirai botnet, which was employed in these attacks,

is entirely made up of IoT devices. During the attack, the Mirai botnet, which means "future" in Japanese, infected 4000 devices each hour, and it is estimated that it now controls over 500,000 devices. The Mirai botnet is well-known for being utilized in 1 terabit per second DDoS attacks, which set a record with 148,000 IoT devices. It mostly hosts CCTV cameras, DVR devices and home routers from 164 different countries (Dobbins, 2016).

According to a report released by the Kaspersky security organization in October 2016, the Hajime botnet had penetrated over 300,000 devices. The Mirai botnet is battling the Hajime botnet, attempting to expand its network by attacking devices on other botnets with malware to gain control of devices. The purpose of a botnet, which is growing day by day, is not yet known. (Millman, 2017)

In April 2017, Unit 42 researchers discovered Amnesia, a new variant of the Tsunami botnet. It exploits a flaw in TVT Digital's DVR devices, which are branded by more than 70 vendors worldwide, to connect to a remote connection that the firm utilizes but does not publicly disclose. Around 227,000 devices have joined the Amnesia botnet network worldwide, including Taiwan, the USA, Israel, Türkiye, and India. This number is expected to be very high today. (Xiao & Zheng, 2017)

A new botnet named Persirai was identified in May 2017. The botnet targets more than 1000 IP Camera models based on numerous Original Equipment Manufacturer (OEM) devices. Trend Micro has detected 120,000 cameras acquired in the Persirai botnet network (Yeh, Chiu, & Lu, 2017).

In June 2017, researchers published a study demonstrating that personal data can be stolen via Fitbit smart wristbands, which come with a significant market share. They used a man-in-the-middle attack on the wristband, allowing them to capture the data before it was transmitted to the cloud servers for processing. (Fereidooni et al., 2017)

The Reaper botnet network, which was said to be more sophisticated than the Mirai botnet, was discovered in October 2017. Unlike the Mirai network, Reaper targets popular brands of routers, IP cameras and network attached storage devices whose security flows have not been discovered yet (Greenberg, 2017).

In March 2018, hackers targeted the Saudi Arabian Oil Company's IoT-based industrial security systems (Perlroth & Krauss, 2018).

A vulnerability was discovered in Amazon's popular video doorbell, Ring, in March 2019, allowing for unwanted home spying. This vulnerability has demonstrated that hackers can gain access to unencrypted audio and video recordings. (Halon, 2019)

In June 2019, security experts discovered Silex, a new malware that spreads by rapidly erasing the firmware of devices. Even though the malware had run only for one day, it managed to deactivate thousands of devices. The software could not be spread further due to the malware's faulty coding. Silex was built by three young people from a European country, according to security expert Ankit Anubhav (TrendLabs, 2019).

A security vulnerability was discovered in February 2020 that might occur during the communications of Philips Hue smart bulbs with other devices. It has been reported that an attacker who exploits this vulnerability may be able to take control of the complete home network. (Owen, 2020)

Nozomi Networks Labs security researchers discovered multiple variants of the Dark Nexus botnet formed out of IoT devices in May 2020 (Pinto, 2020).

The malware aimed to infect as many IoT devices and Linux servers as possible, as per the researchers that found the Kaiji botnet network in May 2020. Kaiji, who seeks to capture devices using SSH brute force attacks, focuses on devices with weak passwords connected to the internet via SSH ports (SecureMac, 2020).

IOT ARCHITECTURE

When the literature is examined, many IoT architecture proposals are encountered. In other words, there is no single accepted architecture like TCP/IP. Despite this, the 3-, 4- and 5-layer architecture approach stands out. The models are given in Figure 1 (Aslan, 2023).
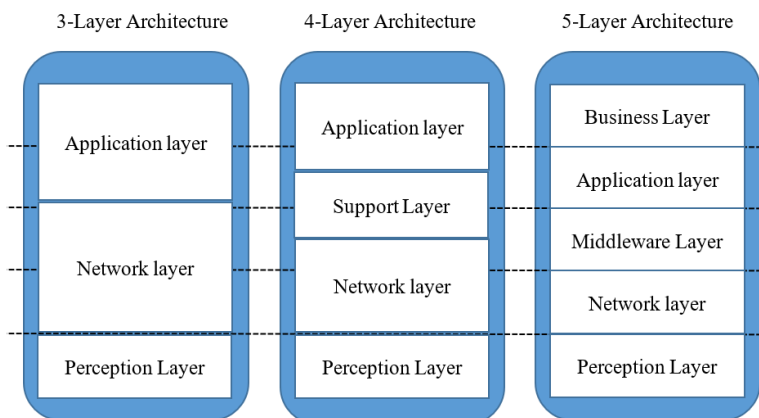
Figure 1: Featured IoT Architectures

Although there is no standard for IoT architectures, each layer uses different technologies and protocols depending on the application being built. In general,

the perception layer is the element of the architecture closest to the hardware and inherits sensors. Figure 2 shows the several types of sensors employed here, and the number of them is growing every day. Medical sensors have hundreds of options such as pulse and heart rate sensor, ECG / EEG sensor, respiratory rate measurement sensor, force sensor used in dialysis machines, oximeter sensor measuring the fraction of hemoglobin saturated with oxygen as per the total hemoglobin levels. Biosensors and chemical sensors, such as pH sensors and glucose sensors, are designed to make various measures and are commonly used in chemistry and biology. Environmental sensors are commonly used to measure sound, acceleration, force, light, pressure, humidity, and gas. This layer also includes cameras, microphones, and sensors such as light proximity and movement in mobile devices.
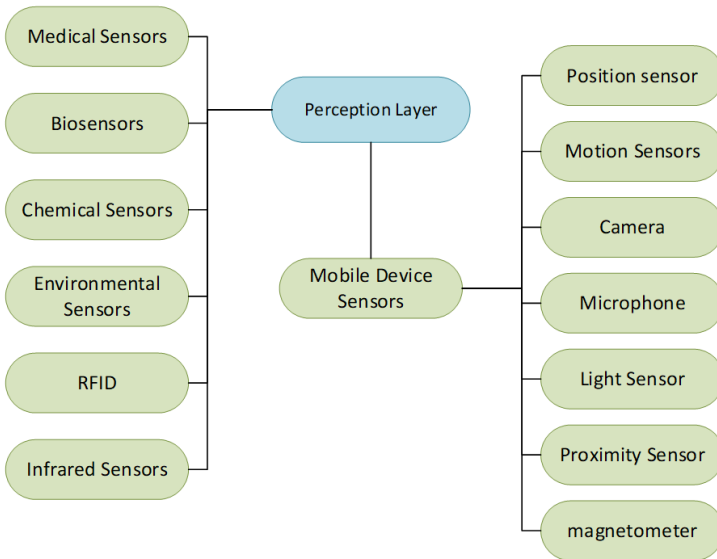
Figure 2: Technologies that can be used in the perception layer.

Many protocols and technologies are defined at the network layer to convey data to the outside environment. Figure 3 depicts the most used ones.
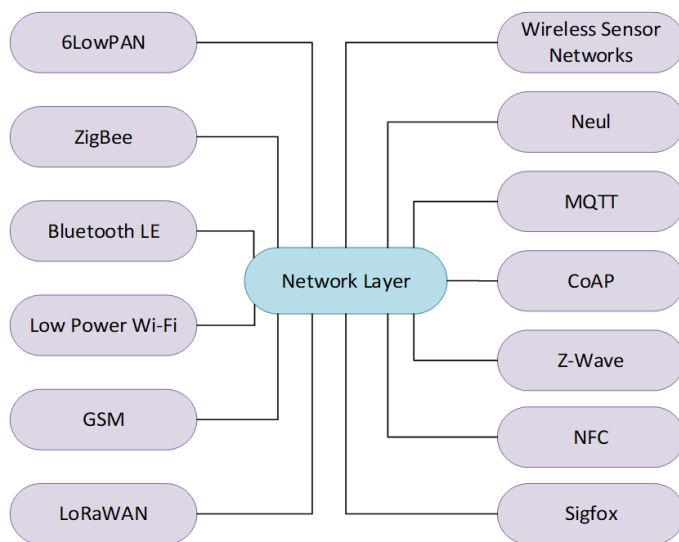
Figure 3: Technologies that can be used in the network layer.

The application layer, as depicted in Figure 4, is related to the IoT application's purpose. Many projects on this topic have been developed and are now being developed around the world. Home automation, fitness tracking, health monitoring, environmental protection, smart cities, and industrial manufacturing are all examples of IoT applications. All of them are defined in the application layer.
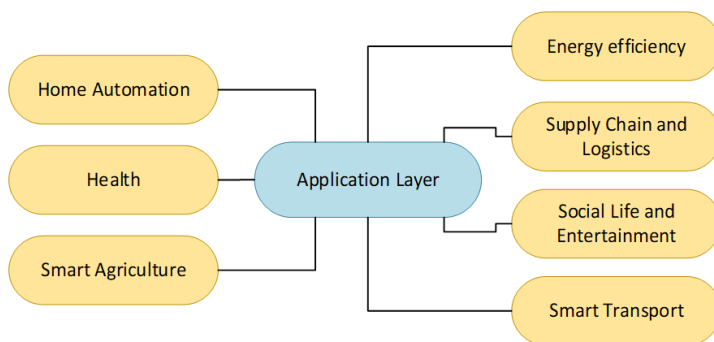
Figure 4: Technologies That can be Used in the Application Layer

THREATS TO THE IOT ARCHITECTURE

The motives of attackers and attacks on IoT devices were discussed in the previous section. According to studies undertaken in this field, threats to IoT applications are classified based on designs and illustrated in Figure 5. The types of attacks that have happened or may happen have been determined based

on layers. Although some reported attacks are directed at traditional computer networks, their functions are evaluated following IoT applications.
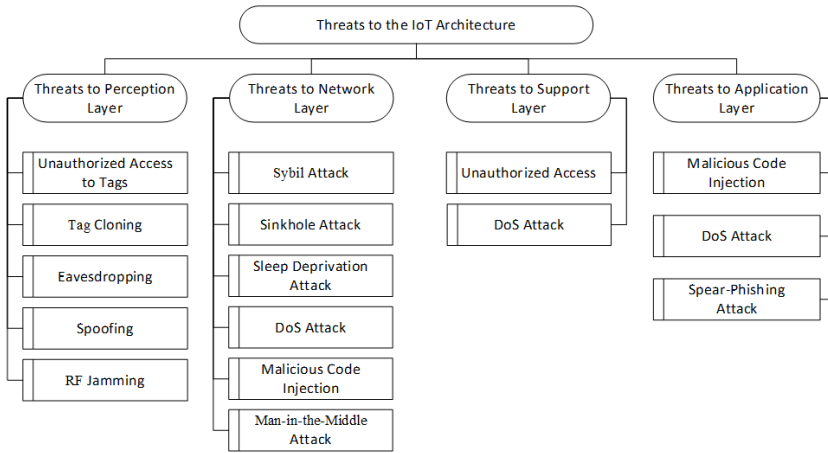
Figure 5: Threats to IoT Architecture

Threats To Perception Layer

The perception layer consists of different sensor technologies such as RFID. These technologies are vulnerable to a variety of risks and threats, which are listed below.

Unauthorized Access to Tags: Since many RFID systems lack an appropriate authentication mechanism, unauthorized individuals can access tags. The attacker has the ability to not only read but also change or delete data (Uttarkar & Kulkarni).

Tag Cloning: Copies of tags that are easily read and reproducible. As a result, it is possible to generate a copy indistinguishable from the original (Uttarkar & Kulkarni).

Eavesdropping: RFID systems, for example, are ideal targets for attackers due to their wireless capabilities. Data sent over the wireless network to the reader is often unencrypted. Attackers can easily obtain this data through listening. (Khoo, 2011).

Spoofing: An attacker sends fake information to RFID systems, fooling the system into thinking the data is coming from a legitimate source. Consequently, the attacker has complete access to the system, leaving it susceptible (Mitrokotsa, Rieback, & Tanenbaum, 2010).

RF Jamming: A large amount of noise signal disrupts RF signal communication in RFID tags. It can be described as a type of DoS (Denial of Service) attack (Li, 2012).

Threats to Network Layer

The network layer is composed of a wireless detector network that securely transfers data from the sensor to the target. Security threats related to the network layer are given below.

Sybil Attack: Sybil is a form of attack in which the attacker manipulates the relevant node for the purpose of providing several credentials. It is frequently used to provide fake network information and confuse other nodes' layouts in the network (Douceur, 2002).

Sinkhole Attack: It is a type of attack in which a compromised node is switched on, and adjacent nodes are forced to deliver data to it. By switching the packet flow in the network to a single direction, all packets can be accessed. While other nodes assume they are sending data to a secure node, network traffic is sent to the attacker. Because the captured node is always active, the IoT devices' energy consumption will increase owing to the nodes (Ahmed, Kanhere, & Jha, 2005).

Sleep Deprivation Attack: Sensor nodes are generally battery-powered devices. When nodes in the network are not transmitting data, they go to sleep to save the battery. Nodes are hindered from sleeping in attacks based on sleep deprivation. The battery life of the nodes declines because of this circumstance, and they become unusable. These attacks can be viewed as denial-of-service (DoS) attacks since they aim to prevent more networks from serving (Bhattasali, Chaki, & Sanyal, 2012).

DoS Attack: It is a sort of attack in which the targeted system is overloaded due to an attacker roaming the network with meaningless traffic, causing the network to become unusable for users (Padmavathi & Shanmugapriya, 2009).

Malicious Code Injection: In this type of attack, the attacker places a malicious code inside a node. At best, malicious code can cripple the network; at worst, the attacker can take control of the entire network (Fulare & Chavhan, 2011).

Man-in-the-Middle Attack: It is a form of attack in which an attacker-controlled node is put between two nodes and treated as if they really were part of the network. As a result, network data will inevitably flow through the attacker's node and be intercepted (Padhy, Patra, & Satapathy, 2011).

Threats to Support Layer

The support layer provides a platform of data storage technologies such as cloud computing for the following application layer. The security threats of this layer are given below.

Unauthorized Access: Unauthorized access to poorly controlled IoT services allows an attacker to gain access to existing data. It is the worst-case scenario. The attacker can delete or control the entire system.

DoS Attack: Data storage or processing platforms can be disabled by denial-of-service attacks occurred at the support layer like in other layers. In this way, the network becomes unavailable (Padmavathi & Shanmugapriya, 2009).

Threats to Application Layer

The apps to be used by the end-user are defined in this layer due to the services given according to the IoT application requirement. All attack threats against the end-user mainly concerns this layer. The particular threats are given below.

Malicious Code Injection: It is a method of injecting malicious malware into a system through an IoT application used by the end-user. In this way, the data of the end-user and, therefore, the system can be obtained. (Farooq, Waseem, Khairi, & Mazhar, 2015).

DoS Attack: Direct attacks on the IoT application, like attacks on other layers, can bring the service to a halt. Not just the IoT system but also the unencrypted end-user data are at risk in these application-level attacks (Farooq et al., 2015).

Spear-Phishing Attack: This type of attack targets the end-user. Spear phishing is a social engineering attack that targets specific individuals and organizations rather than the millions of people attacked in mass attacks. The system attempted to be accessed through the IoT system's usage information once the person's information was collected (Farooq et al., 2015).

CONCLUSION

Despite the fact that IoT applications significantly impact human production and lifestyle, they pose substantial security concerns. Interoperable systems are expected to be the key theme of the second quarter of the 21st century. At this point, security must take priority. In IoT applications, only 2% of device traffic is transferred in encrypted form. This circumstance jeopardizes the security of personal and corporate data. The study presented several cybersecurity violations. Every year, security experts discover botnet networks containing thousands of IoT devices. Many attacks are expected to be carried out across these networks soon. Furthermore, it was discovered that DDOS attacks were frequently employed when searching the subject. Unlike traditional attacks, however, we may state that the goal of these operations is to capture the network besides disabling it.

Within the context of the research, threats to IoT applications are characterized according to architectural layers. As a result, attacks on the perception layer can capture the device, whilst attacks on the network layer can capture communication and data. Nowadays, it is not possible to ensure 100% security, unfortunately. That being the case, communication in IoT systems based on the network, particularly those utilized for industrial and personal data transmission, must be encrypted.

REFERENCES

Ahmed, N., Kanhere, S. S. & Jha, S. 2005. The Holes Problem in Wireless Sensor Networks: A Survey. ACM SIGMOBILE Mobile Computing and Communications Review, 9, 4-18.

Aslan, F. Y., & Aslan, B. Comparison of IoT Protocols with OSI and TCP/IP Architecture. International Journal of Engineering Research and Development, 15(1), 333-343.

Bawany, N. Z., Shamsi, J. A. & Salah, K. 2017. DDoS Attack Detection and Mitigation Using SDN: Methods, Practices, and Solutions. Arabian Journal for Science and Engineering, 42, 425-441.

Beltov, M. 2016. New Linux Trojan NyaDrop targets IoT Devices.

Bhattasali, T., Chaki, R. & Sanyal, S. 2012. Sleep Deprivation Attack Detection in Wireless Sensor Network. International Journal of Computer Applications, 40, 19-25.

C´ardenas, A. A., Amin, S. & Sastry, S. (2008). Research Challenges for the Security of Control Systems. Hot topics in security 2008 San Jose, CA, USA. 1-6.

Cisco visual networking index: Forecast and trends, 2017–2022, Cisco WhitePaper.

Dobbins, R. 2016. Mirai IoT botnet description and DDOS attack mitigation. NetScout.

Douceur, J. R. The sybil attack. International Workshop on Peer-to-Peer Systems, 2002. Springer, 251-260.

Farooq, M., Waseem, M., Khairi, A. & Mazhar, S. 2015. A critical analysis on the security concerns of internet of things (IoT). International Journal of Computer Applications, 111, 1-6.

Fereidooni, H., Classen, J., Spink, T., Patras, P., Miettinen, M., Sadeghi, A. R., Hollick, M. & Conti, M. Breaking fitness records without moving: Reverse engineering and spoofing fitbit. International Symposium on Research in Attacks, Intrusions, and Defenses, 2017. Springer, 48-69.

Fulare, P. S. & Chavhan, N. 2011. False data detection in wireless sensor network with secure communication. International Journal of Smart Sensors and AdHoc Networks (IJSSAN), 1, 66-71.

Greenberg, A. 2015. After jeep hack, Chrysler recalls 1.4 m vehicles for bug fix.Wired, Conde Nast.

Greenberg, A. 2017. The Reaper Botnet Has Already Infected a Million Networks. Wired, Conde Nast.

Halon, E. 2019. Israeli experts expose security flaw in Amazon's Ring Doorbell. Jerusalem Post.

Kaiji malware: a new IoT threat. SecureMac. SecureMac.

Khoo, B. RFID as an enabler of the internet of things: issues of security and privacy. Internet of Things (iThings/CPSCom), 2011 International Conference on and 4th International Conference on Cyber, Physical and Social Computing, 2011. IEEE, 709-712.

Krebs, B. 2014. Target hackers broke in via HVAC company. Krebs on Security.

Krebs, B. 2016. Krebs On Security hit with record DDoS. Krebs On Security.

Li, L. Study on security architecture in the internet of things. Measurement, Information and Control (MIC), 2012 International Conference on, 2012. IEEE, 374-377.

Millman, R. 2017. Hajime malware now has 300,000 strong botnet at disposal say researchers.

Mitrokotsa, A., Rieback, M. R. & Tanenbaum, A. S. 2010. Classification of RFID attacks. Gen, 15693, 73-86.

Owen, M. 2020. Philips Hue smart bulb allows hackers to attack your network. blog, Trend Labs. appleinsider.com: Quiller Media.

Padhy, R. P., Patra, M. R. & Satapathy, S. C. 2011. Cloud computing: security issues and research challenges. International Journal of Computer Science and Information Technology & Security (IJCSITS), 1, 136-146.

Padmavathi, G. & Shanmugapriya, D. 2009. A survey of attacks, security mechanisms and challenges in wireless sensor networks. International Journal of Computer Science and Information Security, 4, 1-9.

Perlroth, N. & Krauss, C. 2018. A cyberattack in Saudi Arabia had a deadly goal. Experts fear another try. New York Times.

Pinto, A. D. 2020. Dark Nexus IoT Botnet: Analyzing and Detecting its Network Activity. Nozomi Networks. Nozomi Networks.

Sethi, P. & Sarangi, S. R. 2017. Internet of things: architectures, protocols, and applications. Journal of Electrical and Computer Engineering, 2017, 1-25.

Trend labs 2019. Silex Malware Bricks IoT Devices with Weak Passwords. blog, Trend Labs.

Unit 42 2020 IoT Threat Report. Palo Alto Networks. Viewed 01 June 2021, https://unit42.paloaltonetworks.com/iotthreat-report-2020.

Chapter 4

Electromagnetic Interference Filters

Elif Merve KÜÇÜKÖNER

Electromagnetic filters are circuits that separate the unwanted signal frequency from the desired signal frequency and suppress the unwanted part of signal. Depending on the frequency threshold of the signal to be suppressed, they can be classified into four categories: low pass, high pass, band pass and band stop filters. A low pass filter is generally preferred to design a filter designed for Electromagnetic Interference (EMI) occurring at high frequencies [1,2].

The inductor and capacitor components that make up EMI filters show low or high impedance values depending on the frequency. These components prevent interference signals from reaching the line because they have high series impedance and low parallel impedance values at the unwanted frequency level. The circuit elements that make up passive EMI filters have undesirable interference parameters - such as equivalent parallel capacitance in inductors and equivalent series inductance in capacitors. Since these parameters do not allow bulk circuit elements to operate correctly at microwave frequencies, filters consisting of inductors and capacitors are not designed for frequencies of 300 MHz and above [1,2].

1. Types of Filters

In literature, the suppression of transmitted and radiated electromagnetic interference is done with low-pass filters. These filters consist of two structures: Common Mode (CM) and Diferantial Mode (DM) filters, as shown in Figure 1.1. While CM filters consist of Y type capacitor and CM shock inductor, DM filters consist of X type capacitor and DM inductor components. There are two important points to look for in the components of EMI filters:

1. The electrical equipment in the test setup must be able to compensate for the nominal voltage and current,

2. HF (High Frequency) characteristic should not change depending on frequency [3].

The EMI filter can be single-layered, as each circuit element has a suppression power of 20 dB/decade. However, in this case, some disadvantages occur. For example, single-layered filters cannot be used when the source and load impedances in the equivalent circuit where the filter is located are different or when 20 dB/decade suppression is not sufficient. Instead, multilayer filters in the form of T, π, CL or LC should be used depending on the load - source impedances and the required suppression ratio. The location of circuit components within the EMI filter is determined depending on the load and source impedances. Capacitors are connected in parallel to the high impedance side, and inductors are connected in series to the low impedance parts, increasing the input loss [3,4].

2. Equivalent Circuit Types of Filtering

Electromagnetic filtering is done by taking into account the two noise components that make up the noise. Therefore, when designing an EMI filter, it is necessary to calculate the filter's capability based on the equivalent circuits of CM and DM noise components given in Figure 2.1 (b) and (c). Additionally, this capability also depends on the input and output impedances. In the test setup, the output of the filter is terminated by Line Impedance Stabilization Network (LISN) with an impedance value of 25 Ω for CM noise and 100 Ω for DM noise. Although the circuit output is simply defined in this way, the source impedance on the equivalent circuit is expressed as a variable because the Device Under Test (DUT) impedance is very difficult to determine.

(a)

(b)

(c)
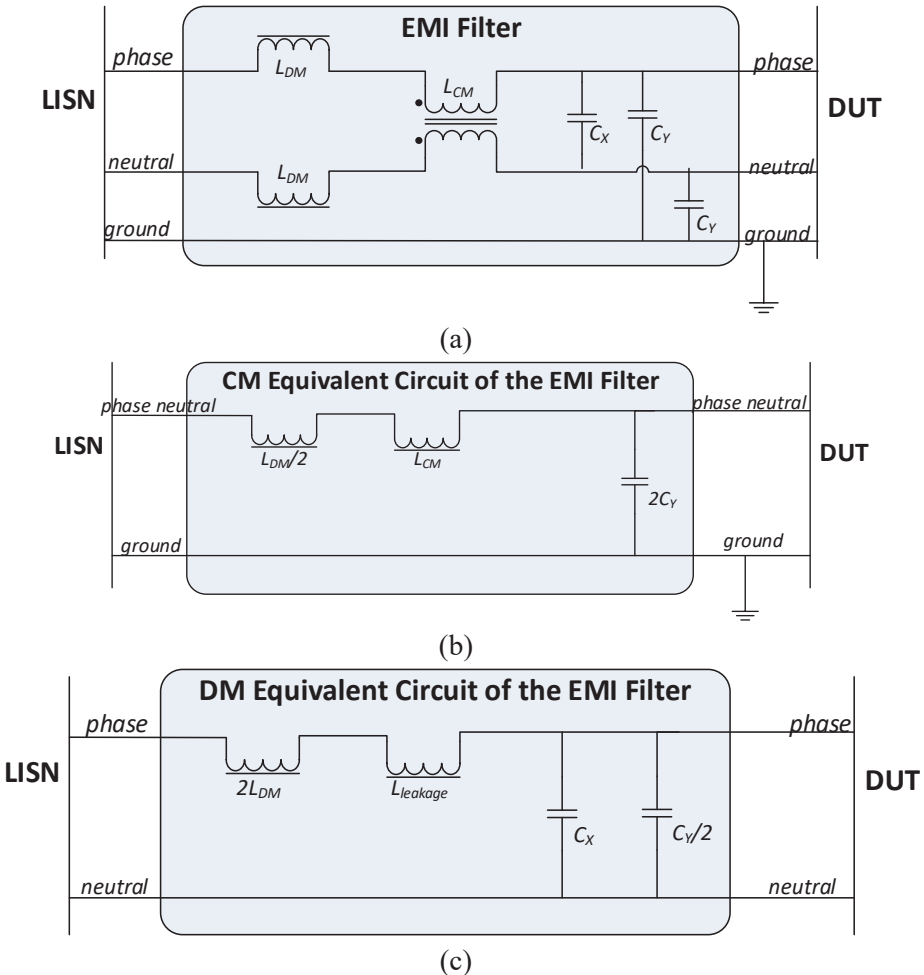
Figure 2.1. Two-structure passive EMI filter (a) electrical equivalent circuit, (b) CM equivalent circuit, (c) DM equivalent circuit

As can be seen from the equivalent circuits in Figure 2.1, although the Y-type capacitor is dominant in CM noise, it attenuates both noises. X type capacitors can only suppress DM noise. DM inductors are effective on both noise components. However, DM causes more attenuation against noise. CM coils are designed to suppress the common mode noise component. However, as seen in Figure 2.1 (c), the leakage inductance they create in the difference mode equivalent circuit contributes to the suppression of DM noise [5].

3. Parts of Filters

Passive EMI filters consist of passive circuit components such as capacitors and inductors, also known as lumped circuit elements. Each circuit element has its own operating conditions and format. Since the filter that is the subject of this study will be designed as a low pass, in such a design, inductors show high impedance values at HF level, while capacitors show low impedance values, preventing noise from advancing to the load.

Even though there are different operating conditions, all filter components must have high HF characteristics. As shown in Figure 3.1 and Figure 3.3, in practice there is an equivalent serial inductor (ESL) in every capacitor and an equivalent parallel capacitor (EPC) in every inductor. These equivalent units are defined as interference on circuit elements. As a result of the mentioned interferences, each filter component resonates at a certain frequency. This frequency is defined as self-resonant frequency (SRF) [3]. The SRF formula is given in Equation (3.1) for the inductor and Equation (3.2) for the capacitor.

$$f_{SRF,L} = \frac{1}{2\pi\sqrt{L \cdot EPC}} \ [Hz] \tag{3.1}$$

$$f_{SRF,C} = \frac{1}{2\pi\sqrt{ESL \cdot C}} \ [Hz] \tag{3.2}$$

Above the SRF, noise parameters increase to a non-negligible level. Because of these parameters, the capacitor starts to behave like an inductor, and the inductor starts to behave like a capacitor. Therefore, the filtering process fails. Another issue that makes this point important is the frequency width of SRF. The SRF of many filter components occurs in the frequency range of 0.15-30 MHz, which is the conduction propagation test range. For this reason, keeping SRF at high values by reducing interference parameters for passive circuit components is of great importance for high HF characteristics [6,7]. However, due to the high HF characteristics of the filter components, a high SRF value

alone may not be sufficient. The resistance of circuit elements to current, wear and temperature is also among the important criteria for filters.

3.1. Capacitors

While a capacitor shows high impedance in low frequency or DC signals such as direct current network currents, it has low impedance in HF signal ranges such as the 0.15-30MHz range where the conduction propagation test is performed. For this reason, in a low-pass filter such as a passive EMI filter, capacitors are always connected in parallel with the noise source. Thus, high frequency noise is prevented from reaching the load by capacitors.

Filter capacitors are called X and Y types according to the points they are connected to. Capacitors connected between phase and neutral lines are called X type capacitors. As can be seen from the equivalent circuit in Figure 2.1 (c), this type of capacitors are only effective in suppressing FM noise components. Since type X capacitors will not be exposed to high voltage differences, capacitance values can be selected without any limitations in design.

The capacitor equivalent circuit is given in Figure 3.1 (a). Here, the equivalent parallel resistance (EPR) can be neglected because it is very large [8]. Thus, the equivalent circuit is as shown in Figure 3.1 (b). Here, ESL is the parasitic inductance parameter that drives the capacitor into resonance and causes the capacitor to behave like an inductor when above the SRF. ESR indicates the impedance value of the circuit component when it reaches resonance [3].

(a)   (b)
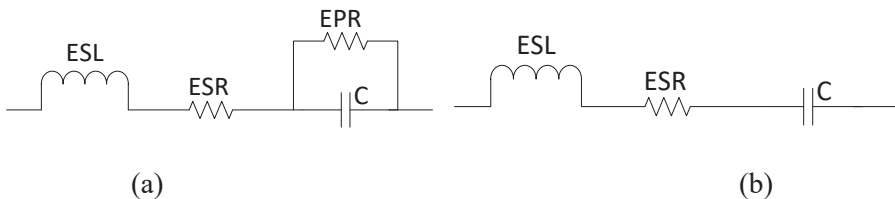
Figure 3.1. Capasitor (a) equivalent circuit (b) EPR neglected [3,7]

3.2. Inductors

Unlike capacitors, inductors have low impedance values in DC and low frequency currents, but they have high impedance values in the HF region where EMI filters are used. Therefore, in the low-pass EMI filtering process, inductors are always connected in series with the noise source.

EMI suppression inductors are divided into two: DM inductor and CM coil inductor. Although DM inductors are designed for DM noise, they have a constant inductance value against all noise components. Therefore, as seen in

Figure 2.1 (b), CM also suppresses noise. Since CM coils have an interconnected structure (Z for Zorro [5]), they reach a certain impedance value depending on the direction and intensity of the magnetic field within the core. As shown in Equation (3.3), a magnetic flux density occurs in a certain core in direct proportion to the number of windings and the line current. Due to the reverse winding directions in CM coils, the same directional current and thus the same directional magnetic flux density occurs as shown in Figure 2.15. The resulting magnetic flux density causes an impedance to emerge, directly proportional to the number of windings and inversely proportional to the current, as seen in Equation (3.4) [9]. Since the magnetic fields created by DM currents of the same value in the choke coils are in opposite directions, they should not cause any impedance under ideal conditions. However, the DM currents of both lines will not show the same value because the phase and neutral line impedances are actually different from each other, thus causing a small leakage impedance as seen in Figure 2.1 (c).

$$\oint B \cdot dl = \mu N I \tag{3.3}$$

$$M = \frac{N}{I} \int B \cdot ds \tag{3.4}$$
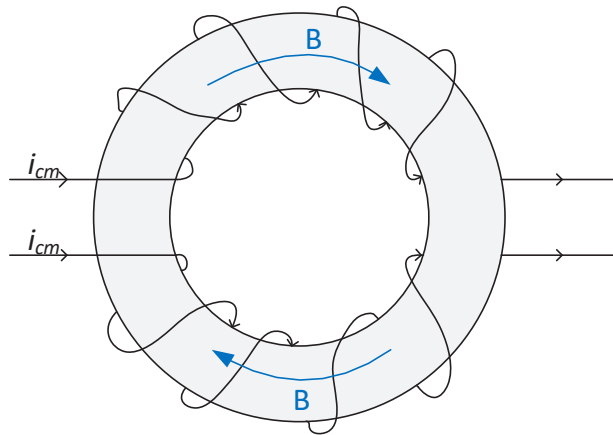
Figure 3.2. CM coil inductor winding

Filter inductors have some disadvantages in the suppression process. Their large structure and HF characteristics being very sensitive to temperature and current cause problems in filtering. In addition, choke coils are very sensitive to magnetic fields that may come from outside. DM inductors may interfere because they operate at high current. Therefore, it may be necessary to shield

the CM choke inside the filter [10]. However, the use of choke coils in filtering is essential, as Y-type capacitors are limited to certain values for safety reasons.

Inductors resonate at much lower frequencies than capacitors. That's why SRF and cancellation techniques are much more important in inductors. Inductors whose equivalent circuit is shown in Figure 3.3 can be neglected in some cases because their ESR is considered too small or their EPR is too large.

(a)   (b)

(c)
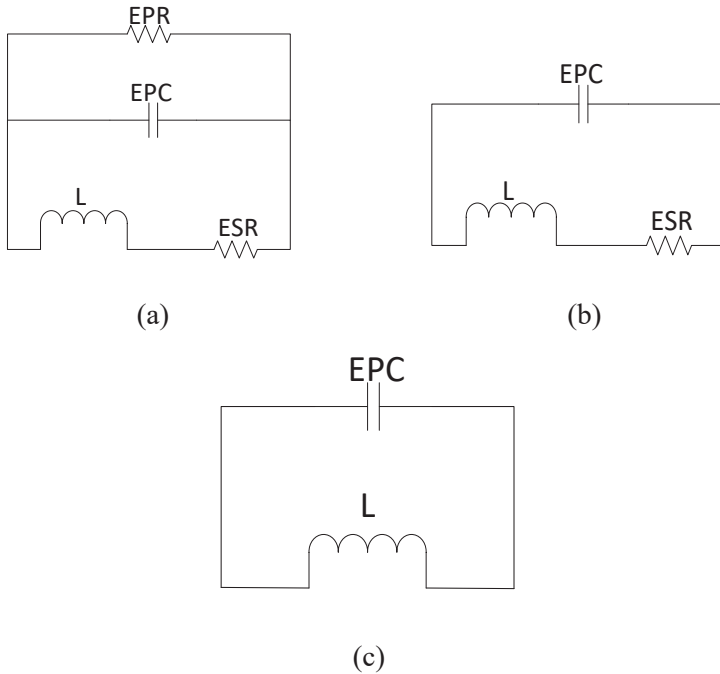
Figure 3.3. Inductor (a) equivalent circuit (b) EPR neglected [3] (c) ESR and EPR are neglected [3,7]

Since the OM choke consists of two windings connected to each other, the EPC parasitic parameter is the sum of the parasitic capacitance occurring between the windings and between the winding-core in this circuit component. The equivalent circuit structure of choke coils is shown in Figure 3.4 (a). The relationship between SRF and interference parameters in chokes and connected inductors is shown in Equation (3.5). As in capacitors, it is necessary to reduce the EPC as much as possible in inductors in order to increase the HF characteristic in filtering. In order to reduce the EPC occurring between the windings, increasing the winding distances or keeping the winding angle above 30° can reduce the EPC [10].

$$f_{SRF} = \frac{1}{2\pi\sqrt{L\left|EPC - \dfrac{C_N}{2}\right|}} \ [\text{Hz}] \qquad\qquad (3.5)$$

(a) (b)
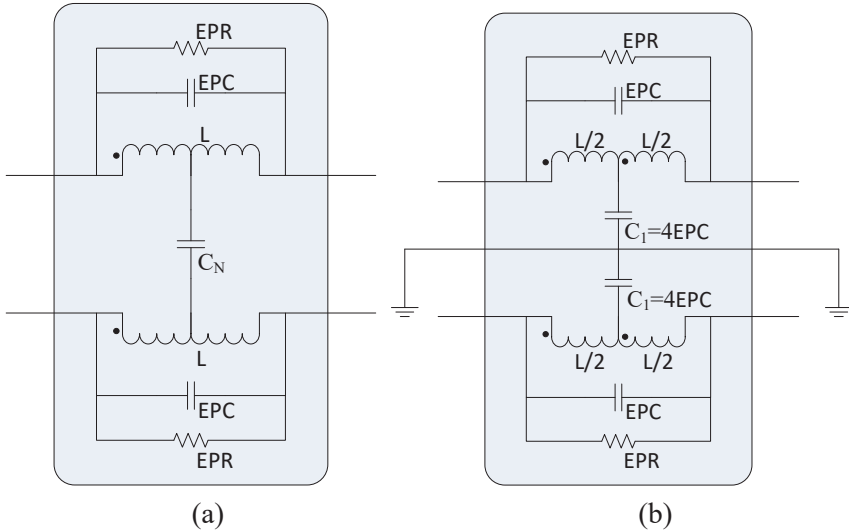
Figure 3.4. Choke coil (a) equivalent circuit,
(b) EPC cancellation method for CM

4. Electromagnetic Interference Filter Design and Simulation

An EMI filter has been designed to suppress the transmission and emission made by the ATX power supply, whose components are detected with a noise separator, at appropriate rates in a certain band range. For this purpose, firstly, using CM and DM noise results, it was determined in which frequency ranges and what amount of suppression ratio was required. Then, the type of filter made and the values of the circuit elements used were determined. Finally, the EMI filter design was carried out in simulation with the determined values.

4.1. Determining Required CM and DM Noise Suppression

The filter that can suppress electromagnetic noise must be designed step by step. First of all, the appropriate cut-off frequency must be determined so that a two-layer filter can completely reduce the noise determined by the 40 dB/decade suppression ratio below the limit. For this, the rate to be suppressed at each frequency should be 6 dB more than the calculated noise.

In order for the designed filter to fully capture the noise generated by the insertion loss, the cut-off frequency at which the suppression will start must be determined correctly. This process can be done geometrically or practically.

There are some values that need to be taken into consideration in order to successfully find the cut-off frequencies of the filter designed for CM and DM noise produced by the ATX power supply under test. These are 168, 235 and 305 kHz in the CM noise component; In the DM noise component, these are the noises occurring between 202 and 404 kHz [11].

It was noted that the CM noise component exceeded the limit by 20.7, 27.55 and 27.75 dBμV at 168, 235 and 305 kHz, respectively. The filter we made with a tolerance value of 6 dB must suppress at least 26.7 dBμV at 168 kHz or 33.55 dBμV at 235 kHz. Through geometric calculations made on MATLAB, it was determined that the cut-off frequency of an EMI filter with a 40 dB/decade ratio that can cover these values should be 34 kHz, as shown in Figure 4.1 [11].
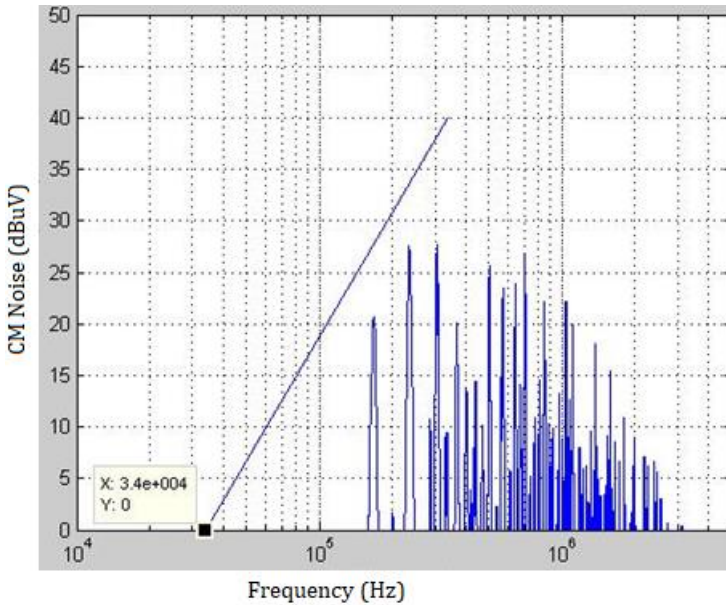
Figure 4.1. CM cut-off frequency [11]

In order to suppress the DM noise component, operations similar to the other noise component must be carried out according to its own values. Therefore, the suppression required in such a filter design should be at least 28.26 dBμV at 202 kHz and at least 36.55 dBμV at 404 kHz. The FM cut-off frequency of the EMI filter, which was designed in line with these needs, was calculated as 39 kHz with geometric calculations made in MATLAB, as shown in Figure 4.2 [11].
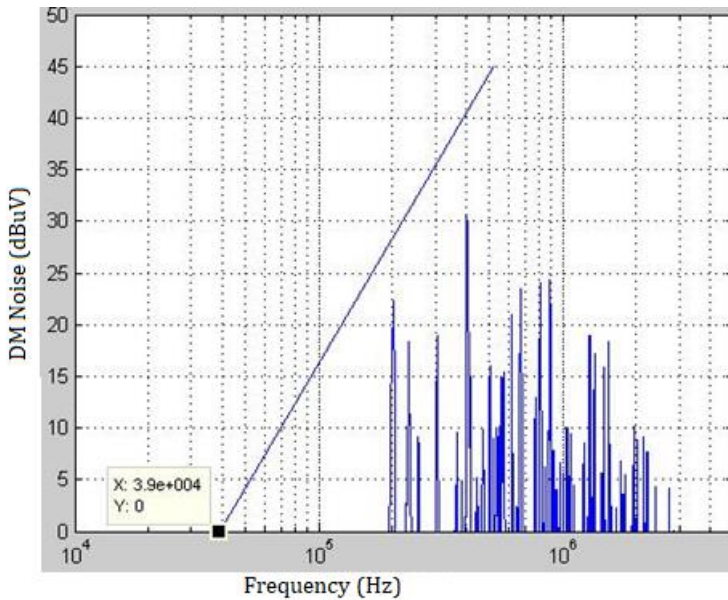
Figure 4.2. DM cut-off frequency [11]

4.2. Determining the Filter Type

The type of EMI filter should be L type as given in Figure 2.1, since two circuit components are selected for each noise component. Thus, since the filter we need to design must have the feature of suppressing high frequencies, inductors showing high impedance values at high frequencies are connected in series to the circuit, and capacitors showing low impedance values at high frequencies are connected in parallel to the circuit to create a filter that gives a low pass response. Considering an inductor noise parameter as EPC and a capacitor noise parameter as ESL, a low-pass filter will work like a band suppression filter. It is necessary to calculate the center frequency and second cutoff frequency of the filter in such a structure [12]. However, in this study, this issue was neglected in the EMI filter design since the measured noise values after 4 MHz did not exceed the limit and therefore there was no need to suppress it.

4.3. Design and Simulation of Filter at AWR Microwave Office

The circuit structure was created after calculating the range that the EMI filter should suppress and the values of the circuit elements that make up the filter. Separate layers were established for each noise component detected in the design and it was shown how these layers affect each other. While the DUT connected to the input of the filter can show high impedance values, the LISN

connected to the output of the filter completes the circuit at low impedance. For this reason, in the EMI filter circuit setup, capacitors are placed at the input of the filter and inductors are placed at the output of the filter in order to balance the impedances.

The structure of the filter circuit is shown in Figure 4.3. The simulation of the designed circuit was carried out on the AWR Microwave Office program and the operation of the circuit was examined [11].
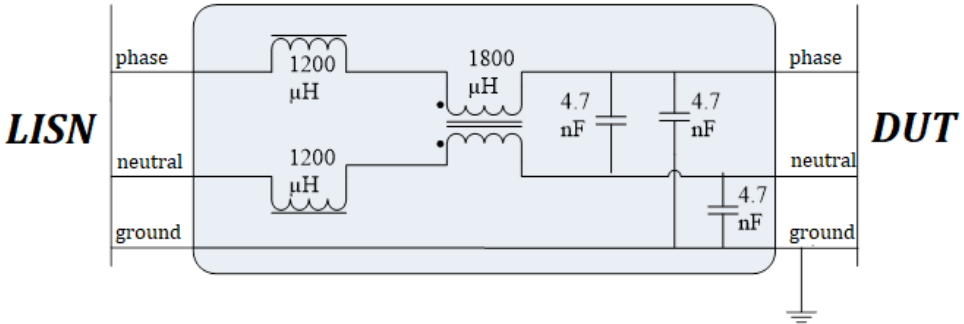
Figure 4.3. Circuit Structure of EMI Filter [11]

DM and CM simulations of the design were made similar to these circuit structures as in Figure 4.6 [11].

(a)   (b)
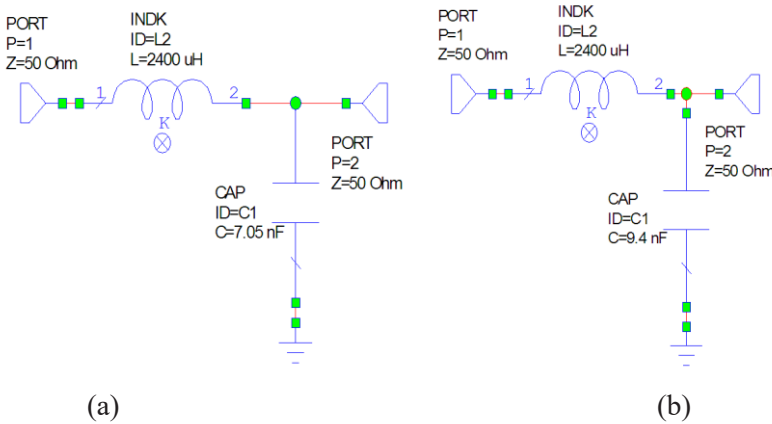
Figure 3.21. (a) DM simulation and (b) CM simulation of EMI filter [11]

REFERENCES

[1] CHEN, R., van WYK, J.D., WANG S. and ODENDAAL, W.G. 2005. Improving the Characteristics of integrated EMI filters by embedded conductive Layers. *Power Electronics, IEEE Transactions* 20 , no. 3 (1): 611 - 619.

[2] DHAR, V.K. 1999. Performance evaluation of power line filter. A case study. *Electromagnetic Interference and Compatibility '99. Proceedings of the International Conference on*.

[3] TIHANYI, L. 2004. EMC in Power Electronics. IEEE Press, Florida.

[4] HARTAL, O. 2002. EMC By Design. Singapore.

[5] OZENBAUGH, R.L. 2001. Emi Filter Design Second Edition. Markel Dekker, Inc., New York.

[6] JIANG, Y., WANG, S., LEE, F.C. and van WYK, J.D. 2008. Equivalent parallel capacitance cancellation for noise reduction application. *Applied Power Electronics Conference and Exposition, 2008. APEC 2008. Twenty-Third Annual IEEE*, 745 - 750.

[7] Wang, S., F.C. Lee, ve J.D. van Wyk. «Design of Inductor Winding Capacitance Cancellation for EMI Suppression.» *Power Electronics Specialists Conference, 2006. PESC '06. 37th IEEE*, 2006: 1 - 7.

[8] Wang, S., F.C. Lee, and W.G. Odendaal. "Using a network method to reduce the parasitic parameters of capacitors." *Power Electronics Specialists Conference, 2004. PESC 04. 2004 IEEE 35th Annual* 1, no. 7 (2004): 304 - 308.

[9] Cheng, D.K. *Fundamentals of Engineering Electromagnetics.* USA: PEARSON, 2014.

[10] Cadirci, I., B. Saka, ve Y. Eristiren. «Practical EMI-filter-design procedure for high-power high-frequency SMPS according to MIL-STD 461.» *Electric Power Applications, IEE Proceedings* - 152 , no. 4 (2005): 775 - 782.

[11] Yalçın, S. «Anahtarlamalı Güç Kaynaklarında Elektromanyetik Girişimin İncelenmesi Ve Elektromanyetik Girişim Süzgeci Tasarımı» Akdeniz University, 2015.

[12] Kotny, J.L., T. Duquesne, ve N. Idir. «EMI Filter design using high frequency models of the passive components.» *Signal Propagation on Interconnects (SPI), 2011 15th IEEE Workshop on* 978-1-4577-0466-6 , no. 12071528 (2011): 143 - 146.

Chapter 5

RFID Applications in Animal Identification and Tracking

Habib DOĞAN[1]

[1] *Assoc. Prof. Dr. , Burdur Mehmet Akif Ersoy University, Gölhisar School of Applied Sciences, Department of Computer Technologies and Information Systems, Gölhisar, Burdur, TURKEY
ORCID: 0000-0001-8685-9569*

ABSTRACT

RFID stands for Radio Frequency Identification, which is a technology that enables objects to be identified using radio frequencies. RFID, one of the automatic identification systems, is a major industry with increasing popularity and use, which is projected to have a market share of 40 billion dollars by 2030 according to published reports. Although its origin and first applications are not very recent, its widespread use has been an adventure of the last 50 years, especially as a result of the development of the chip industry in electronics and miniaturization. The fact that it does not require a line of sight with objects like other automatic identification systems, allows multiple readings, and enables reading and identification from long distances are some of the issues that increase its use in the identification and tracking of objects. It is not possible to put a limit to the areas of use and it is completely dependent on the technological skills of designers and technology developers. In this study, the use of RFID in animals is examined and examples of RFID applications recently used in the identification and tracking of animals are emphasized. The fact that active RFID tags allow the addition of sensors has led to the increased use of different sensors to enhance tracking to obtain data on animal health, etc., and to improve efficiency. Various challenges faced in RFID applications despite its widespread use are also mentioned at the end of the study.

Keywords: RFID, animal identification, animal tracking, rumen bolus

1. **What is RFID?**
a. **History**

RFID (Radio Frequency Identification) technology is an electronic automatic identification system that allows identification and remote monitoring of objects by adding a tag to them. Its operation is related to the electromagnetic fields emitted by radio frequency waves. The induction principle discovered by Faraday in the mid-19th century and the radio and radar technologies that developed later formed the basis of this technology. (Ahson and Ilyas, 2017). While the induction principle discovered by Faraday explains the connection between the tag and the reader in the near field, the connection between the tag and the reader at long distances is based on the principle of backscattering electromagnetic waves, which forms the basis of radar technology.

RFID first entered the literature with Harry Stockman's article "Communication by Means of Reflected Power" published in 1948. In the Second World War, the identification of airplanes as friends or foe was provided by the information obtained from the backscatter signals obtained from the tags placed on the airplanes (Lehpamer, 2012). After this first effective use of RFID technology, the use of RFID systems began to increase in the 1960s due to developments in electromagnetic theory. EAS (electronic article surveillance), developed in 1964 to prevent the theft of products in stores and books in libraries, was the first widespread RFID application. Descriptive information is loaded on the label placed on the product, and the label on the product, which is tried to be taken out without removing the label, is detected by the reader antennas at the exit point and the alarm circuit is activated. EAS tags contain one bit of information and are used only to identify the product. Today, this system is widely used in most shopping centers. The 1970s were the beginning of the micro-electronics era in electronics, when thousands of electronic components were brought together in a chip, and RFID applications increased considerably with this miniaturization process. By the 1980s, transportation and railway control in the US and most European countries were equipped with RFID systems, projects for the identification and tracking of animals were accelerated, and toll road crossings were automated with this technology. Depending on these developments, many sectors are now offering RFID-based solutions, applications in many different fields are emerging, and it is becoming possible to talk about an industrial solution that is growing and is expected to reach a market share of 40 billion dollars in 2030 (URL-1).

When we look at automatic identification systems, RFID systems are most similar to barcode systems but offer many different advantages compared to barcode technology. In solutions such as barcode, OCR, voice recognition, and

biometrics, the tag and the reader must be in the line of sight. In RFID systems, the absence of such an obligation is seen as a great advantage. Many features such as reading many tags at the same time, storing more data, allowing different sensor applications, allowing reading from greater distances, allowing the information in the tag to be changed when desired, and not being affected by environmental conditions can be counted among the advantages of RFID systems over other automatic identification systems. The disadvantages of RFID systems include price and security threats. However, the decrease in label prices due to the development of technology and the decrease in security problems with the increase in standardization are gradually reducing these disadvantages (Çıbuk and Marasli, 2015).

b. Structure and operation

RFID system generally consists of a tag and a reader. In addition to these two main components, the program part, which represents the software dimension of the work, can be considered as a separate component. Tags are structures that are placed on objects and contain information, and simply consist of a chip where the information is stored and an antenna that will provide communication with the reader. When tags are classified according to their structure, they can be evaluated in 3 categories: passive, semi-active, and active tags. Passive tags do not have a power unit. In other words, such tags use the signals from the reader to work. Semi-active tags have a power supply, but this power supply is used to supply the hand-electronic circuits in the tag. Communication is provided by signals from the reader (Dobkin, 2012). Since they switch to active mode with the signal from the reader, these types of tags are preferred due to their longer battery life compared to active tags that send signals continuously. Figure 1 shows a general RFID system. Since there is no power supply in passive tags, the dimensions can be kept to a minimum, and they can be used for a lifetime unless they are physically damaged and broken. In the case of active tags, the power source is the biggest lifetime determining factor. With the development of battery technology, the lifetime of active tags is increasing. In addition, the biggest advantage of active tags over passive tags is the ability to communicate over longer distances and the ability to add sensors to the tags. Different types of RFID tags are displayed in Figure 2. The possibility of inter-tag communication in active tags makes them more attractive for different uses.
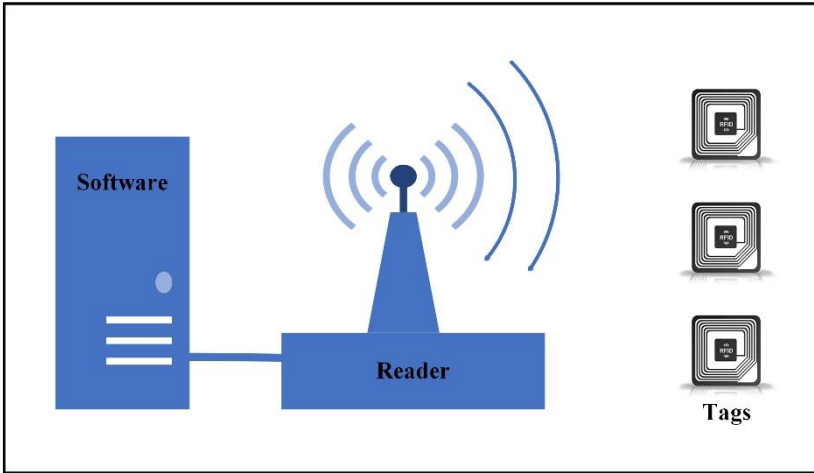
Figure 1. The general structure of the RFID system
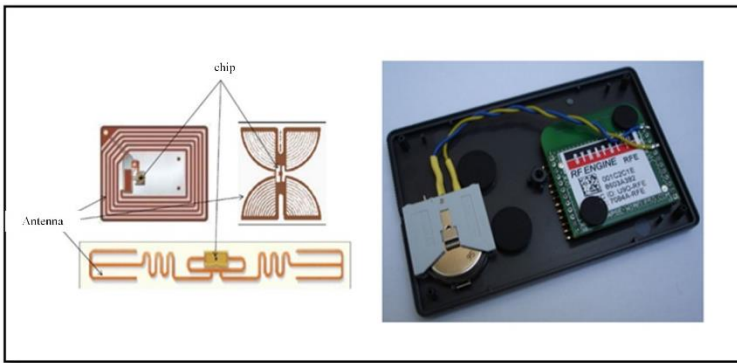
Figure 2. Examples of active and passive RFID tags

It is also possible to categorize tags differently as readable, readable/writable, and writable/re-writable. Read-only labels are generally passive labels. Information is written on such labels during production and is never changed again. Writable tags, on the other hand, are tags where the data obtained during use can also be processed and stored in the tag. These have a larger memory size but are costlier economically than the others.

The operating frequencies of RFID systems are generally ISM (Industrial, Scientific, Medical) bands and may vary from country to country. The reason for choosing these bands is that they allow unlicensed operation. Since the response of materials at different frequencies will be different, it is necessary to select the operating frequency according to the working environment. For example, at high frequencies, attenuation in the material environment will be higher. The penetration rate of low frequencies in metal materials will be higher than high

frequencies. Such issues must be considered in RFID system design and the frequency at which the system design can work best must be selected. Table 1 shows RFID frequencies and their advantages and disadvantages. At low frequencies, the tag and the reader communication is realized by inductive coupling, while at high frequencies communication is realized by electromagnetic coupling. While low frequencies exhibit better omnidirectional communication capability, are less affected by metals and liquids, have a slow reading speed, allow short-distance communication, and are problematic in mass readings, it is seen that as you go up to high frequencies, the reading distance and speed increase, the effect of metals and liquids is high. It is advantageous for multiple readings at the same time. Figure 3 shows inductive and electromagnetic coupling. The power values given in Table 1 are limited to 4W for the USA and 2W EIRP (Equivalent Radiated Power) for the European Union Countries.

RFID (Radio Frequency Identification)				
Properties	LF Low-Frequency	HF High-Frequency	UHF Ultra-High Frequency		MW Microwave Frequencies
Frequency	125-134 KHz	13,56 MHz	433 MHz	856-960 MHz	2,45 &5,8 GHz
Tag Type	Passive	Passive & Semi-active	Active	Passive-Active	Passive-Active
Reading Distance	0-10 cm	0-30 cm	30-100+ m	0-30+ m	0-100+ m
Usage areas	Animal tracking, access control, applications in metals and liquids.	Library, DVD, Personnel cards	Mining, construction, automobile, monitoring with sensors, animal monitoring	Supply chain, pharmaceutical industry, electronic ticketing, product tracking, race timing	Railways, vehicle tracking
Advantages	Standards are globally established, with good results in metal and liquid media.	Standards are in place, more memory	Very high communication distance, high data transmission rate, reading multiple tags simultaneously, lower cost at readers	Longer communication distance, different options in tag size types, high data transmission rate, ability to read multiple tags simultaneously.	Longer communication distance, different options in tag size types, high data transmission rate, ability to read multiple tags simultaneously
Disadvantages	Very short communication distance, low memory, low data transmission rate	Short communication distance, low transmission rate	High label cost, complex software, negative impact from metals and liquids	Lower data quantity rate in writing, negative interaction with metals and liquids	High cost
Permissible Field Strength	72 dB μA/m max	60 dB μA/m max	10-100 mW	0,1-4 W	0,5-4 W

Table 1. Comparison of RFID frequencies

(a)

(b)
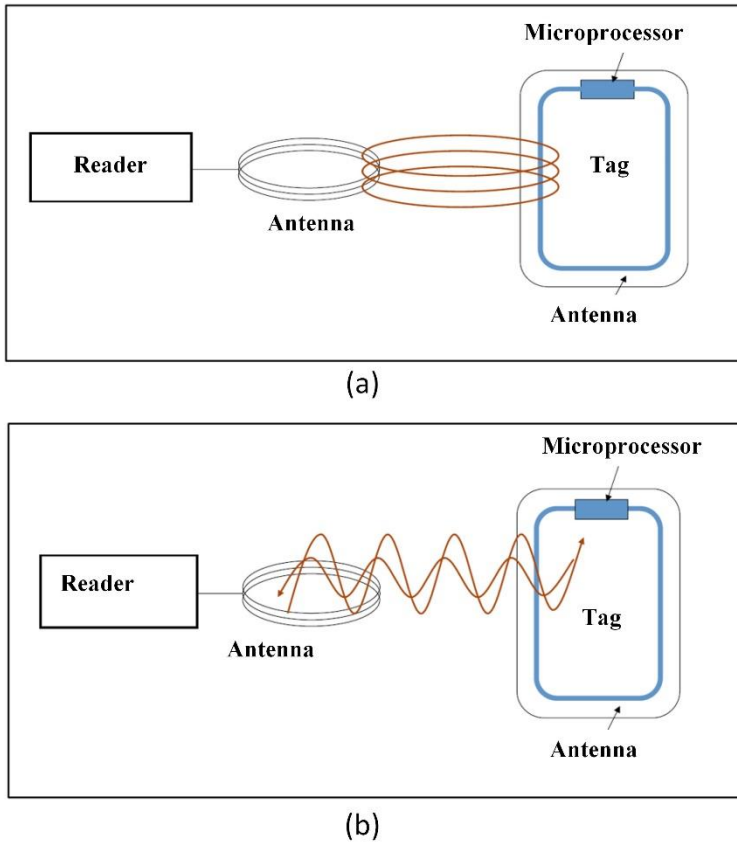
Figure 3. Sort of communication between RFID tags and reader (a) inductive coupling (b) electromagnetic coupling

In addition, the frequency values given in Table 1 may be in different band ranges for each country. This is entirely related to how the relevant authorities of that country regulate the ISM band. For example, in Japan the UHF band is 950-956 MHz, in South Korea it is 908.5-922 MHz, in the US it is 902-928 MHz and in the European Region, it is 865-868 MHz.

The level of signals in an RF system is affected by several factors. These include the transmission power of the reader, cable losses, antenna gain, losses due to distance, losses due to obstacles (walls, different materials, liquids, etc.) between the reader and the tag, and losses due to reflection and scattering. Considering all these losses, designing the system in an optimum way and selecting the tag and antenna types accordingly have an important role in the efficient operation of the system. Choosing a tag that is not suitable for the working environment, using the wrong antenna, and not choosing the system

parameters correctly will increase the cost and reduce the efficiency of the system.

c. Usage Areas

Considering the point of progress that RFID technology has reached today, the question of in which areas it can be used is entirely up to the skill and knowledge of the practitioner. Advances in technology have reduced the size and brought different solutions to the speed problem, and it remains only to evaluate the relationship with other technologies in the use of this technology in the desired area. The fact that the system is more complex than other automatic identification systems and requires a certain establishment cost may disable RFID systems in very small-scale applications. However, RFID solutions come to the forefront in applications where multiple reading, fast data communication, high reading distances, and economic costs are solved. As the standardizations related to this technology settle into a certain order, the increase in the usage areas of RFID technology will continue at a faster pace. Looking at the general applications, the sectors where RFID systems are used intensively can be listed as follows.

- Product supply management
- Pharmaceutical industry
- File tracking
- Access control
- Animal identification and tracking
- Automatic ticketing
- Jewelry sector
- Logistics tracking
- Book and DVD tracking
- Textile industry
- Factory automation
- Inventory tracking
- Vehicle monitoring
- Highways
- Parking lots
- Real-time location detection systems
- Race timer applications

Many different and specific areas can be added to these usage areas. As mentioned before, the usage area of RFID technology depends on the ability of the implementers to use this technology. In general, in addition to many advantages such as reducing labor costs, preventing theft, enabling tracing in

origin tracking, and saving time, the biggest problem of RFID systems for users is that the standards are not fully established for certain situations and may cause privacy problems that may arise from a security vulnerability. However, it can be easily said that these problems will gradually decrease depending on the technological developments in this sector.

d. RFID Standards

In addition to the label costs, the inability to establish a complete standard has also been a factor in the widespread use of RFID technology long after its first use. The fact that most countries set different frequency zones as standards for themselves and require different technical specifications is the factor that limits the use of RFID products developed in one country in other countries. This is a situation that prevents widespread use. Establishing a standard for such technologies will increase the compatibility and interchangeability between products, which will increase the demand for RFID products. In addition, the continuous development of this technology, how it will be integrated with new technologies (5G, artificial intelligence, etc.), and protection needs in issues such as security, privacy, and encryption make standardization mandatory.

In general, RFID standards are set by ISO, and Auto-ID Center, while NFC standards are also set in addition to ISO standards. ISO sets standards for common features related to RFID components such as tag data formats, security features, and performance tests. Examples include ISO 14443, ISO 15693, and ISO 18000. EPC (Electronic Product Code) products developed by the Auto-ID center are intended for numerical identification and are similar to the barcode identification structure in barcode technology but are more comprehensive. Figure 4 shows the EPC structure and its similarity with the barcode. Although 64 and 96-bit EPCs have been developed, the 96-bit structure is more widely used. Some examples of standards developed by EPC Global are EPC Tag Data Standard Version 1.9, which specifies tag data standards, Low-Level Reader Protocol (LLRP), known as the low-level reader protocol, Reader Management 1.0.1 Class 1 Generation 2 UHF Air Interface Protocol Standard (for 860-960 MHZ), known as the reader management standard. The use of RFID components in NFC applications has resulted in the development of related standards in this field. Finally, standard development efforts are ongoing for different extensions used for passive RFID systems operating in the 860-960 MHz UHF band and referencing ISO and EPC Gen2 by the RAIN RFID Alliance.
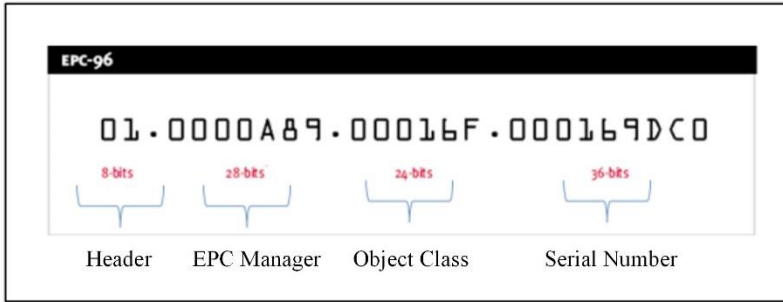
(a)
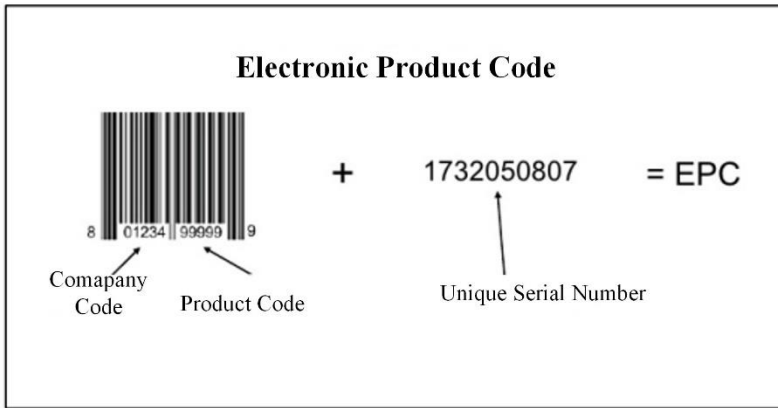
(b)

Figure 4. (a) EPC structure, (b) Similarity with barcode structure.

2. RFID Technology Applications in Animals

The identification of animals is a subject that has been tried since the first human communities, it started in the early times in order to know the owners of the animals and was used to find the real owner of the animal in case of loss or theft of animals. It is known that this identification process is also related to the domestication of animals. When we look at the types of identification made in the past, it is seen that identification was made in different forms such as tattooing, branding, ear notch, and ear tags, and recently this identification has shifted to electronic identification. In addition to these, it is also known that identifications based on the biometric characteristics of animals are also made. These traditional identification types are shown in Figure 5.
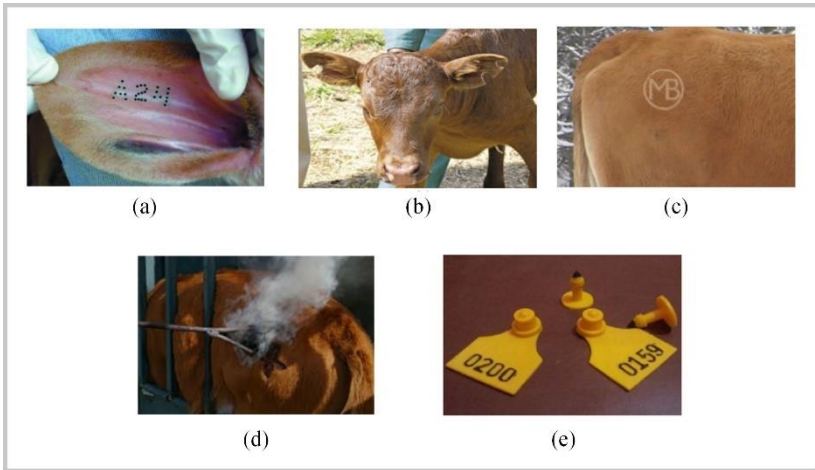
Figure 5. Traditional animal identification methods. (a) tattooing (b) ear notch (c) cold stamping (d) hot stamping (d) ear tag.

Although such traditional identification methods were a solution in the past when the number of animals was small, today, the increase in the number of animals on farms, the automation of most processes, and the introduction of many monitoring systems to increase efficiency have resulted in the inadequacy of such identifications.

The following problems are often encountered with traditional methods.

- Tattoos may change over time.
- Paint and stamping may become illegible due to ambient pollution.
- Ear notches may be interpreted differently by others.
- Ear tags can fall off, get lost, or even be cheated (Dziuk, 1999).

Tracking and locating animals in an automated and efficient way compared to traditional methods is important for food safety, security policies, monitoring of natural migration events due to different reasons, food-borne risk assessment, laboratory behavioral analysis, and detection and tracing of the origin of recent common animal-borne diseases (Catarinucci et al., 2013). Furthermore, accurate and positive identification of animals is predicted to increase farm trade, prevent theft and fraud, and facilitate the tracing of animals and animal products. Accurate identification will provide us with reliable information when working with, trading, or monitoring animals (Dziuk, 1999). The inadequacy of traditional methods in the detection of mad cow (BSE- Bovine Spongiform encephalopathies,), foot and mouth disease (FMD fibromuscular dysplasia), and swine fever (swine-fewer) diseases, which are widespread, especially in the European Union region, and the increasing demand of consumers for safe food

have been the accelerating factors for authorities to seek new technologies compared to traditional methods (Marchant, 2002).

Considering that all stakeholders from producers to consumers will be affected by an animal identification system, it is clear that this system will play an important role in the following issues.

- Reducing labor costs,
- Rapid identification of the origin of diseases,
- Early disease detection,
- Preventing commercial losses,
- Preventing fraud in subsidies,
- For genetic purposes and validation in production.

Therefore, the system is to be designed; with the following should have features such as.

- Easy to apply,
- Permanence,
- Providing accurate, fast, and affordable information,
- Animal friendly
- Minimal affecting from environmental conditions.

The advantages of the secure identification system to be established can be listed as follows.

- Consumers gain assurance in food safety and quality,
- Economic benefits for farm owners and the country,
- Product suppliers and restaurants can offer better quality products to their customers,
- Epidemic control and monitoring of animal diseases (Marchant, 2002).

Considering all these, it is seen that this type of system desired in animal tracking can be achieved with electronic identification methods. In this context, Radar, GPS, and RFID systems that offer reliable and cost-effective solutions in more complex use cases such as animal tracking stands out. It is seen that active RFID tags are used especially for tracking and monitoring farm animals in closed environments, while passive tags are used for tracking smaller laboratory animals (Catarinucci et al., 2013).

The use of RFID technology for animal identification started in the 1970s. Different organizations in European Union countries and North America have conducted prototype studies to integrate these systems into animals. In the first tests, passive RFID systems were used in the early 1970s by John Bridle in the UK, and similar tests were carried out in the Netherlands. An injectable system was first designed in animals in 1976 to track ruminants' ruminations. The work

done at this time was presented to the scientific world at a symposium in the Netherlands in 1976 (Rossing, 1999). When we look at the historical use, electronic identification systems, which were first seen in animals in the form of belts worn around the neck, started to be seen in the form of ear tags and tags placed under the skin following the development of technology. In addition to the ear area, the feet, genital area, and tails of animals have also been among the areas where these tags have been used. Due to the close relationship of animal diseases with temperature and pH ratio in the stomach, passive tags for identification and active tags containing sensors for monitoring have been used in the rumen region of animals. RFID tags used in this region are commonly referred to as rumen bolus (Castro et al., 2010). Although most applications have been made on domestic animals such as cows, sheep, and goats, wild animals and even fish have been identified and tracked with RFID identification systems (Floyd, 2015). Experimental rats, which are used extensively in tests in the field of health (Volk et al., 2014), and zoos can also be shown as examples of areas where RFID technology is applied in animals (Karlsson et al., 2010). Figure 6 shows the regions where RFID tags are used in animals (Caja et al., 2016).
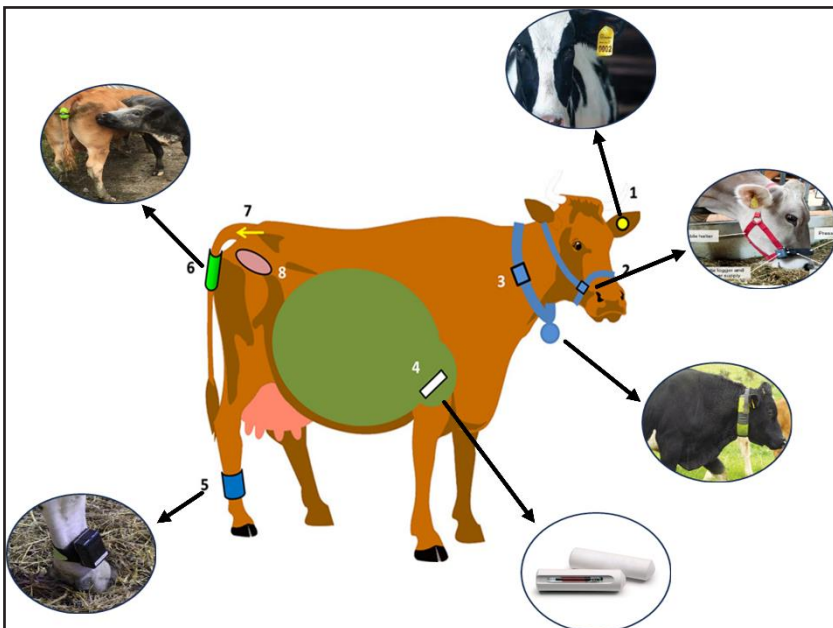
Figure 6. Locations of use of electronic tags for animal identification.

Among the electronic identification tags shown in Figure 6, RFID tags designed in the form of ear tags numbered 1 are currently the most widely used

identification tags. Apart from this, the most common tags are the so-called bolus tags used in the area numbered 4. Passive and active types of boluses are widely used, passive tags are generally designed at low frequencies and are used for identification purposes, while active tags are designed to operate in the high-frequency region and are generally used for monitoring by adding sensors. Injectable tags placed under the skin are generally preferred for the identification of cats and dogs. The most important reason why injectable tags are not preferred for edible animals is the high probability of the tag mixing with the carcass meat. Ear tags are widely used in most countries due to their cost. In some countries, electronic identification in the form of a double ear tag is also used in case of falling and theft.

Looking at the frequency distribution, it is seen that RFID tags, which are generally used in animals due to the negative interaction of the UHF band with metals and liquids, are concentrated in the LF and HF region and are in the form of passive tags. The ISM band of 433-434 MHz is the frequency region where active tags are used and are generally preferred in applications with sensors. Figure 7 shows some of the RFID tag types used in animals. Rumen bolus tags are placed in the rumen region of the animals by using a specially designed apparatus through the mouth. A magnet is added to the tag for weighting. The reason why a magnet is generally preferred instead of another material is the desire to prevent damage to the internal organs of the animal by ensuring that parts such as metal nails and wires that the animals accidentally swallow by mixing with grass or feed are captured by this label. Weight and size are important parameters for rumen boluses. The size should be such that it does not prevent the animal from swallowing easily. In addition, since there is a risk of excretion of labels that do not exceed a certain weight through the excretory system, such labels should be of a weight that will allow them to collapse and remain in the reticulum area.
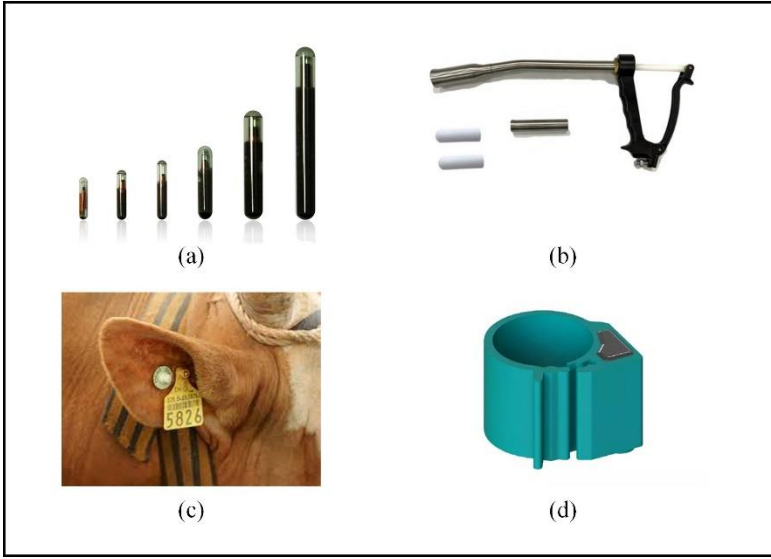
Figure 7. Some RFID tags used for animal identification (a) injectable (b) rumen bolus tag and application apparatus (c) ear tags (d) wristband.

As a result of the inadequacy of the existing identification systems upon the outbreak of animal-borne diseases, studies on alternative identification and monitoring systems were rapidly initiated, and as a result, RFID-based animal identification systems, which are now required by most countries, have been put into use. Table 2 shows the animal identification systems used in some countries.

Ülke	Sistem	Başladığı Yıl
UK	Cattle Tracing System (CTS)	1998
Australia	National Livestock Identification System (NLIS	2000
Canada	Canadian Cattle Identification Agency (CCIA)	2002
Switzerland	Animal Tracking Corporation	2006
USA	National Animal Identification System (NAIS)	2002
Brasil	the Brazilian Bovine and Bubaline Identification and Certification System (SISBOV)	2002
Argentine	Argentine Animal Health Information System (SGS)	2007
Japan	*Individual Identification of Cattle*	2003
South Korea	Beef Traceability System	2008
New Zeland	National Animal Identification and Tracing (NAIT)	2012
Turkey	Animal Information System	2002/2011

Table 2. Animal identification systems in some countries (Zealand, M.B.N. ,2009)

When the identification systems of the countries given in Table 2 are examined in detail, it is seen that some of them have made RFID technology compulsory, while in some others, studies have been initiated to make it

compulsory in the future. For example, in New Zealand, the Animal Identification system has been in place since 1993 before NAIT was introduced, but with NAIT, electronic identification was made compulsory, and the animal was tracked from birth to death or slaughter. In Turkey, while electronic identification was introduced for cats and dogs, it became mandatory to tag bovine animals with ear tags in 2002 and ovine animals in 2011. These ear tags are not electronic identification, but only the use of a barcode-like numbering system on ear tags. Electronic identification and tracking of animals provide advantages in aspects such as the following.

- Remote access to identification data,
- Eliminating the hassle of dealing with paperwork,
- Fast access to statistical data,
- Early diagnosis of animal diseases,
- Healthy and fast tracing of origin,
- Reduction in labor costs,
- Time savings,
- Correct monitoring of animals.

For this reason, in most countries, both official and unofficial organizations are rapidly working towards the widespread adoption of electronic identification. Very large-scale projects have been supported to determine how the electronic identification tags will be used, their dimensions, etc., and according to the results of these projects, the best electronic identification tag has been tried to be determined. The IDEA (Identification électronique des animal) project, which is the largest of these projects, was initiated in 6 member countries together after the disease spread to a very large area as a result of the inability to quickly identify the origin of the disease in animal-related epidemics seen in the European Union countries after the 1990s. Nearly 1 million animals were used in the project, different types of electronic tags were tested and the results were shared. In the project, 32,000 subcutaneous, 255,000 ear tags, and 630,000 bolus type tags were used. At the end of the project, the recovery rate for bolus and ear tags had been 99.5%, while the loss rate for subcutaneous tags had been more than 2%. Recovery rates were very high compared to the traditional ones and it has been stated that the most reliable labeling would be achieved with the bolus type (Ribo et al., 2001).

A bolus apparatus is used for the oral administration of bolus-type electronic tags. Many studies have been conducted to determine which size, weight, and form of bolus will give good results in which animals (Garin et al., 2003, Falllon 2001, Cappai et al., 2014, Ghirardi et al., 2006, Antonini et al. 2006, Casto and

Garin, 2010). Studies have shown that there is no negative effect and eliminated the doubts about whether bolus-type tags harm milk and meat production, fat level in milk, pregnancy status, weight gain, and rumination due to direct interaction with the animal body(Fallon, 2001). It has been stated that only the rumen mucosa can be affected by bolus movements, injury lesions may develop, albeit very slightly, and the rumen bacterial population may be affected due to electromagnetic effect, so the frequency of reading should be low (Antonini et al., 2006). It has also been shown that the bolus diameter and size should be adjusted depending on the size of the animals in which the boluses will be used, and the specific gravity of the boluses should be high to prevent them boluses from being expelled from the rumen. It was emphasized that trying to swallow boluses of inappropriate size may cause throat lesions in animals (Ghirardi et al. 2006). The application of electronic ear tags and bolus-type tags is shown in Figure 8.
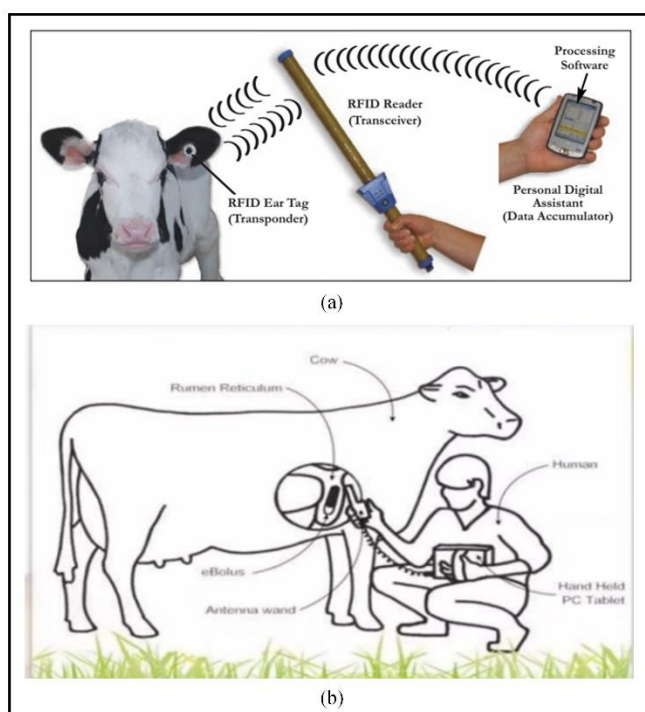
Figure 8. Application of ear tag and bolus type RFID tags (a) ear tag (b) rumen bolus type tag (Grooms, 2007).

The use of RFID technology for identification purposes in animals has increased the studies that this technology can be applied together with sensors for

animal monitoring. The first electronic monitoring studies in animals were initiated for the detection and monitoring of rutting periods in cattle. Different monitoring methods were studied and different solutions were developed for different animals. For example, GPS transmitters were placed on the ankles of pigeons to track them, and different wild animals were monitored with the same method. In addition to the monitoring of wildlife, efforts to monitor marina and marine animals have continued to increase. Since the meat and milk yield of farm animals directly affects economic costs, many experimental studies have been carried out in this field. Monitoring the ruminating, estrus, and feeding habits of animals has led to valuable data in terms of livestock breeding. Based on this, different sensors were attached to the ankles and tails of the animals to detect and manage the changes in the estrus period.

In particular, the directly related of animal diseases to rumen temperature and rumen pH has led farmers to implement practices to monitor rumen values. Pregnancy, heat stress, estrus, drinking behavior and udder inflammation also provide insightful data on rumen temperature. Health and comfort of animals also cause changes in rumen temperature (Kılıç, 2010). On the other hand, Sub Acute Ruminal Acidosis (SARA) is known as a disease related to rumen pH (Hamilton et al., 2019). This disease, which is shown as the most common cause of economic loss in animals, is said to prevent billions of dollars of damage (Enemark, 2010). This disease occurs when the rumen pH value is below a certain value (<5.5) for a long time. It is important for animal health to monitor the rumen pH value and to intervene quickly in case of a decrease in this value. Due to this decrease in pH value, problems such as the following may occur in animals (Gasteiner, 2012).

- Breathing problems,
- Rumenitis
- Laminitis
- Abomasum shift
- Decreased body condition.

Monitoring of this pH is traditionally accomplished either orally or by taking fluid from the animal's rumen through a cannula channel. Figure 9 shows the traditional methods of gastric fluid collection.
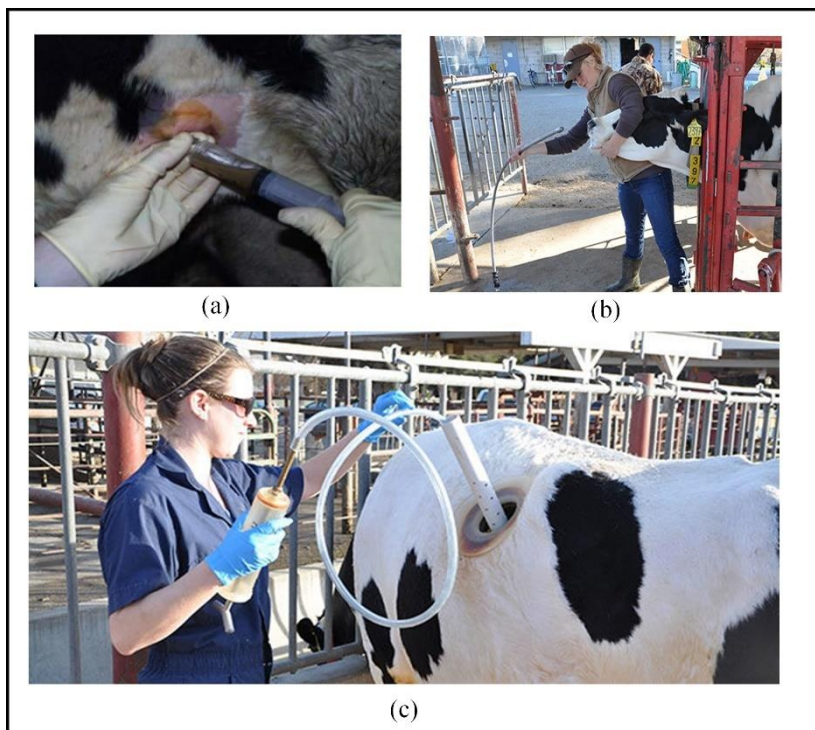
Figure 9. Traditional methods of gastric fluid collection. (a) from the abdominal cavity using a syringe, (b) orally (c) using a cannula (URL-2).

In these traditional methods, the animal is stressed and some injuries may occur. Especially the cannula method is a method that can only be applied on a few animals in farms with a large number of animals for research purposes. Instead, with the development of RFID technology, there have been increasing studies in recent years to add sensors to bolus type tags used for identification purposes. With the temperature and pH sensors added to the RFID bolus tag, which is swallowed orally and placed in the reticulum part of the rumen area, rumen temperature and pH values can be monitored instantaneously. In the first studies, due to the contamination of pH sensors with rumen fluid and deterioration of their calibration, data could be obtained properly for 1-3 months and then deviations in values occurred, but these periods have increased considerably today due to the sensor technology that has developed over time (Mottram, 2009; Phillps et al., 2010, Nogues 2014, Dogan et al., 2018). The biggest problem in this type of monitoring is battery life and sensor technology. Studies on battery life have been carried to very advanced levels today, and pH measurements are now evolving from classical measurements to measurements

using optical technology. As a result, these periods can now be easily given commercially as 3+ years. Figure 10 shows a cannula operation and the pH data obtained from the RFID tag with sensor designed as a result of the operation (Dogan et al., 2018). The pH values given in Figure 10c clearly show the changes in pH values after feeding. In this way, by continuing to monitor pH values at certain intervals, it is ensured that disease-causing conditions are detected in advance and intervened quickly. This results in preventing economic losses due to animal diseases to a certain extent. Studies have also been conducted on whether the electromagnetic waves emitted from these devices will harm the animal (Dogan et al., 2017, Dogan et al., 2019) and it has been shown that the signal power emitted from the tags is too small to cause any damage to the biological tissues of the animals. In addition, with such studies, ideas have been obtained about the optimization of values such as the placement, number and power of the elements to be found in the RFID system to be installed in a farm.
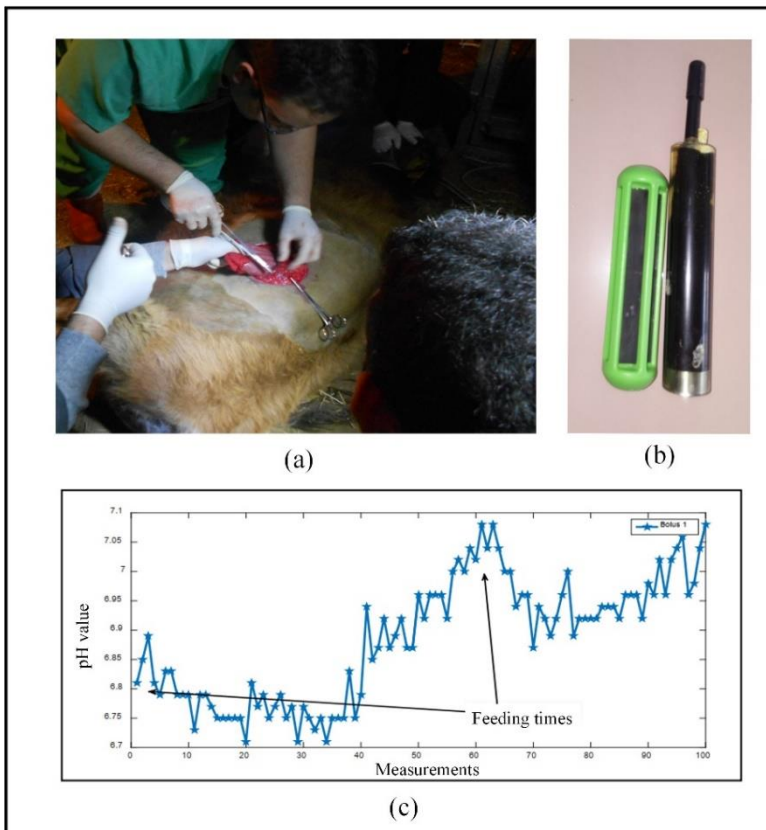
Figure 10. (a) Cannula insertion with surgical operation, (b) active RFID tag with pH and temperature sensors, and (c) pH data from this tag.

Currently, many companies commercially sell tags that enable monitoring of the rumen environment by adding sensors to RFID tags. Some of these tags have been developed after long research and use technologically advanced sensor technology. These rumen pH boluses, which previously provided a short period of efficient working time, have now been reduced in price to very affordable levels and their working time has been extended sufficiently. Table 3 shows a comparison of some of the commercially available pH boluses. In academic studies, comparisons of such boluses with each other have also been included, and it has also been found that accurate information is not given for a very long time as stated in the catalogs (Schori and Muenger, 2022, Han et al., 2022). Considering the sensor technology used, it is noteworthy that the commercial product moowbolus in Table 3 has a lifetime of 3+ years and the pH technology is based on optic. As technology improves, these studies will lead to longer lasting and more accurate tags, and animals will be monitored from many different angles in a healthy way and solutions will be produced. Apart from these products, many research organizations continue to develop such devices (URL-3). Changes in sensor technology need to be applied to this field in order for such labels containing glass-containing pH sensors to have more minimal dimensions and longer lifespan.

Product								
Commercial name	eCow	moonsyst	smaxtec	moow	datamars	autag	fafia	caisley
Purpose of use	tracking	tracking	tracking	tracking	identification	identification	identification	identification
Animals	cattle	cattle	cattle	cattle	sheep, cattle	cattle	sheep, cattle	sheep, cattle
Sensors	ruminal temperature and pH	ruminal temperature and pH	ruminal temperature and pH	ruminal temperature and pH	-	-	-	-
Size and weight	25 mm X 130 mm	32 mm X 100 mm	35 mm X132 mm	-	20 gr, 52 gr, 72 gr	22 gr, 52 gr,72 gr 12mmX 55mm 20mmX 67mm	19mmX 67mm 11mmX 57mm 67,5 gr, 19,5 gr	-
Life span	5 months	6+ years temperature 90 days pH	5 months	3+ years	-	-	-	-
Producer country	UK	Hungary	Austria	Hungary	Switzerland	Netherlands	China	Germany

Table 3. Comparison of some commercially available RFID rumen bolus tags

3. Results

Identification and tracking of animals for different purposes has been a field that has been tried to be realized in a healthy way since ancient times. The phenomenon of identification, which started in order to adopt valuable animals such as horses and to prevent possible theft, has found application in different societies with very different identification methods. Before modern times, traditional identification methods were sufficient due to many factors such as the number of animals, the lack of need for identification and follow-up of wild animals leading a natural life, and the unknown causes of animal-borne diseases. However, the increasing number of herds and the emergence of major epidemics of animal origin have led individuals and institutions to research on different identification systems. As a result of all these studies, it has been concluded that animals can be identified with different electronic technologies, and even by adding different sensors, animals can be monitored with tags to be attached to the animals and valuable data can be obtained from this monitoring in terms of both economic and health. Especially at the end of the 1990s, epidemics such as mad cow, swine flu and avian flu in Europe and other parts of the world accelerated these studies.

The concept of radio frequency identification, the theoretical foundations of which were laid at the end of the 19th century based on electromagnetic waves, showed its first applications especially during World War II, and exploded after the 1970s due to the rapid development in electronic technology. RFID technology, which is mentioned as a market worth 40 billion dollars in the coming years, has been a technology preferred by most countries in animal identification and tracking for the time being, and the legal basis for the identification of all animals with this system has been established, partly compulsory and partly voluntary. With the use of RFID in animals, it is thought that the productivity of farms will be maximized, farm conditions will be optimized in competitive industries, farm management practices will become easier, and quality will increase. Remote tracking of animals with tags added with different sensors will enable the detection of diseases very quickly and keep the spread to a minimum level as it will accelerate the detection of origin. As a result of the farm automation to be provided with RFID, many manual work and processes will be automated and the paperwork burden will be reduced. As a result, there will be significant reductions in labor costs. Applications with sensors, which currently have the chance to be applied in very large farms, will be the RFID products that we will encounter in most farms in the future thanks to the reduction of costs and the increase in their lifetime. The fact that many countries make RFID identification mandatory in primary identification will cause companies investing

in this field to increase their investment capacity and intensify their work. As people's predisposition to technology increases, it is expected that the use of such electronic methods will increase instead of traditional methods.

RFID technology has become one of the most suitable technologies not only for identification purposes but also for monitoring animals for health and other purposes. In addition to tracking wild animals and bird flocks using GPS, sensors added to bolus-type RFID tags developed for livestock can be used to systematically and continuously monitor the estrus status, rumen temperature and pH values of animals. Especially the direct relationship of animal diseases with rumen temperature and pH values makes studies in this field more valuable. Today, many companies have added temperature and pH sensors to rumen boluses for commercial sale. It is seen that the lifetime of such labels depends especially on their batteries, and this lifetime will increase depending on the developing battery technology. Since pH measurement has a very important place in the prevention of diseases such as SARA, companies have been continued to add sensors to the labels to measure pH value, which is a difficult measurement system besides temperature. The fact that the pH sensors used in most commercial products contain a conventional glass membrane has been seen as a factor that prevents their lifetime and minimization. Especially the need for calibration after a certain period of time in such pH meters is the most negative side of such products. Depending on the developing sensor technology, it is seen that classical pH measurements will evolve to optopHmeter technology and in this way, they will have much longer lifetimes than the existing ones. Depending on this development, in the farms of the future, not only RFID products for identification purposes, but also RFID tags with many different sensors in addition to pH and temperature sensors will be encountered. It is thought that all this intensive electronic identification and monitoring will reduce economic losses related to animals, increase the comfort of animals, increase milk and meat yields, automate and facilitate the management of farms, and create positive contributions in many respects.

REFERANSLAR

Ahson, S. A., & Ilyas, M. (2017). RFID handbook: applications, technology, security, and privacy. CRC press.

Lehpamer, H. (2012). RFID design principles. Artech House.

Cibuk, M., & Marasli, F. (2015). RFID Technology and Usage Areas. *Bitlis Eren University Journal of Science and Technology*, 4(2), 249-275.

Dobkin, D. (2012). The rf in RFID: UHF RFID in practice. Newnes.

Dziuk P., (1999). Positive, accurate animal identification. Animal Reproduction Science, 79, 319-323.

Catarinucci, L., Colella, R., Mainetti, L., Mighali, V., Patrono, L., Pieretti, S., & Tarricone, L. (2013). An RFID tracking system supporting the behavior analysis of colonial laboratory animals. *International Journal of RF Technologies*, *5*(1-2), 63-80.

Marchant J., 2002. Secure Animal Identification and Source Verification, JM Communications UK.

Rossing W., 1999. Animal Identification: Indtroduction and history. Computers and Electronics in Agriculture, 24, 1-4.

Castro N., Martín D., Castro A., Arguello A., Capote J., Caja G., 2010. Suitability of electronic mini boluses for early identification of goat kids and effects on growth performance and development of the reticulorumen. JANIM SCI, 88, 3464-3469.

Floyd, R. E. (2015). RFID in animal-tracking applications. *IEEE Potentials*, *34*(5), 32-33.

Volk, T., Gorbey, S., Bhattacharyya, M., Gruenwald, W., Lemmer, B., Reindl, L. M., & Jansen, D. (2014). RFID technology for continuous monitoring of physiological signals in small animals. *IEEE Transactions on Biomedical Engineering*, *62*(2), 618-626.

Karlsson, J., Ren, K., & Li, H. (2010, December). Tracking and identification of animals for a digital zoo. In *2010 IEEE/ACM Int'l Conference on Green Computing and Communications & Int'l Conference on Cyber, Physical and Social Computing* (pp. 510-515). IEEE.

Caja G., Castro-Costa A., Knight C.H., 2016. Engineering to support well-being of dairy animals. Journal of Dairy Research, 83, 136-147.

Zealand, M. B. N. (2009). Review of Selected Cattle Identificationand Tracing Systems Worldwide.

Ribó O., Korn C., Meloni U., Cropper M., De Winne P., Cuypers P., 2001. IDEA: a large-scale project on electronic identification of livestock. Rev. sci. tech. Off. int. Epiz.,20 (2), 426-436

Garin D., Caja G., Bocquier F., 2003. Effects of small ruminal boluses used for electronic identification of lambs on the growth and development of the reticulorumen. J ANIM SCI, 81, 879-884.

Ghirardi, J., Caja G., Flores C., Garı´n D., Herna´ndez M., Bocqui F., 2006. Suitability of electronic mini boluses for early identification of lambs. J ANIM SCI, 85, 248-257.

Antonini C., Trabalza M., Franceschini R., Mughetti L., Acuti G., Asdrubali G., Boiti C., 2006. In vivo mechanical and in vitro electromagnetic side effects of a ruminal transponder in cattle. JANIM SCI, (84-11), 3133-3142.

Cappai M. C., Picciau M., Nieddu G., Bitti M.P.L, Pinna W., 2014. Long term performance of RFID technology in the large-scale identification of small ruminants through electronic ceramic boluses: Implications for animal welfare and regulation compliance. Small Ruminant Research, 117, (2–3), 169–175.

Castro N., Martín D., Castro A., Arguello A., Capote J., Caja G., 2010. Suitability of electronic mini boluses for early identification of goat kids and effects on growth performance and development of the reticulorumen. JANIM SCI, 88, 3464-3469.

Fallon R.J. 2001. The development and use of electronic ruminal boluses as a vehicle for bovine identification. Revue Scientifique et Technique Office International, 20(2), 480-490.

Ghirardi, J., Caja, G., Garín, D., Casellas, J., and Hernández M., 2006. Evaluation of the retention of electronic identification boluses in the forestomachs of cattle. Journal of Animal Science, 84(8), 2260–2268.

Grooms, D. (2007). Radio frequency identification (RFID) technology for cattle.

Kilic, U. (2011). Use of wireless rumen sensors in ruminant nutrition research. *Asian Journal of Animal Sciences*, *5*(1), 46-55.

Hamilton, A. W., Davison, C., Tachtatzis, C., Andonovic, I., Michie, C., Ferguson, H. J., ... & Jonsson, N. N. (2019). Identification of the rumination in cattle using support vector machines with motion-sensitive bolus sensors. *Sensors*, *19*(5), 1165.

Enemark J.M.D., 2008. The monitoring, prevention and treatment of sub-acute ru minal acidosis (SARA). A review. The Veterinary Journal, 176, 32-43.

Gasteiner, J., Guggenberger, T., Häusler, J., & Steinwidder, A. (2012). Continuous and long-term measurement of reticuloruminal pH in grazing dairy cows by an indwelling and wireless data transmitting unit. *Veterinary medicine international*, *2012*.

Mottram T., 2010. Is a lifetime Rumen monitoring Bolus Possible? The First North American Conference on Precision Dairy Management.

Mottram T., Lowe J., McGowan M., Phillips N., 2008. Tecnical Note: A wireless telemetric method of monitoring clinical acidosis in dairy cows. Computer and Electronics in Agriculture, 64, 45-48.

Nogues A., 2013. Commercial Benefits of Routine Monitoring of Rumen pH in Dairy Cows in Southwest England. https://www.ecow.co.uk/wpcontent/uploads/ 2013/09/farm Bolus - results.pdf. Erişim Tarihi:28.06.2017

Philips N. and Mottram T., 2010. Continuous Monitoring of Ruminal pH using Wireless telemetry. Animal Production Science, 50, 72-77.

Dogan, H., & Yavuz, M. (2018). A new wireless bolus sensor with active RFID tag to measure rumen pH. *Fresenius Environmental Bulletin*, *27*(2), 1031-1037.

Dogan, H., Basyigit, I. B., Yavuz, M., & Helhel, S. (2019). Signal level performance variation of radio frequency identification tags used in cow body. *International Journal of RF and Microwave Computer-Aided Engineering*, *29*(7), e21674.

Dogan, H., Basyigit, I. B., Yavuz, M., & Helhel, S. (2017, November). UHF wave attenuation throughout the cow body. In *2017 10th International Conference on Electrical and Electronics Engineering (ELECO)* (pp. 1046-1049). IEEE.

Schori, F., & Muenger, A. (2022). Assessment of two wireless reticulo-rumen pH sensors for dairy cows. *AGRARFORSCHUNG SCHWEIZ*, *13*(2), 11-16.

Han, C. S., Kaur, U., Bai, H., Dos Reis, B. R., White, R., Nawrocki, R. A., ... & Priya, S. (2022). Invited review: Sensor technologies for real-time monitoring of the rumen environment. *Journal of dairy science*, *105*(8), 6379-6404.

URL-1. https://www.marketsandmarkets.com/Market-Reports/rfid-market-446.html?gclid=CjwKCAjwr_CnBhA0EiwAci5siomqlEA8-jqmur_cRnkY_elgm2yL5G5bJexFmxfw-OXocQZHSSzjOBoCVMkQAvD_BwE

URL-2. https://www.agproud.com/articles/21026-collection-of-rumen-fluid

URL-3. https://www.edi.lv/en/projects/mazcenas-boluss-spurekla-parametru-monitoringam-un-agrinai-subakutas-spurekla-acidozes-sara-diagnostikai-govim-2/

Chapter 6

International Studies on Vehicle Inspection and The Current Turkish Example in Practice

Hicri YAVUZ[1]

[1] *Assist. Prof. Dr.; Afyon Kocatepe University, Vocational School of Afyon, Department of Engine Vehicles and Transportation Technology, hicriyavuz@aku.edu.tr ORCID ID: 0000-0001-8427-5164*

ABSTRACT

In daily life, vehicles traveling on highways play a significant role in the transportation sector. In addition to passenger or cargo transportation tasks, these vehicles can also carry out particular tasks with specially equipped vehicles. Special-purpose vehicles include school vehicles, ambulances, fire trucks, funeral vehicles, cranes, etc. They also require special equipment for other purposes that we have yet to mention. These vehicles wear out during use, and due to this wear and tear or natural operation, they can perform differently than when they first entered the traffic. In some vehicles, various features are required depending on their class, and these features must be provided during operation. For all these reasons, vehicles must be inspected at specific intervals starting from the date of entry into traffic, depending on the features they provide and their use. Vehicle inspection procedures and periods vary depending on the country in which they are located, and vehicle inspection is mandatory in most countries. In addition to reducing traffic accidents by inspecting vehicles, the requirement that factors such as exhaust emissions be at specific values within the standards also contributes to protecting the environment. International severe studies have been conducted by scientists and researchers on vehicle inspection, and the findings of these studies are presented with their results. This study includes research on vehicle inspection systems that vary from country to country. Afterward, explanations were made about vehicle inspection procedures, inspection times, inspection results, and the general characteristics of these institutions regarding the example of Turkey. This country has made reformative changes in vehicle inspection. The Turkish example was chosen because comprehensive vehicle inspection is carried out for this sector in the world, and there is no compromise on procedures and legal procedures in this regard. As a result, this study tried to raise profound awareness about vehicle inspection, and the work and procedures specific to the subject were summarized.

Keywords: Vehicle inspection, Vehicle technology, Vehicle safety, Traffic safety, Accident

1. INTRODUCTION

Today, vehicles have a significant place in the transportation sector in terms of cargo transportation and passenger transportation. With the development of technology, upper-segment vehicles that provide comfort and speed with many different features are being produced. Although this development entered our lives in a very short time with hybrid and electric vehicles, studies on vehicles with autonomous and semi-autonomous driving capabilities continue unabated. As in every sector, in the vehicle sector, it is a must for users to carry out periodic maintenance without interrupting the operation of the vehicle in order to provide service. Manufacturers make recommendations regarding maintenance periods and recommend that vehicles be maintained for various distances or periods of use. Manufacturers give users a warranty period and require periodic maintenance of the vehicles to be uninterrupted during this period. Although periodic maintenance varies depending on the type of engine with which the vehicle is driven, it includes oil filter maintenance in internal combustion engines, brake systems etc., depending on changing times. It is a process that also includes the control of systems. It is entirely at the drivers' initiative to carry out these maintenance processes. If vehicle users comply with these periods and perform regular maintenance, the vehicle's economic life will increase, and the vehicle will be safer.

The part we explained above is a phenomenon that occurs entirely under the driver's responsibility. However, people are not individuals when moving in traffic, and they use the highways together with other drivers. Delaying maintenance times and not replacing the parts that need to be replaced on time may result in undesirable situations that may jeopardize the safety of other vehicles. In this process, state legislators impose various mandatory inspections for vehicle owners. Vehicle owners must comply with these conditions. If these conditions are not complied with, legal sanctions such as criminal proceedings or banning vehicles from traffic are applied. For vehicles to technically continue to circulate in traffic, vehicles must be inspected at times determined by vehicle type, varying from country to country. The authorized bodies of the states inspect the vehicles and check whether this process is realized. Since the vehicle sector is dynamic, it is normal for the conditions to change according to the current conditions in these mandatory processes. This is already a necessity due to the structure of the sector.

Vehicles are subjected to many tests to ensure safety at the first stage of the manufacturing process. Due to these tests, they do not cause any technical danger for a certain period when they first enter traffic. During the traffic circulation process, wear and fatigue of the parts occur due to effects such as use, climate,

and road conditions. Periodic inspections of vehicles are carried out in most countries to determine the impact of such adverse conditions on traffic safety. During these periodic inspections, it is checked whether motor vehicles have internationally determined technical competence. Periodic inspection is essential for traffic safety, fuel consumption, and environmental protection. The number of motor vehicles worldwide is increasing without slowing down, serious investments are being made in this field, and noise and emission environmental pollution are increasing due to the increasing number. For all these reasons, vehicle owners need to have these inspections (Eroğlu, 2009).

Various studies are being carried out to minimize the losses in traffic accidents worldwide. These studies can be summarized as increasing public transportation, realizing road designs for safe and comfortable transportation, creating updated policies, and designing various vehicle systems that increase driver and passenger safety. Traffic accidents occur due to human factors and vehicle, road, and environmental conditions. Research has determined that the human factor has the largest share of these conditions. However, in some accident cases, while driver error can be reduced with advanced safety systems, the risk may increase in adverse environmental conditions (Yavruoğlu, 2019). According to World Health Organization data, an average of 1 million 350 thousand people dies annually worldwide, and approximately 78 million suffer socioeconomic losses due to injuries. For this reason, traffic accidents are called a public health problem. The basis of social life is based on mobility. Based on this result, road transportation is indispensable, and traffic safety is seen as a global problem threatening human life. The basic principle in traffic safety should be the protection of life safety. In order to keep negative environmental impacts on highways under control, vehicle, traffic, property, and life safety must be ensured. In order to control these facts, it is mandatory in most countries for vehicles in traffic to undergo a standard inspection and control (Köylü, 2022).

In the following subheadings of this section, in addition to including some scientific studies carried out by researchers on the subject, current issues regarding vehicle classes, inspection periods, inspection processes, and essential points taken into consideration in vehicle inspection will be touched upon in the example of Turkey.

2. SCIENTIFIC STUDIES CONDUCTED ON VEHICLE INSPECTION

Most countries have different legal regulations regarding vehicle inspection. These regulations aim to increase traffic and vehicle safety and reduce environmental pollution caused by exhaust emissions. Factors such as the

development level of the countries, highway parking, and the physical condition of the vehicles play an essential role in these regulations. In the legal regulation's governments make on this subject, issues such as the technical checks that need to be carried out according to vehicle class, whether private or state institutions should carry out these operations, and the period during which the vehicles will be inspected are determined. Government officials and researchers are constantly researching what measures can be taken to reduce accidents through vehicle inspection checks. Because technology is developing rapidly, inspection processes appropriate to these developments should be established, and the system should be kept up to date. This section includes some studies on vehicle inspection in different countries in different locations and at different development levels around the world.

By collecting annual inspection data from Nanjing, China, factors related to emission degradation due to variables, including vehicle features and usage conditions, were determined. The machine learning algorithm revealed the importance of these variables for the subject and their impact on the test results. In the study, the average lifespan of vehicles used as passenger cars in China is 12.9 years, and if this situation is taken into account in the inspected vehicles, more than 5.7% of the vehicles should be converted into scrap. The average mileage of the evaluated vehicles is 105.800 km. The four-level emission standard set in China was 150.000 km in China I/II, 110.000 km in China III, 80.000 km in China IV, and 54.621 km in China V standards. It has been determined that the mileage information of some of the vehicles built here, for example, some 23-year-old vehicles, is lower than the new model vehicles. It has been determined that there is a linear relationship between vehicle age and cumulative km. This result is because taxi-type vehicles used for commercial purposes require regular maintenance, and regular maintenance effectively reduces emission rates. The other reason for this result is that since there is no legal sanction regarding mileage information, errors that may arise regarding mileage will affect the result. However, reaching a definitive conclusion regarding km information is difficult. Because it is difficult to determine whether km values have been reduced or not. Vehicles with high mileage due to vehicle age have higher emission rates and are likelier to fail inspection than older vehicles. It should also be noted that regularly maintained vehicles are more likely to pass the emission test. Vehicles produced with high emission standards have a higher inspection rate. Vehicles that are 10-17 years old and have more than 120.000 km have a higher tendency to fail the inspection (Tu et al., 2022).

In a study conducted in Norway, researchers stated that increasing the number of technical inspections effectively reduced the number of accidents. Based on

the latest data, they stated that a 20% increase in inspections reduced the number of accidents by 4-6%. In Norway, under EU directives, roadside inspections are carried out on vehicles carrying heavy loads by experts from the highway's authority. In these inspections, vehicle weight and braking performance are measured in vehicles. The inspection results show that defects are considered minor, major, or dangerous. If the defect is in the dangerous group, the vehicle is detained until the defect is corrected, and the vehicle is not allowed to be used on the highways until the defect is corrected. Although the number of technical inspections performed varies yearly, in the last years when this study was conducted, it was determined that the annual rate varied between 0.8 and 1.2, approximately once a year for a vehicle carrying heavy loads. Researchers stated that although technical inspections are essential in reducing the number of accidents, more awareness is needed about technical inspections and densities. While the original study estimated that doubling the number of inspections could reduce the number of accidents by 6.7%, the reanalysis estimated that the number of accidents would decrease by 4.9% because the confidence interval was too small. According to the replication analysis, the reduction in accidents was estimated at 21.2%, revealing that the effect of technical inspections is significant in preventing accidents. In Norway, roadside stations are equipped with technically higher-level inspection equipment, allowing better braking performance testing than before. However, researchers argue that technical inspections cannot eliminate the resulting defects. They stated that this was because the number of technical inspections increased, but more than this increased rate would be required. It has been stated that increasing technical inspection inspections of heavy goods vehicles is very effective in reducing the number of accidents (Elvik, 2023).

In some European countries, the lifetime efficiency of particle filters, which essentially prevent the spread of particulate matter, is determined by measuring the number of solid particles at low idle during the technical inspection of vehicles. Researchers have studied the efficiency of these measuring devices (Melas, Vasilatou, Suarez-Bertoa, & Giechaskiel, 2023). As a result of the increase in demand for private and commercial vehicles, the automotive industry develops and contributes to controlling the vehicle's technical condition. With this contribution, the technical condition of the vehicles is better, and the vehicles perform their duties better. States are obliged to ensure the safety of life and property of their citizens. In order to ensure the safety of life and property, the minimum technical requirements that vehicles on the highways must meet are determined, and periodic inspections determine whether these requirements are met. Every EU state must provide this system within the scope of EU directives.

The primary purpose here is to allow vehicles with technical competence to navigate in traffic. According to EU directives, technical inspection describes the examination and evaluation of the system's condition, component, or separate technical structure that makes up a vehicle. After this inspection, defects are evaluated in the vehicle. From these evaluations, the vehicle is sufficient to travel on the highways, the technical condition of the vehicle is sufficient, and there may be acceptable minor defects or incompatibilities that do not affect the safety of the vehicle and the environment. Another defect is allowing the vehicle to temporarily travel on the highways due to defects that may endanger the vehicle's safety or the environment. If a defect is detected in the vehicle that would endanger road vehicle safety, the vehicle will not be allowed to travel on the highways. Since the technical inspection system is implemented with the same rules in every country, the inspection statistical results should be similar for every country. To test this hypothesis, researchers examined examination results from 2019. As a result of this review, they determined that the average technical roadworthiness inspection results do not depend on the average age of the vehicle fleet. They determined that although the number of severe and dangerous defects of the vehicles increased with the age of the vehicles, this situation was not valid interstate. It has been stated that the most crucial factor in this depends on the specific conditions, approach, and determination of standards of the countries where the examinations are carried out. For all these reasons, it has been stated that every country should try to create an inspection system of the best standard to prevent the circulation of vehicles unsuitable for traveling on the highways (Hudec, Šarkan, & Czodörová, 2021).

Heavy vehicle accidents are a significant cause of severe and fatal injury accidents in Australia. In order to reduce and prevent this situation, vehicle inspection programs have been implemented to reduce and manage the factors resulting from severe vehicle defects. In this study, researchers statistically investigated the effectiveness of periodic heavy vehicle inspection in Queensland, Australia, and its effects on the factors that cause accidents and their severity. In the research area, all heavy vehicles are subject to mandatory periodic inspections every 6 to 12 months, depending on the vehicle type and purpose of use. Theoretically, this study develops a model by empirical evaluation of the relationship between periodic vehicle inspection, the factor that caused the accident, and the severity of the accident, and for updating and improving existing policies. This study covers the periodic vehicle inspections in the specified region between June 2009 and December 2013. This study has practical implications as well as theoretical implications. Practical implications include problems such as the driving behaviour of vehicle users, non-compliance with rules, and alcohol

consumption, which have less impact on the periodic inspection of vehicles. It has been stated that the periodic inspection habits of drivers are very effective in accidents, and vehicle inspection facilities should provide driving safety instructions towards this goal, conduct training and evaluations, pay more attention to these drivers, and conduct campaigns and information to raise awareness. Shorter periodic inspection intervals can be an essential factor in reducing defects, and instead of annual inspection, six-monthly inspection intervals and strengthening of inspection regulations have been suggested. Another factor in accidents is driver-related factors such as fatigue, fast driving, driving without a license, advancing age, and, most importantly, drunk driving. More effective policies and controls are needed to prevent these. The limitation of this study is that it focuses on the impact of some specific aspects of periodic vehicle inspection, and the data used is limited for various reasons. In future studies, it may be beneficial to focus on periodic inspections on the causes of inspection failure and on vehicles in other regions (Assemi & Hickman, 2018).

Many problems, such as the lack of standardization regarding the periodic inspection of vehicles in the United Arab Emirates, the lack of frequent calibration of the test equipment in the inspection institutions, their different characteristics, the lack of test equipment, the operation of the inspection institutions by private enterprises, and the inconsistencies in vehicle inspection practices were identified by researchers through a survey. Researchers have determined significant differences in the daily working hours of vehicle inspection centers, weekly working hours, the number of personnel performing inspection, the number of vehicles inspected daily, and the time spent for inspection. It has been stated that inspection costs may differ for each emirate for reasons such as inspection duration and number of inspections. Although devices that measure emission values are available in almost all centers, the devices that should be used to determine the brake status are only available in some inspection stations. Exhaust emissions and brake-related defects are the most common defects in inspection institutions, followed by chassis. Defects such as paint differences, modifications, and lighting errors are less common. It has been stated that the general problem in these organizations is the lack of inspection standards, the organizations being private and not inspected, the lack of devices capable of measuring in all organizations, and the inability to perform the calibration process, which is a determining factor in the measurement results. In the survey conducted, it was stated that the public should be informed about the inspection and that some institutions are crowded, and some are quiet. The number of personnel and working hours may be decisive in these matters. The surveyed inspectors stated that the engine condition should be checked, smoke emissions

in diesel vehicles are essential and should be examined, and although organizations are considering external inspection, most of the inspectors stated that the inspections are sufficient in terms of safety. Inspectors also stated that it is necessary to be able to inspect exhaust measurements on a mobile basis on highways. It has been stated that there are differences between inspection centers in exhaust emission levels and that there are no regulations regarding nitrogen oxides, which is essential in most developed countries where standards are different in various emirates. In the feedback received from vehicle owners, there are requests such as increasing the number of personnel in inspection institutions, making inspection periods biannual instead of annual, checking spare tires, checking fire extinguishers, and reducing inspection costs. The authors stated that the official and civil authorities in the country should contribute to standardization and a more modern inspection process, stricter standards should be established for exhaust emissions, and the devices should be available in all inspection institutions. As a result, the researchers stated that there needed to be more consistency among the inspection bodies that inspected the specified standards (Selim, Maraqa, Hawas, & Mohamed, 2011).

In a study on vehicle inspection in New Zealand, researchers conducted a study on the effects of inspecting vehicles that are six years old twice a year instead of once a year. The decrease in vehicle malfunctions with inspection frequency was estimated along with the safety impact value compared to the cost. It has been determined that inspecting vehicles older than six years old every six months instead of once a year reduces accident rates. In some countries, including New Zealand, when the vehicle owner changes, the prerequisite for obtaining a license for the vehicle is that the vehicle be subjected to periodic inspection. This study, conducted by researchers, aimed to determine whether shortening the vehicle inspection period is justified in terms of safety compared to the cost. Cost-benefit evaluations were made based on comparing implementation costs, considering the social costs, and assessing injuries and deaths. Although reducing the inspection period from 1 year to 6 months provides benefits in terms of safety, the costs of inspection procedures exceed the benefit-cost. In order to cover the cost rates, a 12% reduction in injury accidents is required, and it has been stated that it is impossible to reduce accidents by this much (Keall & Newstead, 2013).

In a study conducted in Japan, the effect of the inspection system implemented in the country on carbon dioxide emissions resulting from automobile-class vehicles was investigated. In the study, a model was created. According to this model, it was stated that the removal of the vehicle inspection system would affect vehicle purchasing behavior in a decreasing way. As a result, it effectively reduces carbon monoxide emissions due to the increase in the average economic

life of the vehicles. If the automobile inspection system in Japan is revised again, the desire of car owners to repurchase vehicles will also cause carbon dioxide emissions to decrease. However, in practice, it is complicated to scrap vehicles at once. For this reason, the authors proposed a modified vehicle inspection system to relieve some of the cost burden that vehicle inspection brings to vehicle owners. Although tax deductions and subsidies for the purchase of environmentally friendly vehicles are essential for popularizing new-generation vehicles, loosening the inspection system for old vehicles will effectively reduce carbon dioxide emissions. Using environmentally friendly vehicles for extended periods will be beneficial in reducing climate change. (Nakamoto & Kagawa, 2018).

A comprehensive periodic vehicle inspection program has been initiated in Norway since 1995 after receiving permission to access the EU internal market. With this study, the authors determined the effect of periodic inspections performed on automobiles, except trucks and buses, on accidents. The data used in the study were taken from a large insurance company and public roads administration in the country. It has been determined that vehicle inspection inspections significantly reduce technical defects in automobiles, but the effect of inspection inspections on accident rates still needs to be found. There may be a tendency for vehicle users to neglect vehicle inspections by vehicle owners who are less concerned about safety. The impact of the findings after the inspection on vehicle owners in terms of behavioural adaptation is discussed. The number of vehicles in Norway is increasing significantly day by day. For this reason, periodic vehicle inspections are also seriously regulated. According to the results obtained by the researchers, technical defects identified after the inspection have a small but statistically significant relationship with the accident rate. Technical deficiencies identified in the vehicle led to the elimination of these defects. It has been determined that vehicles passing the inspection process slightly increase the accident rates, even if they do not decrease. It raises the question of whether these findings mean anything and whether a weak analysis model was applied due to insufficient data. Investigative data from the insurance company may need to be of better quality due to underreporting, whether the accident was reported, and the age of the vehicle. Poor quality data may have been provided because another person caused the accident instead of the vehicle owner registered with the insurance company. There is also a rather complex and unclear situation with the drivers. Looking at the evidence, the authors think that the low mean value problem does not affect their analysis. Vehicle drivers who do not care much about safety do not care about the impact of the vehicle traveling in traffic under appropriate technical conditions on accidents. However, the research shows that

vehicle technical proficiency is practical in the analysis of selectively considering unsafe vehicle drivers. As a result of the inspection, vehicle owners' ability to eliminate severe defects may lead to the perception that the vehicle is safer than before. However, there is no data available to test this conclusion (Christensen & Elvik, 2007).

Researchers in Riyadh, Saudi Arabia, have determined how simple methods can be used to improve the workflow processes applied in vehicle inspection. The workflow processes currently used in the vehicle inspection process were determined in the study, and how long this process took was determined. The current process could be completed quickly by making simple changes. Studies were carried out on vehicle inspection processes, personnel numbers, inspection area, time taken for customers to pay fees and tow the vehicle to the appropriate area, and time management related to all these. If the vehicle passes the inspection after all these processes, the inspection will be terminated by attaching a label to the vehicle. If the vehicle does not pass the inspection, a period will be given to eliminate the defects, and the inspection process will begin again. It is predicted that the efficiency will increase to approximately 175% with simple changes in this entire process, without causing any increase in cost or with a slight increase (Al-Saleh, 2011).

In order to develop the vehicle inspection program in Lebanon, in August 2001, the government issued a new regulation making the inspection of vehicles older than three years old mandatory and introducing various obligations. These features included vehicle inspection and regulation of fines. A scenario-based approach survey was developed regarding the theoretical environment and the potential results of the vehicle inspection program. With this change, policymakers have faced several challenges. The first of these difficulties is selecting the institution to be inspected, and the other is making the vehicle repair mandatory in case of a technical deficiency or imposing emission taxation. Various suggestions were presented due to the survey conducted with vehicle drivers. While 32% disagree with these suggestions, 32% disagree about repairing the vehicle at the station where the fault is detected, paying the inspection fee in the inspection areas, and the reliability of the state-run vehicle, while 34% agree. 61% of the respondents stated that the state should inspect private inspection companies. In the section on air pollution, 89% of the participants stated that inspection programs would be effective, while 43% stated that this would be costly. With this study, it was stated that it would be more appropriate to eliminate the defects of vehicles deemed inadequate during inspection rather than collect taxes on emission rates (Kazopoulo, Kaysi, & El Fadel, 2007).

While in France, in the vehicle inspection program introduced in 1986, inspection was mandatory only for second-hand sales. In 1992, it became mandatory for all cars over five years old, and after 1996, for all cars over four years old. During the inspection, the functional status of the vehicle's brake system and other systems and the correct functioning of the emission system on the vehicle are checked. It focuses on the effectiveness of measures to reduce emissions and uses reasonably simple models to represent domestic vehicle transaction behaviour. Aggregate or discrete two-wave panel data typically used in these studies cannot be used to separate the effects of the policy measure from the effects of the economy because they need more data to estimate the individual parameters of the effects of interest. The policy measure changes between two points in time, but the economy also changes, creating a correlation between the two. Ignoring the latter in the model estimation will lead to the coefficient estimate of the policy measure also representing the effects of the economy. Two factors can be separated if a more extended panel data set is available. However, if panel data are aggregated, they may hinder a complete understanding of individuals' behaviour because aggregate models cannot fully capture the vehicle transaction behaviour of individual households. In this study, the effects of policy measures and economies on household vehicle transaction behaviour are examined from a disaggregated perspective, taking into account the effects of factors that are not stable over time, such as household characteristics and the country's economy. As a result of the research, accelerating the scrapping of a vehicle through a vehicle inspection system effectively encourages vehicle owners to dispose of their old vehicles. In addition, granting grants by the state for scrap vehicles will also contribute to reducing emission rates (Yamamoto, Madre, & Kitamura, 2004).

Shortly after the Clean Air Law amendment was adopted in the USA in 1990, various regulations were published regulating motor vehicle maintenance and inspection procedures. These laws were quickly repealed because they only required test-only inspections and narrowly defined testing procedures. As a result, the federal government gave states flexibility to try different programs. Most states have implemented practices covering remote sensing devices. As detection devices fell short of expectations, computer-aided inspections from in-car diagnostic equipment replaced traditional exhaust emission tests. Experience has shown that this method complements rather than replaces exhaust-based tests (Eisinger & Wathern, 2008).

The effects of injuries resulting from vehicle accidents were examined by periodic vehicle inspection and frequent tire pressure checks. This study stated that vehicle inspections performed every six months were necessary, and the car

accident injury study in New Zealand was analysed. As a sample, vehicles involved in accidents in which a person was hospitalized and died were selected in each case. Interviews were conducted with 588 randomly selected drivers. Accidents in which a person is injured, or dies are higher in vehicles that have not been inspected. For all these reasons, the authors ultimately suggested that vehicle inspection procedures should continue from their current location and that inspection procedures should be used in other areas (Blows, Ivers, Connor, Ameratunga, & Norton, 2023).

The maintenance and inspection processes that are mandatory by countries include regular testing of vehicles on the highways and the elimination of non-conformances if there is a violation of emission regulations. Inspection and maintenance processes require testing at regular intervals to determine whether emission rates comply with standards. In vehicles determined to be defective, the defects must be corrected. In North America, mandatory vehicle inspection and maintenance periods are a widely accepted process for reducing air pollution. In this study, instead of subjecting the vehicles to these processes in a very short time, a cost function estimate was made to enable these processes to take place more reasonably for cost reduction. A cost reduction curve estimate was created for the clean driving program around Toronto. It has been stated that even a minimal decrease in the cost with the model can lead to a significant decrease in the costs reflected on the driver. It is envisaged that this cost-saving will provide resources to reduce urban air pollution (Moghadam & Livernois, 2010).

3. TÜRKIYE'S EXAMPLE IN VEHICLE INSPECTION WITH CURRENT PRACTICES

Until 1985, periodic inspection of vehicles in Turkey was carried out by a joint commission consisting of representatives of the Highways and Police Department and the Turkish Drivers and Automobile Federation. After this date, vehicle inspections were carried out in facilities affiliated with the General Directorate of Highways, camping trailers, or non-institutional areas. In 2003, vehicle inspection stations in Turkey were included in the scope of privatization. In 2005, a tender for privatizing vehicle inspection stations was held, paving the way for private companies to carry out this activity. By Article 34 of the Highway Traffic Law No. 2918, vehicle inspection is mandatory (Yavruoğlu, 2019). In Turkey, in addition to periodic vehicle inspections, inspections involving different vehicle registration groups carried out by the private sector and the public, as well as exhaust, taximeter, and tachograph controls, are also carried out, and these controls contribute to traffic and vehicle safety (Köylü, 2022).

Vehicle inspection stations in Turkey must comply with the TS EN ISO/IEC 17020 General Criteria for the Operation of Various Types of Inspection Bodies (Type A inspection body) standard and be accredited and continue to be accredited during the activity period. Tools and equipment to be used in inspection services are always kept active. Although some exceptions depend on the vehicle class, inspection devices should always be active (Official Newspaper, 31356, 2021). Many legislations have been created for road vehicles by the relevant traffic law articles in Turkey. Legal regulations for vehicles on the highway are listed below (Toklucu, 2020).

✓ Highway Traffic Law No. 2918 and Highway Traffic Regulation
✓ Regulation on the Opening and Operation of Vehicle Inspection Stations
✓ TS EN ISO 17020 Standard
✓ School Bus Vehicles Service Regulation
✓ Regulation on the Transport of Dangerous Goods by Road
✓ Regulation on Advertisements on Commercial Vehicles
✓ Decision on the Procedures and Principles to be Applied in the Issuance of Commercial License Plates
✓ Regulation on Manufacturing, Modification and Assembly of Vehicles (AİTM)
✓ Regulation on Type Approval of Motor Vehicles and Trailers (MARTOY)
✓ Type Approval Regulation for Two or Three Wheeled Motor Vehicles (MOTOY)
✓ Regulation on Type Approval for Wheeled Agricultural or Forestry Tractors (TORTOY)
✓ Approval of Motor Vehicle Brakes (ECE-R13)
✓ Type Approval Directive (71/320/EC) on Braking Devices of Certain Classes of Motor Vehicles and Their Trailers

According to the information compiled from Aksu's (Aksu, 2020) study, the vehicle definitions described in Turkey are in Table 1.

Table 1: Vehicle definitions described in Turkey (Aksu, 2020)

Automobile: It is the name given to a motor vehicle designed to transport people with a maximum of nine seats, including the driver.	**Minibus:** It is a motor vehicle with a minimum of 10 and a maximum of 17 seats, including the driver, designed to transport people.
Pickup truck: The name given to a motor vehicle designed to carry loads whose maximum loaded weight does not exceed 3500 kg.	**Truck:** Vehicles used to carry loads with a maximum loaded weight of more than 3500 kg, which can be defined as a closed or open superstructure, are called trucks.
Bus: It is a vehicle used for passenger transportation that can carry at least 18 or more passengers, including the driver, in which trolleybuses are considered in this class.	**Tractor:** It is the name given to the vehicles used to tow vehicles called trailers and semi-trailers.
Off-Road Vehicle: The name given to a vehicle whose front and rear axles are engine-driven and designed to carry passengers or cargo.	**Special Purpose Vehicle:** These vehicles are designed for particular purposes and are modified with projects called modification projects per their purpose.
Personnel Service Vehicle: It is used to transport private or public personnel with minibuses or buses.	**Public Service Vehicle:** These vehicles are used to transport school students and can also be used in shuttle transportation.
Camping Vehicle: It is the name given to motor vehicles in which the vehicle's interior has been modified for holiday purposes and has the necessary equipment for holiday purposes.	**Trailer:** It is a non-motorized vehicle pulled by motor vehicles for cargo and human transportation.
Semi-Trailer: It is a non-motorized vehicle carried by a tow truck.	**Lowbed:** It is a semi-trailer with different weights, lengths, and widths.
Light Trailer: A vehicle referred to as a non-motorized trailer or semi-trailer with a maximum weight of up to 750 kg.	**Rubber Tire Tractor:** It is the name given to an agricultural vehicle that can pull a trailer or semi-trailer.

3.1. Tools and Equipment That Must be Mandatory in Control Institutions During Vehicle Inspection

Vehicle inspection stations can provide fixed and mobile services in Turkey. All fixed and mobile vehicle inspection stations must have brake, headlight, tire tread depth, gas leak, and noise measuring devices. In stations where only motorcycle inspection will be carried out, brake test equipment, headlights, and tire tread depth measuring devices must be available. In addition to the obligation to have the devices mentioned above, it is also essential that they are in working

order at all times (Official Newspaper, 31356, 2021). As a requirement of this regulation at vehicle inspection stations, gas leakage measurement devices, tire tread depth callipers, brake testers, mobile brake testers for vehicles that cannot be measured with the brake tester, load unit for load simulator, heavy vehicle steering clearance device, traction system measuring gauges, There is a manometer for air brake system tests, a tape measure for dimension measurements, a headlight adjustment measuring device, an exhaust emission device and a noise measuring device for measuring noise levels. With these devices and equipment, the necessary checks and measurements for vehicle inspection are carried out. While the measurements made by some of these devices are transferred to the computer, manual measurements such as meters and manometers are carried out and evaluated by the technician (Toklucu, 2020). Minimum width, height, and length values are determined in Turkey for vehicle inspection procedures. A dimension-measuring device with a laser measuring system is used to perform this control. This measurement is performed on heavy vehicles (Trucks, Trailers, and semi-trailers) (Aksu, 2020).

3.2. Vehicle Inspection Periods

With the use of vehicles, problems arise in which parts of the vehicle expire, become damaged, wear out, or wear out over time. These adverse situations not only endanger the safety of the vehicle but also endanger traffic safety. Depending on the likelihood of this danger occurring, it may also increase the severity of the accident in the event of an accident. All the defects listed above do not appear suddenly, and a particular process is required for these defects to appear. As the vehicle ages, many damages and malfunctions are more likely to occur in passenger or heavy vehicles. Any malfunction or damage in these parts will cause the vehicle to move unsafely in traffic (Özçelik, 2021). According to the regulations implemented in Turkey, inspecting the vehicle at the periodic times given in Figure 1 is mandatory (Official Newspaper, 31356, 2021).

Private and official cars	• After the first three years of age and every two years thereafter
Rubber wheel tractors	• After the first three years of age and every three years thereafter
Two or three wheeled vehicles	• After the first three years of age and every two years thereafter
All other motor vehicles, trailers and semi-trailers	• At the end of the first year of life and annually thereafter

Figure 1: Vehicle inspection periods

3.3. Technical Specifications of Motor Vehicles and Systems Checked During Vehicle Inspection

The vehicle's size, acceleration, weight, capacity, occupation area, speed, and power characteristics are classified as general characteristics. In contrast, the mechanical parts, vision elements, electrical system, tire characteristics, model, and age characteristics are classified as unique (Eroğlu, 2009). Unique characteristics are taken into account during vehicle inspection. It is a general name used for all vehicle operating systems, including mechanical parts. This system includes critical systems for the vehicle, such as the engine, power transmission, motion transmission, and braking system. Vision elements are parts such as mirrors and windows that guide the driver while driving the vehicle. Tire features are among the most essential features of the vehicle. Among these features, the size of the tire, its mounting in the direction of rotation, and the tread depth not being below a specific value attract attention. Among the model and age information, age information is a feature that depends on the wear and tear of the vehicle throughout use. As the age of the vehicle increases, it becomes necessary to check its technical adequacy. In addition to day and night lighting, the electrical system is essential for all living and inanimate objects in the vehicle in case of fire. Considering all these features, the content that the vehicle inspection procedure will cover is determined. In vehicle inspections in Turkey, the general systems specified in Table 2, which vary according to vehicle class, are legally (Official Newspaper, 31356, 2021) required to be tested.

Table 2: Systems that must be checked during vehicle inspection.

Number	System
1	Brake systems
2	Steering wheel
3	Vision Features
4	Lamps, Reflectors and Electrical Equipment
5	Axles, wheels, tires, suspension
6	Chassis and chassis connections
7	Other equipment
8	Noise pollution
9	Additional controls
10	vehicle promotion

3.4. Check Order of Systems Checked During Vehicle Inspection

With the work order created by using the information of the vehicle registration certificate, the vehicle is inspected after checks such as the license plate, chassis and engine number, vehicle brand and model, vehicle group, colour of the vehicle, purpose of use, type label information, number of seats are carried out in the defined inspection area. The technician starts the process (Özçelik, 2021). The titles explained in the lower sections were compiled from the comprehensive study conducted by Özçelik (Özçelik, 2021). Although the control order can be changed according to the inspection site condition to avoid missing checks in the inspection procedure, it generally takes place in this process.

3.4.1. Vehicle Chassis and Engine Numbers

These are also called vehicle identification checks. It is checked whether the chassis and engine number are similar to the numbers specified in the registration certificate, which is the document containing vehicle information in Turkey, where the vehicle's features are stated.

3.4.2. Vehicle Type Label

Vehicles traveling on highways must have signs called type labels placed by the manufacturer. The type label must contain the manufacturer's information: the type approval number, the chassis number, the maximum loaded weight of the vehicle, the maximum loaded weight with the trailer, and the axle weights.

3.4.3. Vehicle Colour Identification

The vehicle's primary colour, which is an essential control in the vehicle description, must match the colour specified in the registration certificate. In this step, colour information is checked.

3.4.4. Registration Plates

It is checked that the license plates installed on the vehicle are the same as the license plate written on the registration certificate.

3.4.5. Engine Pool Controls

Whether the parts in the part called the engine pool, which is usually under the vehicle's front hood, are fixed or not, liquid gas, etc. Leakage checks and shock absorber connection checks are carried out on the lines.

3.4.6. Brake System controls

Factors such as deviation between right and left brake forces, runout, tightness, and brake efficiency are determined by the service brake measurement results of the vehicle. In handbrake measurements, tightness, deviation and efficiency factors are taken into account. The vehicle is taken to the brake tester and waited for 2-3 seconds before braking. If braking force is obtained on the brake tester even though no braking is applied, it is decided that the brakes are tight or there is a fault with the bearing. It is decided whether there are various defects such as deviation, ovality, and runout in the axle regarding the application of force on the brake pedal, that is, braking. Brake values are automatically recorded on the computer.

3.4.7. Lighting Controls

Lighting control is essential for vehicles, especially in attracting attention when traveling at night or changing direction. In the lighting control, lighting equipment such as parking lights, dipped beams, high beams, fog lights, lamps used for signalling, brake system lamps, reversing lamps, and third brake lamps are controlled. In the controls, detailed checks are provided, such as whether the colour the lighting lamps should reflect is working effectively.

3.4.8. Front, Rear and Side Protection Frames

Although it varies depending on the vehicle class, installing a front protection bar for vehicles is possible. When the front guard bar is installed, it should not reduce the field of view of the vehicle, it should not disrupt the work of lighting, license plate, towing equipment, etc., and its installation should be suitable. It

should be of a nature that will not harm people in case of an accident (there should be no sharp corners, pointed edges, etc.).

3.4.9. Glass controls

According to the standards established in Turkey, considering international standards, it is mandatory to use so-called safety glasses in vehicles that go into traffic after 01.01.2003. These checks are carried out within the scope of vehicle inspection, and the required features are checked.

3.4.10. Sub-Controls

Sub-checks are among the essential checks for vehicle inspection. In addition to visual checks by the technician descending into the canal, the front and rear axles of the vehicle are lifted with a jack, and the wheel axle connections are checked in detail. This control checks gearbox connections in the steering system, steering bellows, hydraulic system steering gearbox, tie rod arms, and tie rod ends for oil leaks. In the suspension system checks, the physical control of the coil springs, the durability of the shock absorber gap connections, whether there is oil leakage, the swing arm connections and the clearance checks in these connections, the ball joint stability and dust bellows checks, the anti-roll bar checks, the tire mounting checks and whether any unapproved modifications have been made is checked. During tire checks, it is checked whether the tire and rim sizes are mutually compatible, whether there are any damages on the tire, whether a tire suitable for the load index and speed index is used, and whether the tire tread depth is within standard limits. In-wheel checks, after lifting the axle with a jack, the wheels are moved left and right to check the tie rod end clearance, and by moving to the point where the wheels touch the ground, the bearing clearance is checked. In the checks made at the bottom of the vehicle, in addition to the checks of the parts in the brake system, brake hoses, and pipes, fuel system parts check according to the vehicle's fuel system, limiter control, if any, exhaust system pipes and parts, axle shaft muscle bellows, shaft element checks, differential and engine oil leaks. Comprehensive checks, such as chassis integrity checks, are provided.

3.4.11. Internal Controls

In-vehicle checks include a comprehensive check, just like under-vehicle checks. It is checked whether the informative warning signs on the instrument panel are fulfilling their duties and whether these systems are working by checking the vehicle's mileage information. Clutch brake pedal stability and anti-slip tire conditions are checked. Detailed seat belt checks are carried out

according to the vehicle class and model year and the obligation dates in the regulation. Heating and ventilation system checks are carried out to check whether these systems, especially the windshield diffuser, are working in addition to checking whether the seats have the capacity specified in the vehicle registration certificate, whether their connections are intact, and whether the assembly of the seat backs and headrests are checked. It is checked whether the windshield wipers are working and whether the windshield washer system, if any, is working. Systems such as vehicle door hinge locks, window jack controls, and the electric window lifting system, if any, are checked. In addition to whether the horn is working, it is checked whether the sound harmony is appropriate. It is determined whether the interior rear-view mirror and the mirrors on both sides fulfil their functions. It checks whether the steering lock mechanism works, whether the steering clearance is within the limit values, and whether the steering wheel, airbags, and systems in the vehicle are checked. Fire extinguisher, first aid kit, reflector, spare tire, etc., should be kept for the vehicle. It is checked whether the elements are usable, their capacities, or whether they contain the mandatory content list. There is no requirement for a spare wheel when there are various alternatives, such as tires that repair themselves in the event of a puncture, self-inflatable tires, self-supporting tires called puncture-proof tires, and tires that will ensure driving continuity.

3.4.12. Headlight Measurement

Headlight adjustment control devices, which must be kept in the inspection areas, check the height and illumination light intensity values of the headlights of appropriate standards. If the headlights are adjusted during headlight measurement, the adjustment knob should be in the zero position.

In addition to these checks in the Inspection of Heavy Vehicles, load-dependent brake system checks, sealing in the air brake system, four-way safety valve, red and yellow coupling tests for tow vehicles, check valves, as well as checks of systems such as pile brake system, tank, dryer, etc. element checks are carried out (Özçelik, 2021).

3.5. Evaluations of Defects Detected During Vehicle Inspection

After the defect mentioned above determinations, defect evaluations are carried out according to the following defect groups determined in Turkey (Official Newspaper, 31356, 2021).

3.5.1. Flawless

It is the definition of a defect in which there are no defects in the vehicle inspection. The inspection process of perfect vehicles is approved by authorized personnel.

3.5.2. Slight Defect

It is the situation where defects or defects that do not require re-inspection are detected during the vehicle inspection. These defects are noted in the inspection report. Vehicle inspection is considered successful. Minor defects are stated, and it is stated that the vehicle owner can have these defects repaired if he wishes.

3.5.3. Serious Defect

It is a situation where defects requiring repair are detected during the vehicle inspection. If these defects and defects are detected, the vehicle owner is given a one-month re-inspection period to correct the defects. During the vehicle inspection, it is checked whether the defects mentioned in the report have been eliminated. If the specified defects are corrected, the vehicle's inspection is approved. Suppose it is determined that any of these defects have not been corrected. In that case, the vehicle inspection will not be approved, and a report will be submitted to the vehicle owner for the vehicle to be re-inspected for a fee.

3.5.4. Unsafe

It is a situation where defects that endanger the safety of life and property are detected during vehicle inspection. The vehicle owner is given a one-month inspection re-inspection period to eliminate the defects and defects in question. The vehicle inspection report includes a statement stating that the vehicle cannot be driven on highways. Only the defect evaluations specified in the inspection report are checked during the re-inspection. If these defects are resolved, the inspection process is deemed successful. If not, the inspection process is deemed unsuccessful. If the inspection process is unsuccessful, the vehicle owner must have his vehicle inspected by paying a fee again.

3.6. Delivering the Inspected Vehicle to its Driver

The vehicle driver whose inspection is completed is informed about the inspection process. If the vehicle has passed the inspection, a stamp is affixed to its license plate, and the inspection report is sent to the electronic environment. Inspection etc. In such cases, without asking for any report from the driver, law enforcement officers can easily see whether the vehicle's inspection has been

approved when they check the vehicle's license plate information from their central systems.

4. RESULTS

Vehicle inspection is an essential issue in all countries around the world. Inspection of vehicles that are effective in accidents should be carried out at specific periods when the vehicle exceeds a certain age, depending on the vehicle class. Although it varies depending on the geography where the vehicles are located, governments make legal regulations regarding vehicle inspection. If these legal regulations are not made, vehicle owners may disrupt maintenance operations, and disruption of vehicle inspections may lead to inevitable consequences. In addition to improving traffic and vehicle safety, another important aspect of vehicle inspection is ensuring the environment's protection in terms of exhaust emissions. Considering that the majority of the vehicle fleet consists of internal combustion engines, another critical issue is how much the environment can be polluted in cases such as fluid leaks that may occur in the vehicle. Research has been conducted by researchers on vehicle inspection from many different perspectives. Some of the researchers focused on accident statistics, some focused on vehicle inspection procedures, some focused on environmental pollution, and some have conducted extensive research on issues such as improvements that can be made in vehicle inspection regionally and shortening the time spent by vehicle inspection technicians in inspection or shortening periodically determined periods. In this study can find detailed information about these studies under the title *Scientific Studies Conducted on Vehicle Inspection*.

In this study, detailed research was conducted on vehicle inspection in Turkey after giving information about the importance of vehicle inspection and international studies. The Turkish example was chosen because of the establishment of a professional vehicle inspection system in this country with an innovative approach, as well as the preparation of a legal basis by the government in accordance with the legal obligations of the European Union. First of all, the inspection process, which was carried out by the state, started to be carried out by the private sector under state supervision. An inspection team consisting of expert personnel has been established in this process. In addition to being composed of competent people in their field, this staff has become more competent through in-service training. The same inspection process was applied for each vehicle, even in different cities, and no compromises were made. It is stipulated by the state that all equipment necessary for inspection must be available in inspection areas and that this equipment must be kept in working

order at all times. Maintenance, control, and calibration are carried out without interruption, and measurement accuracy is ensured. In addition, introducing the requirement for these inspection bodies to be accredited ensures that the understanding of quality inspection is not compromised. You can find information about the checks made on vehicles related to the inspection process in Turkey in the sections of this study under the title of *Turkey Example in Vehicle Inspection with Current Practices*. The vehicle inspection process in Turkey can make a positive contribution to developing countries. The inspection process implemented in Turkey is being tried to be made more transparent and more accurate, both with the innovative requests brought by the government and with the innovations brought by the private company that is very expert in vehicle inspection and carries out this process. Depending on technology development, for example, air brake systems performed in heavy vehicle inspections may be performed with automation systems with additional software and systems rather than under the control of technicians. The additional software and automation systems explained here by giving examples can be expanded further. In addition to minimizing possible technician errors that may occur during the vehicle inspection process, these systems can also contribute to reducing the cost of vehicle inspection operations by shortening the vehicle inspection time and ultimately reducing the waiting time of customers.

REFERENCES

Aksu, B. (2020). *Design of Alb Tester for Heavy Vehicle Brake Systems* (MS Thesis). Selçuk University, Konya.

Al-Saleh, K. S. (2011). Productivity improvement of a motor vehicle inspection station using motion and time study techniques. *Journal of King Saud University - Engineering Sciences*, *23*, 33–41. https://doi.org/10.1016/j.jksues.2010.01.001

Assemi, B., & Hickman, M. (2018). Relationship between heavy vehicle periodic inspections, crash contributing factors and crash severity. *Transportation Research Part A: Policy and Practice*, *113*, 441–459. https://doi.org/10.1016/j.tra.2018.04.018

Blows, S., Ivers, R. Q., Connor, J., Ameratunga, S., & Norton, R. (2023). Does periodic vehicle inspection reduce car crash injury? Evidence from the Auckland Car Crash Injury Study. *Australian and New Zealand Journal of Public Health*, *27*(3), 323–327.

Christensen, P., & Elvik, R. (2007). Effects on accidents of periodic motor vehicle inspection in Norway. *Accident Analysis and Prevention*, *39*, 47–52. https://doi.org/10.1016/j.aap.2006.06.003

Eisinger, D. S., & Wathern, P. (2008). Policy evolution and clean air: The case of US motor vehicle inspection and maintenance. *Transportation Research Part D: Transport and Environment*, *13*, 359–368. https://doi.org/10.1016/j.trd.2008.05.001

Elvik, R. (2023). Effects on accidents of technical inspections of heavy goods vehicles in Norway: A re-analysis and a replication. *Journal of Safety Research*, *84*, 212–217. https://doi.org/10.1016/j.jsr.2022.10.021

Eroğlu, Ü. T. (2009). *Investigating Technical Conditions of Vehicles in Traffic* (MS Thesis). Sakarya University, Sakarya.

Hudec, J., Šarkan, B., & Czodörová, R. (2021). Examination of the results of the vehicles technical inspections in relation to the average age of vehicles in selected EU states. *14th International Scientific Conference on Sustainable, Modern and Safe Transport*, *55*, 2–9. Elsevier B.V. https://doi.org/10.1016/j.trpro.2021.07.063

Kazopoulo, M., Kaysi, I., & El Fadel, M. (2007). A stated-preference approach towards assessing a vehicle inspection and maintenance program. *Transportation Research Part D: Transport and Environment*, *12*, 358–370. https://doi.org/10.1016/j.trd.2007.04.002

Keall, M. D., & Newstead, S. (2013). An evaluation of costs and benefits of a vehicle periodic inspection scheme with six-monthly inspections

compared to annual inspections. *Accident Analysis and Prevention*, *58*, 81–87. https://doi.org/10.1016/j.aap.2013.04.036

Köylü, S. B. (2022). *Feasibility Analysis for Inspection and Control Applications in The Automotive Industry* (MS Thesis). Afyon Kocatepe University, Afyon.

Melas, A., Vasilatou, K., Suarez-Bertoa, R., & Giechaskiel, B. (2023). Laboratory measurements with solid particle number instruments designed for periodic technical inspection (PTI) of vehicles. *Measurement: Journal of the International Measurement Confederation*, *215*(112839), 1–11. https://doi.org/10.1016/j.measurement.2023.112839

Moghadam, A. K., & Livernois, J. (2010). The abatement cost function for a representative vehicle inspection and maintenance program. *Transportation Research Part D: Transport and Environment*, *15*, 285–297. https://doi.org/10.1016/j.trd.2010.02.009

Nakamoto, Y., & Kagawa, S. (2018). Role of vehicle inspection policy in climate mitigation: The case of Japan. *Journal of Environmental Management*, *224*, 87–96. https://doi.org/10.1016/j.jenvman.2018.07.028

Official newspaper, 31356. , Official newspaper, 31356 § (2021).

Özçelik, A. (2021). *Design, Realization and Application of the Four-Waysafety Valve Tester for heavy Vehicle Brake Systems* (Ms. Thesis). Selçuk University, Konya.

Selim, M. Y. E., Maraqa, M. A., Hawas, Y. E., & Mohamed, A. M. O. (2011). Assessment of vehicle inspection and emission standards in the United Arab Emirates. *Transportation Research Part D: Transport and Environment*, *16*(4), 332–334. https://doi.org/10.1016/j.trd.2011.01.004

Toklucu, M. (2020). *Design of Sealing Tester for Heavy Vehicle Air Brake Systems* (MS Thesis). Selçuk University, Konya.

Tu, R., Xue, L., Meng, C., Xu, L., Li, T., & Chen, H. (2022). Identifying specifications of in-use vehicles failing the inspection/maintenance emission test. *Transportation Research Part D: Transport and Environment*, *108*(103327), 1–16. https://doi.org/10.1016/j.trd.2022.103327

Yamamoto, T., Madre, J. L., & Kitamura, R. (2004). An analysis of the effects of French vehicle inspection program and grant for scrappage on household vehicle transaction. *Transportation Research Part B: Methodological*, *38*, 905–926. https://doi.org/10.1016/j.trb.2004.02.001

Yavruoğlu, B. A. (2019). *Investigation of Periodic Vehicle Inspection System in Turkey* (M. Sc. Thesis). Gazi University, Ankara.

Chapter 7

A Cost-Effective Healthcare Mobile Application Toward Early Diagnosis of Heart Murmur

Huseyin COSKUN[1]

[1] *Asst. Prof. , Kütahya Health Sciences University, Computer Engineering Department, huseyin.coskun@ksbu.edu.tr ORCID No: https://orcid.org/0000-0002-8380-245X*

ABSTRACT

In this study, a novel mobile software application that can run on Android-based mobile devices has been designed and developed to classify murmur heart sounds using the support vector machines method. The occurrence of heart sounds with murmur at specific age groups and certain conditions may be symptoms of serious health problems. In order to detect this situation, an Android-based mobile application has been designed and implemented with the JAVA programming language by considering the characteristic specialties of mobile devices. First, the heart sound signals have been normalized to develop the application. After that, low and high pass filters of Butterworth, Chebyshev-II, and Elliptic were utilized to remove unwanted data from extra systole heart sounds. It is observed that Chebyshev-II and Elliptic filters are more successful in denoising. When all this is considered, Elliptic was selected for use in the mobile application because it has less runtime. After that, the features vector was obtained with wavelet transformation operation. Finally, Gentle Boost, Gradient Boosting, Neural Network, and K-Nearest Neighbors classification methods have been employed on mean, variance, covariance, standard deviation, maximum value, minimum value, median value, most frequent values, detail coefficients length of features. It was determined that the classification success of the developed application was 87%, according to error matrice. The application was presented to the opinions of cardiologists for evaluation.

Keywords – heart sound, murmur, classification, mobile application, gentle boost

INTRODUCTION

According to WHO (World Health Organization), heart diseases or cardiovascular diseases (CVD) are in first place among the causes of death worldwide. More than other reasons, most people lose their lives yearly because of heart disease. In 2004, nearly 17.1 million people died, representing 29% of all deaths; in 2015, nearly 17.7 million people, representing 31% of all global deaths, died due to heart diseases. Nevertheless, unfortunately, the number is expected to be 23.4 million in 2030 (Mathers and Loncar 2005). In Europe, heart disease creates 42% of all deaths, and expenditure for treatment of heart diseases is almost 192 billion € in total(Allender et al. 2008). Cardiovascular disease, listed as the underlying cause of death, accounts for nearly 801,000 deaths in the US. That is about 1 of every 3 deaths in the US. Direct and indirect costs of cardiovascular diseases and stroke are estimated to total more than $316 billion, including health expenditures and lost productivity in the US (AHA 2017). Early diagnosis of heart disease is crucial in treatment and is vital for preventing the disease. Heart sounds are one of the related basic medical techniques doctors use in diagnosis. Doppler ultrasonography and ECG (Electrocardiography) require time and expert knowledge. Auscultation is one of the primary medical information which doctors use. A Phonocardiogram (PCG) signal can be defined as recording the sounds resulting from these acts. Diseases arising from cardiac valves and auricles are detected through heart sounds instead of EKG. Mobile devices can be carried easily. Generally, they are not as highly equipped as laptops and desktops. Considering their features, methods with low hardware features are required to analyze and classify heart sounds quickly. In this context, a mobile application was developed to prepare the infrastructure for the clinical decision support system, which is planned to be developed quickly with information from other cardiac information. The workflow of the study is as follows. The Related Work section examines the studies on which methods are used in filtering, feature extraction, and classification in applications developed between 2010-2023. The materials section defines normal and murmured heart sounds, their symptoms, and the diseases they cause. In the Method section, the pre-processing and filtering methods are described in detail, and the shape of the filtering results is given. Frequency domain features as a feature extraction method are explained in detail. In this context, Gentle Boost and Gradient Boosting classification methods not used in the literature were chosen. The design and implementation section gives the application's development steps and flow chart. The results section gives the classification result of normal and murmur heart sounds on the figure and application screen. The classification of normal and murmur heart sounds on the mobile device is discussed in the discussion and

conclusion section. The comments of the physicians who tested the application were given and discussed in detail. The positive and negative aspects of the applications in this direction are explained in detail.

RELATED WORK

The analysis and processing of heart sound on mobile devices have shown parallelism with use in the widespread development of mobile device. Regarding studies in mobile heart sound applications, these apps focus on obtaining, monitoring, storing, sharing, analyzing heart sounds, and education about auscultation issues. Güraksın et al. (Güraksn, Ergün, and Deperlioğlu 2011) have classified heart sounds using ANN (artificial neural network) on a pocket computer that can run Windows OS. Shin et al., (Shin et al. 2013) have developed a stethoscope system that can record heart sounds and calculate heart rate from the sound based on a smartphone. Their proposed system has been designed to acquire the heart sounds using the iPhone or iPad apps, record the acquired data on a real-time basis, display the heart sounds in a graph, and allow listening to the acquired sounds. Springer et al., (Springer et al. 2014) have developed a mobile app for rheumatic heart disease. They have addressed signal quality classification, which achieved 90%, and heart sound segmentation with 93.5% F-score. Gradolewski (Gradolewski and Redlarski 2014) et al., have designed a wavelet-based denoising method that removed noises from PCG signals recorded by mobile devices in noisy environments. These noises have variable character; therefore, Gradolewski et al., have used Coif5 wavelet at the 10th decomposition level with the use of a mini maxi threshold selection algorithm and mln rescaling function. Grinchenko et al., (Grinchenko et al. 2014) have developed a mobile monitoring device for electronic auscultation, recording and sort in human life activity sounds which is obtained with stethoscope using special software on a smart phone. The information of patients can be transferred to central server over internet with this device. The stethoscope component has been developed based on electronic stethoscope EPhON-08. Amiri et al., (Amiri et al. 2015) have developed a diagnostic mobile app called PhonoSys to analyze PCG signal using Random Forest. In their study, PCG signals from 120 newborns who are either healthy or with cardiac abnormalities have been diagnosed by using PhonoSys. They used an electronic stethoscope connected to a mobile device in the data acquisition step and a 3rd order band-pass Butterworth filter with cut-off frequencies at 50-200 Hz to filter the original PCG in Pre-processing step. The sensitivity of classification for pathological murmur was 96.8% with a specificity of classification of 98.4%. Sinharay et al., (Sinharay et al. 2016) have developed digital stethoscope and its mobile app based on smartphone for poor or

developing countries where healthcare centers are scarce. Patients have to travel a long distance to visit the clinic. The motivation of this work is to enable the heart patients to send their heart sound to doctor's chamber/ hospitals from their home instead of traveling all the way to hospitals/clinics. The data files can also be sent to a server by using this app. Reynolds at al., (Reynolds et al. 2017) have developed a mobile app for testing an electronic stethoscope prototype which has been developed by themselves for recording PCG signal. Their app has been designed in order to denoise sound signal through Wavelet Filters. In the mobile app, denoising using Wavelet transform, orthogonal Daubechies 5 (db5) with a decomposition level 2 and a low pass IIR (Infinite Impulse Response) filter whit cut-off frequency of 1.5 KHz. Sulistyanto, (Sulistyanto 2016) has developed a mobile app in Android to classification of 40 PCG signal with tricuspid regurgitation, aortic valve stenosis. This app uses Fast Fourier Transform (FFT) to spectral analysis and Artificial Neural Network (ANN) for classification. The classification result has been obtained as a 97.5%. Bentley et al., (Deng and Bentley 2012) have developed an external hardware used to create iStetoscope. iStetoscope uses the combined output of iPhone's microphone, motion sensors and camera to get a much more accurate reading than a simple acoustic stethoscope, then it shows the heart's form on the iPhone's display. When the studies which are given above is examined, it will be seen that there is no any study towards the classification of murmur heart sound on mobile device using Gentle Boost and Gradient Boosting and Wavelet for feature extraction. Although all these studies and methods are used, the absence of a mobile app is remarkable in the context of the methods used in this study. Therefore, with the aim of contributing to heart sound classification studies, considering wide-spreading of mobile apps usable, it is seen that the requirement of develop a mobile app with the aim of classification of different heart sound types with different features extraction methods.

MATERIALS AND METHODS
Normal and Heart Sounds with Murmur

Heart sounds result from the vibrations of heart valves between auricle and ventricle. A normal heart sound is like the sounds "lub dub, lub dub" sounds. In medicine, "lub" is named as S_1 sound while "dub" sound is called as the S_2 sound. Every "lub dub" sound is one beat. Normal heart can have 60 - 100 beats in a minute. Figure 1.shows normal heart sound, S1, S2 parts and "lub dub" sound pattern.
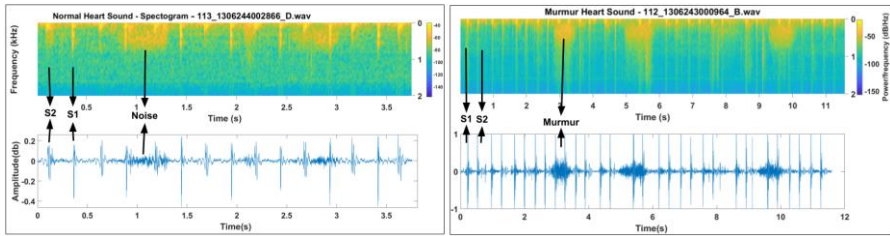
Figure 1: Normal heart sound S1, S2 sections (top) and heart sound with murmur (bottom)

Range between inception of S_1 and S_2 sounds are called as systole. Inception of S_2 sound and starting of the S_1 sound again is called as diastole. Systole range between S_1 and S_2 sounds in a normal heart follow the range of diastole between every beat. This situation is shown in
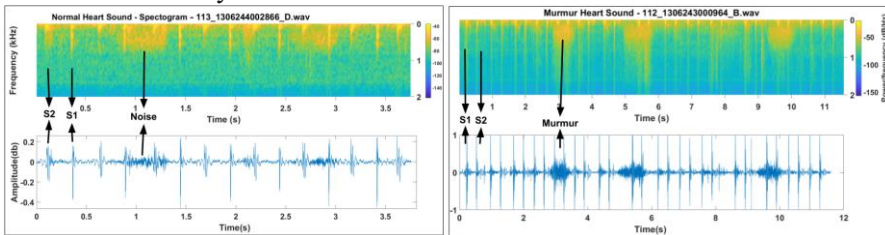
Figure 1 presenting heart sound diagram. Cardiac information in heart sounds includes low frequency ingredients. The frequency spectrum of a normal S1 sound is known to contain peaks in the low frequency range (10 to 50Hz) and mid-frequency range (50 to 140Hz) (Huiying, Sakari, and Iiro 1997). The frequency spectrum of a normal S2 sound is known to include peaks in the low frequency range (10 to 80Hz), mid frequency range (80 to 200Hz), and high frequency range (220 to 400Hz) (Rangayyan and Lehner 1987). Heart sounds are consisted of cardiac information besides various high frequency body noises. One of these sounds is murmurs. Heart murmurs are swishing or swishing sounds made by rapid, choppy blood flow in the heart (Pelech 1998). The murmurs are generally low frequency from 20 Hz- 150 Hz, on the contrary some murmurs may be as high as 500 Hz to 2000 Hz (Rennert, Morris, and Barrere 2004). Therefore, murmurs may occur along S1 and S2 or in the region between them. This situation is shown in Figure 1.

The Incidence of Murmurs in Humans
A heart murmur is caused by rapid, fluctuating blood flow in the heart. A heart murmur may occur in the following situations: When the heart fills with blood

(diastolic murmur), When your heart empties (systolic murmur), or throughout the heartbeat (continuous murmur) (Dijkema, Leiner, and Grotenhuis 2017). A harmless murmur usually occurs in a person with a typical heart. Innocent heart murmurs frequently occur in newborns and children (Frank and Jacobe 2011). Events that can cause a harmless heart murmur include: febricity, lack of healthy red blood cells (anemia), overactive thyroid, rapid growth stages of adolescence, intense physical activity or exercise, pregnancy. Harmless murmurs may disappear over time. Sometimes it can last a lifetime without causing serious health problems. Harmful murmurs may occur in children with congenital heart defects (Frank and Jacobe 2011). Heart valve problems in adults can cause harmful murmurs (Dijkema et al. 2017). Causes of noisy murmurs include holes in the wall or chamber of the heart, deformations occurring in heart shunts, and deformation of heart valves over time.

Preparing Dataset, Pre-processing & Filtering

It is observed that datasets consisting of biomedical data can generally be unbalanced due to the insufficiency of samples representing classes. It is inevitable to create unbalanced datasets in heart sound datasets, especially in rare cases such as murmurs and extra beats compared to normal beats. In dataset used in this study, there are two types of heart sounds including 200 normal, 66 murmured, these sounds were recorded by using Digiscope digital stethoscope (Deng and Bentley 2012). In order to create a balanced data set, data augmentation was made by using fewer murmur sounds and the number of heart sounds of both types was equalized.

During auscultation with an electronic stethoscope, sounds such as lung sound, body movement, and even environmental sounds mixed with heart sound make noise (Zhao, Shen, and Ren 2013). If these noises aren't extracted from heart sounds accuracy of features belonging to these sounds can be affected (Zhao et al. 2013). Hearty sounds must be normalized before extraction of the noise. Heart sounds were normalized with the statement in Equation-1(Sung et al. 2015).

$$x_{norm}[n] = \frac{x[n] - \min(|x[n]|)}{\max(|x[n]|) - \min(|x[n]|)} \tag{1}$$

If the studies of heart sound filtering and normalization is examined, it has been seen that different filtering methods such as Butterworth, Elliptic, Chebyshev, Bessel, wavelet, notch (band-stop) filter are applied on heart sound to remove unwanted sound (Aimukhanbetov et al. 2017; Malik et al. 2017; Strunic et al. 2007; Tsai and Chou 2012; Wang and Li 2016).
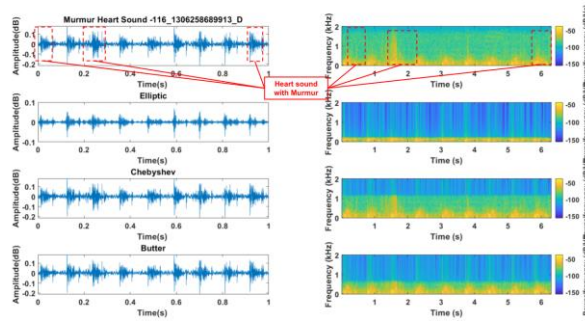
Figure 2: Heart sound with murmur, Elliptic, Chebyshev and Butter filtering results (right), spectrum of heart sounds after filtering (left)

It was noticed by Butterworth and Chebyshev-II are the best, fastest, and simple filters for extraction of noises from heart sounds (Cherif, Mostafi, and Debbal 2014; Coskun, Yigit, and Deperlioglu 2016; Smith and others 1997). The filter order has been selected as 10 degrees for all filter methods. The cut-off frequency is 50 Hz in Butterworth filter. The stopband attenuation is 30 db and stop band edge frequency is 50 Hz in Chebyshev-II filter. The peak-to-peak passband ripple is 0.1, stopband attenuation is 30 db and passband edge frequency 50 Hz for Elliptic filter. With the same values, Butterworth, Chebyshev-II and Elliptic filters within mobile program which developed in JAVA were applied to some murmur heart sounds in heart sounds data base. In Figure 2, it is observed that Chebyshev and Elliptic filters are more successful in denosing. In Figure 2, noise extraction was shown with red arrow mark. Taking into consideration all of the obtained data and, Elliptic was selected to be used in the mobile application. In Figure 2, it can be seen that the yellow regions in the spectrum graphs represent heart sounds (S1, S2). Green areas represent noisy sounds. In the filtering results, it is seen that the green regions disappear, and the blue regions appear. These results visually demonstrate that noisy sounds are separated from heart sounds.

Feature Extraction

For any class of data that will be classified in classification applications, differentiating features peculiar to the related class should be used to allow class members to bunch in their own regions. These features are called as attributes. The feature extraction aims to transform data into data series with lower dimensions representing the data or decreasing calculation processes (Phua et al. 2008). In the classification method, the feature extraction process that yielding the smallest class diameter and the biggest distance among classes should be found. In digital sound classification processes selection of attribute data series,

which belongs to time and frequency characteristics of the signal, is important for finding a high-level accuracy value (Liang et al. 2005). With Fourier Transform (FT) the signal is differentiated into complex exponential functions that have different frequencies. The frequency resolution is gained with FT very well, but no time resolution is gained for non-continuous signals (Chen et al., 2020). Because of this, it cannot be determined that which frequency component is in the given time interval. Although Short-term Fourier Transform (STFT) somewhat compensates for this deficiency, the resolution problem related to window width is a negative aspect of this method (Say et al., 2002). Because, in some cases the window width should be changed in order to gain a more detailed resolution. If a window with narrow dimensions is used a poor frequency resolution will be gained. With increasing window dimensions, the frequency resolution improves but the time resolution became worsen (Say et al., 2002). Because the window dimensions are fixed in STFT, an attribute vector cannot be gained at requested precision. Wavelet transform is a technique that can separate sound signals into different frequency data and represent every data in its resolution at its scale (Zhang et al. 2001). Wavelet transform of a signal, a function of time, is related to frequency and time variables. Wavelets provide a more precise transform technique for time frequency analysis. The ability of wavelet transforms which is for carrying out variable window dimensioning as it is wide for low frequencies and narrow for high frequencies for time-frequency analysis of continuous signal shows its superiority on other methods (Daubechies 1990). Continuous Wavelet Transform (CWT) calculates the integral for total period of values that are gained by multiplication of main wavelet with values gained by offsetting and scaling of main wavelet. CWT also can be defined as the transformation that scaling and offsetting variables which take continuous values. As a result of this calculation wavelet coefficients according to time placement and scale value are calculated. Because calculation load is excessive in CWT, calculation efficiency gets lower and operation time gets longer. CWT can be expressed mathematically as follows:

$$\psi_{a,b}(t) = \frac{1}{\sqrt{a}} \, \psi\left(\frac{t-b}{a}\right) \tag{2}$$

In Equation-2, if $a > 0$, $a, b \in \mathcal{R}$, a shows scaling variable, b shows transform variable, $x(t)$ shows the value of signal at time t, ψ shows wavelet function (main wavelet), $1/\sqrt{a}$ shows normalisation factor and finally $W(a, b)$ shows wavelet transform of the signal. In Discrete Wavelet Transform (DWT) the variables of scaling and offsetting takes discrete values. So, better

calculation efficiency can be attained by analysing the signal in defined scales and in this way, results as correct as results of CWT can be gained. In DWT, offsetting and scalings are performed by using powers of two and dyadic wavelet transform is gained. Discrete Wavelet Transform is expressed as follows:

$$\psi_{j,k}(t) = 2^{-\frac{j}{2}} \psi\left(2^{-j}.t - k\right) \tag{3}$$

In Equation-3, if $a = 2^j$, $b = k.2^j = k.a$, $j, k \in Z^2$, j and k are scaling and transform integers, respectively. DWT functions form an orthogonal group. DWT coefficients are calculated by this mathematical expression (Mahmoodabadi et al. 2006).

$$c_{j,k} = 2^{j/2} \int_{-\infty}^{\infty} f(x).\psi\left(2^j x - k\right) dx \tag{4}$$

DWT signals should gradually be separated into high and low frequencies (Mallat 1999). In order to calculate changes with high frequency in sound signal, it is filtered through high pass filters and detail coefficients are calculated. In order to calculate changes with low frequency, approximation coefficients are calculated by using low pass filters.

$$cA_n = y_{high}[k] = \sum_{n=-\infty}^{\infty} x[n].g[2k - n] \tag{5}$$

$$cD_n = y_{low}[k] = \sum_{n=-\infty}^{\infty} x[n].h[2k - n] \tag{6}$$

In order to separate the signal into different frequency divisions, level approximation and detail coefficients are gained according to k steps, by taking the power of $x[n]$ in Equations 5 and 6 by high pass and low pass filters consequently. For $k = 1$, first level approximation coefficients (cA$_1$) represent the high scale and low frequency components of the signal. First level detail coefficients (cD$_1$) represent the low scale high-frequency components of the signal. Because after the first level filtering the highest frequency in the signal will be $\pi / 2$ instead of π after the first level filtering, according to Nyquist criteria half of the samples in the signal can be eliminated according to Nyquist criteria.
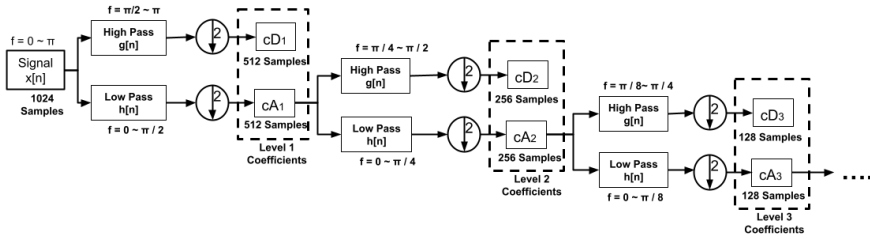
Figure 3: Wavelet tree, approximation and detail level coefficients

Because of this, the signal is applied down-sampling with 2 as seen in Figure 3. Assuming that the starting signal has 1024 samples and a component of 1000 Hz at most, all frequencies above 500 Hz will be terminated by using low pass filter as defined in the Equation 6. After this process, value of the highest frequency decreased by half, half of the samples, which are 512, in the signal are deleted and omitted. Number of the samples is halved. Because half of the frequencies are deleted by low pass filtering, as a result of down-sampling scale doubles, the resolution is decreased by half due to down-sampling scale doubles. As a result, the detail coefficients produced are smaller and as they are formed by high pass filtering, they are unnecessary coefficients with high frequency. Approximation coefficients formed by low pass filtering are smaller than original signal and have the values that can almost represent the original signal (Mallat 1999). The level number of separations into coefficients is determined by k in $2k$ expression in the Equation 5 and 6. If the signal processed has 1024 value, tenth level coefficients of the signal can be gained at most, because 210 equals 1024. If two filter outputs at the same separation level are added by applying up-sampling to the signal and filtering through combination filters, original $x(n)$ signal will be gained. A signal that wavelet transform is applied can be formed again from wavelet coefficients. Because of this, it is assumed to be a more effective method in data compression, noise removal and attribute extraction.

Figure 4: Normal heart sound and wavelet detail coefficients

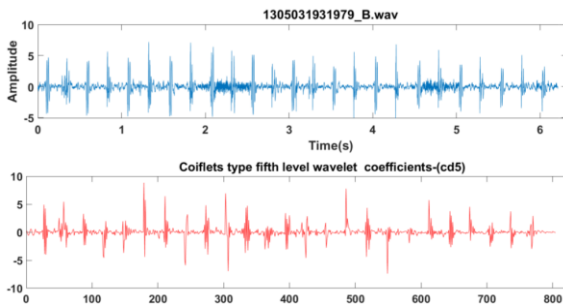Although there is no definite information as to which wavelet type should be used in literature, while selecting wavelet type that was wanted to use on signal, the similarity of signal and wavelet type is considered generally. Therefore, coiflets wavelets have been chosen which is the most similar to heart sound. The coiflets type fifth level wavelet coefficients (cD5) have been used or feature extraction. Basic statistical features were extracted from the obtained detail coefficients. The statistical features are following mean value, variance, covariance, standard deviation, maximum value, minimum value, median value, most frequent values, detail coefficients length. The coif5 type sixth level wavelet detail coefficients (cD_5) obtained with the developed mobile application; original heart sound signal (s) are presented in Figure 4.

Classification Algorithms

Gentle Boost, K-Nearest Neighbors (KNN), Gradient Boosting, and Neural Network (NN) methods, frequently used classifiers in this context in the literature, were preferred to classify the created features. Since a mobile application was developed in this book chapter, the theoretical dimension of the classification methods is not explained in detail. Since classification methods are thought to be helpful in adapting algorithms to software, it is thought that it would be better to present the algorithms instead of their theoretical dimensions. Gentle Boosting is a boosting algorithm. It is an ensemble learning technique that combines the predictions of multiple weak learners (usually decision trees or stumps) to create a strong learner. In Gentle Boosting, each data point in the training set is assigned a weight that reflects its importance. All data points are initial equal weights (El Morr et al. 2022). After each round of training, the weights of the misclassified data points are increased, while the weights of the correctly classified points are decreased. Each weak learner's contribution to the final prediction is weighted based on its performance during the final prediction. Weak learners that perform well are given more influence in the final prediction (Vinod and Rao 2020). Gentle Boosting introduces an adaptive learning rate, which controls the contribution of each weak learner. This adaptive learning rate ensures that the boosting process is gentler and less aggressive than standard AdaBoost. It helps prevent overfitting and can make the algorithm more robust. Gentle Boosting aims to find a "soft margin" solution for the classification problem, which means it tolerates some misclassification of data points to avoid overfitting. Like other boosting algorithms, Gentle Boosting trains weak learners sequentially. In each round, it focuses on the data points that were misclassified in the previous round.

The Gentle Boost algorithm was first proposed by Friedman et al (Friedman, Hastie, and Tibshirani 2000). It incorporates the features of AdaBoostM1 and LogitBoost. Gentle Adaboost is a modified version of the Real AdaBoost algorithm. It uses a weighting scheme that utilizes a margin function that decays more slowly than the exponential function used by the Adaboost algorithm. There is a substantial similarity between updating the weights of the Gentle AdaBoost algorithm and updating the LogitBoost algorithm. The loss function measures how well a model fits each training example in the data set. Gentle Adaboost minimizes the exponential loss function of Adaboost using Newton steps (Friedman et al. 2000). However, its numerical optimization is tuned differently. Like LogitBoost, each weak learners fits a regression model to the response values $y_n \in \{-1, +1\}$.

For an N-dimensional Z dataset, while
$Z = \{z_1, z_2, \ldots\ldots., z_N\}$ with $z_i = (x_i, y_i)$,
$x_i \in X$ and $y_i \in \{-1, +1\}$
assuming, $Z = (x_1, y_1), (x_2, y_2), (x_3, y_1), (x_4, y_1), \ldots\ldots (x_i, y_i)$,
$i = 1,2,3\ldots, N$ and weights
$W_t(i) = \{ w \mid 1/n \}$ and $F(x) = 0$,

Gentle Boost algorithm is presented in Figure 5 (Zhang and Ma 2012). The Gentle AdaBoost Algorithm is currently considered the most successful boosting algorithm due to its stability and robustness to noisy data.

REPEAT $t = 1, \ldots T$

1) Fit the regression function $F_t(x)$ by weighted least-squares of y_i to x_i with weights $w_t(i)$.
2) UPDATE $F(x) \leftarrow F(x) + F_t(x)$.
3) SET $w_t(i) \leftarrow w_t(i) \exp(-y_i f_t(x_i))$ and renormalize to $\sum_t^\square w_t = 1$.

OUTPUT $sign[F(x)] = sign[\sum_t^T F_t(x)]$.

Figure 5: GentleBoost algorithm

Gradient Boosting is a powerful ensemble learning algorithm widely used in machine learning for classification and regression tasks. It builds an ensemble of decision trees sequentially, where each tree corrects the errors made by the previous ones. Gradient Boosting is a boosting algorithm that combines the predictions of multiple weak learners (typically decision trees) to create a strong learner (Saupin 2022). Unlike bagging methods like Random Forest, boosting methods focus on improving the model iteratively. Gradient Boosting trains decision trees sequentially. It starts with a single decision tree, and each

subsequent tree is trained to correct the errors (residuals) of the previous trees. This leads to a reduction in the overall prediction error. The "Gradient" in Gradient Boosting refers to using gradient descent optimization to minimize the loss function. It optimizes the model's parameters by moving toward steepest descent in the loss function space. Gradient Boosting allows flexibility in choosing different loss functions depending on the problem, such as mean squared error for regression and deviance (logarithmic loss) for classification. The choice of the loss function influences the algorithm's behavior (Vandeput 2021). Gradient Boosting introduces a learning rate hyperparameter that controls the contribution of each tree to the final prediction. Lower learning rates result in more robust models but require more trees for the same performance. Gradient Boosting can provide insights into feature importance by analysing how much each feature contributes to reducing the loss function. This can help in feature selection and understanding the dataset. Gradient Boosting is a boosting algorithm based on loss function gradients. The gradient of the loss function for a single sample is called the residual. Briefly, it represents the capture error between the correct and predicted labels (Friedman 2001). This error or residual measures the amount of misclassification; unlike AdaBoost, which uses weights instead of residuals, gradient boosting uses these residuals directly. Therefore, gradient boosting is considered another sequential ensemble method that aims to train weak learners on residuals (i.e., gradients) (Kunapuli 2022). For an N-dimensional Z dataset, while $Z = \{z_1, z_2, \ldots \ldots, z_N\}$ with $z_i = (x_i, y_i)$, $x_i \in x$ and $y_i = -g_m(x_i)$ assuming $\psi(y, f)$ is loss-function and $h(x, \theta)$ base-learner model. Gradient Boosting algorithm is presented in Figure 6 (Friedman 2001; Natekin and Knoll 2013).

SET $F_0(x) = 0$
REPEAT $t = 1, \ldots. T$
  1) Compute gradient $-gt(x)$
  2) Fit a new base-learner
$$a_m = argmin_{a,\beta} \sum_{i=1}^{N} [-g_t(x) - \beta h(x_i; a)]^2$$
  3) Find the best gradient descent step-size
$$\rho_t = argmin_p \sum_{i=1}^{N} \psi[y_i, F_{t-1}(x_i) + \rho h(x_i; a_m)]$$
  4) Set the function estimate
$$F_m(x) \leftarrow F_{m-1}(x) + \rho_m h(x; a_m)$$
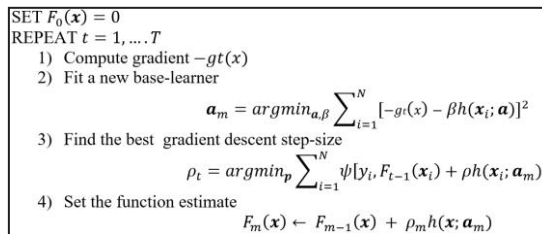
Figure 6: Gradient Boosting algorithm

Since boosting algorithms are based on decision trees, in this algorithm, $h(x; a_m)$ is a small regression tree, for a regression tree the parameters a_m are the splitting variables, locations, and the terminal node means of the individual trees. Steepest descent which represents ρ_t is one of the simplest of the frequently used numerical minimization methods. (Friedman 2001). Gentle Boosting and

Gradient Boosting are both ensemble learning techniques that aim to improve predictive performance by combining the outputs of weak learners, typically decision trees, but they differ in their approach. Gentle Boosting employs an adaptive learning rate and a soft-margin philosophy, making it more resilient to noisy data and outliers, and iteratively corrects errors cautiously (Vinod and Rao 2020). On the other hand, Gradient Boosting, including algorithms like XGBoost and LightGBM, optimizes model parameters using gradient descent, iteratively fitting decision trees to minimize a specified loss function, often leading to higher predictive accuracy but at the cost of increased computational complexity and sensitivity to noisy data. KNN is a simple and intuitive machine-learning algorithm for classification and regression tasks. KNN is based on the principle that similar data points tend to belong to the same class or have similar values. It's a non-parametric and instance-based learning algorithm, so it does not make assumptions about the underlying data distribution. The "K" in KNN represents the number of nearest neighbors to consider when making a prediction (Kramer 2013). For classification, KNN finds the K data points closest to the new data point in the training set and assigns the class label that occurs most frequently among those neighbors. For regression, it averages the target values of the K nearest neighbors to predict the target value for the new data point. KNN relies on a distance metric (e.g., Euclidean distance) to measure the similarity between data points. The choice of distance metric can significantly impact the algorithm's performance. The choice of the value of K is a critical hyperparameter in KNN. A small K can make the algorithm sensitive to noise. In contrast, a large K can make it less sensitive but potentially introduce bias (Kramer 2013). KNN is considered a "lazy learner" because it does not build an explicit model during training. Instead, it memorizes the entire training dataset and performs computations at prediction time. KNN can be computationally expensive, especially with large datasets, as it requires computing distances to all training samples for each prediction. KNN is instance-based, using the entire training dataset during prediction (Rhys 2020). In contrast, model-based algorithms, like decision trees or neural networks, build explicit models during training. Neural networks, also known as artificial neural networks (ANNs), are a class of machine learning algorithms inspired by the structure and functioning of the human brain. They have gained immense popularity for their ability to solve complex problems in various domains. Neural networks use a feedforward mechanism to make predictions or classifications and backpropagation to update the model's weights during training. Backpropagation minimizes a specified loss function by adjusting the network's parameters through gradient descent. Each artificial neuron in a neural network applies an activation function to the weighted sum of

its inputs. Common activation functions include the sigmoid, hyperbolic tangent (tanh), and rectified linear unit (ReLU). Since KNN and Neural Network methods represent 2 different machine learning approaches, they were used for comparison purposes to evaluate these boosting classification methods. For the Gentle Boost algorithm, parameter values of learner type, decision tree, maximum number of splits, 5, the number of learners, 800, and learning rate 0.05 were used. For the Gradient Boosting algorithm, the number of trees, 150, limit depth individual tree, 5, minimum subset size, 3, number of learners, 800 and learning rate 0.05 parameter values were used. For the KNN algorithm, the number of neighbors, 10, distance metric, Euclidean, distance weight, 3, Squared inverse and data standardization parameter values were used (Coskun 2023). The NN has nine inputs, one-hundered hidden layers, two-hundered neuron in hidden layers and two output layers. Data division feature random, training function scaled conjugate gradient (SCG), Levenberg-Marquardt optimization method, and cross-entropy are used in the networks. The activation function is ReLU, and 500 the maximal number of iterations were used to train. The error goal has been limited to 0.001 (Coskun, Deperlioglu, and Yigit 2017a, 2017b; Coskun and Yigit 2018). The weights and biases are initialized using the Nguyen-Widrow method. For all classifiers, 15% of the data was used as validation and test data. The training model has been tested with data not previously used in training. Therefore, test data is entirely different from training data. All models were validated through a 5-fold cross-validation process to evaluate the predictive ability as it allows the classifier to operate without bias and avoids the overfitting problem. The cross-validation was performed without data sharing between training and validation data to avoid overtraining. In order to measure the performances of each model, a multi-class confusion matrix which is defined in (Coskun et al. 2022) and the ROC curve, is created, and Accuracy (A), Recall (R), precision (P), F1-score (F), Balanced Accuracy, AUC (Area Under Curve), and Specificity (S) indicators are calculated to evaluate performance (Coskun et al. 2022).

IMPLEMENTATION

In this study, an application was developed for mobile devices in order to distinguish murmur-patterned heart sounds and normal heart sounds. As the first step, recorded heart sounds of different lengths were rearranged on the same length for making classification over these heart sounds. In the training data file, nine data are in each line. These columns carry the statistical attribute values obtained in the attribute phase.
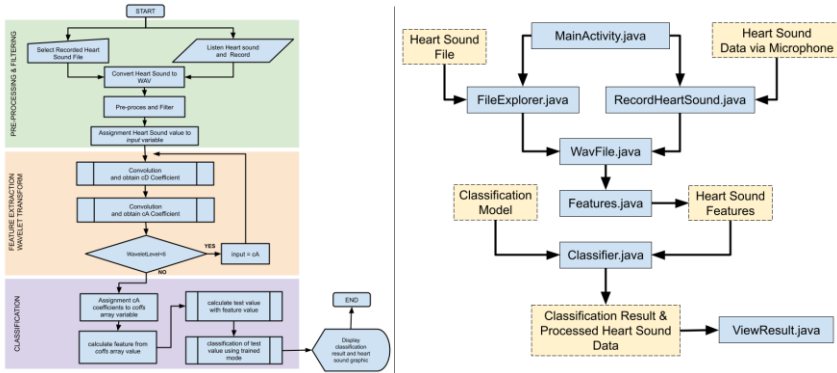
Figure 7 Flowchart of mobile application working (left), working architecture of application code file (right)

Also, the variety of heart sounds which was categorized was done physically to give more information about the process. Flow chart belonging to the application was given in the Figure 7. It has been aimed to use the application in many mobile devices. Therefore, I was planned the development of the mobile application is on the Android operating system in order to make it usable by more people because Android operating system is used in approximately 85% of mobile devices around the world according to Strategy Analytics and Statica (Statcounter Global Stats 2023; Statista 2023). The programming language of the mobile application is selected as JAVA because it will be used in devices which have Android™ operating system and it is most used programming language across the world (Github 2023). Basic working architecture of code files of JAVA, belonging to the application are shown in the Figure 7 . Source codes files in performance architecture of the application and their basic functions are explained in.

Table 1: Application code files and their functions

File Name	Function
MainActivity: It is code file related to the home screen of the application. It includes codes for selecting recorded heart sounds file or codes in which processes of recording heart sounds take place.	
FileExplorer: It includes recorded heart sounds or codes used for selecting heart sounds process in the data set of heart sounds. The application controls the selected files such as WAV (Waveform Audio File Format). It sends the address of the selected file to WavFile class.	
RecordHeartSound: It allows recording heart sounds via microphone of the mobile device. Heart sounds are recorded on 44100 sampling rate and channelled WAV file in dual as Stereo type. It sends the address of recorded file to WavFile class.	
WavFile: It allows reading recorded sounds as WAV and sends the data belonging to files it read in the class of Analyser.	
Features: It approves pre-treatment on the purpose of classification of sounds data belonging to sounds file in WAV format. It enables Filtering and Wavelet transform. Also, it obtains data related to attribution and it sends the attribution data to the Classifier for classification.	
Classifier: It allows classifying the features with Classifier Model. Then it sends the obtained result and processed data of the sound to the class: ViewResult	
ViewResult: It includes the result of heart sound classification and graphical display.	
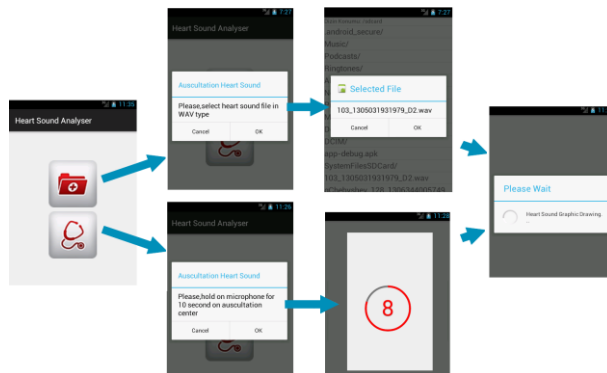
Figure 8: Interface of listening heart sound (bottom) and selection of recorded heart sound (top)

With this application the users can distinguish heart sounds or record them via microphone of the mobile device as pushing stethoscope signal within 10 seconds. The mobile app interfaces for recorded heart sounds and listening of heart sounds and operation steps are presented in Figure 8.

RESULTS AND DISCUSSION

The results are discussed under the headings of measuring classification performance and using the mobile application.

Classification

The distribution of training data is given in Figure 9.
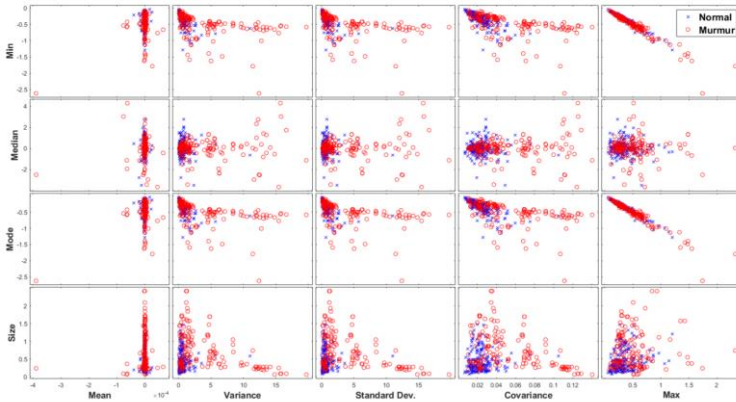
Figure 9: Features distributions

When the distribution of the data is examined, it is seen that they overlap each other for all attributes. In this respect, it can be seen that the problem that is the subject of the study is a problematic classification problem.
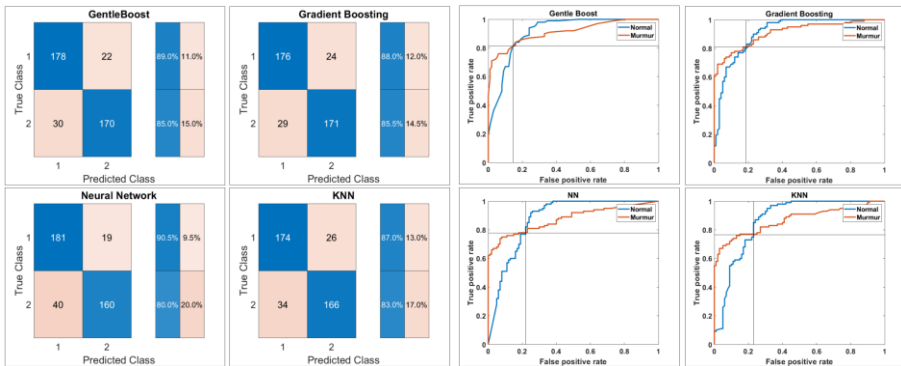
Figure 10: Confuison matrices (left) and ROC curves of models (right)

It can be seen that the most discriminative features are variance, covariance, and maximum value. For the classification of heart sounds, confusion matrices for all models are presented in Figure 10.When the confusion matrices are examined, it is seen that the samples are mainly classified according to their classes. When the classification performance metrics in Figure 11 are examined,

it is seen that all the algorithms show close classification performance, and the Gentle Boost algorithm has the best values.
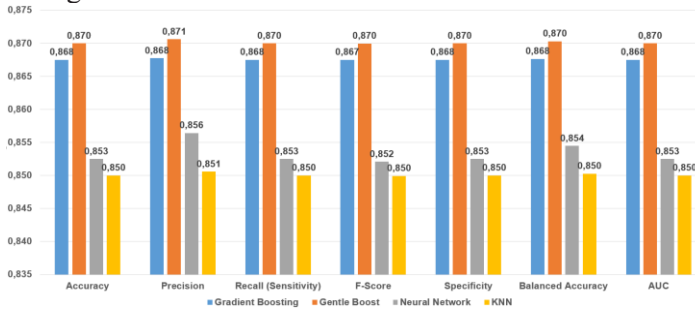
Figure 11: Classification performance analysis

The ROC curves belonging to the models with the highest accuracy values for evaluating the accuracy values are presented in Figure 10 . The earliest and shortest approach is in the Gentle Boost algorithm. When the ROC graphs are examined, it is seen that all models approach the upper left corner point (0,1). In addition, the fact that the murmur class samples approach the (0,1) point first compared to the normal class samples in all models is a supporting indicator that the model accuracies are qualified. It can be said that the results in the ROC chart is evidence of the accuracy values obtained by the models.
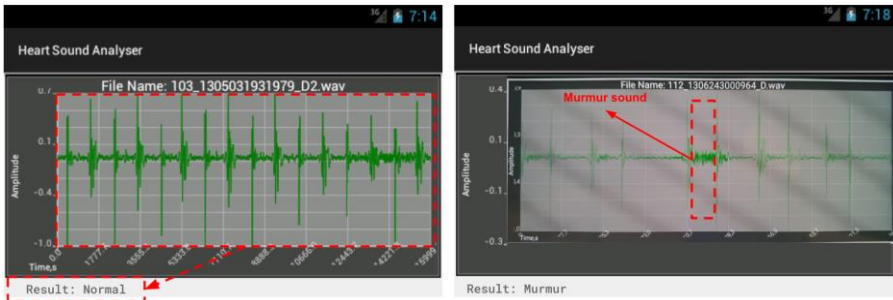
Figure 12: Interface of the graphical display of heart sound and classification results, normal (left), murmur (right)

Mobile Application

Selected or acquired heart sound records are classified using Features and the Classifier classes. Moreover, the classification results are shown on the screen. The graphical display and result on the classification interface are given in Figure 12. The Application's work order done via microphone and stethoscope was given in Figure 13, In Figure 13-a and Figure 13-b, Dark EvoPad T7016 tablet and Samsung Note 4 model smart phone was used respectively. The Android 4.0.3 and 5.1.1 version is working on these devices respectively. It has been observed that the application works in different versions of Android operating

systems. It would be understood that the app can be used in both cheap and expensive mobile device. The microphone box (MB) has been used to connect microphone and stethoscope pipe.
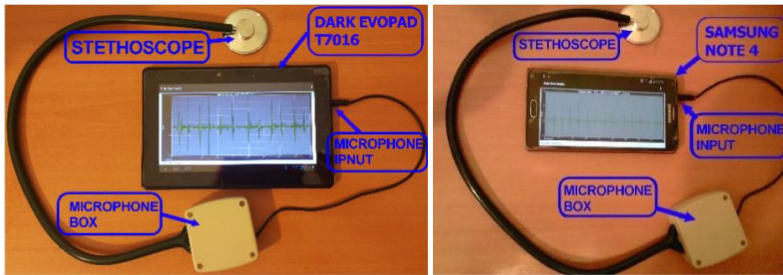
Figure 13: Working system of application on tablet (left), Working system of application on mobile phone (right)

It has been designed to make soundproof insulation of microphone in stethoscope pipe. There are materials which have soundproof feature inside it. The materials consist of acoustic foam. The more successful classification results have been gained in the auscultation experiments which have been used MB.

Cardiologists' Comments and Suggestion

Also, the physicians' who works in Uşak State Hospital views about app have been collected. The physicians' views have been discussed in discussion section.

#1: The app is practical. The usage of the app is easy and faster, not complicated. It will be better if there are more functions of the app. There are just display, record and classification. There should be feature as segmentation, sharing, recording of heart sound graphics and storing basic patient information. (Male-44 years old)

#2: The usage of the app is easy generally and it is fairly usable for initial study. There should be a classification feature of other heart diseases. Because a physician will not use this app for only one heart disease which it is non-critical. The app must instant visualization not offline or visualization after recording. (Female-38 years old)

#3: The application caught my attention. But I think recognizing only murmurs and normal heart sounds is good for a start. But in addition, it would be better to have a magician who combines characteristics such as age, gender, etc. in order to reveal the causes of the murmur sound. The application seems open to development. (Male-36 years old)

#4: It is insufficient for the application only to classify murmur and normal heart sounds. A physician may not want to use the application just to classify

these sounds. It would be better to have features that analyze heart rate, S1, S2 segmentation and their number. Considering its recognition rate and features, I can say that it is a positive but generally inadequate application for the beginning. (Female-48 years old)

CONCLUSION AND FUTURE WORKS

A mobile application has been developed for the use of cardiologists or ordinary person who doubt themselves for the early diagnosis of heart sounds containing murmur. Thanks to the developed mobile application recorded heart sounds can be classified as heart sounds recorded by microphone of the mobile device or heart sounds recorded by an electronic stethoscope. Compared to similar mobile applications based on heart sound analysis and provided in Android application shop, the developed mobile application is practical; it comes into prominence with its simple interface and usage. Thus, it can be used both by normal users and doctors.   Thanks to this mobile application, the following operations can be done:

- storing and monitoring of heart sounds,
- classification of heart sounds that are external recorded and can be listened to instantly from certain listening centers,
- graphical display of classification results belonging to murmur heart sounds.

In this study, Gentle Boost, Gradient Boosting, Neural Network and KNN methods have been utilized to classification. The different machine learning methods to comparison of them can be tried to better classification results. Furthermore, if some physician's views are considered, new features can be added to the app such as segmentation, sharing and instant visualization. Also, the option can be added to select different filtering, feature extraction and classification methods for furthering the app and to get better classification results. Thus, the heart sound will be able to segment easily, and the segmentation of heart sound will become more observable. Besides, if developed mobile applications can share the recorded voices and the classification results over the internet, evaluating the results of these records by the physician will be much easier. Thus, the heart sounds result of someone using application will be evaluated by physicians before going to the hospital.

REFERENCES

AHA. 2017. "heart disease and Stroke Statistics 2017 At-a-Glance."

Aimukhanbetov, Erzhan A., Erkebulan S. Kunesbekov, Maulenbek T. Abdulkhairov, Daulen N. Koishybaev, and Aidana S. Kyzdarbekova. 2017. "Development of a Channel for Recording Phonocardiograms in Electronic Stethoscopes." Pp. 355–59 in *2017 International Conference" Quality Management, Transport and Information Security, Information Technologies"(IT&QM&IS)*.

Allender, Steven, Peter Scarborough, Viv Peto, Mike Rayner, Jose Leal, Ramon Luengo-Fernandez, and Alastair Gray. 2008. "European Cardiovascular Disease Statistics." *European Heart Network* 3:11–35.

Amiri, Amir Mohammad, Giuliano Armano, Amir Mohammad Rahmani, and Kunal Mankodiya. 2015. "PhonoSys: Mobile Phonocardiography Diagnostic System for Newborns."

Chen, Y., Wei, S., & Zhang, Y. (2020). Classification of heart sounds based on the combination of the modified frequency wavelet transform and convolutional neural network. *Medical & Biological Engineering & Computing*, *58*, 2039–2047.

Cherif, L. Hamza, M. Mostafi, and S. M. Debbal. 2014. "Digital Filters in Heart Sound Analysis." *International Journal of Clinical Medicine Research* 1(3):97–108.

Coskun, Huseyin. 2023. "Human Sitting Postures Classification Based on Angular Features with Fuzzy-Logic Labeling." Pp. 611–19 in *International Conference on Applied Engineering and Natural Sciences*. Vol. 1.

Coskun, Huseyin, Omer Deperlioglu, and Tuncay Yigit. 2017a. "Ekstra Sistol Kalp Seslerinin MFKK Öznitelikleriyle Yapay Sinir Ağlari Kullanilarak Siniflandirilmasi." *2017 25th Signal Processing and Communications Applications Conference, SIU 2017*. doi: 10.1109/SIU.2017.7960252.

Coskun, Huseyin, Omer Deperlioglu, and Tuncay Yigit. 2017b. "Implementation of Wavelet Transform Extrasystole Heart Sound with Convolution Method for Feature Extraction." in *2017 25th Signal Processing and Communications Applications Conference, SIU 2017*. Institute of Electrical and Electronics Engineers Inc.

Coskun, Huseyin, and Tuncay Yigit. 2018. "Artificial Intelligence Applications on Classification of Heart Sounds." Pp. 146–83 in *Nature-Inspired Intelligent Techniques for Solving Biomedical Engineering Problems*. IGI Global.

Coskun, Huseyin, Tuncay Yigit, and Omer Deperlioglu. 2016. "Effect of Filter Selection on Classification of Extrasystole Heart Sounds via Mobile Devices." Pp. 1–5 in *2016 IEEE 10th international conference on application of information and communication technologies (AICT)*.

Coskun, Huseyin, Tuncay Yiğit, İsmail Serkan Üncü, Mevlüt Ersoy, and Ali Topal. 2022. "An Industrial Application Towards Classification and Optimization of Multi-Class Tile Surface Defects Based on Geometric and Wavelet Features." *Traitement Du Signal* 39(6):2011–22. doi: 10.18280/TS.390613.

Daubechies, Ingrid. 1990. "The Wavelet Transform, Time-Frequency Localization and Signal Analysis." *IEEE Transactions on Information Theory* 36(5):961–1005.

Deng, Yiqi, and Peter J. Bentley. 2012. "A Robust Heart Sound Segmentation and Classification Algorithm Using Wavelet Decomposition and Spectrogram." Pp. 1–6 in *Workshop Classifying Heart Sounds, La Palma, Canary Islands*.

Dijkema, Elles J., Tim Leiner, and Heynric B. Grotenhuis. 2017. "Diagnosis, Imaging and Clinical Management of Aortic Coarctation." *Heart* 103(15):1148–55. doi: 10.1136/HEARTJNL-2017-311173.

Frank, Jennifer E., and Kathryn M. Jacobe. 2011. "Evaluation and Management of Heart Murmurs in Children." *American Family Physician* 84(7):793–800.

Friedman, Jerome H. 2001. "Greedy Function Approximation: A Gradient Boosting Machine." *The Annals of Statistics* 29(5):1189–1232.

Friedman, Jerome, Trevor Hastie, and Robert Tibshirani. 2000. "Additive Logistic Regression: A Statistical View of Boosting (With Discussion and a Rejoinder by the Authors)." 28(2):337–407. doi: 10.1214/AOS/1016218223.

Github. 2023. "The Top Programming Languages." Retrieved September 13, 2023 (https://octoverse.github.com/2022/top-programming-languages).

Gradolewski, Dawid, and Grzegorz Redlarski. 2014. "Wavelet-Based Denoising Method for Real Phonocardiography Signal Recorded by Mobile Devices in Noisy Environment." *Computers in Biology and Medicine* 52:119–29.

Grinchenko, Victor, Alexander Artemiev, Anatolii Makarenkov, Anastasiia Makarenkova, Valery Oliynik, Rustam Nabiev, Oleg Gurenko, Vladymyr Gnateiko, and Anna Glazova. 2014. "Mobile End-User Solution for System of Monitoring of Respiratory and Cardiac Sounds." Pp. 299–302 in *2014 IEEE 34th International Scientific Conference on Electronics and Nanotechnology (ELNANO)*.

Güraksn, Gür Emre, Uçman Ergün, and Ömer Deperlioğlu. 2011. "The Analysis of Heart Sounds and a Pocket Computer Application via Discrete Fourier Transform." *Fourier Transforms: New Analytical Approaches and FTIR Strategies*.

Huiying, Liang, Lukkarinen Sakari, and Hartimo Iiro. 1997. "Heart Sound Segmentation Algorithm Using Wavelet Decomposition and Reconstruction." *Annual International Conference of the IEEE Engineering in Medicine and Biology - Proceedings* 4:1630–33. doi: 10.1109/IEMBS.1997.757028.

Kramer, Oliver. 2013. *Dimensionality Reduction with Unsupervised Nearest Neighbors*. Springer.

Kunapuli, Gautam. 2022. *Ensemble Methods for Machine Learning* . Manning Publications.

Liang, Bai, Hu Yaali, Lao Songyang, Chen Jianyun, and Wu Lingda. 2005. "Feature Analysis and Extraction for Audio Automatic Classification." Pp. 767–72 in *2005 IEEE International Conference on Systems, Man and Cybernetics*.Vol. 1.

Mahmoodabadi, S. Z., A. Ahmadian, M. D. Abolhasani, M. Eslami, and J. H. Bidgoli. 2006. "ECG Feature Extraction Based on Multiresolution Wavelet Transform." Pp. 3902–5 in *2005 IEEE Engineering in Medicine and Biology 27th Annual Conference*.

Malik, B., N. Eya, H. Migdadi, M. J. Ngala, R. A. Abd-Alhameed, and J. M. Noras. 2017. "Design and Development of an Electronic Stethoscope." Pp. 324–28 in *2017 Internet Technologies and Applications (ITA)*.

Mallat, Stéphane. 1999. *A Wavelet Tour of Signal Processing*. Elsevier.

Mathers, Colin D., and Dejan Loncar. 2005. "Updated Projections of Global Mortality and Burden of Disease, 2002-2030: Data Sources, Methods and Results." *Geneva: World Health Organization* 10.

El Morr, Christo., Manar. Jammal, Hossam. Ali-Hassan, and Walid. EI-Hallak. 2022. *Machine Learning for Practical Decision Making : A Multidisciplinary Perspective with Applications from Healthcare, Engineering and Business Analytics*. Springer.

Natekin, Alexey, and Alois Knoll. 2013. "Gradient Boosting Machines, a Tutorial." *Frontiers in Neurorobotics* 7(DEC):63623.

Pelech, A. N. 1998. "THE CARDIAC MURMUR: When to Refer?" *Pediatric Clinics of North America* 45(1):107–22.

Phua, Koksoon, Jianfeng Chen, Tran Huy Dat, and Louis Shue. 2008. "Heart Sound as a Biometric." *Pattern Recognition* 41(3):906–19.

Rangayyan, Rangaraj M., and Richard J. Lehner. 1987. "Phonocardiogram Signal Analysis: A Review." *Critical Reviews in Biomedical Engineering* 15(3):211–36.

Rennert, Nancy J., Rebecca Morris, and Candice C. Barrere. 2004. "How to Cope with Scopes: Stethoscope Selection and Use with Hearing Aids and Cls." *Hearing Review* 11(2):34–41.

Reynolds, Jorge, José Forero, Juan Botero, Vivian Leguizamón, Luis Ramirez, and Carlos Lozano. 2017. "Electronic Stethoscope With Wireless Communication to a Smart-Phone, Including a Signal Filtering and Segmentation Algorithm of Digital Phonocardiography Signals." Pp. 553–56 in *VII Latin American Congress on Biomedical Engineering CLAIB 2016, Bucaramanga, Santander, Colombia, October 26th-28th, 2016*.

Rhys, Hefin I. 2020. *Clustering Based on Density: DBSCAN and OPTICS - Machine Learning with R, the Tidyverse, and Mlr*.

Saupin, Guillaume. 2022. *Practical Gradient Boosting A Deep Dive*. AFNIL.

Say, O., Dokur, Z., & Olmez, T. (2002). Classification of heart sounds by using wavelet transform. *Proceedings of the Second Joint 24th Annual Conference and the Annual Fall Meeting of the Biomedical Engineering Society][Engineering in Medicine and Biology*, *1*, 128–129.

Shin, Ji Yun, Sehi L'Yi, Dong Hyun Jo, Jin Ho Bae, and Tae Soo Lee. 2013. "Development of Smartphone-Based Stethoscope System." Pp. 1288–91 in *2013 13th International Conference on Control, Automation and Systems (ICCAS 2013)*.

Sinharay, Arijit, Deb Ghosh, Parijat Deshpande, Shahnawaz Alam, Rohan Banerjee, and Arpan Pal. 2016. "Smartphone Based Digital Stethoscope for Connected Health–A Direct Acoustic Coupling Technique." Pp. 193–98 in *2016 IEEE First International Conference on Connected Health: Applications, Systems and Engineering Technologies (CHASE)*.

Smith, Steven W., and others. 1997. "The Scientist and Engineer's Guide to Digital Signal Processing."

Springer, David B., L. J. Zühlke, B. M. Mayosi, L. Tarassenko, and G. D. Clifford. 2014. "Mobile Phone-Based Rheumatic Heart Disease Diagnosis."

Statcounter Global Stats. 2023. "Mobile Operating System Market Share Worldwide." Retrieved September 13, 2023 (https://gs.statcounter.com/os-market-share/mobile/worldwide).

Statista. 2023. "Global Mobile OS Market Share 2023." Retrieved September 13, 2023 (https://www.statista.com/statistics/272698/global-market-share-held-by-mobile-operating-systems-since-2009/).

Strunic, Spencer L., Fernando Rios-Gutiérrez, Roc\'\io Alba-Flores, Glenn Nordehn, and Stanley Burns. 2007. "Detection and Classification of Cardiac Murmurs Using Segmentation Techniques and Artificial Neural Networks." Pp. 397–404 in *2007 IEEE symposium on computational intelligence and data mining*.

Sulistyanto, Muhammad Priyono Tri. 2016. "Rancang Bangun Smart Digital Mobile Stethoscope Berbasis Pada Sistem Mobile Device." *SMARTICS Journal* 2(1):1–6.

Sung, Po Hsun, William Reid Thompson, Jieh Neng Wang, Jhing Fa Wang, and Ling Sheng Jang. 2015. "Computer-Assisted Auscultation: Patent Ductus Arteriosus Detection Based on Auditory Time-Frequency Analysis." *Journal of Medical and Biological Engineering* 35(1):76–85.

Tsai, Ming-Jong, and Wen-Yang Chou. 2012. "Fast Implementation Method of a Wideband Butterworth Band Pass Filter for Signal Acquisition of Human Heart Sound." 中國機械工程學刊 33(5):457–66.

Vandeput, Nicolas. 2021. *Data Science for Supply Chain Forecasting*.

Vinod, Hrishikesh D., and C. Radhakrishna (Calyampudi Radhakrishna) Rao. 2020. *Financial, Macro and Micro Econometrics Using R*.

Wang, Xinpei, and Yuanyang Li. 2016. "Improving Classification Accuracy of Heart Sound Recordings by Wavelet Filter and Multiple Features." Pp. 1149–52 in *2016 Computing in Cardiology Conference (CinC)*.

Zhang, Cha, and Yunqian Ma. 2012. "Ensemble Machine Learning." *Ensemble Machine Learning*. doi: 10.1007/978-1-4419-9326-7.

Zhang, Yu, Yuanyuan Wang, Weiqi Wang, and Bin Liu. 2001. "Doppler Ultrasound Signal Denoising Based on Wavelet Frames." *IEEE Transactions on Ultrasonics, Ferroelectrics, and Frequency Control* 48(3):709–16.

Zhao, Zhidong, Qinqin Shen, and Fangqin Ren. 2013. "Heart Sound Biometric System Based on Marginal Spectrum Analysis." *Sensors 2013, Vol. 13, Pages 2530-2551* 13(2):2530–51. doi: 10.3390/S130202530.

Chapter 8

Effect of Electrolyte Parameters on PEMFC Outputs

Hüseyin KAHRAMAN[1], İdris CESUR[2]

1 Dr. Öğr. Üyesi.; Sakarya Uygulamalı Bilimler Üniversitesi, Teknoloji Fakültesi, Makina Mühendisliği Bölümü. huseyink@subu.edu.tr ORCID No: 0000-0003-3322-9904
2 Doç. Dr.; Sakarya Uygulamalı Bilimler Üniversitesi, Teknoloji Fakültesi, Makina Mühendisliği Bölümü. icesur@subu.edu.tr ORCID No: 0000-0001-7487-5676

INTRODUCTION

Fuel cells have emerged as a promising and environmentally friendly alternative to traditional energy conversion technologies, offering high efficiency and low emissions. Among various types of fuel cells, Proton Exchange Membrane Fuel Cells (PEMFCs) have garnered significant attention due to their suitability for various applications, ranging from transportation to stationary power generation. PEMFCs operate on the principle of converting chemical energy from hydrogen and oxygen into electrical energy through an electrochemical process, with the aid of a proton-conducting polymer electrolyte membrane (Shrivastava et al. 2020).

The performance of PEMFCs is inherently tied to the behavior of the electrolyte, as it directly influences key electrochemical processes, including proton conduction, water management, and gas diffusion. This paper seeks to delve into the intricate relationship between electrolyte physical parameters and PEMFC performance, shedding light on the fundamental aspects that govern the efficiency and stability of these power sources (Yang et al. 2021). Figure 1. Shows a PEMFC components.
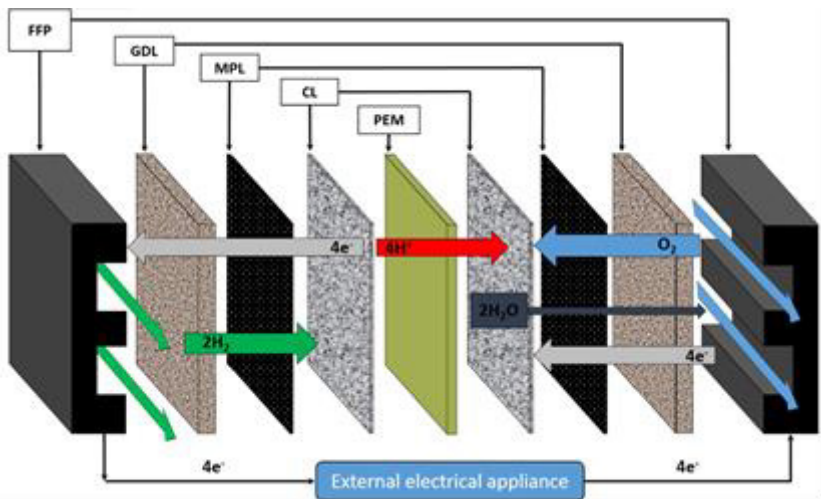
Figure 1: PEMFC components adopted from (Xing et al. 2019). (FFP: Flow field plate, GDL: Gas diffusion layer, MPL: Micro porous layer, CL: Catalyst layer, PEM: Polymer electrolyte membrane - electrolyte)

The physical parameters of the electrolyte encompass a range of properties, such as the ionomer content, ionomer-to-filler ratio, membrane thickness, porosity, and morphology (Wang et al. 2021). These parameters collectively influence the proton conductivity, water retention ability, mechanical strength,

and gas permeability of the membrane, all of which play pivotal roles in determining the overall performance of a PEMFC. Understanding how variations in these parameters impact the cell's behavior is crucial for optimizing PEMFC designs and advancing their practical applications (Kot et al. 2021).

Furthermore, the environmental conditions under which PEMFCs operate, such as temperature and humidity, also exert a significant influence on the electrolyte's physical properties. The interplay between these external factors and the inherent characteristics of the membrane material necessitates a comprehensive investigation to unravel the intricate dynamics at play (Nanadegani, Lay, and Sunden 2019).

In this study, we will systematically explore and analyze the effect of different electrolyte physical parameters on PEMFC performance. Our study aims to contribute to the existing body of knowledge in the field by providing valuable insights into the optimization of PEMFCs for enhanced efficiency, durability, and practical utility. By elucidating the complex relationships between electrolyte properties and fuel cell performance, we seek to facilitate the development of more efficient and sustainable energy solutions, fostering a cleaner and greener future.

Ion Conductivity

Ion conductivity is a crucial factor in the operation of PEMFCs. The ion conductivity, especially proton conductivity in the case of PEMFCs, plays a significant role in their performance and efficiency.

In PEMFCs, protons (H^+ ions) are transported through the proton exchange membrane (PEM) from the anode to the cathode. This transport of protons is what generates the electrical current. The higher the ion conductivity of the membrane, the more efficiently it can transport protons, leading to improved cell performance. This phenomenon can be seen schematically in Figure 2.
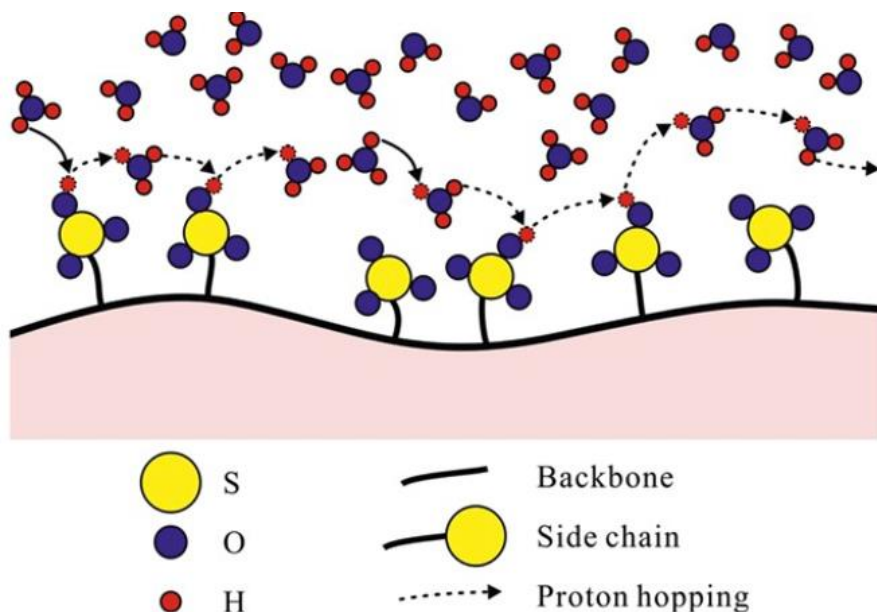
Figure 2: Ion transport mechanism for a PEM electrolyte. Adopted from (Hu et al. 2017)

Ion conductivity affects the ohmic losses within the cell. Ohmic losses occur due to the resistance encountered by protons as they move through the PEM. Higher ion conductivity reduces these losses, ensuring that more of the electrical energy generated is available for useful work.

Regarding the relationship between PEM electrolyte width and ion conductivity: Generally, as the thickness (width) of the PEM increases, the ion conductivity tends to decrease as seen in Figure 3. This is because a thicker membrane presents a longer path for ions to travel, leading to higher resistance. Thinner PEMs are often preferred in PEMFCs as they offer lower resistance to proton transport, resulting in higher efficiency and better performance.
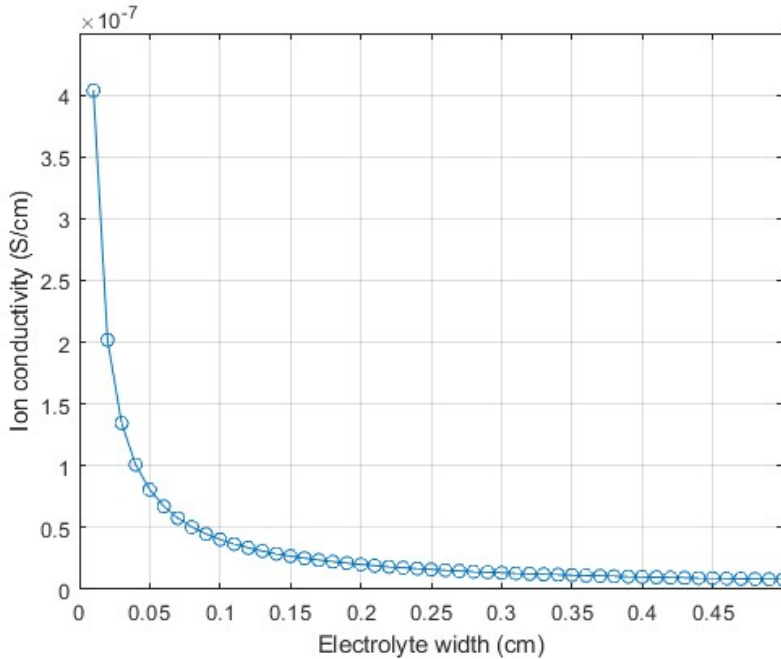
Figure 3: Electrolyte thickness (cm) versus ion conductivity (S/cm)

Ion conductivity is temperature dependent. Figure 4 shows the effect of temperature (between 25-80°C) to membranes ion conductivity. An increase in temperature typically leads to an increase in ion conductivity. This property is important because PEMFCs often operate at elevated temperatures to enhance their performance. A membrane with good ion conductivity will maintain efficient proton transport even at higher operating temperatures.
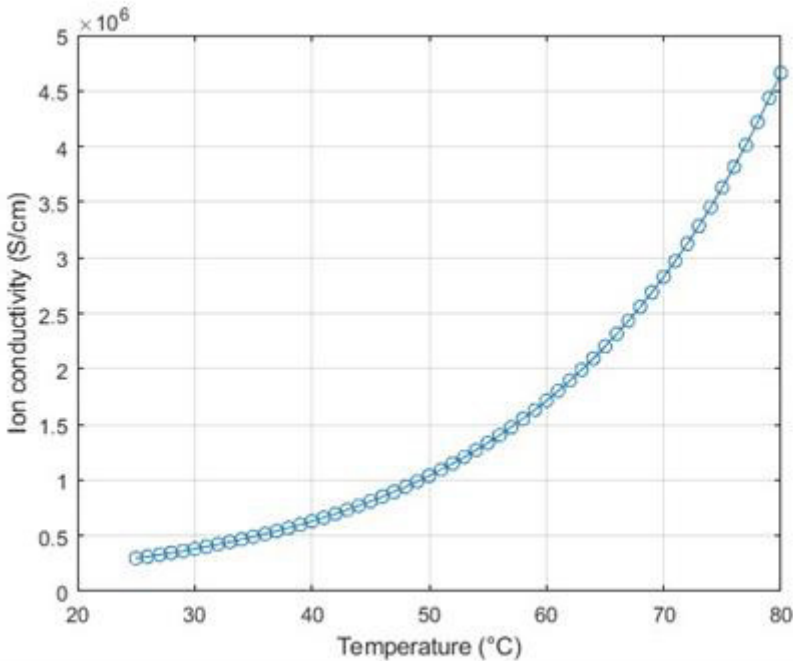
Figure 4: The effect of cell temperature to membrane ion conductivity.

PEMFCs require water for their operation, and the ion conductivity of the PEM affects water management within the cell. The PEM must strike a balance between allowing enough water for proton conduction and not becoming too saturated, which can block proton transport. The choice of PEM material and its ion conductivity properties are critical in achieving this balance. The relationship between water content and electrolyte ion conductivity in a PEMFC is fundamental to understanding and optimizing the cell's operation. Water content within the PEMFC directly impacts its overall performance and efficiency. Water content plays a crucial role in facilitating the transport of protons (H+ ions) within the proton exchange membrane. Adequate water content is necessary to maintain proton conductivity, ensuring efficient ion transport across the membrane. Finding the right balance of water content is essential. Excess water can lead to flooding of the membrane, inhibiting gas diffusion and reducing ion conductivity. Conversely, insufficient water content can limit proton transport and decrease ion conductivity. The relationship between water content and ion conductivity is often non-linear. Figure 5 shows this phenomenon. At low water content levels, ion conductivity may decrease due to limited proton availability, while at high water content levels, it can decrease due to flooding and increased resistance.
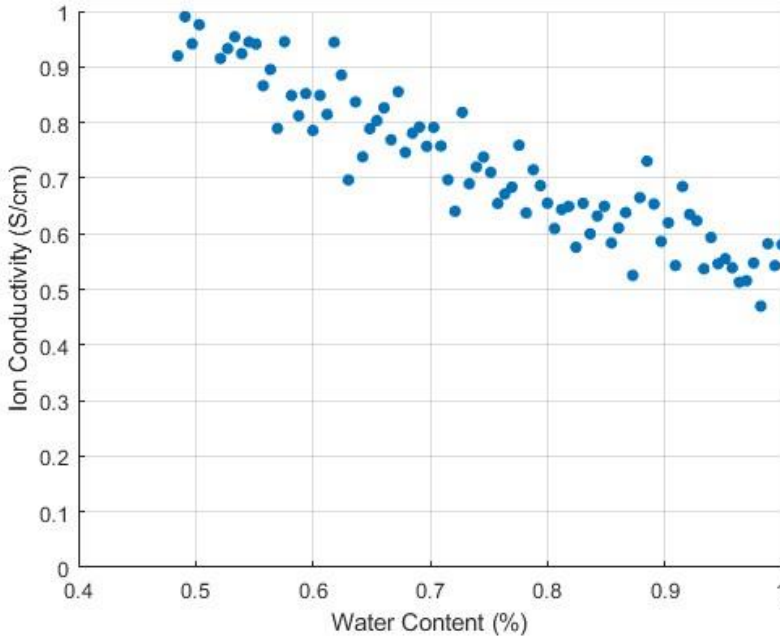
Figure 5: Relationship between water content and membrane ion conductivity.

CONCLUSION

In this study, we have systematically investigated the influence of three crucial factors, namely membrane thickness, temperature, and water content, on the ion conductivity of PEMFC membranes. These factors play pivotal roles in determining the performance and efficiency of PEMFCs, making their comprehensive understanding essential for the advancement of this promising energy conversion technology. Our research revealed several important findings:

- Membrane Thickness: We observed a clear inverse relationship between membrane thickness and ion conductivity. As the thickness of the PEMFC membrane increased, ion conductivity decreased.
- Temperature: Temperature exhibited a significant positive impact on ion conductivity. As the temperature of the PEMFC increased, ion conductivity improved markedly. This behavior can be explained by the enhanced kinetic energy of protons and ions at higher temperatures, leading to more efficient proton transport.

- Water Content: Water content was found to have a complex, non-linear relationship with ion conductivity. At low water content levels, ion conductivity decreased due to limited proton availability. Conversely, at high water content levels, ion conductivity decreased as a result of flooding and increased resistance. This intricate relationship underscores the importance of precise water management within PEMFCs to strike a balance between hydration and flooding for optimal ion transport.

These findings collectively highlight the intricate interplay of membrane thickness, temperature, and water content in influencing PEMFC membrane ion conductivity. Achieving the right balance among these factors is essential for optimizing PEMFC performance and efficiency.

REFERENCES

Hu, Y., X. Li, L. Yan, and B. Yue. 2017. 'Improving the Overall Characteristics of Proton Exchange Membranes via Nanophase Separation Technologies: A Progress Review'. *Fuel Cells* 17(1):3–17. doi: 10.1002/fuce.201600172.

Kot, Anna, Dominik Dorosz, Marta Radecka, and Katarzyna Zakrzewska. 2021. 'Improved Photon Management in a Photoelectrochemical Cell with Nd-Modified TiO2 Thin Film Photoanode'. *International Journal of Hydrogen Energy* 46(22):12082–94. doi: 10.1016/j.ijhydene.2020.05.094.

Nanadegani, F. S., E. N. Lay, and B. Sunden. 2019. 'Effects of an MPL on Water and Thermal Management in a PEMFC'. *International Journal of Energy Research* 43(1):274–96. doi: 10.1002/er.4262.

Shrivastava, Udit N., Avital Zhegur-Khais, Maria Bass, Sapir Willdorf-Cohen, Viatcheslav Freger, Dario R. Dekel, and Kunal Karan. 2020. 'Water Content and Ionic Conductivity of Thin Films of Different Anionic Forms of Anion Conducting Ionomers'. *The Journal of Physical Chemistry C* 124(43):23469–78. doi: 10.1021/acs.jpcc.0c04278.

Wang, X. R., Y. Ma, J. Gao, T. Li, G. Z. Jiang, and Z. Y. Sun. 2021. 'Review on Water Management Methods for Proton Exchange Membrane Fuel Cells'. *International Journal of Hydrogen Energy* 46(22):12206–29. doi: 10.1016/j.ijhydene.2020.06.211.

Xing, Lei, Weidong Shi, Huaneng Su, Qian Xu, Prodip K. Das, Baodong Mao, and Keith Scott. 2019. 'Membrane Electrode Assemblies for PEM Fuel Cells: A Review of Functional Graded Design and Optimization'. *Energy* 177:445–64. doi: 10.1016/j.energy.2019.04.084.

Yang, Xiaokang, Jiaqi Sun, Guang Jiang, Shucheng Sun, Zhigang Shao, Hongmei Yu, Fangwei Duan, and Yingxuan Yang. 2021. 'Experimental Study on Critical Membrane Water Content of Proton Exchange Membrane Fuel Cells for Cold Storage at −50 °C'. *Energies* 14(15):4520. doi: 10.3390/en14154520.

Chapter 9

Digital Twin: An Approach to Artificial Intelligence-Enabled Wireless Networks

Sercan YALÇIN[1], Hüseyin VURAL[2]

[1] *Assoc. Prof..; Adıyaman University, Engineering Faculty, Computer Engineering. svancin@adiyaman.edu.tr ORCID No: 0000-0003-1420-2490*

[2] *Asst. Prof..; Adıyaman University, Engineering Faculty, Computer Engineering. hvural@adiyaman.edu.tr ORCID No: 0000-0001-9290-6317*

INTRODUCTION

A digital twin (DT) is a virtual representation or a digital replica of a physical object, process, or system. It is created by capturing and integrating real-time data from sensors, Internet of Things (IoTs) devices, and other sources, along with relevant contextual information (Attaran and Celik, 2015: 100165). DTs enable real-time monitoring, analysis, and simulation of the physical counterpart, providing valuable insights, predictive capabilities, and decision support. Future generation wireless networks, such as 5G and beyond, are envisioned to support unprecedented levels of connectivity, data rates, and diverse applications (Siddiqui et al., 2023). To realize the full potential of these networks, intelligent management and optimization approaches are required. In this context, the concept of DT has emerged as a promising technology that combines virtual representations and artificial intelligence (AI) techniques to enhance the intelligence and efficiency of wireless networks. A DT for intelligence-based future-generation wireless networks leverages real-time data collection from network devices, sensors, and management systems to create a virtual replica of the network (Fuller et al., 2020: 108952; Liu et al., 2021:346]. This virtual representation is integrated with AI algorithms, including machine learning (ML), deep learning (DL), and reinforcement learning (RL), to enable advanced analytics, predictive modeling, and optimization. By analyzing network data and patterns, the DT provides insights into network performance, predicts potential issues, and facilitates proactive decision-making. The DT enhances network planning and optimization by simulating different scenarios and evaluating the impact of network parameters. It enables predictive maintenance by detecting anomalies, predicting equipment failures, and optimizing maintenance schedules. Spectrum management benefits from DTs by dynamically allocating and optimizing frequency bands based on spectrum availability and demand (Khan et al., 2022:2230; Barricelli et al., 2019: 167653; Minerva et al., 2020:1785). Furthermore, DTs contribute to IoT network management, network security, traffic prediction, and virtual testing and validation. The integration of DT technology with intelligence-based future-generation wireless networks opens up new possibilities for optimizing network performance, ensuring reliable connectivity, and adapting to dynamic network conditions. It empowers network operators and administrators with valuable insights, automated decision support, and efficient resource allocation. However, challenges such as data privacy, scalability, and real-time synchronization between the physical network and the DT need to be addressed to fully realize the potential of this technology (Wu et al., 2021: 13789; Dinter et al., 2022: 107008). By creating a virtual replica of the network and leveraging AI algorithms, DTs enable intelligent network

management, optimization, and decision-making. They contribute to improved network performance, enhanced user experience, and efficient utilization of network resources in the evolving landscape of wireless communication (D'Amico et al., 2022:613).

In recent studies, several areas and applications of DTs have emerged in the context of wireless networks (Consilvio et al., 2019:1; Errandonea et al., 2020: 103316). DTs are utilized for network planning and optimization tasks, such as determining optimal base station locations, antenna configurations, and network capacity planning. By simulating different scenarios and analyzing the impact of network parameters, DTs assist in optimizing coverage, capacity, and quality of service for wireless networks. DTs are employed for predictive maintenance of wireless network infrastructure. By analyzing data from network devices, sensors, and historical maintenance records, DTs can detect anomalies, predict equipment failures, and recommend proactive maintenance actions. This helps in reducing downtime, optimizing maintenance schedules, and improving network reliability. DTs play a role in optimizing spectrum utilization and management (Picone et al., 2021: 100661). They can analyze spectrum availability, interference patterns, and traffic demand to dynamically allocate and optimize frequency bands. DTs help mitigate interference issues, improve network performance, and maximize spectrum efficiency. DTs are applied in managing and optimizing the IoT networks. By creating DTs of IoT devices and their connectivity, it becomes possible to monitor device behavior, analyze data patterns, and optimize network performance. DTs assist in managing device configurations, handling scalability challenges, and ensuring reliable connectivity for IoT applications (Minerva et al., 2020:1785). DTs contribute to enhancing network security in wireless networks. By creating digital replicas of network infrastructure and applying AI algorithms, DTs can monitor network traffic, detect anomalies, and identify potential security threats. DTs aid in real-time threat detection, incident response, and network security management (Wu et al., 2021:13789).

In summary, while several studies have explored DT frameworks, AI techniques, and wireless network optimization, limited research has specifically addressed the integration of DT, AI, LoRa protocol, and spectrum sensing management in the context of wireless 5G networks. Errors related to LoRa node identification, transmission, and reception are decreased via effective spectrum management.

RELATED WORKS

According to Rasheed et al. (2019), DTs are adaptive models of complex systems. DTs are becoming a more realistic possibility thanks to recent advancements in computing pipelines, multiphysics solvers, AI, big data cybernetics, data processing, and management tools. In a variety of applications, DTs are currently a significant rising trend. Also known as synchronized virtual prototypes, device shadows, mirroring systems, avatars, and computing gigantic models. In order to encourage the modularization of interdisciplinary systems and overcome basic hurdles, DTs play a transformative role not just in how we design and manage cyber-physical intelligent systems. Alexopoulos et al. (2020:429) emphasized that by creating a suitable training data set and automatically labeling it using a simulation toolchain, the DT's model can be leveraged to speed up the ML training phase while minimizing human involvement. These artificial datasets can be expanded and cross-validated utilizing a large amount of real-world data with little to no use. In order to actualize the multidisciplinary integration of information and communication technology (ICT) in crisis informatics and disaster response, Fan et al. (2021: 102049) researched and offered a vision of a catastrophe city DTs idea. To improve situation assessment, decision-making, and coordination among various stakeholders and hence increase insight into the dynamics of complex disaster response and humanitarian assistance, AI algorithms and approaches must be incorporated. Yurkevich and Stepanovskaya (2021) proposed a neural model created for digital air traffic control. The components of this technique are connected to wireless 4G and 5G networks, and it embraces the idea of a physical self-organizing social network of a distributed organization and technical system. This method has the advantage of a sophisticated integration with hybrid AI and a very promising analysis and management principle. Li et al. (2021) went into great length on the traits, the most cutting-edge makeup, and the corresponding constraints of the future DTs in the aerospace industry. They presented the aero DTs in three dimensions. The community conducting research and development on aviation DTs may benefit from these, which include interaction, standardization, and cognitive. They assisted in quadrupling the effectiveness of current and upcoming aeronautical systems and related procedures. Bécue et al. (2020:4482) proposed a novel cognitive modeling and cooperative simulation environment. To assess the human behavior models and security testing skills in aerospace, they introduced holistic DTs and AI technologies. Finally, they showed how to use holistic DTs and AI technologies to deliver new services for optimizing and recovering future factories. Grigoropoulos and Lalis (2020:1) provided an analog environment and support for DTs for a platform that makes it easier to manage and run drone-based

applications on a standard drone architecture. The platform and the functions of the apps running on it can first be thoroughly tested in the simulation environment before being deployed to the real world. When apps are deployed, the DT is used to identify gaps and expected behaviors between them. When the simulation test is run or no errors have been detected, this information can be used as an error indicator. Xiong, et al. (2021:3751) investigated a DT-driven aviation engine predictive maintenance framework and found an Implicit DTs (IDTs) model to enhance the effectiveness of engine predictive maintenance. The validity of the model is assessed by comparing virtual and real data assets. By combining the data-driven DL method with the Long Short-Term Memory (LSTM) model and using an illustration of an aviation engine, the approach's utility is shown. Angin et al. (2020:77) suggested AgriLoRa, a low-cost farmland DT system, for intelligent agriculture. In order to identify plant illnesses, weed clusters, and nutritional deficits in plants, AgriLoRa uses a wireless sensor network (WSN) installed in agricultural areas in conjunction with cloud servers that run computer vision algorithms. In a study, Dangana et al. (2022:9039) investigated the behavior of Narrow Band (NB)-IoT wireless communication in an indoor industrial setting. A situation in the industrial sector was modeled and simulated using Wireless Insite software. Their study looked at how this situation or environment affects the physical layer of the NB-IoT's communication characteristics. In this context, signal-to-noise ratios (SNRs) in the environment, throughput levels among terminals as well as between terminals and transceiver towers, the power received at signal destination locations, and distances between terminals and transceivers are taken into account. Gao et al. (2023: 104835) studied the time delay of bridge DT services in relation to communication and computation complexity, exposing the different influences of their order. They proposed an AIoT-informed DT communication architecture. To reduce communication complexity in the framework, the information hierarchy and two-way communication can be used. A Petri net is used to illustrate the proposed framework's data flow and robustness. Additionally, the framework is cross-platform integrated into a generic DT and tested with various situations. The findings show that in comparison to other bridge DTs now in use, the proposed framework has high efficiency, low latency, and superior fault tolerance, which can improve the effectiveness and safety of bridge O&M, particularly in situations where communication is limited.

WIRELESS 5G NETWORKS AND LoRa STANDARD

Wireless 5G network refers to the fifth generation of wireless network technology, which is designed to provide faster data transmission, lower latency,

higher capacity, and more reliable connectivity compared to previous generations. It is an advanced wireless network technology that aims to meet the increasing demands of modern applications, such as IoTs, virtual reality (VR), augmented reality (AR), and high-definition video streaming (Fu et al., 2018:58; You et al., 2019:21301).

The wireless 5G network consists of 5G base stations that transmit and receive data to and from user devices. These base stations are equipped with advanced antenna technologies to provide high-speed wireless connectivity. The user devices, such as smartphones or IoT devices, communicate with the base stations wirelessly, allowing users to access various applications and services with improved performance (Oever, 2023:102442). The wireless 5G network utilizes higher frequency bands, advanced modulation techniques, and beamforming to enable faster data transmission rates and lower latency. It also employs advanced network management techniques, such as network slicing, to allocate network resources efficiently and provide customized services to different types of applications and users. Overall, the wireless 5G network offers enhanced connectivity and enables a wide range of innovative applications and services that require high-speed, low-latency, and reliable wireless communication (Li et al., 2017).

LoRa, short for Long Range, is a low-power, wide-area networking (LPWAN) technology designed for long-range wireless communication. It operates in unlicensed frequency bands, typically using sub-GHz frequencies, and is known for its ability to provide long-range connectivity while consuming minimal power (Yalçın, 2023:5433).

In the DT wireless 5G network spectrum sensing scheme, LoRa can be utilized for specific reasons:

- Long Range Sensing: LoRa's long-range capabilities make it suitable for spectrum sensing in wireless networks, including 5G. By deploying LoRa-based devices as sensors, the DT can gather spectrum-related data across a wide area, providing comprehensive information for spectrum management and optimization.
- Low Power Consumption: The low-power nature of LoRa devices allows for prolonged sensing operations without draining excessive energy. This is essential for continuous spectrum monitoring and ensures the sustainability of the proposed DT scheme.
- Chirp Spread Spectrum (CSS): LoRa utilizes CSS modulation, which spreads the signal over a wide frequency range. This modulation technique allows LoRa devices to achieve long-range communication and high resistance to noise and interference.

- Adaptive Data Rate (ADR): LoRa-based LPWANs employ data rate techniques to optimize the data rate and power consumption based on the signal strength and distance between devices. This operation dynamically adjusts the communication parameters to maintain an optimal balance between range, data rate, and energy efficiency.
- Robustness and Penetration: LoRa exhibits excellent robustness against interference and can penetrate through obstacles such as walls and buildings, ensuring reliable connectivity even in challenging environments.
- Wide Coverage: LoRa's ability to cover large areas facilitates spectrum sensing in a distributed manner. By deploying LoRa-based sensors strategically, the DT can monitor the spectrum usage across a wide range, capturing variations and patterns in different locations.

By integrating LoRa-based LPWANs into the DT architecture for wireless 5G network spectrum sensing, the scheme can leverage LoRa's long-range communication, low power consumption, and wide coverage to collect spectrum data efficiently and accurately (Zhang et al., 2022:2100228; Tendeng et al., 2018:23). This data can then be utilized for spectrum management, optimization, and decision-making within the DT system, ultimately enhancing the performance and efficiency of wireless 5G networks. LoRa operates in the unlicensed spectrum and provides long-range communication with low power consumption. On the other hand, 5G is a cellular network technology that operates in licensed spectrum bands, offering high-speed connectivity and supporting various use cases beyond IoT. As such, there isn't a direct combination of 5G and LoRa in terms of protocol integration. However, it is possible to consider scenarios where a hybrid network architecture combines the capabilities of both technologies to address diverse connectivity requirements. In such cases, 5G can be used for high-speed data transmission and LoRa can be utilized for low-power, long-range IoT communication. The 5G base station provides high-speed connectivity to 5G user devices, enabling applications that require fast data transmission, such as video streaming or real-time communication. The 5G network operates in licensed spectrum bands and supports advanced features like network slicing and low latency. On the other hand, the LoRa gateway connects to LoRa devices, which are typically low-power IoT sensors or devices (Nurelmadina et al.,2021:1). It is suitable for IoT applications that require long battery life and connectivity in remote areas. In a hybrid scenario, the 5G and LoRa networks can be interconnected to provide seamless connectivity for different use cases. In the proposed framework, the 5G network was used for

high-speed data transfer and control of IoT devices, while LoRa was utilized for low-power, wide-area network applications that require long-range connectivity.

3.1. Operation and Designing of the DT framework.

In this section, the DT architecture for 5G wireless network management with LoRa communication protocol, is explained along with the relationships between its components:

a) Data Collection Layer: The Data Collection Layer is responsible for gathering real-time data from various sources within the 5G network, including base stations, user devices, sensors, and LoRa gateways. This data includes network performance metrics, signal strength, device statuses, environmental conditions, and LoRa-specific parameters such as SNR and packet error rate (PER).

b) Data Ingestion and Pre-processing: The collected data from the Data Collection Layer is ingested into the DT platform and undergoes pre-processing. This stage involves data cleaning, normalization, filtering, and transformation to ensure the quality and consistency of the data. For LoRa-specific data, additional pre-processing steps may include decoding LoRaWAN messages and extracting relevant information.

c) Data Storage and Management: The pre-processed data is stored in a suitable database or data management system. This allows for efficient storage, retrieval, and query operations on both historical and real-time network data. The stored data includes 5G network parameters, LoRa-specific metrics, device information, and environmental data.

d) Integration of 5G Network Data: The DT incorporates data from the 5G network, including information from 5G base stations, user devices, and network management systems. This data provides insights into network performance, user experience, and resource utilization within the 5G network.

e) Integration of LoRa Network Data: The DT integrates data from the LoRa network, which includes information from LoRa gateways, LoRa devices, and IoT sensors. This data enables monitoring of IoT device connectivity, sensor data collection, and overall performance of the LoRa network.

f) AI and Analytics Layer: The AI and Analytics Layer consists of various AI techniques such as ML, DL, and statistical analysis algorithms. These algorithms analyze the collected data to extract insights, detect patterns, and predict network behavior. The AI models are trained using historical data to provide accurate predictions and optimizations for 5G network management with LoRa.

In the AI and Analytics layer of the wireless network's DT, a Convolutional Neural Network (CNN) can play a significant role in analyzing and processing the collected data. CNN is a DL algorithm specifically designed to make it well-suited for various applications in the wireless network domain. Here is further information in the AI and Analytics layer of the DT:

- Anomaly Detection: CNNs were used to detect anomalies or unusual patterns in network data in this study. By training on normal network behavior, CNNs can learn to identify deviations from the expected patterns, such as network intrusions, security breaches, or performance anomalies. This aids in early detection and mitigation of potential network issues. A mathematical model is designed for fault detection using an AI-based wireless network.

- Network Modeling and Simulation: The Network Modeling and Simulation component creates a virtual replica or model of the 5G wireless network with integrated LoRa communication. This model captures the network topology, connectivity, device configurations, and the impact of LoRa parameters. Simulation techniques are employed to simulate different scenarios and evaluate the performance of the network under various conditions.

- Control and Optimization: The Control and Optimization component takes inputs from the AI models, simulation results, and user interactions to drive intelligent decision-making and optimization actions. It enables automated or semi-automated control and optimization of network parameters, device configurations, LoRa gateway placement, and LoRa channel allocation to improve the overall performance, capacity, and reliability of the 5G network with LoRa.

Overall, the CNN-based AI and Analytics layer empowers the DT to extract valuable insights, make informed decisions, and optimize network operations in wireless networks. By leveraging the capabilities of DL, CNNs enable intelligent analysis of complex data, leading to improved network performance, enhanced security, and better user experience. Fig. 1 represents the proposed framework.
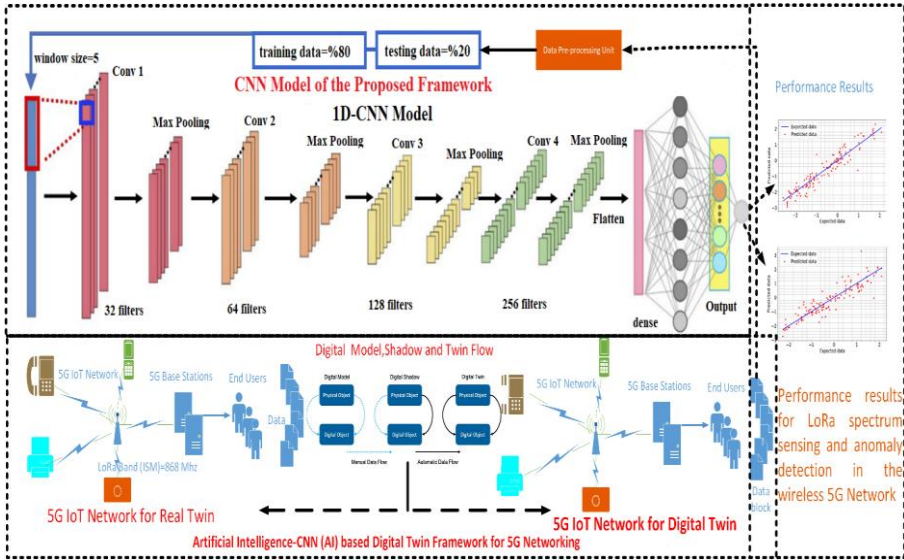
Figure 1: The proposed framework: AI-CNN based DT framework for wireless 5G networks.

In the proposed model, 4 convolution and max pooling layers are used based on the 1D-CNN structure. These layers are combined in the dense layer after the flatten layer and transferred to the output layer. Filters of 32, 64, 128, and 256 are considered, respectively. An AI-based (CNN) system of 5G and LoRa network has been established. As seen in Fig. 1, the digital mirror block consists of model, shadow, and flow mirroring. The physical (real) and digital (virtual) data in the 5G network obtained using the DT are compared and forwarded to the CNN layer for training. 80% of the total data is set for training and the rest for testing. In the output layer, the expected and predicted values of the data are analyzed. The relationships between these components involve the flow of data and information. The Data Collection Layer feeds real-time data to the Data Ingestion and Pre-processing stage, which then delivers the pre-processed data to the Data Storage and Management component. The AI and Analytics Layer utilizes the stored data for analysis and generates insights, which are then visualized and presented through the Visualization and User Interface component. The Control and Optimization component takes inputs from AI models, simulation results, and user interactions to drive network optimization actions, thus completing the feedback loop. In this way, the proposed DT architecture for 5G wireless network management with LoRa communication protocol enables efficient monitoring, analysis, and optimization of network performance, device configurations, and LoRa-specific parameters. It leverages AI techniques, simulation capabilities,

and user-friendly interfaces to enhance decision-making and improve the overall management of 5G networks incorporating LoRa technology. By integrating the 5G and LoRa networks within the DT framework, network operators can have a holistic view of their wireless infrastructure. They can optimize resource allocation, identify potential issues, and make data-driven decisions for network management and optimization in a hybrid environment.

4. THE MATHEMATICAL MODELING OF A DT FOR WIRELESS 5G NETWORK

The mathematical model of a DT for a wireless 5G network involves various components and their relationships. Here is the proposed mathematical representation of the DT model:

a) Network Topology: Consider $G(V, E)$ as the network topology, where V is the set of network nodes (LoRa devices) and E is the set of links connecting these nodes. Each node $v \in V$ is associated with its coordinates (x_v, y_v) in the network.

b) Signal Propagation Model: The signal propagation model determines the path loss and interference between nodes. Define $P_l(v_i, v_j)$ as the path loss between nodes v_i and v_j, which depends on factors such as distance, antenna characteristics, and environmental conditions. The interference level between nodes v_i and v_j is denoted as $I(v_i, v_j)$.

c) Spectrum Sensing: Spectrum sensing measures the occupancy and availability of the spectrum bands. Consider $O(v_i, b)$ as the occupancy status of spectrum band b at node v_i, where $O(v_i, b) = 1$ indicates the band is occupied, and $O(v_i, b) = 0$ represents an available band.

d) Resource Allocation: Resource allocation involves assigning spectrum bands, transmit power, and other network resources to optimize network performance. Represent $R(v_i, b)$ as the allocated resources for node v_i on spectrum band b. This includes the allocated transmit power, bandwidth, modulation scheme, and coding rate.

e) Performance Metrics: Various performance metrics can be considered, such as throughput, latency, energy efficiency, and coverage. Let $P(v_i)$ denote the achieved throughput at node v_i, and $T(v_i)$ represent the latency experienced by node v_i.

f) Optimization Objective: The objective of the DT model is to optimize network performance based on specific criteria. Let $f(O, R)$ be the objective function representing the optimization goal, which can be formulated as a minimization or maximization problem.

g) Constraints: There may be various constraints in the DT model, such as maximum transmit power limits, interference thresholds, and quality of service requirements. These constraints can be represented as mathematical inequalities or equations.

The proposed mathematical model of the DT for a LoRa wireless 5G network incorporates these components and their relationships to simulate, analyze, and optimize network operations. It provides a mathematical framework to study the interactions between different network elements, predict network behavior, and optimize resource allocation to achieve desired network performance. The specific formulation of the mathematical model may vary depending on the objectives, constraints, and performance metrics considered in a particular DT implementation.

The proposed mathematical modeling of a DT for fault detection in a wireless network typically involves capturing the relationship between the sensor measurements and the occurrence of faults or anomalies. The proposed mathematical model for fault detection in a wireless network, is presented as:

a) LoRa sensor node measurements: The sensor measurements are considered as $v_1, v_2, \dots v_{N_s}$ where N_s represents the number of LoRa nodes in the network. These measurements are related to the physical volt amounts ranging from -3 to 3 of the LoRa sensor nodes, which are considered homogeneous and of the same type in the network. In fact, although there are many different types of nodes in IoT 5G networks and the physical variable environment data these nodes detect, the battery voltage values of low power consuming nodes are taken as the basis in this study. The obtained data in the network is passed through a pre-processing operation such as filtering before being trained.

b) Fault Detection Model: The specific form of the proposed fault detection model depends on the three-step approach.

- Training and Validation: The fault detection model requires training and validation using historical sensor data. This involves collecting a dataset that includes both normal operating conditions and known fault instances. The dataset is used to train the model to distinguish between normal and faulty situations. The model is then validated on unseen data to assess its performance.

- Decision Threshold: In threshold-based approaches, a decision threshold is defined to determine when a fault is detected. The threshold λ was set to the system for wireless network application.

- Alarm Generation: When a fault is detected, an alarm can be generated to notify the network administrator or appropriate personnel. The alarm can

be in the form of a notification, message, or any other mechanism that indicates the presence of a fault.

The fault detection model captures the relationship between the sensor measurements and the fault detection variable. This can be done by comparing the measured values with expected or predicted values. The goal is to detect faults or anomalies in the sensor measurements. This has been performed by the proposed algorithm.

The absence or presence of an end user in the network sensing area is determined by the two hypotheses H_0 and H_1. Eq (1) gives the signal D_i that the LoRa node i received signal by the DT user.

$$D_i = \begin{cases} n_i & H_0 \\ c_i\,R_i + n_i & H_1 \end{cases} \tag{1}$$

where D_i is the signal that the digital end user i perceives, R_i is the transmitted signal by a real end-user i, c_i is the channel amplitude gain, and n_i is the additive white gaussian noise (AWGN). According to the H_0 hypothesis, there is no end user and the received signal sample D_i is made up entirely of noise. Contrarily, the noise and the signal broadcast after the c_i channel are likewise present in the signal received according to the H_1 hypothesis. Examining the signal acquired during the fault detection technique is necessary to select between binary hypotheses (Nurelmadina et al., 2021:1; Khan et al., 2019:1). The presence of a digital end user and its signal can only be determined by measuring the power considered in the frequency band and comparing it to a number of thresholds. The test static T_s for signal/data detection of the LoRa node, which ascertains whether the end user is active or not, is defined in Eq. (2).

$$T_s = \frac{1}{N_s}\sum_{i=1}^{N_s} |f_v(v_1, v_2, \dots v_i)\,|^2 \tag{2}$$

where f_v is defined for the fault detection variable in terms of $v_1, v_2, \dots v_i$ measurements, N_s is the number of LoRa node signal samples. The tests are expressed in Eqs. (3) and (4) with the test static T_s for both of the hypotheses H_0 and H_1, respectively (Khan et al., 2019:1; Yalçın 2022:4526).

$$T_s|H_0 \sim G(w_a^2, \frac{w_a^4}{N_s}) \tag{3}$$

$$T_s|H_1 \sim G(w_t^2 + w_a^2, \frac{(w_t^2 + w_a^2)^2}{N_s}) \tag{4}$$

where G is Gaussian distribution, w_t^2 and w_a^2 denote the variances of the forwarded data signal and AWGN, respectively. If $(T_s > \lambda | H_1)$ and $(T_s > \lambda | H_0)$, Eqs. (5) and (6) are satisfied, and the probability of detection P_d and the false alarm (fault signal) P_a are presented by Eqs. (5) and (6).

$$P_d = Q\left(\frac{\lambda - w_a^2(1+\Upsilon)}{\frac{w_a^2(1+\Upsilon_S)}{\sqrt{N_S}}}\right) \tag{5}$$

$$P_a = Q\left(\frac{\lambda - w_a^2}{\frac{w_a^2}{\sqrt{N_S}}}\right) \tag{6}$$

where Υ represents the SNR of the end user's signal measured, $Q()$ defines the Gaussian function, and λ is the threshold value. Finally, fault detection function f_d is presented in Eq.(7).

$$f_d = P_d \sim P_a \tag{7}$$

where f_d is defined for the fault detection, which indicates the presence (f_d= 1) or absence (f_d = 0) of a fault, as given in Eq.(8). Here, $\sim$ is the operator that creates the output of the decision (classifier) between P_d and P_a, performed by the proposed CNN model.

$$fault = \begin{cases} 0, & if \ f_d = 0 \\ 1, & if \ f_d = 1 \end{cases} \tag{8}$$

By incorporating this mathematical model into the DT framework, the DT continuously monitors the sensor measurements, applies the fault detection model, and generates alerts when anomalies or faults are detected. This enables proactive fault management and improves the overall reliability and performance of the DT-based wireless network.

5. DISCUSSION AND FUTURE ASPECTS

Inference in the field of DT for intelligence-based future-generation wireless networks reveal the tremendous potential and advancements made in leveraging this technology. By combining virtual replicas with AI techniques, DTs offer a transformative approach to network management, optimization, and decision-making in wireless networks. Significant progress has been made in several key areas. DTs have been successfully applied to network planning and optimization,

allowing for the simulation of different scenarios and evaluation of network parameters. Predictive maintenance has benefited from DTs by enabling proactive fault detection and optimization of maintenance schedules. Moreover, DTs have played a vital role in IoT network management, network security, traffic prediction, and virtual testing and validation. The integration of AI techniques, such as ML, DL, and RL, with DTs could enhance network intelligence.

In the near future, several studies can be performed in wireless networks with DT to advance network management, optimization, and overall performance. We can give some potential areas of research:

- Network Planning and Optimization: DT can be utilized for network planning and optimization, considering factors such as coverage, capacity, interference, and user demand. Studies can focus on developing algorithms and techniques to optimize network deployment, antenna placement, frequency planning, and resource allocation for improved network performance.

- Spectrum Management and Dynamic Spectrum Access: DT can enable studies on dynamic spectrum management techniques, including spectrum sensing, spectrum sharing, and spectrum allocation. Researchers can explore AI-based algorithms to optimize spectrum utilization, minimize interference, and enable efficient coexistence of different wireless technologies.

- Resource Allocation and Quality of Service (QoS) Management: Studies can investigate resource allocation techniques within the DT framework, aiming to enhance QoS for different applications and user requirements. This includes developing algorithms for dynamic resource allocation, load balancing, traffic prioritization, and adaptive modulation and coding schemes.

- Security and Privacy: DTs can be leveraged to study security and privacy aspects in wireless networks. Research can focus on developing intrusion detection and prevention mechanisms, authentication protocols, encryption techniques, and privacy-preserving solutions to safeguard network infrastructure, user data, and IoT devices.

- Edge Computing (EC) and Network Function Virtualization (NFV): DTs can facilitate research on the integration of EC and NFV concepts into wireless networks. Studies can explore the placement of virtualized network functions, edge caching strategies, and dynamic offloading mechanisms to enhance network performance, reduce latency, and support emerging applications such as IoT, AR, and VR.

- Energy Efficiency and Green Networking: Studies can focus on energy-efficient design and operation of wireless networks within the DT framework. Researchers can investigate techniques to optimize energy consumption, develop power-aware routing protocols, and explore energy harvesting solutions for sustainable and green networking.

These are just a few examples of the studies that can be conducted in wireless networks with DT in the near future. With the continuous evolution of wireless technologies and the increasing complexity of network management, the DT approach provides a promising avenue for research and innovation in optimizing network performance, enhancing user experience, and enabling advanced wireless applications.

6. CONCLUSION

In this book chapter, a DT framework based on AI for wireless 5G networks with LoRa protocol which presents a promising approach is proposed to detect the faults in the network. By integrating AI techniques within the DT architecture, the framework enables efficient data collection, analysis, and decision-making processes. The use of LoRa protocol for spectrum sensing adds an additional layer of flexibility and scalability to the framework. Through the deployment of LoRa-based sensors, real-time spectrum-related data can be gathered, facilitating accurate fault detection. The AI algorithms applied within the DT framework allow for the identification of interference sources, prediction of spectrum usage patterns, and strategies, which reduce faults or sensor disorders in the wireless network. The proposed DT framework can offer a foundation for future research and development in the field, opening doors for practical implementation and real-world deployments of AI-driven DT solutions for wireless 5G networks.

REFERENCES

Alexopoulos K., Nikolakis N., and Chryssolouris G. (2020). Digital twin-driven supervised machine learning for the development of artificial intelligence applications in manufacturing. *Int J Comp Integ M*., 33(5), 429–439.

Angin, P., Anisi, M.H., Goksel, F., Gursoy, C. and Buyukgulcu, A. (2020). AgriLoRa: A Digital Twin Framework for Smart Agriculture. *Journal of Wireless Mobile Networks, Ubiquitous Computing, and Dependable Applications (JoWUA)*, 11(4), 77-96.

Attaran, M. and Celik, B.G. (2023). Digital Twin: Benefits, use cases, challenges, and

opportunities. *Decision Analytics Journal*. 6(80),100165.

Barricelli, B. R., Casiraghi, E. and Fogli, D. (2019). A Survey on Digital Twin: Definitions, Characteristics, Applications, and Design Implications. *IEEE Access*. 7, 167653-167671.

Bécue, A., Maia, E., Feeken, L., et al. (2020). A new concept of digital twin supporting optimization and resilience of factories of the future. *Applied Science*. 10(13), 4482.

Consilvio, A., Sanetti, P., Anguìta, D., Crovetto, C., Dambra, C., Oneto, L., Papa, F., and Sacco, N. (2019). Prescriptive maintenance of railway infrastructure: from data analytics to decision support. *6th International Conference on Models and Technologies for Intelligent Transportation Systems (MT-ITS)*, pp. 1-10.

D'Amico, R.D., Erkoyuncu, J.A., Addepalli, S., Penver, S. (2022). Cognitive digital twin: An approach to improve the maintenance management. *CIRP Journal of Manufacturing Science and Technology*. 38, 613-630.

Dangana, M., Ansari, S., Asad, S.M, Hussain, S., Imran, M.A. (2022). Towards the Digital Twin (DT) of Narrow-Band Internet of Things (NBIoT) Wireless Communication in Industrial Indoor. Environment. *Sensors*. 22(23), 9039.

Dinter, R., Tekinerdogan, B., Catal, C. (2022). Predictive maintenance using digital twins: A systematic literature review. *Information and Software Technology*. 151, 107008.

Errandonea, I., Beltran, S., and Arrizabalaga, ´ S. (2020). Digital Twin for maintenance: a literature review. *Comput. Ind.* 123, 103316.

Fan, C., Zhang, C., Yahja A., et al. (2021). Disaster City Digital Twin: A vision for integrating artificial and human intelligence for disaster management. *International Journal of Information Management*. 56: 102049.

Fu, Y., Wang, S., Wang, C. –X, Hong, X. and McLaughlin, S. (2018). Artificial Intelligence to Manage Network Traffic of 5G Wireless Networks. *IEEE Network*. *32(6), (pp. 58-64)*.

Fuller, A., Fan, Z., Day, C., and Barlow, C. (2020). Digital Twin: Enabling Technologies, Challenges and Open Research. *IEEE Access. 8, (pp. 108952-108971)*.

Gao, Y., Li, H., Xiong, G. and Song, H. (2023). AIoT-informed digital twin communication for bridge maintenance. *Automation in Construction*. 150, 104835.

Grigoropoulos, N., Lalis, S. (2020). Simulation and digital twin support for managed drone applications. *IEEE/ACM 24th International Symposium on Distributed Simulation and Real Time Applications (DS-RT). (pp. 1–8)*.

Khan, L. U., Han, Z., Saad, W., Hossain, E., Guizani, M. and Hong, C. S. (2022). Digital Twin of Wireless Systems: Overview, Taxonomy, Challenges, and Opportunities. *IEEE Communications Surveys & Tutorials*. 24 (4), 2230-2254.

Khan, M. S., Jibran, M., Koo, I., Kim, S. M. and Kim, J. (2019). A Double Adaptive Approach to Tackle Malicious Users in Cognitive Radio Networks. *Wireless Communication and Mobile Computing*. Vol.2019,2350964, p. 9.

Li, L., Aslam, S., Wileman, A., et al.(2021). Digital Twin in Aerospace Industry: A Gentle Introduction. IEEE Access, 10, 9543–9562.

Li, R., Zhao, Z., Zhou, X., et al. (2017). Intelligent 5G: when cellular networks meet artificial intelligence. *IEEE Wirel Commun*. 24: 175–183.

Liu, M., Fang, S., Dong, H. and Xu, C. (2021). Review of digital twin about concepts, technologies, and industrial applications. *Journal of Manufacturing Systems*. 58 (Part B), 346-361.

Minerva, R., Lee, G. M. and Crespi, N. (2020). Digital twin in the IoT context: A survey on technical features, scenarios, and architectural models. *Proc. IEEE*. 108(10), pp. 1785–1824.

Nurelmadina, N., Hasan, M.K., Memon, I., Saeed, R.A., Ariffin, K.A.Z., Ali, E.S., Mokhtar, R.A., Islam, S., Hossain, E., Hassan, M.A. (2021). A Systematic Review on Cognitive Radio in Low Power Wide Area Network for Industrial IoT Applications. *Sustainability*. 13,1-22.

Oever, N. (2023). 5G and the notion of network ideology, or: The limitations of sociotechnical imaginaries. *Telecommunications Policy*. 47(5), 102442.

Picone, M., Mamei, M. and Zambonelli, F. (2021). WLDT: A general purpose library to build IoT digital twins. *SoftwareX*. 13, 100661.

Rasheed, A., San, O., and Kvamsdal, T. (2019). Digital twin: Values, challenges and enablers. arXiv preprint arXiv., 1910, 01719.

Siddiqui, M., Kahandawa, G., and Hewawasam, H.S. (2023). Artificial Intelligence Enabled Digital Twin For Predictive Maintenance in Industrial Automation System: A Novel Framework and Case Study. *2023 IEEE International Conference on Mechatronics (ICM) (pp. 1-6)*, Loughborough, United Kingdom.

Tendeng, R., Lee, Y., Koo, I. (2018). Implementation and Measurement of Spectrum Sensing for Cognitive Radio Networks Based on LoRa and GNU Radio. *International Journal of Advanced Smart Convergence*. 7(3), 23-36.

Wu, Y., Zhang, K., and Zhang, Y. (2021). Digital twin networks: A survey. *IEEE Internet Things J*. 8(18), 13789–13804.

Xiong, M., Wang, H., Fu, Q., et al. (2021). Digital twin–driven aero-engine intelligent predictive maintenance. *Int J Adv Manuf Tech.* 114, 3751–3761.

Yalçın, S. (2022). An improved genetic algorithm approach to spectrum sensing for long range based cognitive radio networks. *Transactions on Emerging Telecommunications Technologies*. 33(9), e4526.

Yalçın, S. (2023). An artificial intelligence-based spectrum sensing methodology for LoRa and cognitive radio networks. *International Journal of Communication Systems*. 36(5), e5433.

You, X., Zhang, C., Tan, X., et al. (2019). AI for 5G: research directions and paradigms. *Sci. China Inf. Sci.* 62, 21301.

Yurkevich, E.V, Stepanovskaya, I.A. (2021). Controlling the security of the airport airspace using the digital twin. *J Phys: Conf Ser*. IOP Publishing, 1864(1), 012128.

Zhang, Z., Wen, F., Sun, Z., Guo, X., He, T. and Lee, C. (2022). Artificial Intelligence-Enabled Sensing Technologies in the 5G/Internet of Things Era: From Virtual Reality/Augmented Reality to the Digital Twin. *Advanced Intelligent Systems*. 4(7), 2100228.

Chapter 10

Assessing the Effect of Hexanol and Di-n-Butyl Ether on Diesel Fuel Characteristics

Mert GULUM[1], Sibel OSMAN[2]

[1] *Assistant Prof. Dr.; Karadeniz Technical University, Faculty of Engineering, Mechanical Engineering Department.*
gulum@ktu.edu.tr ORCID No: 0000-0002-1792-3499
[2]*Lecturer Dr. Eng.; Ovidius University of Constanta, Faculty of Applied Sciences and Engineering, Department of Chemistry and Chemical Engineering.*
sibel_o@yahoo.ro ORCID No: 0000-0003-0160-6699

ABSTRACT

Diesel engines play an important role in transportation, construction, and agriculture sectors, and power generation. However, due to the depletion of fossil fuels' reserves and their harmful emissions, clean and sustainable alternative fuels for diesel engines are playing an increasingly important role. In this context, this study investigates the potential of n-hexanol and di-n-butyl ether as alternative fuels to diesel fuel by examining their fuel properties. The investigated fuel properties include density, copper strip corrosion, oxidation stability, sulfur content, ash content, and carbon residue. Eight binary blends of diesel fuel with n-hexanol and di-n-butyl ether at varying concentrations (5%, 10%, 15%, and 20% v/v) are prepared, and their properties are measured and compared to the international standards. The results of this study demonstrate that both n-hexanol and di-n-butyl ether can improve the properties of diesel fuel. The density values of binary blends fall within the acceptable range specified by EN 590 standard. The copper strip corrosion test shows low corrosiveness for all blends, meeting the Class 1 criteria set by EN 590. Oxidation stability is enhanced with the addition of n-hexanol and di-n-butyl ether, leading to diminished total insolubles in the binary blends. Sulfur content in the blends diminishes compared to pure diesel fuel, complying with the sulfur content limit of 10 mg/kg specified by EN 590. Ash content reduces in both n-hexanol and di-n-butyl ether blends, meeting 0.010% (m/m) limit set by EN 590. Carbon residue values remain below 0.1% (m/m) for all binary blends, meeting 0.30% (m/m) maximum threshold of EN 590. Finally, n-hexanol and di-n-butyl ether blends show promise as oxygenated additives for diesel fuel, enhancing diesel fuel properties without exceeding international standard. In future research, the engine performance, combustion, and emissions of diesel engines fuelled with these binary blends under various operating conditions can be focused on.

Keywords: Diesel engine, Fuel property, Diesel fuel, Di-n-butyl ether, Hexanol

INTRODUCTION

Diesel engines are among the primary sources of power worldwide. Given the escalating exhaustion of fossil fuels' reserves and harmful emissions resulting from their combustion, it is imperative for researchers to discover environmentally friendly and sustainable alternative fuels to diminish global reliance on fossil fuels [1, 2]. In this context, in recent years, there has been a growing surge of research interest directed towards higher alcohols and ethers.

n-Hexanol ($C_6H_{14}O$) represents a higher alcohol containing a linear chain of six carbons. This colorless liquid shows slight solubility in water, while it is miscible with diethyl ether and ethanol. The blending of hexanol with biodiesel will result in the enrichment of fuel-rich regions with hydroxyl group radicals. These radicals exhibit catalytic capabilities in promoting the oxidation of hydrocarbon species, thus preventing soot growth reactions. Hexanol lies in its potential as a desirable additive for diesel fuel. This potential stems from its higher heating value (39.1 MJ/kg), elevated cetane number (23), enhanced blend stability with diesel fuel, and reduced hygroscopic nature (less corrosive) in comparison to lower alcohols, such as ethanol and methanol. Hexanol's properties, including density (821 kg/m^3), and viscosity (3.33 mm^2/s at 40°C), more closely resemble those of diesel fuel compared to other alcohols. The oxygen content (wt.%), flash point, boiling point, and vapor pressure of n-hexanol are 15.70%, 58°C, 157°C, and 1 mmHg, respectively. Moreover, n-hexanol represents a type of second-generation biofuel that is produced through the conversion of waste, biomass, or waste syngas generated by industries into fuels [3-8].

Di-n-butyl ether (DBE, $C_8H_{18}O$) emerges as a promising high-reactivity oxygenated candidate with elevated cetane number (up to 100), calorific value (38.7 MJ/kg), volatility (vapor pressure of 6.4 mbar), and lower viscosity (0.64 mm^2/s at 40°C) and density (770 kg/m^3 at 20°C). DBE has a faster spray breakup due to the high volatility, and low surface tension (22.2 mN/m) as well as viscosity. The boiling point and flash point of DBE are 141°C (180-360°C for diesel fuel) and 25°C, respectively. DBE is not soluble in water, which is an advantage in terms of preventing corrosion in engines. The production of DBE can be achieved through the etherification process of n-butanol, which makes it a potentially renewable additive. Given its notable oxygen content (12.3% m/m), DBE presents an appealing substitute for diesel fuel, which carries the potential to decrease smoke emissions [9-13]. Moreover, according to the study given in Ref. [14], the high reactivity of DBE leads to higher thermal efficiency and lower HC and CO emissions.

Fuel properties directly affect performance, emissions, cold flow behaviors, storage period, safety, carbon deposits, and stability and degradation characteristics. For example, density stands as a key property, given its interrelation with cetane number and heating value. Moreover, since diesel engines meter fuel injection volumetrically, fluctuations in density directly affect engine power and fuel consumption. Furthermore, density plays a role in the initiation of injection, injection pressure, and spray characteristics [15, 16]. The copper corrosion test is employed to measure the fuel's potential to corrode fuel system components, especially those made of copper or copper allows. The degree of copper corrosion stands as a vital performance indicator for fuels, given their consistent interaction with metal vessels throughout storage and transportation [17-19]. Fuel's oxidation stability is a crucial characteristic, as the oxidative breakdown of the fuel could result in diminished fuel quality, engine performance, and storage period. In other words, oxidation stability represents a physical property that elucidates the aging tendencies of fuels while they are being transported and stored [20, 21]. An important parameter among diesel fuel properties is sulfur content, which is a key factor in fuel standards. Advanced engine after-treatment systems (diesel particulate filter, lean NO_X trap, and selective catalytic reduction) are affected by fuel sulfur content. Fuels with low sulfur content improve the diesel particulate filter performance. However, the sulfur content of diesel fuel leads to higher sulfate emissions, which increases the total particulate matter emissions [22, 23]. Ultra-low sulfur diesel fuel loses its inherent lubricity characteristics, which results in increased friction within the fuel pump system, and excessive wear on injectors. Carbon residue is the measure of the tendency of a fuel to produce carbon deposits on injector tips, valve seats, and combustion chamber walls [24]. Finally, ash content can result from oil, water-soluble metallic compounds, natural gums, or extraneous solids (dirt and rust), and it can cause blockage of the engine filter [25, 26].

In the existing literature, researchers have more focused on the studies on the effects of n-hexanol and di-n-butyl ether blends with diesel fuel on performance, combustion, and emission characteristics for diesel engines [9, 12, 27-29]. However, the experimental studies of fuel properties of n-hexanol and di-n-butyl ether blends have been less performed. More studies need to be carried out in terms of the fuel properties of n-hexanol and di-n-butyl ether blends before their effects on performance and emissions are investigated. In order to overcome this gap in the existing literature, in this study, the fuel properties noted above (density, copper strip corrosion, oxidation stability, sulfur content, ash content, and carbon residue) of diesel fuel-n-hexanol and

diesel fuel-di-n-butyl ether blends are measured to examine whether they meet international standards.

MATERIALS and METHODS
Preparation of binary blends

In order to carry out this research, n-hexanol ($C_6H_{14}O$) (≥98 %) and di-n-butyl ether ($C_8H_{18}O$) (≥99%) are purchased from the Sigma-Aldrich. These chemicals are subject to no further purification and are used as soon as the bottles are opened. Diesel fuel (DF), which is used as a base fuel to prepare binary blends, is provided by a refinery owned by a local company (Constanta) and does not contain additives. The properties of DF are listed in Table 1. The used DF meets the EN 590 standard.

Table 1: The properties of DF

Property	Units	Method	EN 590 Limits		DF
			Minimum	Maximum	
Density at 15°C	kg/m^3	EN ISO 12185:1996	820	845	842.2
Kinematic viscosity at 40°C	mm^2/s	EN ISO 3104:1996	2.000	4.500	3.0727
Water content	% (m/m)	EN ISO 12937:2000	-	0.020	0.0065
Sulfur content	mg/kg	EN ISO 20846:2019	-	10.0	8.6
Flash point	°C	EN ISO 2719:2016	>55.0	-	61
Cetane number	-	EN ISO 5165:2020	51.0	-	51.6
Carbon residue	% (m/m)	EN ISO 10370:2014	-	0.30	<0.1
Ash	% (m/m)	EN ISO 6245: 2002	-	0.010	0.0016
Cold filter plugging point	°C	EN 116:2015	-	+5 (Summer) -15 (Winter)	-5
Copper corrosion (3h at 50°C)	-	EN ISO 2160	Class 1		1b
Oxidation stability	g/m^3	EN ISO 12205:1999	-	25	8.9
Distillation 250°C	% (v/v)	EN ISO 3405:2019	-	<65	29
Distillation 350°C	% (v/v)		85	-	94
Distillation 95% (v/v)	°C		-	360	357

A total of 8 blends (4 diesel fuel-n-hexanol and 4 diesel fuel-di-n-butyl ether blends) as well as the unblended DF are tested in this study. The oxygenated

components (n-hexanol and di-n-butyl ether) are blended with DF in volumetric proportions of 5%, 10%, 15%, and 20%. Each blend designation is abbreviated with a letter code and a number, as listed in Table 2. All binary blends are prepared on the day of the experiment and kept in a freezer to minimize evaporative losses. These binary blends are perfectly miscible, and no separation is observed.

Table 2: Prepared binary blends

Binary blend	Blending fuel percentage (by volume)
HX5	DF (95%)+ n-hexanol (5%)
HX10	DF (90%)+ n-hexanol (10%)
HX15	DF (85%)+ n-hexanol (15%)
HX20	DF (80%)+ n-hexanol (20%)
DBE5	DF (95%)+ di-n-butyl ether (5%)
DBE10	DF (90%)+ di-n-butyl ether (10%)
DBE15	DF (85%)+ di-n-butyl ether (15%)
DBE20	DF (80%)+ di-n-butyl ether (20%)

Methods

The density, copper corrosion, oxidation stability, sulfur content, ash content, and carbon residue are determined for DF and each blend in accordance with international standards (Ovidius University). The list of equipment used in this study along with their technical specifications and their test methods are presented in Table 3. These properties are measured thrice for each sample. To allow for a better evaluation of the qualities of the studied binary blends, DF is used as a comparative sample.

Table 3: The methods and equipments used for the determination of the property of binary blends

Properties	Standard method	Equipment	Repeatability	Reproducibility
Density	ASTM D4052/ EN ISO 12185	Anton Paar - SVM 3000	0.00005 g/cm^3	0.0001 g/cm^3
Oxidation stability	EN ISO 12205	STANHOPE-SETA	$5.4 \cdot (x/10)^{0.25}$	$10.6 \cdot (x/10)^{0.25}$
Copper corrosion (3h at 50ºC)	EN ISO 2160	SETA OXICOR	-	-
Sulfur content	EN ISO 20846:2019	XPlorerSulhur Analyzer,Trace Elemental Instruments	0.6	1.9
Ash content	EN ISO 6245:2002	Bunsen gas bulb/Carbolite oven	0.003%	0.005%
Carbon residue	EN ISO 10370:2014	Micro method MCRT-140, Petroleum	$0.03161 \cdot (x+3)$	$0.04681 \cdot (x+3)$

x: Experimental data

RESULTS and DISCUSSION

Density at 15°C

The density values of the diesel fuel-n-hexanol (DF-HX) and diesel fuel-di-n-butyl ether (DF-DBE) blends are measured at 15°C and presented in Figure 1. It is observed that density decreases with the increase of HX and DBE concentrations in the blends because the densities of di-n-butyl ether (770 kg/m^3) and n-hexanol (821 kg/m^3) are lower than that of DF (842.2 kg/m^3). HX blends have density values between 837 and 840.6 kg/m^3 while DBE blends have density values between 828 and 838.5 kg/m^3. The densities of HX5, HX10, HX15, and HX20 are 0.19%, 0.33%, 0.47%, and 0.62% lower than that of DF, respectively. The densities of DBE5, DBE10, DBE15, and DBE20 are 0.44%, 0.85%, 1.27%, and 1.69% lower than that of DF, respectively. As shown in Figure 1, DBE blends experience the most significant decrease. The densities of all binary blends comply with the values set by the EN 590 norm (820 and 845 kg/m^3).
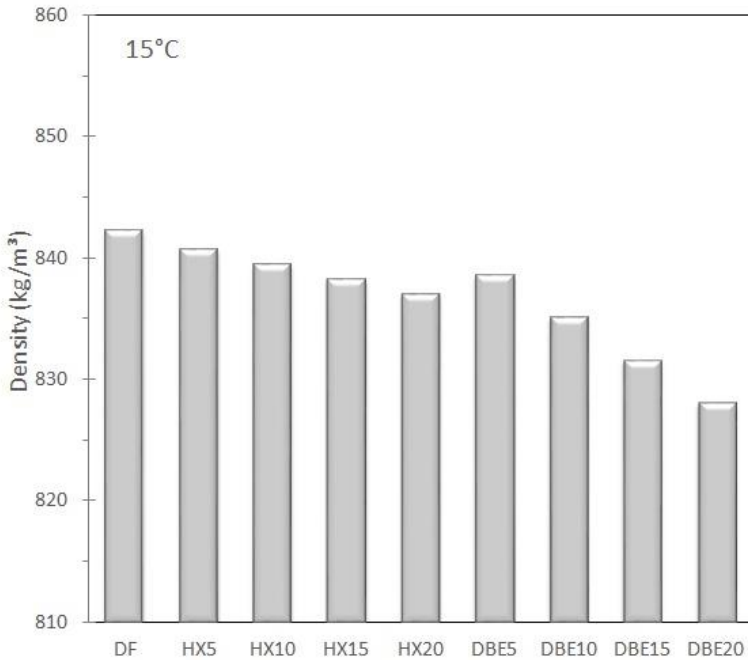
Figure 1: Densities of DF-HX and DF-DBE blends

Copper strip corrosion at 50°C

Copper strip corrosion is a property in determining the tendency of a fuel to corrode the engine fuel system components made up of copper, zinc, and bronze [24]. For copper corrosion, DF-HX and DF-DBE blends give the same results. In other words, the copper strip presents the same color after being heated at 50°C (Class 1). It is found that all samples have a low degree of corrosiveness and comply with the limit as defined in EN 590. This result is attributed to the fact that n-hexanol is less hygroscopic and corrosive, and DBE is not soluble in water [13, 30, 31].

Oxidation stability

Oxidation stability is a parameter that describes the degradation tendency of a fuel under some conditions (the presence of heat, oxygen, water, metal ions, and other impurities) [32]. The main oxidation products are peroxides and hydroperoxides. [33, 34]. Since oxidative stability affects fuel quality, oxidation stability quality requirements have been included in the EN 590 for diesel fuel [35]. To determine the amount of deposits that may potentially be developed from the degradation of a fuel, EN ISO 12205 test is used in this study. The test determines the total amount of filterable and adherent (non-filterable, gum) insolubles [36].

Figure 2 presents the oxidation stability of DF-HX and DF-DBE blends. In the case of all fuel blends, their total insolubles decrease with increasing HX and DBE content (i.e. the oxidation stability improves). DBE5 is found to contain filterable and adherent insolubles of a total of 8.7 g/m^3. Similar values are obtained for DBE10, with the content of filterable and adherent insolubles having the value of 8.5 g/m^3. In the case of DBE15 and DBE20, the values are measured as 8.1 g/m^3 and 7.5 g/m^3, respectively. These results show a 2.25%, 4.49%, 8.99%, and 15.73% decrease, compared with the initial value of insolubles of DF (8.9 g/m^3). Moreover, HX5, HX10, HX15, and HX20 exhibit 8.8 g/m^3, 8.6 g/m^3, 7.7 g/m^3, and 7.4 g/m^3 total insolubles, respectively. According to these results, there is a 1.12%, 3.37%, 13.48%, and 16.85% decrease in the deposits (filterable and adherent) for HX5, HX10, HX15, and HX20, compared to the initial value of insolubles of DF (8.9 g/m^3). As a result, all binary blends meet EN 590 standard in terms of oxidation stability (maximum 25 g/m^3). In the case of DF, the formation of deposits is caused by the presence of fuel compounds containing nitrogen and sulfur, reactive olefins, and organic acids which are precursors of macromolecular structures having limited solubility [37]. The addition of HX and DBE has led to the formation of a low amount of deposits. In other words, the alcohol and ether slow down the hydrocarbon degradation.
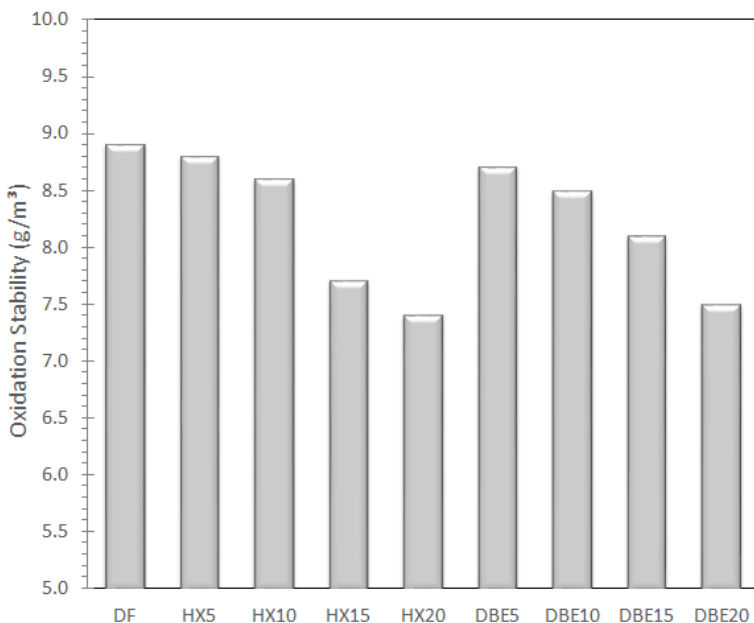

Figure 2: Oxidation stabilities of DF-HX and DF-DBE blends during storage

Sulfur content

Figure 3 shows the sulfur contents of DF-HX and DF-DBE blends. The sulfur contents of HX5, HX10, HX15, and HX20 blends are measured to be 8 ppm, 7.2 ppm, 6.8 ppm, and 6 ppm, respectively. According to the results, there is a 6.98%, 16.28%, 20.93%, and 30.23% decrease in the sulfur content of HX5, HX10, HX15, and HX20 blends, compared to the initial value of sulfur content of DF (8.6 ppm). For DBE5, DBE10, DBE15, and DBE20 blends, the sulfur content values are measured to be 8.4 ppm, 8.1 ppm, 7.3 ppm, and 6.2 ppm. The sulfur contents of DBE5, DBE10, DBE15, and DBE20 blends are 2.33%, 5.81%, 15.12%, and 27.91% lower than that of DF (8.6 ppm). According to the results, all blends are in accordance with the EN 590 standard in terms of sulfur content (maximum limit of 10 mg/kg).
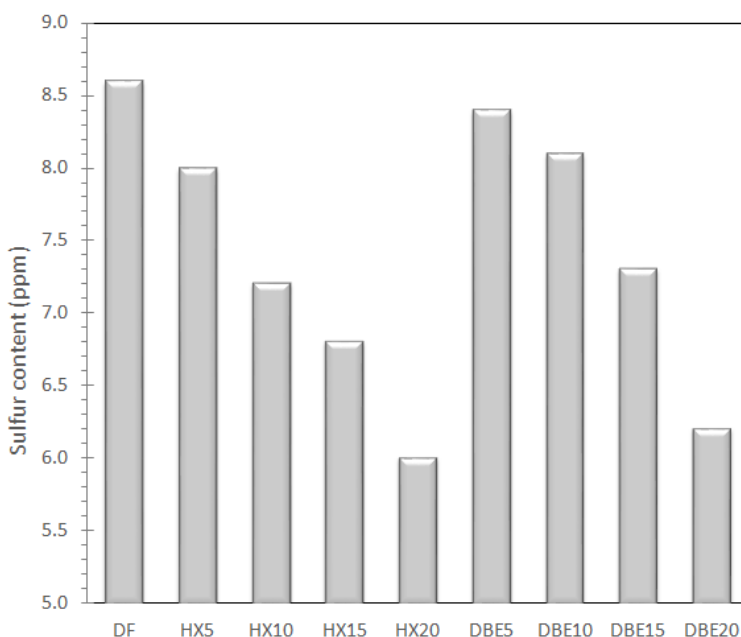
Figure 3: Sulfur content of DF-HX and DF-DBE blends

Ash content

Figure 4 shows the ash contents of DF-HX and DF-DBE blends. The ash content of HX5, HX10, HX15, and HX20 blends is measured as 0.0014% m/m, 0.0012% m/m, 0.0011% m/m, and 0.0010% m/m, while the ash content of DBE5, DBE10, DBE15, and DBE20 blends is measured as 0.0015% m/m, 0.0014% m/m, 0.0013 m/m, and 0.0012% m/m, respectively. Results exhibit that HX blends have a decrease of 12.5%, 25%, 31.25%, and 37.5%, and DBE blends have a decrease of 6.25%, 12.5%, 18.75%, and 25% in the ash content,

compared to DF (0.0016% m/m). It is concluded that the use of HX and DBE as an additive would contribute towards lessening the ash content. All blends are in accordance with EN 590 standard in terms of ash content (maximum limit of 0.010% m/m).

Figure 4: Ash content of DF-HX and DF-DBE blends
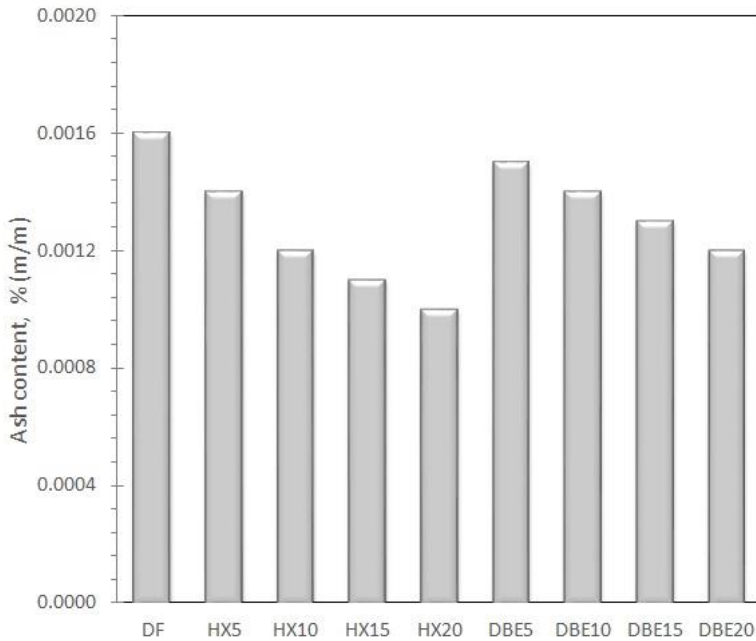
Carbon residue

The amount of carbon residue is a measure of the tendency of a fuel to form carbonaceous deposits in engines, causing hot spots leading to stress, corrosion, or cracking [38]. Most of the deposits are found in the nozzles of fuel injectors. There is a correlation between carbon content in fuel and deposits, which is why a carbon residue test is used [39]. The carbon residue of DF is <0.1% (m/m). All binary blends have also carbon residue values lower than 0.1% (m/m). According to the results, the blends meet EN 590 standard in terms of carbon residue (maximum limit of 0.30% m/m).

CONCLUSIONS

Hexanol and di-n-butyl ether have risen as promising oxygenated candidates for diesel engines due to their favorable properties. Owing to its elevated volatility and low surface tension, along with its low viscosity, di-n-butyl ether exhibits an accelerated spray breakup. It has high a cetane number (up to 100).

It has a notable oxygen content (12.3% m/m), which decreases the potential smoke emissions. Moreover, n-hexanol exhibits higher heating value, cetane number, and blend stability with diesel fuel, compared to lower alcohols. The main conclusions from this study are listed as follows:

- The density values of HX5, HX10, HX15, and HX20 are 0.19%, 0.33%, 0.47%, and 0.62% lower than that of DF, respectively. Similarly, the density values of DBE5, DBE10, DBE15, and DBE20 are 0.44%, 0.85%, 1.27%, and 1.69% lower than that of DF, respectively. Blends containing HX show density values ranging between 840.6 and 837 kg/m^3, while blends containing DBE show density values ranging between 838.5 and 828 kg/m^3. The densities of both DF-HX and DF-DBE blends conform to the density standard set by the EN 590 regulation.

- In terms of copper strip corrosion, both the DF-HX and DF-DBE blends exhibit identical outcomes. In other words, all samples exhibit low corrosive effects, adhering to the stipulated limit as outlined in EN 590 (Class 1).

- There is a reduction of 2.25%, 4.49%, 8.99%, and 15.73% in the total insolubles values of DBE5, DBE10, DBE15, and DBE20, compared to DF. Moreover, there is a decrease of 1.12%, 3.37%, 13.48%, and 16.85% in the total insolubles for HX5, HX10, HX15, and HX20, respectively, compared to DF. Consequently, all blends satisfy EN 590 standard concerning oxidation stability.

- The sulfur content in HX5, HX10, HX15, and HX20 decreases by 6.98%, 16.28%, 20.93%, and 30.23%, respectively, compared to DF. For DBE5, DBE10, DBE15, and DBE20, the sulfur content is 2.33%, 5.81%, 15.12%, and 27.91% lower than that of DF. According to the results, all blends comply with EN 590 standard in terms of sulfur content (maximum limit of 10 mg/kg).

- HX5, HX10, HX15, and HX20 show a reduction in ash content by 12.5%, 25%, 31.25%, and 37.5%, while DBE5, DBE10, DBE15, and DBE20 exhibit a decrease of 6.25%, 12.5%, 18.75%, and 25% compared to DF. All blends conform to the EN 590 standard with respect to ash content, which has a maximum limit of 0.010% (m/m).

- Binary blends exhibit carbon residue values below 0.1% (m/m), which shows that they are in compliance with EN 590 standard concerning carbon residue (maximum threshold of 0.30% m/m).

As a future study, for a better understanding and application of DF-HX and DF-DBE blends as alternative fuels, their effects on engine performance, combustion, and exhaust emissions of diesel engines under various operating conditions can be studied. Optimum blending ratios can be determined using machine learning methods. Since economic sustainability and commercial viability are very important, cost analysis of these blends can be performed.

REFERENCES

[1] Liu, J., Huang, Q., Ulishney, C., & Dumitrescu, C. E. (2022). Comparison of random forest and neural network in modeling the performance and emissions of a natural gas spark ignition engine. Journal of Energy Resources Technology, 144(3), 032310.

[2] Tan, D., Wu, Y., Lv, J., Li, J., Ou, X., Meng, Y., ... & Zhang, Z. (2023). Performance optimization of a diesel engine fueled with hydrogen/biodiesel with water addition based on the response surface methodology. Energy, 263, 125869.

[3] Thomas, J. J., Nagarajan, G., Sabu, V. R., Manojkumar, C. V., & Sharma, V. (2022). Performance and emissions of hexanol-biodiesel fuelled RCCI engine with double injection strategies. Energy, 253, 124069.

[4] Nour, M., Sun, Z., El-Seesy, A. I., & Li, X. (2021). Experimental evaluation of the performance and emissions of a direct-injection compression-ignition engine fueled with n-hexanol–diesel blends. Fuel, 302, 121144.

[5] De Poures, M. V., Sathiyagnanam, A. P., Rana, D., Kumar, B. R., & Saravanan, S. (2017). 1-Hexanol as a sustainable biofuel in DI diesel engines and its effect on combustion and emissions under the influence of injection timing and exhaust gas recirculation (EGR). Applied Thermal Engineering, 113, 1505-1513.

[6] Campos-Fernandez, J., Arnal, J. M., Gomez, J., Lacalle, N., & Dorado, M. P. (2013). Performance tests of a diesel engine fueled with pentanol/diesel fuel blends. Fuel, 107, 866-872.

[7] Murcak, A., Haşimoğlu, C., Çevik, İ., Karabektaş, M., & Ergen, G. (2013). Effects of ethanol–diesel blends to performance of a DI diesel engine for different injection timings. Fuel, 109, 582-587.

[8] Pandian, A. K., Munuswamy, D. B., Radhakrishanan, S., Devarajan, Y., Ramakrishnan, R. B. B., & Nagappan, B. (2018). Emission and performance analysis of a diesel engine burning cashew nut shell oil bio diesel mixed with hexanol. Petroleum Science, 15, 176-184.

[9] Garcia, A., Monsalve-Serrano, J., Villalta, D., Zubel, M., & Pischinger, S. (2018). Potential of 1-octanol and di-n-butyl ether (DNBE) to improve the performance and reduce the emissions of a direct injected compression ignition diesel engine. Energy Conversion and Management, 177, 563-571.

[10] Frigo, S., Pasini, G., Caposciutti, G., Antonelli, M., Galletti, A. M. R., Gori, S., ... & Arnone, L. (2021). Utilisation of advanced biofuel in CI internal combustion engine. Fuel, 297, 120742.

[11] Ahmad, S., Jafry, A. T., Haq, M. U., Asif, M., Ahmad, K., & Zafar, F. U. (2023). Experimental study of castor biodiesel ternary blends with ethanol, butanol, diethyl ether and dibutyl ether in a diesel engine. Journal of Thermal Analysis and Calorimetry, 148(3), 927-941.

[12] Wang, Q., Yin, S., & Ni, J. (2021). The effects of n-pentanol, di-n-butyl ether (DBE) and exhaust gas recirculation on performance and emissions in a compression ignition engine. Fuel, 284, 118961.

[13] Thion, S., Togbé, C., Serinyel, Z., Dayma, G., & Dagaut, P. (2017). A chemical kinetic study of the oxidation of dibutyl-ether in a jet-stirred reactor. Combustion and Flame, 185, 4-15.

[14] Zubel, M., Pischinger, S., & Heuser, B. (2017). Assessment of the full thermodynamic potential of C8-oxygenates for clean diesel combustion. SAE International Journal of Fuels and Lubricants, 10(3), 913-923.

[15] Alptekin, E., & Canakci, M. (2008). Determination of the density and the viscosities of biodiesel–diesel fuel blends. Renewable Energy, 33(12), 2623-2630.

[16] Tesfa, B., Mishra, R., Gu, F., & Powles, N. (2010). Prediction models for density and viscosity of biodiesel and their effects on fuel supply system in CI engines. Renewable Energy, 35(12), 2752-2760.

[17] Arun, S. B., Karthik, B. M., Yatish, K. V., Prashanth, K. N., & Balakrishna, G. R. (2023). Green synthesis of copper oxide nanoparticles using the Bombax ceiba plant: Biodiesel production and nano-additive to investigate diesel engine performance-emission characteristics. Energy, 274, 127345.

[18] Linglin, L., Fashe, L., Huicong, Z., Yaozong, D., & Wenchao, W. (2023). Efficient removal of alkali and alkaline earth metals from biodiesel using Ion-exchange resin: Performance and mechanism. Separation and Purification Technology, 323, 124485.

[19] Micayabas, K. C. C., Tingalan, D. R., Pacturan, K. N., Singgil, D. J. B., Saldo, I. J. P., Casas, R. Y., & Peñafiel-Dandoy, M. J. (2023). Comparative assessment of mixed biodiesel and commercial diesel on a dual fuel mode generator. American Journal of Energy Research, 11(3), 117-127.

[20] Khan, E., Ozaltin, K., Spagnuolo, D., Bernal-Ballen, A., Piskunov, M. V., & Di Martino, A. (2023). Biodiesel from rapeseed and sunflower oil: effect of the transesterification conditions and oxidation stability. Energies, 16(2), 657.

[21] Rajamohan, S., Gopal, A. H., Muralidharan, K. R., Huang, Z., Paramasivam, B., Ayyasamy, T., ... & Hoang, A. T. (2022). Evaluation of oxidation stability and engine behaviors operated by Prosopis juliflora biodiesel/diesel fuel blends with presence of synthetic antioxidant. Sustainable Energy Technologies and Assessments, 52, 102086.

[22] Tan, P. Q., Hu, Z. Y., & Lou, D. M. (2009). Regulated and unregulated emissions from a light-duty diesel engine with different sulfur content fuels. Fuel, 88(6), 1086-1091.

[23] Karonis, D., Lois, E., Zannikos, F., Alexandridis, A., & Sarimveis, H. (2003). A neural network approach for the correlation of exhaust emissions from a diesel engine with diesel fuel properties. Energy & Fuels, 17(5), 1259-1265.

[24] Kakati, J., Gogoi, T. K., & Pakshirajan, K. (2017). Production of biodiesel from Amari (Amoora Wallichii King) tree seeds using optimum process parameters and its characterization. Energy Conversion and Management, 135, 281-290.

[25] Momin, M., & Deka, D. C. (2015). Fuel property of biodiesel and petrodiesel mix: experiment with biodiesel from yellow oleander seed oil. Biofuels, 6(5-6), 269-272.

[26] Belagur, V. K., & Chitimi, V. R. (2013). Few physical, chemical and fuel related properties of calophyllum inophyllum linn (honne) oil and its blends with diesel fuel for their use in diesel engine. Fuel, 109, 356-361.

[27] Babu, D., & Anand, R. (2017). Effect of biodiesel-diesel-n-pentanol and biodiesel-diesel-n-hexanol blends on diesel engine emission and combustion characteristics. Energy, 133, 761-776.

[28] Duraisamy, S., Kasirajan, L., Krishnamoorthy, S., Kadasari, R., & Tiruchengode, R. C. (2020). Performance test and emission characteristics of diesel fuel blended with n-Hexanol. Thermal Science, 24(1 Part B), 557-564.

[29] Singh, A. K., Khan, M. M., & Pali, H. S. (2021, November). Investigation of 1-hexanol diesel blends on performance, combustion and emission characteristics of a diesel engine. In Journal of Physics: Conference Series (Vol. 2062, No. 1, p. 012028). IOP Publishing.

[30] EL-Seesy, A. I., Kayatas, Z., Takayama, R., He, Z., Kandasamy, S., & Kosaka, H. (2020). Combustion and emission characteristics of RCEM and common rail diesel engine working with diesel fuel and ethanol/hydrous ethanol injected in the intake and exhaust port:

Assessment and comparison. Energy Conversion and Management, 205, 112453.

[31] Kumar, B. R., & Saravanan, S. (2016). Use of higher alcohol biofuels in diesel engines: A review. Renewable and Sustainable Energy Reviews, 60, 84-115.

[32] Kumar, S., Yadav, K., & Dwivedi, G. (2018). Impact analysis of oxidation stability for biodiesel & its blends. Materials Today: Proceedings, 5(9), 19255-19261.

[33] Karavalakis, G., Karonis, D., & Stournas, S. (2009). Evaluation of the oxidation stability of diesel/biodiesel blends using the modified rancimat method. SAE International Journal of Fuels and Lubricants, 2(1), 839-849.

[34] Karavalakis, G., & Stournas, S. (2010). Impact of antioxidant additives on the oxidation stability of diesel/biodiesel blends. Energy & Fuels, 24(6), 3682-3686.

[35] CEN (2010). Automotive fuels-diesel-requirements and test methods. EN 590. Brussels: Comité Européen de Normalisation.

[36] Beck, Á., Pölczmann, G., Eller, Z., & Hancsók, J. (2014). Investigation of the effect of detergent–dispersant additives on the oxidation stability of biodiesel, diesel fuel and their blends. Biomass and Bioenergy, 66, 328-336.

[37] Odziemkowska, M., Czarnocka, J., & Wawryniuk, K. (2018). Study of stability changes of model fuel blends. in: Ceper, B. A., and Yıldız, M. (Eds.), Improvement Trends for Internal Combustion Engines, IntechOpen. ISBN: 978-953-51-3892-1.

[38] https://www.mbie.govt.nz/assets/ee29238801/reviewing-aspects-of-the-engine-fuel-specifications-regulations-2011.pdf?. Ministry of business, innovation & employment. Reviewing aspects of the engine fuel specifications regulations 2011. ISBN 978-0-908335-31-2. Accessed: 07.09.2023.

[39] Bezergianni, S., & Dimitriadis, A. (2013). Comparison between different types of renewable diesel. Renewable and Sustainable Energy Reviews, 21, 110-116.

Chapter 11

A Metal of Innovation: The History of Titanium Use in Biomedical Applications

Muhammet Taha ACAR[1]

[1] *Asst. Prof.; Erzincan Binali Yildirim University, Engineering Faculty, Mechanical Engineering Department. taha.acar@erzincan.edu.tr*

ABSTRACT

Titanium, a lustrous and resilient metal known for its remarkable strength-to-weight ratio and biocompatibility, has revolutionized the field of biomedical engineering and healthcare.

Titanium, a remarkable metal known for its exceptional properties, has become an integral part of various industries, from aerospace to healthcare. Its high strength-to-weight ratio, corrosion resistance, and biocompatibility make it a sought-after material. To better understand and utilize titanium, it is essential to delve into its classification based on different factors.

Titanium, a lightweight and corrosion-resistant metal, has revolutionized the field of biomedical engineering over the past few decades. Its unique combination of properties makes it an ideal choice for a wide range of medical devices and implants. From dental implants to joint replacements, titanium has become an integral material in modern healthcare.

However, to maximize their performance and biocompatibility, surface modifications are often necessary. Surface coating methods offer a versatile approach to achieve biocompatible structures longevity of implants.

Keywords: Titanium, Biomedical Applications, Surface treatments

INTRODUCTION

The history of titanium's use in biomedical applications is a compelling narrative of scientific innovation and technological advancement intersecting with the realm of healthcare. Titanium, a metal renowned for its exceptional properties, has emerged as a pivotal player in transforming the landscape of medical devices and implants (Kumaravel et al., 2021). This journey through time takes us from its early discovery and exploration to its contemporary prominence as a fundamental material in improving the quality of life for countless individuals.

The story begins with the isolation of titanium as an element in the late 18th century, a feat achieved through the tireless efforts of chemists and metallurgists. However, it wasn't until the mid-20th century that titanium's unique attributes, including its remarkable strength-to-weight ratio, corrosion resistance, and biocompatibility, captured the attention of the medical community (Hecht, 2010).

The pivotal moment in titanium's integration into medicine came with the development of titanium alloys, such as Ti-6Al-4V, which offered a perfect combination of mechanical strength and biocompatibility. These alloys became the foundation for a wide array of medical applications, ranging from orthopedic implants to dental prosthetics (Roach, 2007).

Throughout the years, the use of titanium expanded beyond the confines of surgical instruments and joint replacements to encompass cardiac implants, spinal devices, and even dental implants that forever transformed the lives of those with missing teeth (Esposito et al., 2008). The rise of 3D printing and advanced manufacturing techniques further accelerated the customization and precision of titanium-based medical solutions, allowing for patient-specific implants and improved surgical outcomes (Guo et al., 2022).

As we traverse this historical journey, we will explore the groundbreaking discoveries, pioneering research, and the collaborative efforts of scientists, engineers, and healthcare professionals that have propelled titanium to the forefront of biomedical applications. This chronicle not only highlights the material's remarkable properties but also underscores its enduring impact on the well-being and quality of life for patients worldwide. In this unfolding narrative, we witness the seamless fusion of science, technology, and medicine, making the history of titanium in biomedical applications a testament to human ingenuity and innovation (Awad et al., 2021).

THE DISCOVERY OF TITANIUM

The discovery of titanium can be attributed to several scientists, but it was the English clergyman and amateur geologist William Gregor who first identified

titanium in 1791(Baker, 2019). He found it while analyzing the mineral ilmenite in Cornwall, England. Gregor initially referred to it as "manaccanite" after the nearby village of Manaccan but later recognized it as a new element and named it "titanium" after the Titans of Greek mythology, reflecting its impressive strength (Jorge et al., 2013).

Early Biomedical Applications

Despite its early discovery, titanium's use in biomedical applications didn't gain traction until the mid-20th century. During World War II, titanium was employed in military and aerospace industries, leading to a deeper understanding of its remarkable properties. In the 1950s, researchers began exploring its potential in medical devices (Tan & Ramakrishna, 2021).

One of the first documented biomedical applications of titanium was in dental implants. In 1952, Swedish orthopedic surgeon Per-Ingvar Brånemark accidentally discovered the metal's affinity for bone tissue when he observed that a titanium chamber he had inserted into a rabbit's leg bone had fused with the bone, a phenomenon he termed "osseointegration"(Citron & Nerem, 2004). This breakthrough laid the foundation for the development of modern dental and orthopedic implants.

Titanium in Orthopedics

The use of titanium in orthopedic implants grew rapidly in the latter half of the 20th century (Van Noort, 1987). Its biocompatibility and mechanical properties made it an ideal material for hip and knee replacements, spinal fusion devices, and bone plates (Levine et al., 2006). These titanium-based implants offered several advantages over traditional materials, including reduced corrosion, increased longevity, and improved patient outcomes (Manivasagam et al., 2010).

Titanium's Role in Cardiovascular Medicine

Titanium has also made significant contributions to cardiovascular medicine. Its biocompatibility and resistance to corrosion make it an excellent choice for heart valve prostheses, stents, and pacemaker casings (Williams, 2008). The use of titanium in these devices has enhanced their performance and durability, ultimately improving the lives of countless individuals with cardiovascular conditions.

Dental and Craniofacial Implants

In the field of dentistry, titanium dental implants have become the gold standard for replacing missing teeth. These implants, which are surgically inserted into the jawbone, provide a stable foundation for prosthetic teeth (Zitzmann & Marinello, 2002). They have revolutionized oral rehabilitation and have had a profound impact on patients' quality of life.

Moreover, titanium's biocompatibility has expanded its use in craniofacial and maxillofacial surgeries, where it is employed to reconstruct facial bones and enhance facial aesthetics. Custom-made titanium implants can be precisely tailored to each patient's unique anatomical needs, ensuring optimal results.

Recent Advances and Future Prospects

As technology and materials science continue to advance, titanium's role in biomedical applications is poised to expand further. Researchers are exploring the use of titanium in 3D-printed implants, tissue engineering, and drug delivery systems (Hua et al., 2021). These innovations hold the promise of improving patient outcomes and expanding the scope of medical treatments.

The history of titanium's use in biomedical applications is a testament to human ingenuity and innovation. From its accidental discovery in the late 18th century to its pivotal role in modern medicine, titanium has transformed healthcare and improved the lives of countless individuals worldwide (Qadri et al., 2020). As science and engineering continue to evolve, we can expect titanium to remain at the forefront of medical advancements, ushering in new possibilities for the future of healthcare.

EXPLORING THE CLASSIFICATION OF TITANIUM MATERIALS

Classification by Grade

One of the primary ways to classify titanium materials is by grade, which is determined by the chemical composition and mechanical properties of the material. The most common titanium grades include**:**

Commercially Pure Titanium (CP): CP titanium is divided into several grades, with Grade 1 to Grade 4 being the most common. These grades contain varying levels of oxygen, nitrogen, carbon, and iron. Grade 1 is the purest form, while Grade 4 contains slightly more impurities. CP titanium is known for its excellent corrosion resistance, formability, and weldability, making it suitable for applications in chemical processing, marine environments, and medical devices (Ronoh et al., 2022).

Titanium Alloys: Titanium alloys are created by adding specific elements such as aluminum, vanadium, and nickel to pure titanium. These alloys are classified into three main categories:

Alpha Alloys: These alloys primarily consist of alpha-phase titanium, making them highly ductile and easy to weld (Boyer, 1996). They are used in industries like aerospace for components requiring high strength and low weight.

Beta Alloys: Beta alloys, which consist mainly of beta-phase titanium, offer an excellent combination of strength and corrosion resistance. They find applications in aerospace and the automotive industry (Cotton et al., 2015).

Alpha-Beta Alloys: These alloys contain a mix of both alpha and beta phases, providing a balance between strength, formability, and weldability. They are commonly used in various industrial and medical applications.

Classification by Form
Titanium materials are also classified by their physical form, which includes:

Titanium Sheets and Plates: These are flat, rectangular pieces of titanium available in various thicknesses. They are used in aerospace, chemical processing, and medical devices, among other industries.

Titanium Bars and Rods: Titanium bars and rods are cylindrical forms of titanium, often used in structural components, fasteners, and medical implants.

Titanium Tubes and Pipes: Titanium tubes and pipes are hollow structures, widely employed in heat exchangers, chemical reactors, and pipelines due to their corrosion resistance and heat transfer properties.

Titanium Wire: Titanium wire is used in welding applications, as well as in the production of springs, orthodontic devices, and jewelry**.**

Classification by Application
Titanium materials find diverse applications across multiple industries. Some of the notable applications include:

Aerospace: Titanium's high strength-to-weight ratio makes it an ideal choice for aircraft components, such as airframes, landing gear, and engine components**.**

Medical and Healthcare: Titanium's biocompatibility and corrosion resistance make it suitable for medical implants like dental implants, orthopedic implants, and surgical instruments.

Chemical Processing: The exceptional corrosion resistance of titanium makes it valuable in chemical processing equipment, including tanks, reactors, and valves**.**

Automotive: Titanium alloys are used in the automotive industry for lightweight components, improving fuel efficiency and performance**.**

The classification of titanium materials is a crucial aspect of understanding and utilizing this versatile metal. By considering factors such as grade, form, and application, engineers and manufacturers can choose the most appropriate titanium material for their specific needs. Whether it's aerospace, medical, or industrial applications, titanium continues to play a pivotal role in advancing technology and improving the quality of life. As research and development in titanium materials continue to evolve, we can expect even more innovative applications in the future.

USE OF TITANIUM IN VARIOUS BIOMEDICAL APPLICATIONS

Titanium, a lightweight and corrosion-resistant metal, has revolutionized the field of biomedical engineering over the past few decades. Its unique combination of properties makes it an ideal choice for a wide range of medical devices and implants. From dental implants to joint replacements, titanium has become an integral material in modern healthcare. In this article, we will explore the incredible versatility and significance of titanium in various biomedical applications (Bosshardt et al., 2017).

Dental Implants

Dental implants have transformed the way people regain their smiles and dental function. Titanium's biocompatibility, strength, and resistance to corrosion make it the preferred material for dental implants (Grandin et al., 2012). When titanium implants are inserted into the jawbone, they fuse with the surrounding bone tissue through a process called osseointegration. This strong bond ensures the stability and long-term success of dental implants, allowing patients to enjoy natural-looking and functioning teeth for many years.

Orthopedic Implants

Titanium is also extensively used in orthopedic implants, such as hip and knee replacements. These implants require materials that can withstand the mechanical stresses of daily activities while minimizing the risk of infection and tissue rejection. Titanium's excellent strength-to-weight ratio, corrosion resistance, and biocompatibility make it a prime candidate for these applications (Verma, 2020). Patients with titanium orthopedic implants experience improved mobility and quality of life.

Surgical Instruments

Titanium's advantageous properties extend to the production of surgical instruments. Instruments made from titanium are not only lightweight but also exceptionally strong and durable. Surgeons and medical professionals benefit from the reduced fatigue associated with lighter instruments during prolonged procedures. Additionally, titanium's resistance to corrosion ensures that these instruments remain sterile and reliable over time.

Cardiovascular Devices

In the realm of cardiovascular medicine, titanium has found its place in the production of stents and pacemakers. Stents, which are used to keep arteries open and prevent blockages, require materials that are both biocompatible and flexible. Titanium's compatibility with bodily tissues and its ability to maintain its structural integrity make it an excellent choice for these life-saving devices.

Prosthetics

Prosthetic limbs and devices have undergone a remarkable transformation, thanks in part to the use of titanium. The metal's lightweight nature, durability, and biocompatibility have made it an ideal material for crafting prosthetic components. This enables amputees to regain mobility and lead active lives.

Imaging and Diagnostic Equipment

Even beyond implants and instruments, titanium plays a vital role in biomedical imaging and diagnostic equipment. It is used in components such as MRI coils and frames for CT scanners. The material's low magnetic susceptibility and high strength make it well-suited for ensuring the accuracy and longevity of these essential medical devices.

Biocompatibility and Allergenicity

One of titanium's key attributes in biomedical applications is its exceptional biocompatibility. Biocompatibility refers to the ability of a material to interact with biological systems without causing harm or triggering an immune response (Brown & Badylak, 2013). Titanium's surface readily forms a biologically inert oxide layer, which minimizes the risk of adverse reactions when it comes into contact with bodily tissues.

Moreover, titanium is non-allergenic, making it suitable for individuals with metal allergies or sensitivities. This feature is particularly advantageous when selecting materials for implants and medical devices, as allergic reactions can lead to complications and discomfort in patients.

The use of titanium in biomedical applications has revolutionized the field of medicine, enhanced patient outcomes and improving the quality of life for countless individuals. Its unique combination of biocompatibility, strength, and resistance to corrosion makes it an ideal choice for a wide range of medical devices and implants. As technology continues to advance, it is likely that titanium will play an even more significant role in shaping the future of healthcare, enabling innovative solutions for complex medical challenges.

SURFACE TREATMENTS FOR TITANIUM MATERIALS: EXPLORING ADVANTAGES AND DISADVANTAGES

Anodizing

Anodization is an electrochemical process that forms a porous oxide layer on the titanium surface, primarily producing titanium dioxide (TiO_2) (Grandin et al., 2012). This method improves osseointegration by increasing surface roughness and wettability. Anodization is cost-effective and environmentally friendly but may lack control over coating thickness.

Advantages:

Enhanced corrosion resistance: The anodized layer acts as a robust barrier against corrosion, making titanium suitable for harsh environments.

Improved wear resistance: Anodizing increases surface hardness, resulting in enhanced durability and wear resistance.

Aesthetic appeal: Anodized titanium offers vibrant color options for decorative and branding purposes.

Disadvantages:

Limited thickness control: Achieving precise and uniform thickness of the anodized layer can be challenging.

Limited color range: Anodized colors may not match specific application needs.

Plasma Spray Coating

Plasma spraying is a widely used technique for coating titanium implants with biocompatible materials such as hydroxyapatite (HA) or titanium nitride (TiN) (Roşu et al., 2012). This method involves melting and spraying the coating material onto the titanium surface. The advantages of plasma spraying include good adhesion, the ability to control coating thickness, and versatility in material choices. However, it may suffer from poor coating uniformity and may require post-treatment to improve adhesion.

Advantages:

Exceptional wear resistance: Plasma-sprayed coatings significantly bolster titanium's wear resistance.

High-temperature performance: Some coatings withstand extreme temperatures, making them ideal for aerospace and industrial uses.

Customizable properties: Engineers can tailor surface properties by selecting different coating materials.

Disadvantages:

Adhesion challenges: Ensuring strong adhesion between the coating and the titanium substrate can be problematic, potentially leading to delamination.

Surface roughness: Plasma spraying can yield a rough surface finish, unsuitable for applications requiring a smooth surface.

Passivation

Passivation is a surface treatment process used to enhance the corrosion resistance of metal surfaces, particularly those made of stainless steel or other corrosion-resistant alloys. The primary goal of passivation is to create a protective oxide layer on the metal's surface, which helps prevent corrosion and improves the longevity of the material (Asri et al., 2017).

Advantages:

Superior corrosion resistance: Passivation eliminates potential contaminants, enhancing titanium's suitability for critical applications.

Biocompatibility: Passivated titanium is highly biocompatible, making it ideal for medical devices.

Disadvantages:

Limited surface modification: Passivation mainly focuses on corrosion resistance and cleanliness, with minimal alteration of mechanical properties.

Limited applicability: Passivation is best suited for applications prioritizing corrosion resistance and biocompatibility.

Nitriding

Nitriding is a surface treatment process used to improve the hardness, wear resistance, and corrosion resistance of metal components, primarily steel. It involves the diffusion of nitrogen atoms into the surface of the material to create a hard and durable outer layer. This process is typically carried out at elevated temperatures in the presence of ammonia gas, and it can be applied to various types of steel and even some other alloys (Santecchia et al., 2015).

Advantages:

Increased hardness: Nitriding significantly boosts surface hardness, rendering titanium more durable and wear resistant.

Enhanced fatigue resistance: Nitrided titanium displays improved fatigue resistance, suitable for components under cyclic loading.

Disadvantages:

Shallow treatment depth: The nitrided layer's depth is limited, potentially offering less protection than other treatments.

Limited color options: Nitriding does not provide color variety for aesthetic purposes.

Physical Vapor Deposition (PVD):

PVD methods, including sputtering and evaporation, create thin, adherent coatings with precise control over composition and thickness. Titanium can be coated with various materials like nitrides, oxides, and diamond-like carbon (DLC). PVD coatings exhibit excellent wear resistance and biocompatibility. Their main disadvantages include the need for specialized equipment and the limitation in coating complex geometries (Geyao et al., 2020).

Advantages:

<u>Precise thickness control</u>: PVD allows for accurate control of coating thickness.

<u>Versatile applications</u>: PVD offers a wide range of coatings, including wear-resistant, decorative, and functional.

<u>Enhanced adhesion</u>: PVD coatings typically exhibit strong adherence to the substrate.

Disadvantages:

<u>Limited coating materials</u>: The choice of coating materials may be restricted, limiting customization options.

<u>Equipment costs</u>: PVD equipment can be expensive to purchase and maintain.

Chemical Vapor Deposition (CVD):

CVD is a high-temperature process that can deposit biocompatible coatings like diamond-like carbon (DLC), titanium nitride (TiN), and titanium oxide (TiO$_2$). CVD coatings are conformal, with excellent adhesion and wear resistance. However, the process is costly, time-consuming, and may require high temperatures, limiting its applicability for certain implants (Schrand et al., 2009).

Advantages:

<u>Conformal coating</u>: CVD ensures uniform coverage even on complex geometries.

<u>Excellent adherence</u>: Coatings generated by CVD tend to have strong bonds with the titanium surface.

<u>Wide material range</u>: CVD offers a broad spectrum of materials for various applications.

Disadvantages:

<u>High process temperatures</u>: CVD often requires high temperatures, which may limit its use with certain materials or substrates.

<u>Equipment complexity</u>: CVD equipment can be intricate and costly to operate and maintain.

Surface treatments serve as a versatile toolkit for optimizing the properties of titanium materials to meet diverse application needs. The selection of a specific surface treatment should be guided by the particular requirements of the project, considering factors such as corrosion resistance, wear resistance, biocompatibility, and aesthetic preferences. While each surface treatment offers

unique advantages and disadvantages, they collectively contribute to expanding the utility of titanium across a wide range of industries and applications.

CONCLUSIONS

In conclusion, the history of titanium's utilization in biomedical applications is a remarkable testament to human innovation and the enduring quest to enhance healthcare and improve the lives of individuals. From its humble beginnings as a newly discovered element to its current status as a cornerstone of modern medical technology, titanium's journey has been marked by scientific curiosity, relentless research, and ingenious engineering.

Through the development of titanium alloys and the application of advanced manufacturing techniques, this exceptional metal has found its way into a multitude of medical devices and implants, offering unmatched strength, durability, and biocompatibility. From orthopedic and dental implants to cardiac devices and spinal instruments, titanium has become an indispensable component in the arsenal of healthcare providers, significantly impacting patient outcomes and quality of life.

As we reflect on this history, it becomes evident that the collaboration between diverse fields, including material science, engineering, and medicine, has been instrumental in shaping the trajectory of titanium's role in healthcare. The ongoing pursuit of excellence in biomedical applications of titanium promises even more exciting innovations and breakthroughs in the future.

In closing, the story of titanium in medicine serves as a vivid reminder of the power of human ingenuity to transform challenges into opportunities. It is a testament to the relentless spirit of discovery that continues to push the boundaries of what is possible, ultimately benefitting patients around the world and enhancing the field of healthcare in profound ways. The history of titanium in biomedical applications is not merely a narrative of metal and machinery; it is a story of hope, healing, and the enduring quest for better health and well-being.

REFERENCES

Asri, R. I. M., Harun, W. S. W., Samykano, M., Lah, N. A. C., Ghani, S. A. C., Tarlochan, F., & Raza, M. R. (2017). Corrosion and surface modification on biocompatible metals: A review. *Materials Science and Engineering: C*, *77*, 1261–1274.

Awad, A., Trenfield, S. J., Pollard, T. D., Ong, J. J., Elbadawi, M., McCoubrey, L. E., Goyanes, A., Gaisford, S., & Basit, A. W. (2021). Connected healthcare: Improving patient care using digital health technologies. *Advanced Drug Delivery Reviews*, *178*, 113958.

Baker, T. N. (2019). Titanium microalloyed steels. *Ironmaking & Steelmaking*, *46*(1), 1–55.

Bosshardt, D. D., Chappuis, V., & Buser, D. (2017). Osseointegration of titanium, titanium alloy and zirconia dental implants: Current knowledge and open questions. *Periodontology 2000*, *73*(1), 22–40.

Boyer, R. R. (1996). An overview on the use of titanium in the aerospace industry. *Materials Science and Engineering: A*, *213*(1–2), 103–114.

Brown, B. N., & Badylak, S. F. (2013). Expanded applications, shifting paradigms and an improved understanding of host–biomaterial interactions. *Acta Biomaterialia*, *9*(2), 4948–4955. https://doi.org/10.1016/j.actbio.2012.10.025

Citron, P., & Nerem, R. M. (2004). Bioengineering: 25 years of progress—but still only a beginning. *Technology in Society*, *26*(2–3), 415–431.

Cotton, J. D., Briggs, R. D., Boyer, R. R., Tamirisakandala, S., Russo, P., Shchetnikov, N., & Fanning, J. C. (2015). State of the art in beta titanium alloys for airframe applications. *Jom*, *67*(6), 1281–1303.

Esposito, M., Grusovin, M. G., Kwan, S., Worthington, H. V., & Coulthard, P. (2008). Interventions for replacing missing teeth: Bone augmentation techniques for dental implant treatment. *Cochrane Database of Systematic Reviews*, *3*.

Geyao, L., Yang, D., Wanglin, C., & Chengyong, W. (2020). Development and application of physical vapor deposited coatings for medical devices: A review. *Procedia CIRP*, *89*, 250–262.

Grandin, H. M., Berner, S., & Dard, M. (2012). A Review of Titanium Zirconium (TiZr) Alloys for Use in Endosseous Dental Implants. *Materials*, *5*(8), 1348–1360. https://doi.org/10.3390/ma5081348

Guo, A. X., Cheng, L., Zhan, S., Zhang, S., Xiong, W., Wang, Z., Wang, G., & Cao, S. C. (2022). Biomedical applications of the powder-based 3D printed titanium alloys: A review. *Journal of Materials Science & Technology*, *125*, 252–264.

Hecht, J. (2010). Short history of laser development. *Optical Engineering*, *49*(9), 091002–091002.

Hua, L., Lei, T., Qian, H., Zhang, Y., Hu, Y., & Lei, P. (2021). 3D-printed porous tantalum: Recent application in various drug delivery systems to repair hard tissue defects. *Expert Opinion on Drug Delivery*, *18*(5), 625–634.

Jorge, J. R. P., Barao, V. A., Delben, J. A., Faverani, L. P., Queiroz, T. P., & Assunçao, W. G. (2013). Titanium in dentistry: Historical development, state of the art and future perspectives. *The Journal of Indian Prosthodontic Society*, *13*, 71–77.

Kumaravel, V., Nair, K. M., Mathew, S., Bartlett, J., Kennedy, J. E., Manning, H. G., Whelan, B. J., Leyland, N. S., & Pillai, S. C. (2021). Antimicrobial TiO2 nanocomposite coatings for surfaces, dental and orthopaedic implants. *Chemical Engineering Journal*, *416*, 129071.

Levine, B. R., Sporer, S., Poggie, R. A., Della Valle, C. J., & Jacobs, J. J. (2006). Experimental and clinical performance of porous tantalum in orthopedic surgery. *Biomaterials*, *27*(27), 4671–4681.

Manivasagam, G., Dhinasekaran, D., & Rajamanickam, A. (2010). Biomedical implants: Corrosion and its prevention-a review. *Recent Patents on Corrosion Science*, *2*(1).

Qadri, Y. A., Nauman, A., Zikria, Y. B., Vasilakos, A. V., & Kim, S. W. (2020). The future of healthcare internet of things: A survey of emerging technologies. *IEEE Communications Surveys & Tutorials*, *22*(2), 1121–1167.

Roach, M. (2007). Base metal alloys used for dental restorations and implants. *Dental Clinics of North America*, *51*(3), 603–627.

Ronoh, K., Mwema, F., Dabees, S., & Sobola, D. (2022). Advances in sustainable grinding of different types of the titanium biomaterials for medical applications: A review. *Biomedical Engineering Advances*, 100047.

Roşu, R. A., Şerban, V.-A., Bucur, A. I., & Dragoş, U. (2012). Deposition of titanium nitride and hydroxyapatite-based biocompatible composite by reactive plasma spraying. *Applied Surface Science*, *258*(8), 3871–3876. https://doi.org/10.1016/j.apsusc.2011.12.049

Santecchia, E., Hamouda, A. M. S., Musharavati, F., Zalnezhad, E., Cabibbo, M., & Spigarelli, S. (2015). Wear resistance investigation of titanium nitride-based coatings. *Ceramics International*, *41*(9), 10349–10379.

Schrand, A. M., Hens, S. A. C., & Shenderova, O. A. (2009). Nanodiamond particles: Properties and perspectives for bioapplications. *Critical Reviews in Solid State and Materials Sciences*, *34*(1–2), 18–74.

Tan, J., & Ramakrishna, S. (2021). Applications of magnesium and its alloys: A

review. *Applied Sciences*, *11*(15), 6861.

Van Noort, R. (1987). Titanium: The implant material of today. *Journal of Materials Science*, *22*, 3801–3811.

Verma, R. P. (2020). Titanium based biomaterial for bone implants: A mini review. *Materials Today: Proceedings*, *26*, 3148–3151. https://doi.org/10.1016/j.matpr.2020.02.649

Williams, D. F. (2008). On the mechanisms of biocompatibility. *Biomaterials*, *29*(20), 2941–2953.

Zitzmann, N. U., & Marinello, C. P. (2002). A review of clinical and technical considerations for fixed and removable implant prostheses in the edentulous mandible. *International Journal of Prosthodontics*, *15*(1).

Chapter 12

Dynamic Substructuring of a Jet Engine Dual Rotor System Based on Receptances

Murat ŞEN[1], Orhan ÇAKAR[2]

[1] *Asst. Prof. Dr.; Firat University, Department of Mechanical Engineering. Elazig, Türkiye, msen@firat.edu.tr ORCID No: 0000-0002-3063-5635*
[2] *Prof. Dr.; Firat University, Department of Mechanical Engineering. Elazig, Türkiye, cakaro@firat.edu.tr ORCID No: 0000-0001-6947-3875*

ABSTRACT

In some mechanical engineering applications such as jet engines, dual rotor systems are widely used. In a dual rotor system used in a jet engine is combined of two rotors one of which is a low-pressure inner rotor and the other is high pressure outer rotor. Although the dynamic properties of each rotor systems (subsystems) are known, the dynamic characteristics of the whole dual rotor system are completely different. Determining the dynamic characteristics of these dual rotor systems is great importance for providing safe operation conditions.

In this study, the dynamic characteristics of a jet engine dual rotor system are obtained by using the dynamic properties of each sub rotor systems. This is achieved by using the FRF (frequency response function) based dynamic sub structuring (structural coupling) method. To prove the validity of the method the results obtained with structural coupling method are compared with the ones obtained for the whole jet engine dual rotor system created with FE (finite element) method.

Keywords: Dual rotor system, natural frequency, frequency response function, structural coupling, Jet engine

INTRODUCTION

In many mechanical engineering applications dual rotor systems can be widely used. The dual rotor systems are created by using different shafts working one inside the other. The inner shaft is supported to the body of the rotor system and the outer shaft is supported to the body and to the inner shaft by different bearings (Şen et al., 2022). In jet engines rotor systems, there are two different shafts working for different pressure compressors and turbines (low pressure and high pressure). Determining the dynamic characteristics of these dual rotor systems is crucial for providing safe operation conditions. Knowing the dynamic characteristics of these systems is important for some model improvement or model updating studies as well. The dynamic characteristics of a mechanical system can be determined by using different approaches such as analytical, numerical or experimental. Analytical methods can be very hard and numerical methods can be very time consuming. For many complex mechanical systems, experimental methods for determining the dynamic characteristics are used and can provide advantage. By performing experimental modal analysis methods dynamic properties such as natural frequencies, anti-resonance frequencies, vibration mode shapes and damping of very complex mechanical systems can be obtained easily (Şen et al., 2022). There are many studies for modeling and determining the dynamic properties of dual rotor systems proposed by many researchers in the literature recently, (Yu et al, 2018; Lu et al., 2021 and Ma et al., 2021) and (Yu et al., 2022; Chen et al. 2022; and Wanga et al., 2019). In this context, Zhang et al. (2020), proposed a FE dual rotor model with misaligned coupling using Timoshenko beam elements comparing the results with experimental studies. Miao et al. (2014), studied on model updating of a dual rotor system and they used the updated model to predict the critical speeds and unbalanced responses of the dual rotor system. Li et al. (2022), proposed a study based on model scaling to predict the dynamic characteristics of a dual rotor system combined of shaft, disk and bolted joints.

In engineering applications, it is very common to obtain the dynamic characteristic of a system by using the dynamic properties of subsystems that make up the whole system. As mentioned above a jet engine is combined with an inner and an outer shaft working together with different rotational speeds. The dynamic characteristics of such a system can be obtained by using the dynamic properties of each the inner and the outer rotor systems. This is within the scope of the study of dynamic sub structuring or structural coupling in structural dynamics (Jin et al., 2019). Systems used in many engineering applications are formed by bringing together many subsystems. Although the

dynamic properties of the subsystems that make up these systems are known, the dynamic properties of the combined system formed as a result of the combination of these subsystems are completely different. The unified system, on the other hand, can have a very complex structure because it consists of many subsystems. Obtaining the dynamic properties of these complex systems can be quite difficult by analytical, numerical or experimental methods. Structural coupling methods are approaches that make this process very easy. By using the dynamic properties of the subsystems, the dynamic properties of the combined and/or complex system can be determined (Pradeepkumar and Nagaraj, 2022). Structural coupling applications provide convenience in many areas such as engineering design, improvement, model updating and design validation studies. In addition, dynamic sub structuring provides easily determining local dynamic behavior of mechanical systems. In this respect, effective methods have been proposed by many researchers (Klerk et al., 2008) studying in the field of structural dynamics especially for a few decades (Hurty, 1960; Craig and Hale, 1987; D'Ambrogio and Sestieri, 2004; and Jetmundsen et al., 1988) from physical, frequency and modal domain methods to coupling of reduced components approaches (Kyrychko et al., 2006; Klerk et al., 2006; and Park and Park, 2004).

Other methods known to be very effective in structural coupling studies are the methods in which FRFs (frequency response functions) are used. In this context, valuable methods proposed by many researchers up to now (Imregun and Robb, 1992; Allen and Mayes, 2007; Gordis, 1994; and Şen and Çakar, 2023) and these methods have been used effectively in structural dynamic studies. Lee and Eun (2014) proposed a sub structuring method uses the FRFs of the interface points for local damage detection of mechanical structures. Roettgen et al. (2016), used transmission simulator method for dynamic sub structuring on a wind turbine by performing modal test on the hub of the wind turbine with a single blade and replicated the structure three times rotated as a circle about the hub and assembled together. D'Ambrogio and Fregolent (2014), studied to identified of the dynamic characteristics of a structural subsystem. They used the dynamic behavior of both the coupled and the remaining part of the residual subsystem.

Dynamic characteristics of joint parameters of coupled systems can also be obtained utilizing dynamic sub structuring techniques. Joints of mechanical systems created by bringing together many subsystems have a very important effect on the overall dynamic properties of the system. For this reason, it is very important to define the dynamics of the joint during the design stages of mechanical systems. Mehrpouya et al. (2013), investigated inverse receptance

coupling method to predict the dynamic properties of the joint modelled with lumped mass, damping and stiffness elements. Ren and Beards (1995) presented a method for determining joint dynamic properties using experimentally measured FRF data. They showed that their method is effective even when noisy experimental data are used.

In this study, the FRFs of a jet engine dual rotor model are obtained by using the FRFs of the inner and the outer rotor models separately. The FRFs of the substructures are combined utilizing dynamic structural coupling method. The obtained FRFs are verified with that of the whole jet engine rotor model created with FE modelling using MATLAB.

THE FE MODEL OF THE JET ENGINE DUAL ROTOR SYSTEM

In this section, the methodology for creating the FE modelling of the jet engine rotor system with equations is given. The FE model of jet engine dual rotor system is illustrated in Figure 1. Here, the jet engine rotor system is created with two rotor systems one is housed inside the other using coupling bearing, which is modelled with spring k_c and damper c_c. The inner and the outer rotor systems represent the low and high-pressure engine rotors respectively. The inner rotor shaft is modelled with 12 Euler-Bernoulli beam finite elements and with springs k_1, k_2 and dampers c_1, c_2 at both ends referring the bearing supports and totally 13 nodes are obtained. There are 2 discs located at node 2 and node 3 for modelling low-pressure compressor and there are 3 discs located at node 10, node 11 and node 12 for modelling the low pressure turbine.

Similarly, the outer rotor shaft is modelled with 8 finite elements and 9 nodes with a spring k_3 and a damper c_3 referring the bearing support between the shaft and the ground. The outer shaft is coupled to the inner shaft with the coupling spring k_c and the coupling damper c_c between node 9 of the inner shaft and node 9 of the outer shaft as seen in Figure 1.
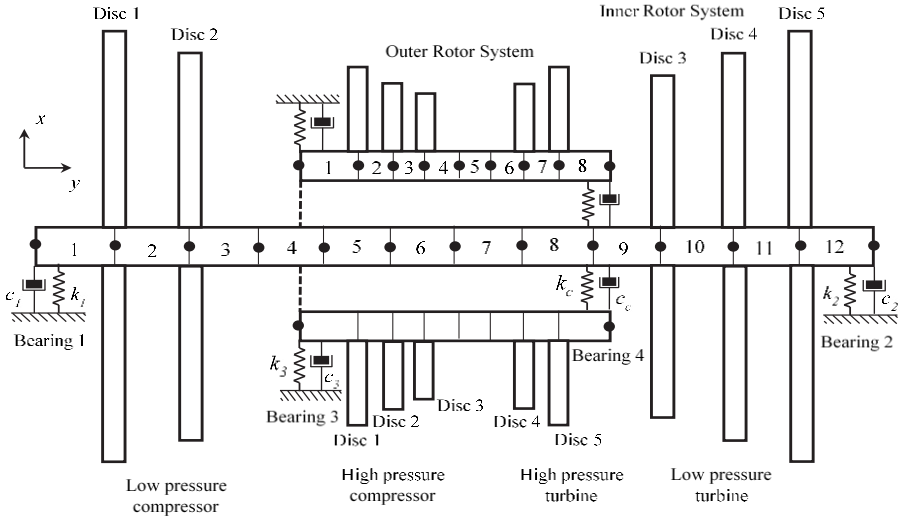
Figure 1: The FE jet engine dual rotor model with low pressure and the high-pressure shafts

The mass and the stiffness matrices for both inner and outer rotor shafts and the whole jet engine rotor shaft are created first. In Figure 2 an Euler Bernoulli beam element is shown with 2 dofs at each node one is translational and the other is rotational.
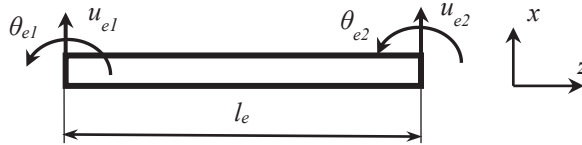

Figure 2: Euler Bernoulli beam element on *x-y* plane

In Figure 2, u_{e1} and u_{e2} represent the translational coordinates, θ_{e1} ve θ_{e2} are the rotational coordinates of each element of the shaft respectively and can be written as follows:

$$\{q_e\} = \{u_{e1}, \theta_{e1}, u_{e2}, \theta_{e2}\}^T \tag{1}$$

Thus, each node has 2 and each beam element has 4 degrees of freedom. Elemental stiffness and mass matrices can be given as:

$$[k]^{(i)} = \begin{bmatrix} k_{11}^{(i)} & k_{12}^{(i)} & k_{13}^{(i)} & k_{14}^{(i)} \\ k_{21}^{(i)} & k_{22}^{(i)} & k_{23}^{(i)} & k_{24}^{(i)} \\ k_{31}^{(i)} & k_{32}^{(i)} & k_{33}^{(i)} & k_{34}^{(i)} \\ k_{41}^{(i)} & k_{42}^{(i)} & k_{43}^{(i)} & k_{44}^{(i)} \end{bmatrix} = \frac{E_i I_i}{l_i^3} \begin{bmatrix} 12 & 6l_i & -12 & 6l_i \\ 6l & 4l_i^2 & -6l_i & 2l_i^2 \\ -12 & -6l_i & 12 & -6l_i \\ 6l_i & 2l_i^2 & -6l_i & 4l_i^2 \end{bmatrix} \quad (i=1,2,...,n) \tag{2}$$

$$[m]^{(i)} = \begin{bmatrix} m_{11}^{(i)} & m_{12}^{(i)} & m_{13}^{(i)} & m_{14}^{(i)} \\ m_{21}^{(i)} & m_{22}^{(i)} & m_{23}^{(i)} & m_{24}^{(i)} \\ m_{31}^{(i)} & m_{32}^{(i)} & m_{33}^{(i)} & m_{34}^{(i)} \\ m_{41}^{(i)} & m_{42}^{(i)} & m_{43}^{(i)} & m_{44}^{(i)} \end{bmatrix} = \frac{\rho_i A_i l_i}{420} \begin{bmatrix} 156 & 22l_i & 54 & -13l_i \\ 22l_i & 4l_i^2 & 13l_i & -3l_i^2 \\ 54 & 13l_i & 156 & -22l_i \\ -13l_i & -3l_i^2 & -22l_i & 4l_i^2 \end{bmatrix} \quad (i=1,2,...,n) \quad (3)$$

Where, E_i, I_i, l_i, ρ_i, and A_i are the modulus of elasticity, moment of inertia of cross-section, length, mass density and cross-section area of the beam elements respectively. $[k_s]^{(i)}$ and $[m_s]^{(i)}$ represent the elemental stiffness and mass matrices. The finite element size is given with n and the matrices can be written for i=1, 2, …, n.

The mass matrix of a single disc located on the rotor shaft can be expressed as follows with the mass and the diametric mass moment of inertia of the disc corresponding the translational and the rotational coordinates respectively.

$$[m_d] = \begin{bmatrix} m_d & 0 \\ 0 & I_d \end{bmatrix} \quad (4)$$

Where m_d and I_d are the mass and the diametric mass moment of inertia of the disc respectively, which can be calculated as

$$m_d = \frac{\rho_d \pi \left(D_d^2 - D_s^2\right) t_d}{4} \quad (5)$$

$$I_d = \frac{\rho_d \pi \left(D_d^4 - D_s^4\right) t_d}{64} + \frac{\rho_d \pi \left(D_d^2 - D_s^2\right) t_d^3}{48} \quad (6)$$

Here, ρ_d, D_d, D_s and t_d represent the mass density, the outer diameter, the inner diameter (also shaft diameter) and the thickness of the disc respectively.

The bearing supports can be assumed to restrict the relevant coordinates of the bearing location according to the bearing type. For long case bearing (clamped boundary condition) translational and rotational coordinates are restricted and for short case bearing (simply supported condition) only the translational coordinate is restricted.

The global mass and stiffness matrices of each rotor system can be obtained considering each element matrices and constraints as shown in Figure 3.
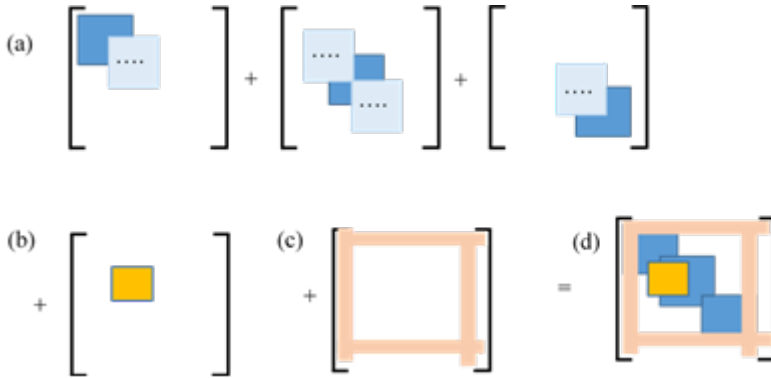
Figure 3: The system matrices; (a) shaft, (b) disc, (c) bearings (constraints), (d) overall system (Friswell et., (2010))

After creating the mass and the stiffness matrices of the inner and the outer rotor systems the equations of motion of each rotor systems can be written as:

$$[M]_1\{\ddot{x}\}_1 + [C]_1\{\dot{x}\}_1 + [K]_1\{x\}_1 = \{F\}_1$$

$$[M]_2\{\ddot{x}\}_2 + [C]_2\{\dot{x}\}_2 + [K]_2\{x\}_2 = \{F\}_2$$

(7)

In Equation 7, the subscripts 1 and 2 represent the inner and the outer shaft of the jet engine dual rotor system respectively. For FE solution of the whole rotor system the global mass and stiffness matrices can be obtained by combining the matrices of the substructures (inner and the outer rotors) given Equation 8.

$$[M] = \begin{bmatrix} [M]_1 & [0] \\ [0] & [M]_2 \end{bmatrix}; \quad [C] = \begin{bmatrix} [C]_1 & [0] \\ [0] & [C]_2 \end{bmatrix}; \quad [K] = \begin{bmatrix} [K]_1 & [0] \\ [0] & [K]_2 \end{bmatrix}$$

(8)

For the whole jet engine dual rotor system, the equation of motion can be written in matrix form as follows:

$$[M]\{\ddot{x}\} + [C]\{\dot{x}\} + [K]\{x\} = \{F\}$$

(9)

For creating the global mass and stiffness matrices, the procedure given in Figure 4 and Figure 5 can be used. The element matrices can be joined to global matrix nested together by adding the parameters of the related coordinates. The mass and the diametric mass moment of inertia values of the discs can be added to related coordinates in the mass matrix. The stiffness values of the bearings (considering only for translational coordinates for convenience) can be added to the global stiffness matrix in the related coordinates. The inner and the outer rotor systems are assumed to be coupled to each other by using coupling spring k_c.
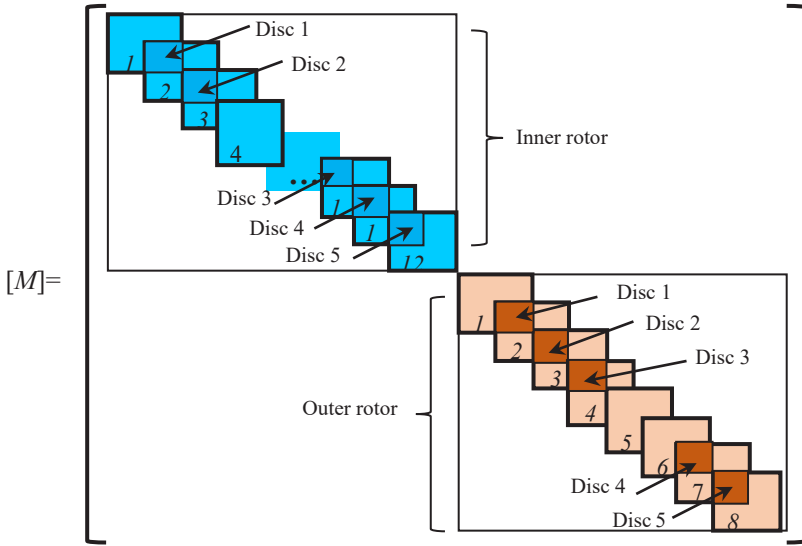
Figure 4: The mass matrix of the jet engine dual rotor system FE model
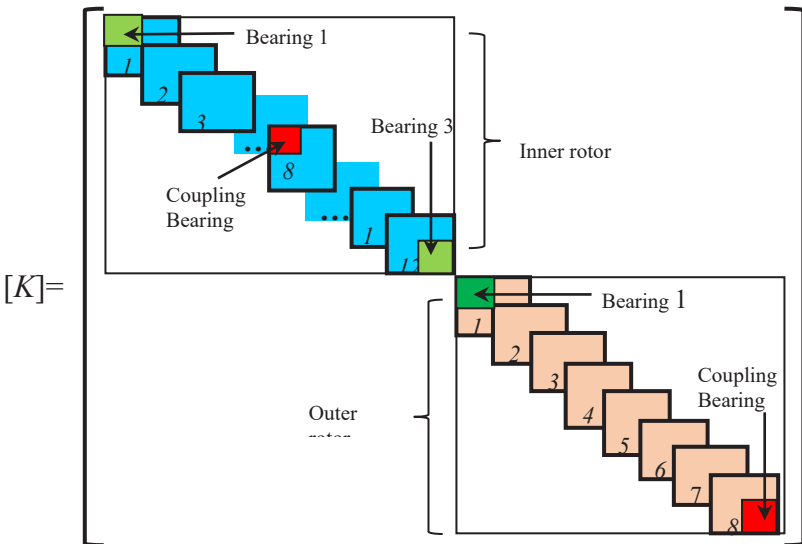

Figure 5: The stiffness matrix of the jet engine dual rotor system FE model

Natural frequencies for bending vibrations of each system (inner rotor system, outer rotor system, whole jet engine rotor system) were obtained from the eigenvalue problem solutions for each system. The FRF graphs of the coupling coordinates where the two rotor systems are connected to each other are shown in the determined frequency range with frequency (Hz)-amplitude (m/N) graphs. By using the FRFs of each subsystem, the FRFs of the general jet

engine rotor system were obtained with the help of the dynamic structural coupling method given in Section 3. The FRF plot obtained with the FE solution is shown in comparison with the FRF plot obtained using the dynamic structural coupling method in Section 4.

STRUCTURAL COUPLING METHOD FOR JET ENGINE DUAL ROTOR SYSTEM

In this section the structural coupling method for obtaining the FRFs of the whole jet engine rotor system by using the FRFs of the inner and the outer rotors systems is given with the formulations. The structural coupling method used in this study is based FRFs. By using the FRFs of the substructure, the FRFs of the coupled system can be obtained.

The FRFs of the coupled system can be represented using the FRFs of the substructures with Equation 10 (Kalaycioglu and Ozguven, 2014).

$$[H]_C = [H]_c \left[[I] + [Z][H]_c \right]^{-1} \tag{10}$$

Where, $[H]_C$, $[I]$, $[Z]$ and $[H]_c$ represents the FRF matrix of the coordinates at the coupling points of the coupled system, the unit matrix, the dynamic stiffness containing the coupling parameters, and the FRF matrix of the coupling coordinates for each subsystem, respectively.

The matrix $[H]_c$ and the coupling parameters of the jet engine dual rotor system belong to the coupling coordinates with dynamic stiffness matrix can be written with Equation 11 and Equation 12.

$$[H]_c = \begin{bmatrix} [H]_{c1} & [0] \\ [0] & [H]_{c2} \end{bmatrix} = \begin{bmatrix} H_{c1c1} & 0 \\ 0 & H_{c2c2} \end{bmatrix} \tag{11}$$

$$[Z] = \begin{bmatrix} k_c & -k_c \\ -k_c & k_c \end{bmatrix} \tag{12}$$

Where, $[H]_{c1}$ and $[H]_{c2}$ represent the FRF matrices of the coupling coordinates of each rotor systems and can be written for this particular rotor system as H_{c1c1} and H_{c2c2} which are the point FRFs of each coupling coordinates of each rotor system. The stiffness values in Equation 12 belong to the coupling coordinates of the rotor systems (node 9 for the inner rotor and node 9 for the outer rotor of the jet engine dual rotor system given with Figure 1).

NUMERICAL SIMULATIONS

For numerical studies, the mass and stiffness matrices for the inner and the outer rotor systems and the coupled jet engine dual rotor system were created as given with Equation 8 and Figures 4-6 above. From the solutions of standard

eigenvalue problems obtained by using the equations of motion given with Equation 7 and Equation 8, the natural frequencies were obtained for the inner, the outer rotor models and for the whole coupled system. With the modal solution, the FRFs of each structure are obtained and two of each are plotted with frequency (Hz)-magnitude (m/N) graphs (Figures 6-13). The physical and the mechanical properties of the rotor system is given with Table 1.

Table 1: The physical and the mechanical properties of the dual rotor system

Parameter	Value
Shaft 1 diameter d_{1o}-d_{1i} (mm)	10-0
Shaft 2 diameter d_{2o}-d_{2i} (mm)	30-20
Shaft 1-2 length (mm)	900-600
Shaft 1-2 mass density (kg/m^3)	7850
Shaft 1-2 Elasticity Modulus (GPa)	210
Rotor 1: Disk 1-2-3-4-5 diameter (mm)	150-130-110-130-150
Rotor 1: Disk 1-2-3-4-5 thickness (mm)	10-10-10-10-10
Rotor 2: Disk 1-2-3-4-5 diameter (mm)	120-100-80-100-120
Rotor 2: Disk 1-2-3-4-5 thickness (mm)	10-10-10-10-10
Rotor 1,2: Disk 1-2-3-4-5 mass density (kg/m^3)	7850
Rotor 1,2: Disk 1-2-3-4-5 Elasticity Modulus (GPa)	210
Bearing 1-2-3-4 stiffness (kN/m)	3000-2000-1000-1000
Bearing 1-2-3-4 damping (Nm/s)	0-0-0-0

The natural frequencies calculated for each rotor system are determined and the frequency values calculated in 0-300 Hz bandwidth are tabulated in Table 2.

Table 2: Natural frequencies for the damped and undamped dual rotor systems

	Natural Frequencies (Hz)							
Mode	1	2	3	4	5	6	7	8
Inner rotor	10.87	28.48	86.01	134.73	194.86	246.52	288.17	-
Outer rotor	43.94	139.64	281.6	-	-	-	-	-
Whole rotor	4.06	26.92	41.86	53.02	127.68	136.83	160.10	215.96

The receptance type FRFs are obtained in 0-300 Hz bandwidth with 0.01 Hz increments. One of obtained point and transfer FRFs were plotted for the inner, the outer and the whole rotor models.
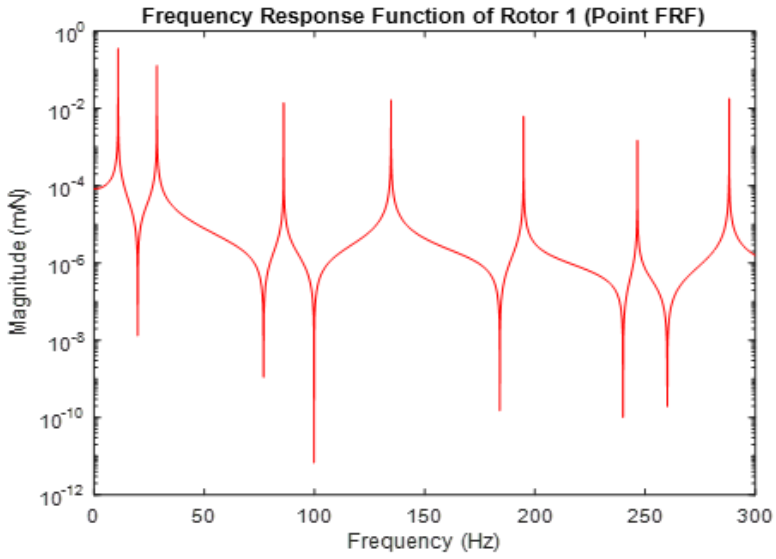
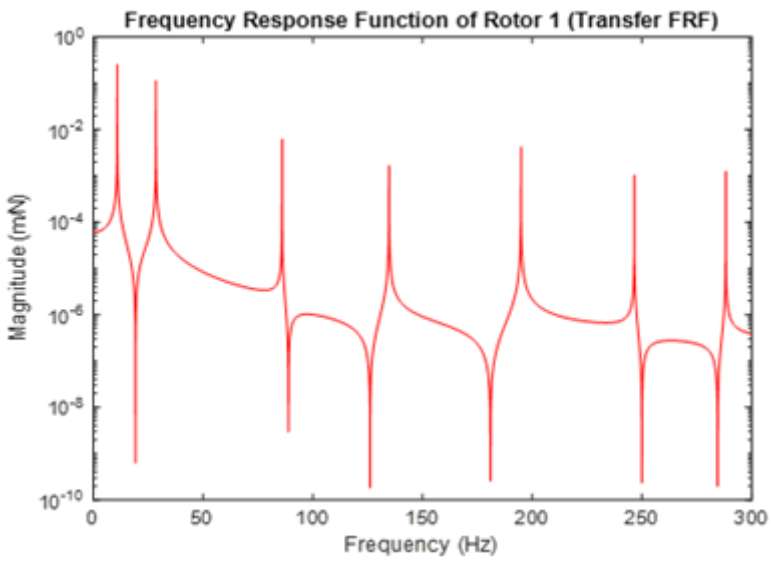**Figure 6:** One of the points FRFs of the inner rotor system (Rotor 1)

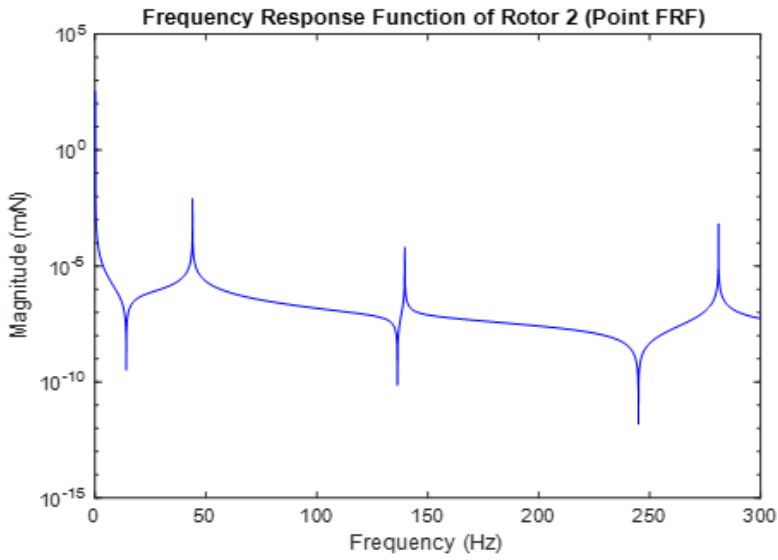**Figure 7:** One of the transfers FRFs of the inner rotor system (Rotor 1)

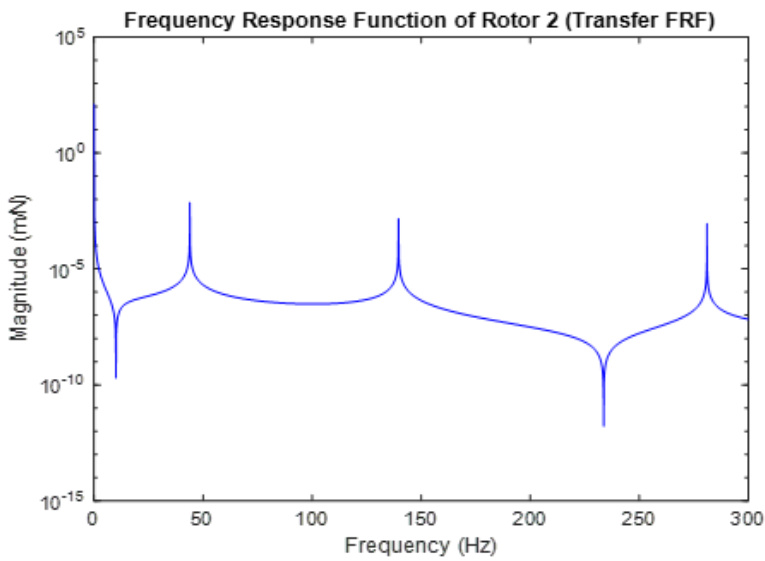**Figure 8:** One of the points FRFs of the outer rotor system (Rotor 2)

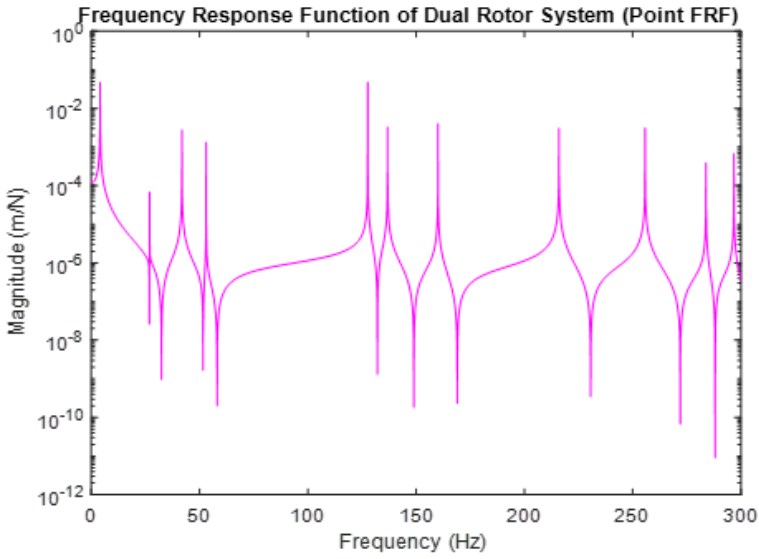**Figure 9:** One of the transfers FRFs of the outer rotor system (Rotor 2)

Figure 10: One of the points FRFs of the whole rotor system (Jet engine rotor)
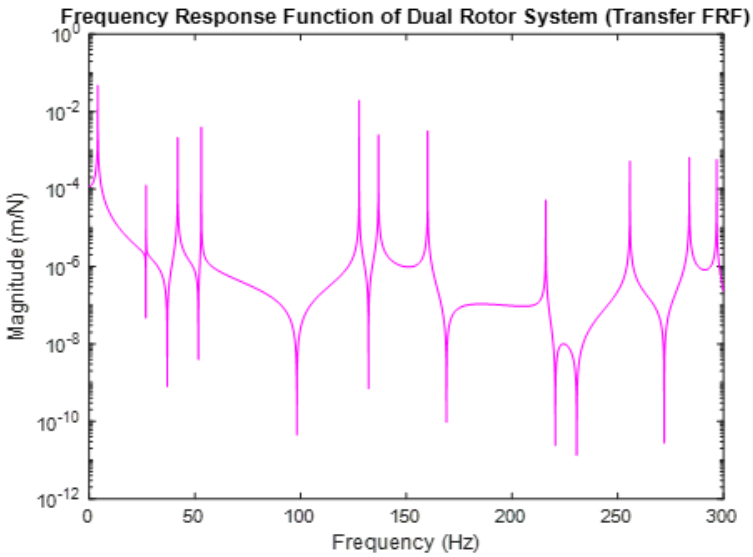

Figure 11: One of the transfers FRFs of the whole rotor system (Jet engine rotor)

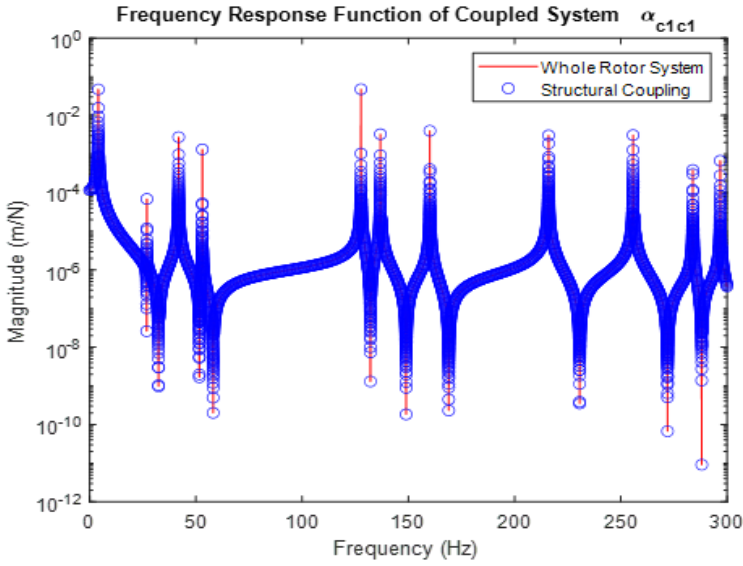**Figure 12:** One of the points FRFs of the whole rotor system- the coupled
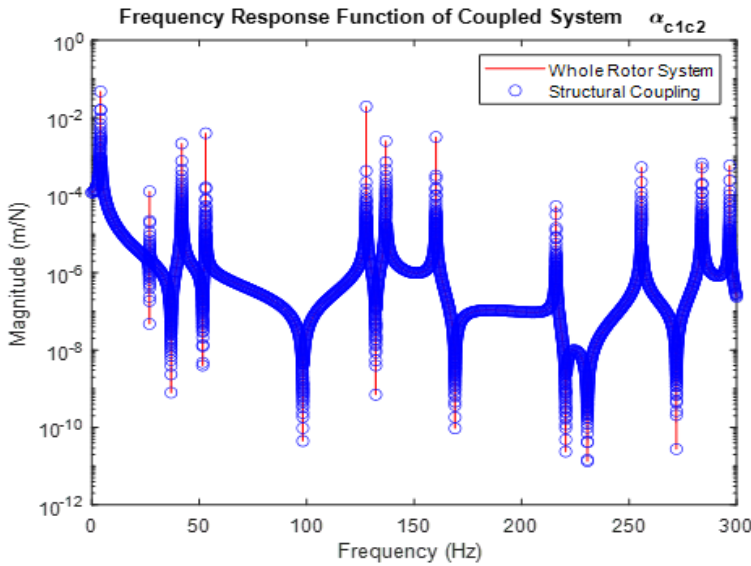rotor system

Figure 13: One of the transfers FRFs of the whole rotor system- the coupled
rotor system

As expected, anti-resonance frequencies are seen after each natural frequencies at point FRF graphs for each rotor system. In Figure 9, one of the point and one of the transfer FRFs belong to the coupling coordinates are seen

for both the whole rotor system created with FE approach (red straight line) and with the structural coupling method (blue round pattern line) comparatively. The FRFs are the same for both cases.

RESULTS AND DISCUSSION

In this study, the structural coupling of a jet engine dual rotor system based on FRFs is presented. The FE models of the inner (low pressure) and the outer (high pressure) rotor systems and the FE model of the whole dual rotor system were created. With standard eigen solution the natural frequencies for the bending vibrations were calculated. Applying modal solutions the receptance type FRFs of each system were obtained and two of each (one point and one transfer) were plotted in 0-300 Hz bandwidth with 0.01 Hz increments. Then the FRFs of the whole rotor system were obtained with the dynamic structural coupling method using the FRFs of the coupling coordinates of the inner and the outer rotor systems. The FRFs of the coupled jet engine rotor system are given obtained with FE approach and dynamic coupling method comparatively in frequency (Hz)-amplitude (m/N) with graphs. According to the obtained results the dynamic structural coupling method can be used effectively for dual rotor systems.

REFERENCES

Allen M., and Mayes R. (2007). Comparison of FRF and Modal Methods for Combining Experimental and Analytical Substructures, Proceedings of the 25th International Modal Analysis Conference, Society for Experimental Mechanics, 269.

Chen L., Zeng Z., Zhang D., et al. (2022). Vibration properties of dual rotor systems under base excitation, mass unbalance and gravity, Applied Sciences,12, 960.

Craig R., and Hale A. (1987). Review of Time-Domain and Frequency Domain Component Mode Synthesis Methods, International Journal of Analytical and Experimental Modal Analysis, 2(2): 59–72.

D'Ambrogio W. and Fregolent A. (2014). Inverse dynamic substruc

turing using the direct hybrid assembly in the frequency domain, Mechanical System and Signal Processing, 45: 360-377.

D'Ambrogio W., and Sestieri A. (2004). Unified Approach to Substructuring and Structural Modification Problems, Shock and Vibration, 11(3): 295–309.

Friswell M. I., Penny J. E. T., Garvey S. D. and et al. (2010). Dynamics of Rotating Machines, Cambridge University Press, New York.

Gordis J. (1994). Structural Synthesis in the Frequency Domain: A General Formulation, Proceedings of the Twelfth International Modal Analysis Conference, Society for Experimental Mechanics, Bethel, CT, 575–581.

Hurty W. C. (1960). Vibrations of Structural Systems by Component Mode Synthesis, Journal of Engineering Mechanics/American Society of Civil Engineers, 86(4): 51–69.

Imregun M., and Robb D. (1992). Structural Modification via FRF Coupling Using Measured Data, Proceedings of the Tenth International Modal Analysis Conference, Society for Experimental Mechanics, Bethel, CT, 1095–1099.

Jetmundsen B., Bielawa R., and Flannelly W. (1988). Generalized Frequency Domain Substructure Synthesis, Journal of the American Helicopter Society, 33(1): 55–65.

Jin Y., Lu K., Huang C., et al. (2019). Nonlinear dynamic analysis of a complex dual rotor-bearing system based on a novel model reduction method, Applied Mathematical Modelling, 75(2019): 553-571.

Kalaycıoğlu T. and Özgüven N. (2014). Nonlinear structural modification and nonlinear coupling Mechanical Systems and Signal Processing, 46, 289–306.

Klerk D., Rixen D., and de Jong J. (2006). Frequency Based Substructuring (FBS) Method Reformulated According to the Dual Domain Decomposition Method, Proceedings of the Fifteenth International Modal Analysis Conference, Society for Experimental Mechanics, 136.

Klerk D., Rixen D. J. and Voormeeren S. N. (2008). General Framework for Dynamic Sustructuring: History, Riview and Clasification of Techniques, AIAA Journal, 46(5): 1169-1181.

Kyrychko Y., Blyuss K., Gonzalez-Buelga A., et al. (2006). Real-Time Dynamic Substructuring in a Coupled Oscillator Pendulum System, Philosophical Transactions of the Royal Society A, Mathematical, Physical, and Engineering Sciences, 462(2068): 1271–1294. doi:10.1098/rspa.2005.1624.

Lee E. T., Eun H. C. (2014). A Model-Based Substructuring Method for Local Damage Detection of Structure, Shock and Vibration, 390769.

Li L., Luo Z., He F., et al. (2022). Similitude for the Dynamic Characteristics of Dual-Rotor System with Bolted Joints, Mathematics 2022, 10(3). https://doi.org/10.3390/math10010003

Lu Z., Zhang S., Chen H., et al. (2021). Nonlinear response analysis for a dual rotor system supported by ball bearings, International Journal of Non-linear Mechanics, 128: 103627.

Ma X., Ma H., Qin H., et al. (2021). Nonlinear vibration response characteristic of a dual rotor bearing system with squeeze film dampers, Chinese Journal of Aeronautics, 34(10): 128-147.

Mehrpouya M., Graham E. and Park S. S. (2013). FRF based joint dynamics modeling and identification, Mechanical Systems and Signal Processing, 39(2013): 265–279.

Miao H., Zang C. and Friswell M. (2014). Model updating and validation of a dual-rotor system, Proceedings of Isma, Model Updating and Correlation.

Park K., and Park Y. (2004). Partitioned Component Mode Synthesis via a Flexibility Approach, AIAA Journal, 42(6): 1236–1245.

Pradeepkumar S. and Nagaraj P. (2022). Dynamic Substructuring Method for Vibration Analysis of Complex, Journal of Vibration Engineering & Technologies, (2022)10: 313–333, https://doi.org/10.1007/s42417-021-00378-8

Ren Y. and Beards C. F. (1995). Identification of Joint Properties of a Structure Using FRF Data, Journal of Sound and Vibration, 186(4): 567–587.

Roettgen D. R., Allen M. S. and Mayes R. L. (2016). Wind Turbine Substructuring Using the Transmission Simulator Method, Sound and Vibration ,11: 14-17.

Şen M. and Çakar O. (2023). An Efficient Method for Structural Coupling of Mechanical Systems by Using Frequency Response Functions, Journal of Vibration and Control, First published online January 17, 2023. https://doi.org/10.1177/10775463231152069

Şen M., Çakar O., and Yiğid O. (2022). Dynamic Analysis of a Dual Rotor System, VI-International Europen Conference on Interdisciplinary Scientific Research, Bucharest, Romania: 1448-1456.

Şen M., Çakar O., and Yiğid O. (2022). Model Reduction and Dynamic Analysis of a Rotor System, VI-International Europen Conference on Interdisciplinary Scientific Research, Bucharest, Romania: 317-329.

Wanga N., Liu C., Jiang D., et al. (2019). Casing vibration response prediction of dual-rotor-blade-casing system with blade-casing rubbing, Mechanical Systems and Signal Processing, 118: 61–77.

Yu P., Hou L., Wang C., et al. (2022). Insights into the nonlinear behaviors of dual rotor system with inter-shaft rub-impact under co-rotation and counter-rotation conditions, International Journal of Non-linear Mechanics, 140, 103901.

Yu P., Zhang D., Ma Y., et al. (2018). Dynamic modeling and vibration characteristics analysis of the aero engine dual rotor system with fan blade out, Mechanical System and Signal Processing, 106: 158-175.

Zhang, H., Huang, L., Li X., et al. (2020). Spectrum analysis of a coaxial dual rotor system with coupling misalignment, Shock and Vibration, 58566341.

Chapter 13

Compilation of Gas Sensing Research of Calix[4]arene-based Nano Thin Films *via* QCM Technique for Dichloromethane and Chloroform Vapors

Erkan HALAY[1,2], Yaser AÇIKBAŞ[3], Rifat ÇAPAN[4]

[1] *Assoc. Prof. Dr. ; Usak University, Department of Chemistry, Scientific Analysis Technological Application and Research Center. erkan.halay@usak.edu.tr ORCID No: 0000-0002-0084-7709*
[2]*Assoc. Prof. Dr. ; Usak University, Banaz Vocational School, Department of Chemistry and Chemical Processing Technologies, Chemical Tecnology Programme. erkan.halay@usak.edu.tr ORCID No: 0000-0002-0084-7709*
[3]*Assoc. Prof. Dr. ; Usak University, Faculty of Engineering, Department of Materials Science and Nanotechnology Engineering. yaser.acikbas@usak.edu.tr ORCID No: 0000-0003-3416-1083*
[4]*Prof. Dr. ; Balikesir University, Faculty of Science, Department of Physics. rcapan@balikesir.edu.tr ORCID No: 0000-0003-3222-9056*

ABSTRACT

Technological development in various industrial branches brings the use of great amounts of chemical with it. Considering the direct/indirect release of vapours of those chemicals to the environment poses a dramatical direct threat to the living organisms and human being, in particular. On that note, the detection of gases and volatile organic compounds through monitoring indoor/outdoor air pollutions in order to help managing industrial processes has been gaining much more importance day by day. Hence, construction of elaborated supramolecular systems has drawn considerable attention. There have been limited interesting and favoured macrocyclic compounds presented due to their readily modification/ functionalization by suitable groups and their cavity structure preparing the way for recognition ability of a variety of target analytes such as ions and molecules. One of these macrocycles, namely calix[4]arenes have been in the centre of attention in order to make available new dimensions in host-guest chemistry. In this chapter, due to these unique characteristics, the application and potential of calix[4]arene supramolecular designs in gas sensors are discussed and it is expected to present new dimensions to the calix[4]arene-based chemical gas sensors by shedding light on scientists working in this domain.

Keywords: Calix[4]arenes; QCM; volatile organic vapours; chemical sensor.

INTRODUCTION

Because air quality is very important for all living organisms on the Earth, gas is an important state of substances. Contrary to this, humankind have caused air pollution via many activities including industrial processes and so the air composition has forced to change by various gases and volatile organic compounds (VOCs) (Li vd., 2020:6364). Those emissions such as greenhouse/toxic gases and VOCs have been burning up negatively on the environment and of course global climate which is a current and sensitive issue (He vd., 2019:4471; Woellner vd., 2018:1704679). Moreover, short-term exposure limits for those gases are recommended by some health agencies, because air pollution may make humans much more vulnerable to diseases like COVID-19 (Asri vd., 2021:18381; Zhang vd., 2020:140244; Fattorini ve Regoli, 2020:114732). Due to the air pollution faced with release of harmful and polluting gases to the environment, monitoring those gaseous species by developing new and effective methods for tracking environmental conditions and monitoring indoor air quality have been still in the spotlight among scientist who care about human welfare (Rasheed ve Nabeel, 2019:213065; Kim vd., 2018:75).

In this direction, several available/routinary instrumental techniques like chromatographic (gas, high/ultra-performance liquid chromatography) and spectrophotometric/spectrometric (UV, fluorescence, IR and mass) ones are used to perform gas detection accurately (Barreto vd., 2021:97; Sanchez vd., 2020:6299; He vd., 2019:3543; Dewulf ve Langenhove, 2002:637). Beside their having accuracy and precision, these related techniques show some disadvantages/drawbacks which of these may have hampered their further development such as requiring time consuming work up steps, high skilled operators, long analysis time and high-power demand along with high cost, particularly. Thus, it has been becoming significant to find user-friendly and inexpensive gas sensing devices and design novel smart sensing materials with superior performance for both gases and VOCs (Kang vd., 2021:130299; Zheng vd., 2021; Acikbas vd., 2018:526).

Thin films are described as material layers with the dimension of few nanometers/micrometers which are built on substrates that exhibit different physical properties due to constrains in their geometries. The sensors have the capability of conducting stable, perfect measurements by using this thin film technology. Hence, over the last two decades, thin film technology has consistently developed in the field of nanoscience/nanotechnologies and as a consequence such thin films have widely employed in the field of optics, biomedical devices and sensor materials fabrication (Elanjeitsenni vd., 2022:022001). Thin film gas sensors are a type of chemical detector fabricated

with the purpose of monitoring indoor/outdoor conditions by detecting gaseous species in the environment (Nazemi vd., 2019:1285). Among various methods (chemical/physical vapour deposition, electrochemical deposition, sputtering, sol-gel technique, printing methods and coating techniques) by which thin film sensors are prepared, Langmuir-Blodgett (LB) coating technique allow the formation/deposition of molecular monolayers, for organic compounds particularly, through supramolecular processes (Oprea ve Weimar, 2020:6707; Ozmen vd., 2014:156; Ariga vd., 2013:6477). In other words, the advantage of the related technique is the ability to control the film density and structure sensitively along with the obtaining anisotropic thin film possibility (Rytel vd., 2022: 118548; Rytel vd., 2020:22380).

Characterization of thin films fabricated in that way, has been mostly made by surface plasmon resonance (SPR) and quartz crystal microbalance (QCM) techniques due to their advantages of label-free and real-time detection along with high sensitivity. Since the optical SPR technique consists of a total internal reflection device using light beam, very sensitive reflected light formed by the change in target compound concentration enables to analyse greatly low concentration of sample (Wang vd., 2019:6801207; Wu vd., 2010:14395; Homola vd., 1999:3). On the other hand, QCM is a much more sensitive, acoustic wave-based device which is capable of measuring mass in nanogram levels due to the fact of changing resonance frequency upon the deposition of a given mass on the QCM electrode (Dehari vd., 2010:175). The QCM coated with various organic compounds, especially macrocyclic ones have been widely investigated for the purpose of using as a gravimetric sensor capable of detecting gas species (Temel ve Tabakci, 2016:221; Mermer vd., 2012:240).

The ability to manipulate the local molecular environment is crucial to access fundamentally new classes of organic functional materials with unprecedented properties and performance (Matsuoka ve Nabeshima, 2018:349). Concordantly, as one of the leading groups of these macrocyclic compounds like crown ethers and cyclodextrins, calixarenes represents the third generation of supramolecular platforms. Calix compounds are bowl-shaped, preorganized architectures and with the increase of the number of phenols in their structure, different sensor properties emerge along with specific interactions of altered size of the cavity (Kumar vd., 2017:129; Özbek vd., 2011:235).

We now review and introduce recent researches regarding supramolecular architectures with calix[4]arene macrocycle produced by host-guest interactions for dichloromethane and chloroform vapors. Moreover, the gas sensing experiments are explained in detail.

VOLATILE ORGANIC COMPOUNDS (VOCs)

People's demand for energy, the requirements in the industry and the rapid increase in the number of vehicles have had many negative reflections on the environment, especially air pollution. Many gases such as CO_2, CO, SO_x, NO_x, NO_x, HCl, NH_3, which are released uncontrollably into the air, ozone depletion, acid rain and global warming, etc. As a result of causing environmental problems, it has disrupted the ecological balance of our world and caused many diseases in living things.

Volatile organic compounds (VOCs) that play an active role in environmental pollution their origin is anthropogenic or natural sources. VOCs, which include dichloromethane, chloroform, benzenes, alcohols, ethers, ketones and the like, have high vapour pressure (10 Pa at 20 °C) and are one of the factors in air pollution due to their harmful and/or toxic structures. Exposure of living organisms to VOCs in our daily life is known to cause various health problems such as slowdown in the functioning of the central nervous system, irritation of the skin and eyes, vomiting, etc., especially in humans and animals (Su ve Hu, 2018:1234). It also increases the risk of mutation and cancer in case of long-term exposure (Hirota vd., 2004:1185). The information about the VOCs selected within the scope of this study is briefly described below.

Dichloromethane

Dichloromethane is a synthetic chemical substance not found in nature. It has a soft, colourless structure. It exists in liquid phase at room temperature. Dichloromethane is used as a solvent in industry. Since its solvent property is very good, it is used in the separation of spice mixtures. It is not used for this purpose today due to its harmful effect on health. The reason for the high concentration of dichloromethane in the environment is that it is industrial and used as a paint remover in homes. Although it is volatile in the air, it is absolutely insoluble in water. Since dichloromethane is very volatile, it cannot hold in the soil. Therefore, when it is released into both soil and water, it passes into the air very quickly. Half of the amount of dichloromethane disappears in a period of 17 to 53 days. Research shows that aquatic organisms and plants cannot store dichloromethane.

Dichloromethane, which is a volatile gas, affects the bodies of living organisms through respiration. In places where dichloromethane is used, paint removers and waste areas resulting from the production of raw materials in the industry are places that adversely affect human health [5]. Dichloromethane causes deep burns on the skin if contacted as a liquid. Dichloromethane damages the autonomic nervous system in humans. When it is present in the atmosphere

in high concentrations (above the required rate in the air), it can cause a decrease in reaction to an event and instability in manual dexterity tasks that require personal dexterity (Karlık, 2004).

Chloroform

Chloroform ($CHCl_3$) is a colourless, sweet-smelling, dense liquid and is a flammable, irritating and dangerous chemical. Chloroform vapour depresses the central nervous system, depresses life and is dangerous to health. Inhaling about 1000 ppm for a short time can cause dizziness, weakness and headache. Continuous exposure to chloroform can damage the liver and may damage kidneys, contact with skin may cause irritation and wounds. Above a certain dose, it may even cause death. For the reasons mentioned, it is recommended that chloroform vapour it is important that it can be detected accurately and at low ppm in the places where it is used.

CALIX[4]ARENE-BASED CHEMICAL SENSOR MATERIALS

Calixarenes are capable of complexing with various organic compounds or ions with different structures due to the ring structures in their structures and the diameters of the cavities varying according to the number of phenolic units. Thanks to these properties, they can be used as molecule or ion carriers. These compounds are in the form of endo- and exo- complexes. Calixarenes form sheets in the aqueous phase by the introduction of hydrophilic groups at the para-position or phenolic oxygen. Such structures are stabilised as monolayers or multilayers after cross-linking reactions. They are converted into suitable carriers using the production of nano thin film methods such as spin coating and Langmuir-Blodgett (LB) thin film technique. Calixarenes are converted into monolayer polymeric carrier materials to form membranes. The phases of these membranes can be changed by looking at the permeability ratio and molecular voids (Brake vd., 1993:65).

In our previous studies, the gas sensing abilities of 25,27-(Dipropylmorpholinoacetamido)-26,28-dihydroxycalix[4]arene and the triazine based calix[4]arene materials were investigated with QCM technique (Acikbas vd., 2017:77); (Halay vd., 2019:2521). The chemical structure of these materials is given in Figure 1.
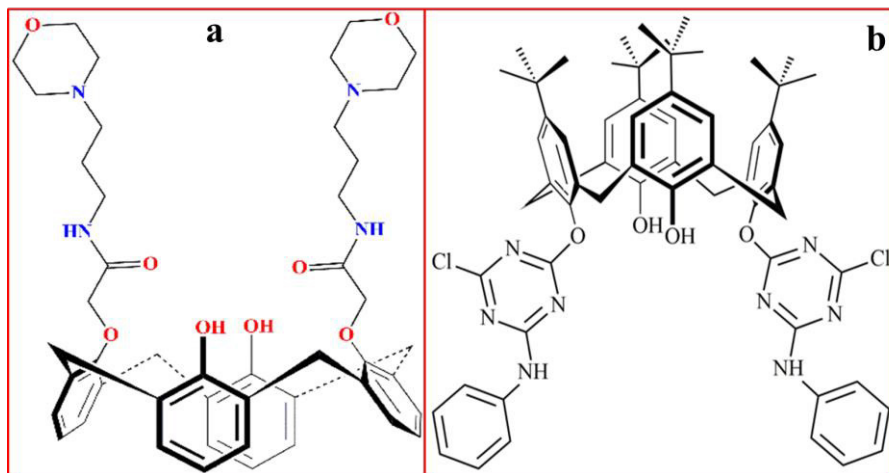
Figure 1. Chemical structure of **a)** 25,27-(Dipropylmorpholinoacetamido)-26,28-dihydroxycalix[4]arene molecule (Acikbas vd., 2017:77)], **b)** The triazine based calix[4]arene molecule (Halay vd., 2019:2521)].

QCM TECHNIQUE

Quartz Crystal Microbalance (QCM) is a high-frequency, surface mass change sensitive method used in different sensor applications. It is based on the determination of changes in resonant frequency (Δf) caused by layers adsorbed on sensor surfaces. Until 1950, the frequency shift, Δf was only qualitatively defined. The necessity to monitor small mass variations led later researchers to investigate more carefully. In 1960 it was realised that the resonant frequency of a quartz crystal depends on the geometrical dimensions of the quartz layer and the thickness of the electrodes. Therefore, manufacturers prepared quartz crystals with a resonant frequency higher than the desired value and then controlled the frequency by controlling the thickness of the existing quartz electrodes (Acikbas vd., 2015:99).

The QCM is a high-frequency, surface mass change sensitive method used in different sensor applications. It is technique is based on the piezoelectric principle and is a simple, high resolution, mass sensitive method with a wide quantification range. QCM is a high-frequency, surface mass change sensitive method used in different sensor applications. It is an electromechanical resonator that converts electrical energy into mechanical energy by electrodes coated with a sensing chemical film (Acikbas vd., 2016:470). QCM system basically consists of three parts: quartz crystal, oscillator and frequency meter (given in Figure 2).
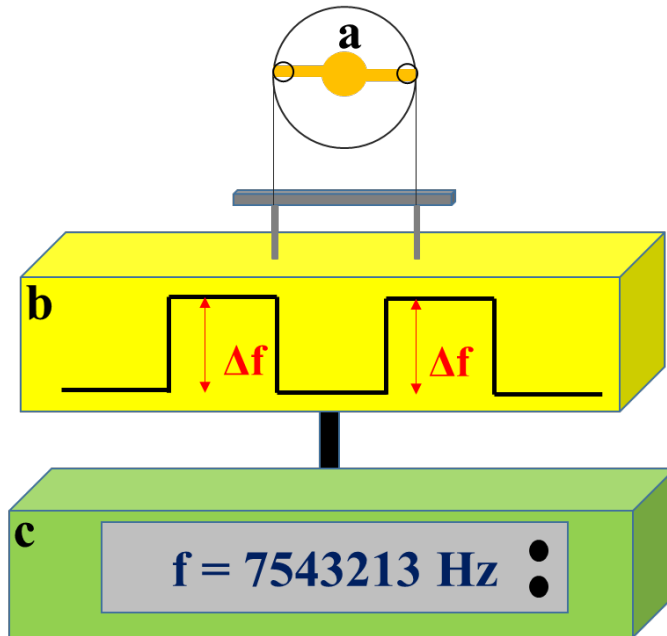
Figure 2. Basic elements of Quartz Crystal Microbalance system: quartz crystal **(a)**, oscillator **(b)** and frequency meter **(c)**.

QCM has nanometric gaps that vary according to the type of coating used. With these gaps, it captures molecules smaller than its own diameter. The mass of the QCM varies according to the amount of molecules captured. With the changing mass, the resonance frequency of the QCM also changes. In this transducer, a frequency change of 1 Hz corresponds to an absorbed mass of 1 ng per cm^2. The desired gas can be detected by a selective chemical interface coated on the QCM. Generally, the closer the size of the molecules is to the size of the coating cavities, the more difficult it is for the molecules to escape from the cavity (Acikbas vd., 2016:470).

Gas Kinetic Measurements via QCM Technique

The interaction of calixarene nano thin film with four different organic vapours is given in Figure 3. Between 0 seconds and 120 seconds, there is air in the experimental environment in the laboratory. At 120 seconds, when organic vapour, which we can express as harmful, is sent to the experimental environment, the changes in the resonance frequency of the crystal are seen from the graph in Figure 3. When harmful organic vapour molecules enter the environment, the resonance frequency shift of the quartz crystal increases rapidly and gradually reaches a minimum value. At this point, as soon as the harmful

organic vapour is introduced into the environment, the change in the resonance of the crystal causes the frequency to take different values quickly. This situation can be explained that the calixarene nano thin film reacts very quickly against harmful organic vapour.

After the frequency shows a variable values, it takes an absolute value approximately. The frequency remains at a constant value during this time period indicates that the calixarene nano thin film interacts with harmful organic vapour. Organic vapour remained in the environment for 120 seconds, fresh air was introduced into the environment at the 4th minute (240th second) and it was observed that the changes in the resonance frequency of the crystal regressed to their previous values. This situation shows that the thin film sensor used in the experimental environment is reversible. If the value of the frequency change in the experimental data is not return to its previous value after the clean air is given, it could be stated that the thin film sensor coated with calixarene material is not reversible.
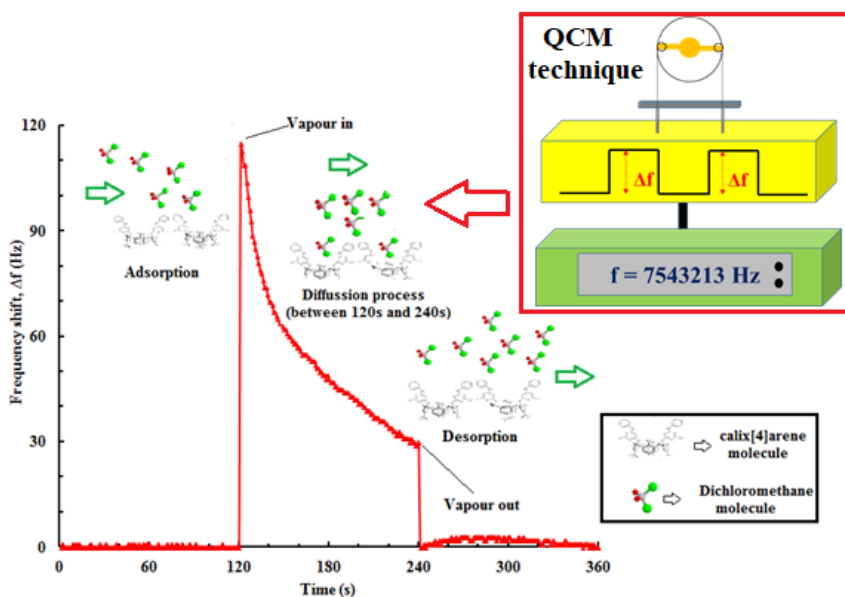
Figure 3. A symbolic presentation of QCM gas kinetic measurements.

In our previous studies, to investigate the chemical sensor properties of 25,27-(Dipropylmorpholinoacetamido)-26,28-dihydroxycalix[4]arene -based nano thin film (Acikbas vd., 2017:77) and the triazine based calixarene nano thin film (Halay vd., 2019:2521) for dichloromethane and chloroform vapours, the kinetic response of calixarene thin film sensor to these vapours is recorded by measuring

the frequency changes as a function of time. The calixarene based nano thin film sensors are periodically exposed to the organic vapours for 2 min, followed by injection of dry air for a further 2 min period. Figure 4 displays the kinetic response of these chemical sensors to the saturated dichloromethane and chloroform vapours.
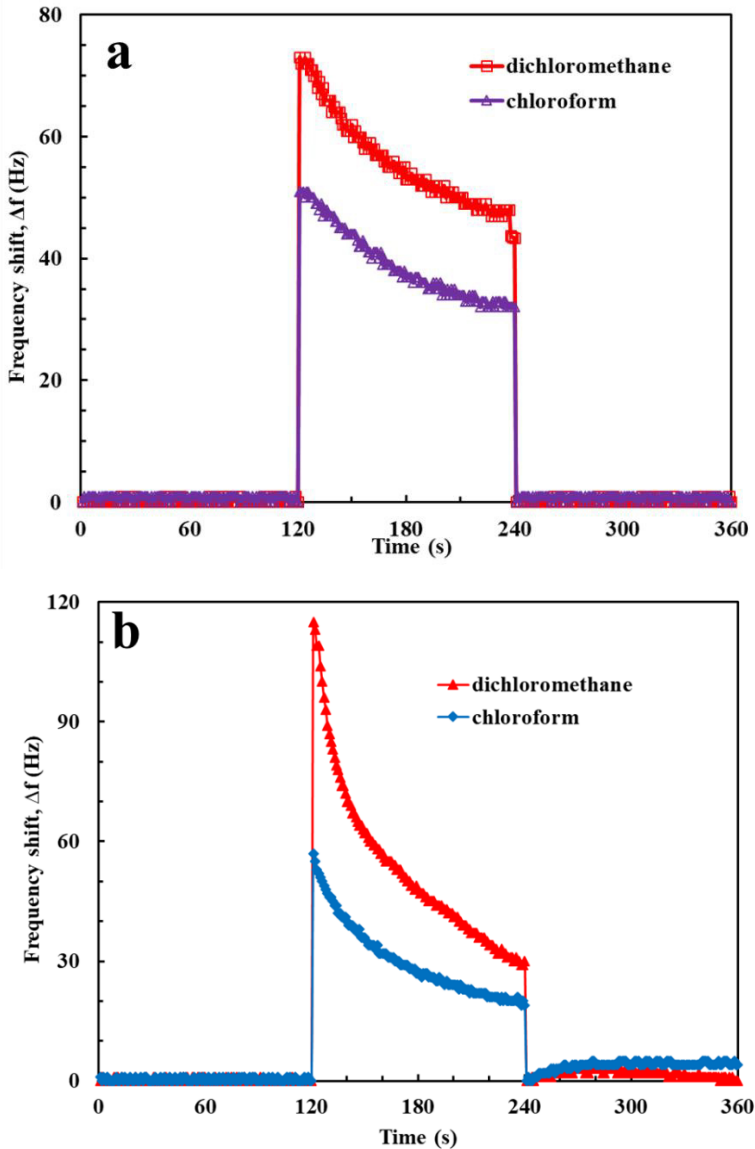

Figure 4. The QCM kinetic measurements of **a)** 25,27-(Dipropylmorpholinoacetamido)-26,28-dihydroxycalix[4]arene -based nano thin film chemical sensor (Acikbas vd., 2017:77) **b)** The triazine based calix[4]arene nano thin film chemical sensor (Halay vd., 2019:2521).

The Response of Calix[4]arene-based QCM Chemical Sensor for Dicholoromethane Vapour at Different Concentrations

The sensitivity of the thin film produced with the triazine based calix[4]arene material was tested by quartz crystal microbalance technique by Halay et al. (Halay vd., 2019:2521). The QCM system starts by introducing dry air into the environment. In Figure 5, there is air on the surface of the medium between 0 and 120 s. At 120 s, 0.5 ml of DCM vapour is taken with the help of an injector and sent to the nano film surface in the gas cell. Between 120 s and 240 s, DCM was seen to spread on the surface of the medium and the film-vapour interaction continued. From this second onwards, the molecules of DCM vapour molecule interacted with the triazine based calix[4]arene molecule and a rapid increase in the resonance change of the QCM crystal was observed. At 240 s, when dry air was reintroduced to the environment, it was seen that the previous ambient conditions were formed. At 360 s, when 1 ml of DCM vapour is given to the same environment again, the changes in the graph are observed. There is a rapid increase in the resonance change in the graph proportional to the amount of vapour supplied to the system and there is DCM vapour in the environment between 360 and 480 s. When dry air is sent to the surface of the environment again at 481 s, the environment is completely purified from DCM vapour. It was seen that the sensor returned to its initial state in the range of 480-600 seconds. At 600 s, the medium is exposed to 1.5 ml DCM and the resonance change is followed. At 720 s, dry air is again sent to the surface of the medium, the medium is completely purified from DCM vapour and the sensor returns to its initial state in the range of 720-840 s. When 2 ml of DCM vapour is given to the same medium again at 840 s, the changes in the graph are observed. Between 840 and 960 s, DCM vapour is present in the environment and at 960 s, when dry air is sent to the surface of the environment again, the environment is completely purified from DCM vapour. It was observed that the sensor returned to its initial state between 960-1080 s. When 2.5 ml of DCM vapour is given to the same environment again at 1081. s, the changes in the graph are observed. Between 1080 and 1200 s, DCM vapour is present in the environment and at 1200 s, when dry air is sent to the surface of the environment again, the environment is completely cleared of DCM vapour. It was observed that the sensor returned to its initial state in the 1200-1320 s range. To summarise briefly, it was found that there was a rapid increase in the resonance change when DCM was added to the medium. It was observed that the result did not change when air/DCM vapours were repeated about five times at different ratios on the thin film surface coated with the triazine based calix[4]arene material. Here, it was concluded that the sensor obtained with the triazine based calix[4]arene synthesis material can

respond quickly to DCM vapour and has both reproducible and reversible properties (Acikbas vd., 2016:18); (Büyükkabasakal vd., 2019:9097).

Some literature information about the QCM-kinetic measurements of calix[4]arene-based QCM-chemical sensor for dichloromethane and chloroform vapours was given in Table 1.
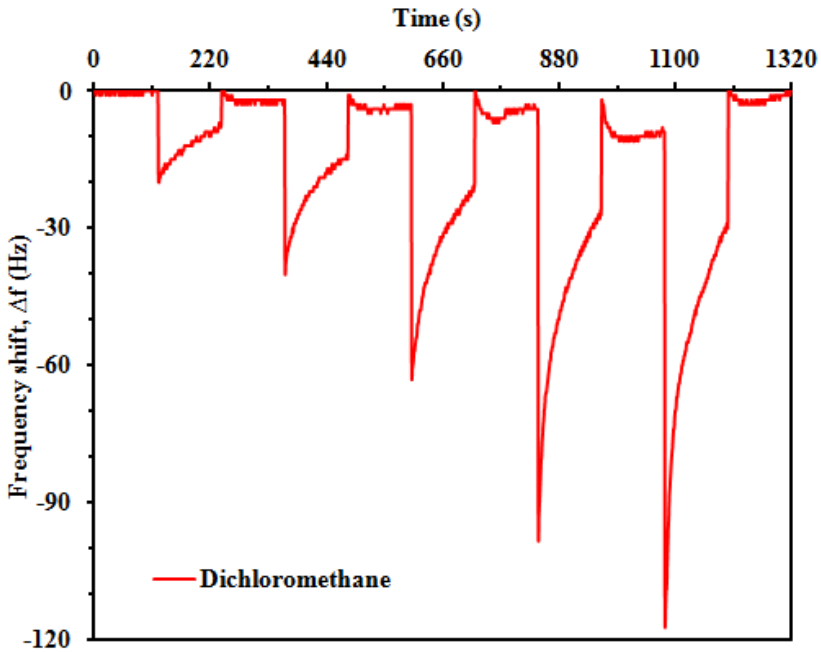
Figure 4. The response of the triazine based calixarene nano thin film sensor to different concentrations of dichloromethane vapour (Halay vd., 2019:2521).

Table 1. QCM-Chemical sensor performances of calix[4]arene-based nano thin films.

P[5]arene-based sensing material	VOCs	Performance (Frequency shift, Hz)	Ref.
The 25,27-(Dipropylmorpholinoacetamido)-26,28-dihydroxycalix[4]arene*)*	Dichloromethane	73	(Acikbas vd., 2017:77)
	Chloroform	51	
The triazine based calix[4]arene	Dichloromethane	115	(Halay vd., 2019:2521)
	Chloroform	57	
The calix[4]arene thiourea decorated with 2-(2-aminophenyl)benzothiazole moiety	Chloroform	154	(Durmaz vd., 2020:4670)
	Dichloromethane	51	

CONCLUSIONS

In the literature, QCM-nano thin film sensors prepared using calix[4]arene materials were interacted with both saturated and different concentrations of dichloromethane and chloroform organic vapours and frequency change values were obtained as a function of time. Depending on the increase in vapour concentrations, an increase in frequency change was also observed. After the QCM nano thin film sensor materials were exposed to organic vapours, the reproducibility capacity of QCM sensor materials was measured by time-dependent measurements. The results obtained in calix[4]arene based thin film sensors revealed that these sensors are self-renewable and have the potential to have multiple uses.

References

Acikbas, Y., Capan, R., Erdogan, M., Yukruk, F. (2015). Characterization and organic vapor sensing properties of Langmuir-Blodgett film using perylendiimide material, *Res. Eng. Struct. Mat.* 2, 99–108.

Acikbas, Y., Dogan, G., Erdoğan, M., Çapan, R., Soykan, C. (2016). Organic vapor sensing properties of copolymer Langmuir-Blodgett thin film sensors, *J. Macromol. Sci. Part A,* 53(8), 470–474.

Acikbas, Y., Cankaya, N., Çapan, R., Erdoğan, M., Soykan, C. (2016). Swelling behavior of the 2-(4-methoxyphenylamino)-2-oxoethyl methacrylate monomer LB thin film exposed to various organic vapors by quartz crystal microbalance technique, *J. Macromol. Sci. Part A,* 53(1), 18-25.

Acikbas, Y., Bozkurt, S., Halay, E., Capan, R., Guloglu, M.L., Sirit, A., Erdogan, M. (2017). Fabrication and characterization of calix[4]arene LangmuireBlodgett thin film for gas sensing applications, *J. Inclusion Phenom. Macrocycl. Chem.* 89, 77-84.

Acikbas, Y., Bozkurt, S., Erdogan, M., Halay, E., Sirit, A., Capan, R. (2018). Optical and vapor sensing properties of calix [4] arene Langmuir-Blodgett thin films with host–guest principles. *Journal of Macromolecular Science, Part A,* 55 (7), 526-532.

Ariga, K., Yamauchi, Y., Mori, T., ve Hill, J. P. (2013). 25th Anniversary article: What can be done with the Langmuir-Blodgett method? Recent developments and its critical role in materials science. *Advanced Materials*, *25*(45), 6477-6512.

Asri, M. I. A., Hasan, M. N., Fuaad, M. R. A., Yunos, Y. M., ve Ali, M. S. M. (2021). MEMS gas sensors: A review. *IEEE Sensors Journal*, *21*(17), 18381-18397.

Barreto, D. N., Kokoric, V., Petruci, J. F. D., ve Mizaikoff, B. (2021). From light pipes to substrate-integrated hollow waveguides for gas sensing: A review. *ACS Measurement Science Au*, *1*(3), 97-109.

Brake, M., Böhmer, V., Krämer, P., Vogt, W. and Wortmann, R. (1993). O-Alkylated p-Nitrocalix[4]arenes, Syntheses, LB-Monolayers and NLO-Properties, *Supramoleculer Chemistry*, 2, 65-70.

Büyükkabasakal, K., Acikbas, S.C., A Deniz, A., Y Acikbas, Y., R Capan, R., M Erdogan, M. (2019). Chemical sensor properties and mathematical modeling of graphene oxide langmuir-blodget thin films, *IEEE Sensors Journal,* 19(20), 9097-9104.

Dehari, Y., Takei, Y., Koyama, S., Nanto, H., ve Seki, S. (2010). QCM gas sensor with organic nanowire film as molecular recognition membrane. *Sensors and Materials*, *22*(4), 175-181.

Dewulf, J., ve Van Langenhove, H. (2002). Analysis of volatile organic compounds using gas

chromatography. *Trac-Trends in Analytical Chemistry*, *21*(9-10), 637-646.

Durmaz, M., Acikbas, Y., Bozkurt, S., Capan, R., Erdogan, M., Ozkaya, C. (2020). A novel calix[4]arene thiourea decorated with 2-(2-aminophenyl)benzothiazole moiety as highly selective chemical gas sensor for dichloromethane vapour. *ChemistrySelect,* 6, 4670–4676.

Elanjeitsenni, V. P., Vadivu, K. S., ve Prasanth, B. M. (2022). A review on thin films, conducting polymers as sensor devices. *Materials Research Express*, *9*(2), 022001.

Fattorini, D., ve Regoli, F. (2020). Role of the chronic air pollution levels in the Covid-19 outbreak risk in Italy. *Environmental Pollution*, *264*, 114732.

Flores-Sanchez, R., Gamez, F., Lopes-Costa, T., ve Pedrosa J. M. (2020). A calixarene promotes disaggregation and sensing performance of carboxyphenyl porphyrin films. *ACS Omega*, *5*(12), 6299-6308.

Halay, E., Acikbas, Y., Capan, R., Bozkurt, S., Erdogan, M., Unal, R. (2019) A novel triazine–bearing calix[4]arene: design, synthesis and gas sensing affinity for volatile organic compounds, Tetrahedron 75(17), 2521–2528.

He, C., Cheng, J., Zhang, X., Douthwaite, M., Pattisson, S., ve Hao, Z. (2019). Recent advances in the catalytic oxidation of volatile organic compounds: A review based on pollutant sorts and sources. *Chemical Reviews*, *119*(7), 4471-4568.

He, Z.-H., Gong, S.-D., Cai, S.-L., Yan, Y.-L., Chen, G., Li, X.-L., Zheng, S.-R., Fan, J., ve Zhang, W.-G. (2019). A benzimidazole-containing covalent organic framework-based QCM sensor for exceptional detection of CEES. *Crystal Growth & Design*, *19*(6), 3543-3550.

Hirota, K., Sakai, H., Washio, M. and Kojima, T. (2004). Application of electron beams for the treatment of VOCs streams. *Ind. Eng. Chem. Res.*, 43, 1185-1191.

Homola, J., Yee, S. S., ve Gauglitz, G. (1999). Surface plasmon resonance sensors: Review. *Sensors & Actuators: B. Chemical*, *54*(1-2), 3-15.

Kang, Z., Zhang, D., Li, T., Liu, X., ve Song, X. (2021). Polydopamine-modified SnO2 nanofiber composite coated QCM gas sensor for high-performance formaldehyde sensing. *Sensors & Actuators: B. Chemical*, *345*, 130299.

Karlık, B. (2004) Tehlikeli ve Zararlı Kokuları Gerçek-Zamanlı Tanıma ve Koku Bilgisinin İletimi, Havacılık İleri Teknolojiler ve Uygulamaları Sempozyumu, Hava Harp Okulu, İstanbul.

Kim, D., Chen, Z., Zhou, L.-F., ve Huang, S.-X. (2018). Air pollutants and early origins of respiratory diseases. *Chronic Diseases and Translational Medicine*, *4*(2), 75-94.

Kumar, S., Chawla, S., ve Zou, M. C. (2017). Calixarenes based materials for gas sensing applications: A review. *Journal of Inclusion Phenomena and Macrocyclic Chemistry*, *88*(3-4), 129-158.

Li, H.-Y., Zhao, S.-N., Zang, S.-Q., ve Li, J. (2020). Functional metal–organic frameworks as effective sensors of gases and volatile compounds. *Chemical Society Reviews*, *49*(17), 6364-6401.

Matsuoka, R., ve Nabeshima, T. (2018). Functional supramolecular architectures of dipyrrin complexes. *Frontiers in Chemistry*, *6*, 349.

Mermer, Ö., Okur, S., Sümer, F., Özbek, C., Sayın, S., ve Yılmaz, M. (2012). Gas sensing properties of carbon nanotubes modified with calixarene molecules measured by QCM techniques. *Acta Physica Polonica A*, *121*(1), 240-242.

Nazemi, H., Joseph, A., Park, J., ve Emadi, A. (2019). Advanced micro- and nano-gas sensor technology: A review. *Sensors*, *19*(6), 1285.

Oprea, A., ve Weimar, U. (2020). Gas sensors based on mass-sensitive transducers. Part 2: Improving the sensors towards practical application. *Analytical and Bioanalytical Chemistry*, *412*(25), 6707-6776.

Özbek, Z., Çapan, R., Göktaş, H., Şen, S., İnce, F. G., Özel, M. E., Davis, F. (2011). Optical parameters of calix[4]arene films and their response to volatile organic vapors. *Sensors & Actuators: B. Chemical*, *158*, 235-240.

Özmen, M., Özbek, Z., Bayrakçı, M., Ertul, Ş., Ersöz, M., ve Çapan, R. (2014). Preparation and gas sensing properties of Langmuir-Blodgett thin films of calix[n]arenes: Investigation of cavity effect. *Sensors & Actuators: B. Chemical*, *195*, 156-164.

Rasheed, T., ve Nabeel, F. (2019). Luminescent metal-organic frameworks as potential sensory materials for various environmental toxic agents. *Coordination Chemistry Reviews*, *401*, 213065.

Rytel, K., Kedzierski, K., Barszcz, B., Biadasz, A., Majchrzycki, L., ve Wrobel, D. (2022). The influence of zinc phthalocyanine on the formation and properties of multiwalled carbon nanotubes thin films on the air–solid and air–water interface. *Journal of Molecular Liquids*, *350*, 118548.

Rytel, K., Kedzierski, K., Barszcz, B., Widelicka, M., Stachowiak, A., Biadasz, A., Majchrzycki, L., Coy, E., ve Wrobel, D. (2020). The influence of diameter of multiwalled carbon nanotubes on mechanical, optical and electrical properties of Langmuir-Schaefer films. *Physical Chemistry Chemical Physics*, *22*(39), 22380-22389.

Su, S. and Hu, J. (2018). Ultrasound assisted low-concentration VOC sensing, *Sens. Actuat. B*, 254, 1234-1241.

Temel, F., ve Tabakçı, M. (2016). Calix[4]arene coated QCM sensors for detection of VOC emissions: Methylene chloride sensing studies. *Talanta*, *153*, 221-227.

Wang, H., Li, W., Huang, J., Su, R., Wang, R., Luo, L., Zhang, Y., Zhang, Z., ve Xue, Q. (2019). Surface plasmon resonance (SPR) sensor based on optimal pre- and post-selection. *IEEE Photonics Journal*, *11*(2), 6801207.

Woellner, M., Hausdorf, S., Klein, N., Mueller, P., Smith, M. W., ve Kaskel, S. (2018). Adsorption and detection of hazardous trace gases by metal-organic frameworks. *Advanced Materials*, *30*(37), 1704679.

Wu, L., Chu, H. S., Koh, W. S., ve Li, E. P. (2010). Highly sensitive graphene biosensors based on surface plasmon resonance. *Optics Express*, *18*(14), 14395-14400.

Zhang, Z., Xue, T., ve Jin, X. (2020). Effects of meteorological conditions and air pollution on COVID-19 transmission: Evidence from 219 Chinese cities. *Science of the Total Environment*, *741*, 140244.

Zheng, J., Noh, H. L., Chun, H. W., Oh, B. M., Lee, J., Choi, S.-K., Kim, E., Jung, D., Lee, W. S., ve Kim, J. H. (2021). Highly sensitive, selective, and rapid response colorimetric chemosensor for naked eye detection of hydrogen sulfide gas under versatile conditions: Solution, thin-film, and wearable fabric. *Sensors & Actuators: B. Chemical*, *341*, 130013.

Chapter 14

Enhancing Classification Accuracy of Pumpkin Seed with Detail Morphological Features and Different Machine Learning Algorithms

Huseyin COSKUN[1]

[1] *Asst. Prof. , Kütahya Health Sciences University, Computer Engineering Department, huseyin.coskun@ksbu.edu.tr ORCID No: https://orcid.org/0000-0002-8380-245X*

ABSTRACT

In this study, classification was carried out using morphological features to recognize the types of pumpkin seeds (Koklu et. al., 2021). New morphological feature values were obtained using the open-access pumpkin seed feature data set. Three different data sets were used, using the features in this study and those in the previous study. Gradient boosting, support vector machine, k-nearest neighbors, and random forest machine learning techniques were used to increase classification success. As a result, models with higher classification metric values than previous study were created.

Keywords: classification, enhancing, morphological features, correlation.

INTRODUCTION

Classification of pumpkin seeds addresses an essential problem in many fields, from the food industry to agricultural practices. Pumpkin seeds attract great attention as a food item that is both rich in nutritional value and available in various types. However, distinguishing features between different species are often not easily detected by eye. In this context, the use of machine learning and image processing techniques can play an essential role in the classification of pumpkin seeds. This study aims to investigate the methods and models that can be used to increase the classification accuracy of two different types of pumpkin seeds used in Koklu's (Koklu et al., 2021) previous study. The use of different classification algorithms with data mining and feature engineering techniques has the potential to provide solutions to such recognition problems. Its results could be significant in various application areas, from food quality control to agricultural productivity. This study is carried out to demonstrate the effectiveness of machine-learning approaches in pumpkin seed classification and to shed light on future research in this field.

METHOD

Koklu et al. In their study, they classified the "Ürgüp Sivrisi" and "Çerçevelik" types of pumpkin seeds. For this classification, they first prepared an experimental environment to obtain images of pumpkin seeds. The schematic of the experimental environment is presented in Figure 1 (Koklu et al., 2021). In the experimental environment, it is seen that bar LEDs are used in the dark box to protect from the lighting in the current working environment. In this way, a constant and controllable light reflection was achieved on the surface of the pumpkin seeds.
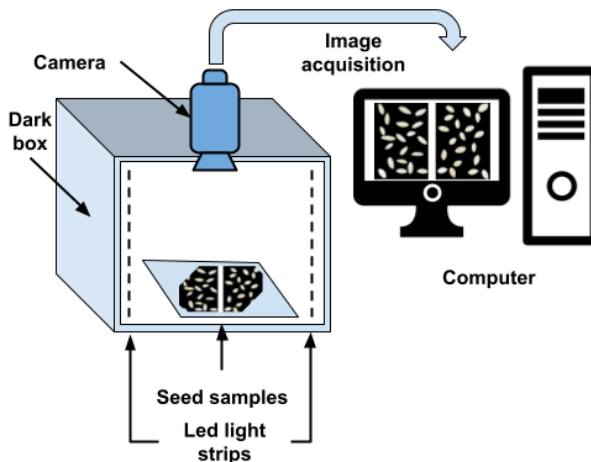

**Figure 1**: Experimental setup for pumpkin seed image acquisition

Koklu et al. (Koklu et al., 2021) used a total of 2500 pumpkin seed images, including 1200 Ürgüp Spikes and 1300 Frames. Sample images are presented in Figure 2 (Koklu et al., 2021).

a) Ürgüp sivrisi   b) Çerçevelik

Figure 2: Pumpkin seed samples

Feature Extraction

In their study, Koklu et al. considered the pumpkin seed image as an ellipse (Koklu et al., 2021). An example of this representation and the properties of an ellipse are presented in Figure 3.
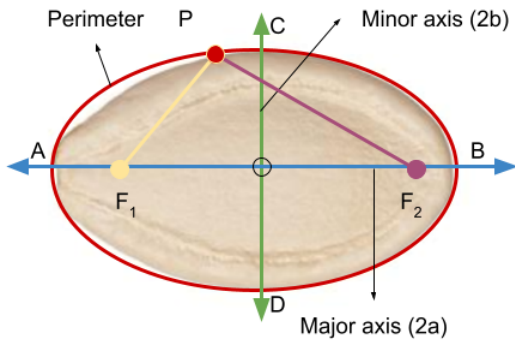
1. Ellipses have two (F_1 , F_2) focal points.
2. An ellipse has a center, and two axes — major axis and minor axis; center is at (0,0), AB is major axis, CD is minor axis.
3. The sum of the distances between any point (P) on the ellipse and the two focal points is constant, and it is equal to the total length of the major axis; here $PF_1 + PF_2 = 2a = L$ is constant.
4. The eccentricity value of all ellipses is always less than one (e < 1)

Figure 3: An ellipse that represented a pumpkin seed

Twelve morphological features of the ellipse representing this image are separated in size and shape and presented with their explanations in Table 1 (Koklu et al., 2021).

Table 1: The geometric and morphological features of pumpkin seed images

No	Name	Explanation	Type	Equation
1	Area (A)	It gave the number of pixels within the borders of a pumpkin seed	Size	-
2	Perimeter (P)	It gave the circumference in pixels of a pumpkin seed	Size	-
3	Major Axis Length (MA)	It gave the circumference in pixels of a pumpkin seed	Size	$2a$
4	Minor Axis Length (MiA)	It gave the small axis distance of a pumpkin seed	Size	$2b$
5	Eccentricity (e)	It gave the eccentricity of a pumpkin seed	Shape	$\sqrt{1 - (b^2/a^2)}$
6	Convex Area (CA)	It gave the number of pixels of the smallest convex shell at the region formed by the pumpkin seed	Size	πab
7	Extent (E)	It returned the ratio of a pumpkin seed area to the bounding box pixels	Shape	-
8	Equiv Diameter (ED)	It was formed by multiplying the area of the pumpkin seed by four and dividing by the number pi, and taking the square root	Size	$2a^2/b$
9	Compactness (C)	It proportioned the area of the pumpkin seed relative to the area of the circle with the same circumference	Shape	$4\pi A/P^2$
10	Solidity (s)	It considered the convex and convex condition of the pumpkin seeds	Shape	A/CA
11	Roundness (r)	It measured the ovality of pumpkin seeds without considering its distortion of the edges	Shape	$4\pi A/\pi L^2$
12	Aspect Ratio (AR)	It gave the aspect ratio of the pumpkin seeds	Shape	$2a/2b$

Koklu et al. (Koklu et al., 2021) used the shape and size features given in Table 1 in his study to classification pumpkin seed images. In addition to these features, 10 attributes given in Table 2 were determined in this study.

Table 2: The morphological features of pumpkin seed images

No	Name	Explanation	Type	Equation
1	Convex Perimeter (CP) (Kumar et al., 2019)	The convex perimeter of an object is the perimeter of the convex hull that encloses the object.	Shape	$2 * (2a + 2b)$
2	Convexity (Cx) (Manik et al., 2016)	This value is the perimeter ratio between convex perimeter of object and the object itself.	Shape	P/CP
3	D (MathMonks.com, 2023)	The semi-distance between the F_1 and F_2	Size	$a * e$
4	Circularity (c) (Park et al., 2020; S. et al., 2021)	The relationship between the area and perimeter of a closed curve is elucidated as compactness of its shape. It ranges between zero and one.	Shape	$4\pi CA/CP^2$
5	Area-2 (MathMonks.com, 2023)	Geometric area of an ellipse	Shape	$\pi * a * b$
6	Perimeter-2 (P2) (Waranusast et al., 2016)	It is defined as the distance around the pumpkin seed edge.	Shape	$\pi \left[3(a + b) - \sqrt{(3a + b)}\right.$
7	Perimeter-3 (P3) (MathMonks.com, 2023)	Geometric perimeter of an ellipse	Shape	$2\pi \sqrt{\dfrac{a^2+b^2}{2}}$
8	Elongation (El) (Manik et al., 2016)	It measures the length of the object. It ranges between zero and one.	Shape	$1 - (b/a)$
9	Rectangularity (R) (Manik et al., 2016)	It illustrates similarity of object shape with rectangular shape. It ranges between zero and one.	Shape	$A/(2a * 2b)$
10	AP Ratio (Gomes Ataide et al., 2020)	It is defined as the ratio between object area and perimeter of the object	Shape	A/P

The convex and morphological drawings belong to sample of pumpkin seed are given in Figure 4.

| The original image | Area (Black pixels) | Perimeter | Convex Area | Convex Perimeter |

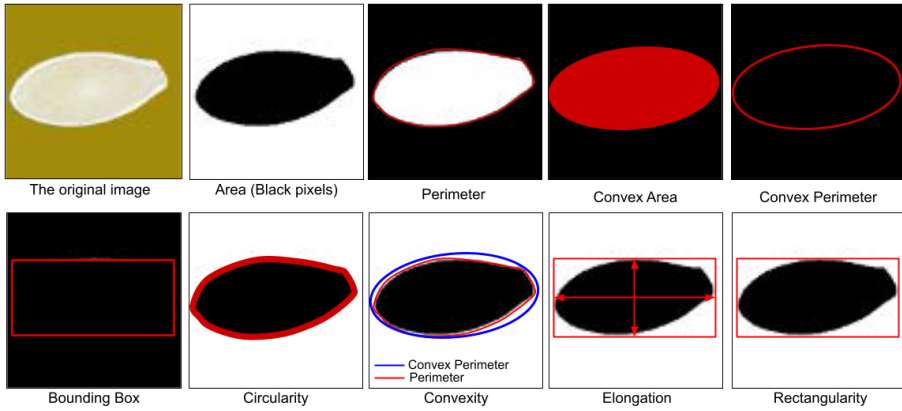| Bounding Box | Circularity | Convexity | Elongation | Rectangularity |

Figure 4: Convex shapes and morphological features of a pumpkin seed

In order to make the morphological features whose values vary between 0-1 more understandable, these features for different geometric shapes are presented in Figure 5. The distribution of the ten features explained in Table 2 according to classes is given in the Figure 6. When this figure is examined, it can be seen that the Circularity and Elongation features are better separated.
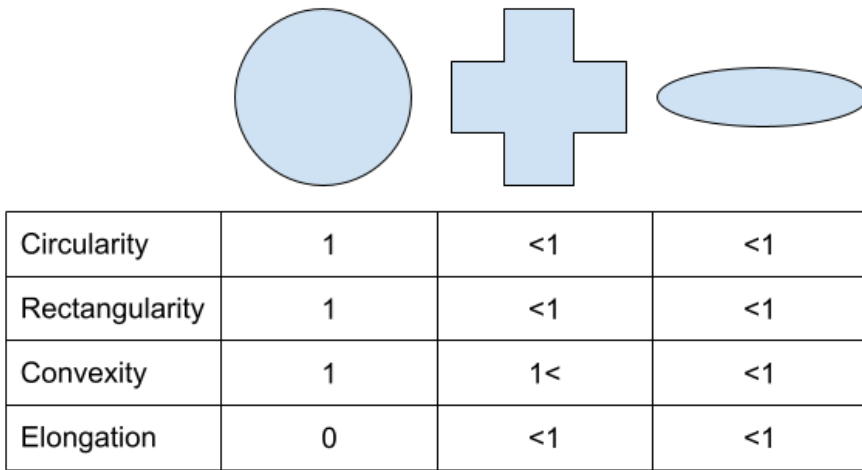

Circularity	1	<1	<1
Rectangularity	1	<1	<1
Convexity	1	1<	<1
Elongation	0	<1	<1

Figure 5: Evaluation of morphological features according to different shapes

The average, standard deviation, maximum, and minimum statistical values of the features in this study were presented in Table 3.
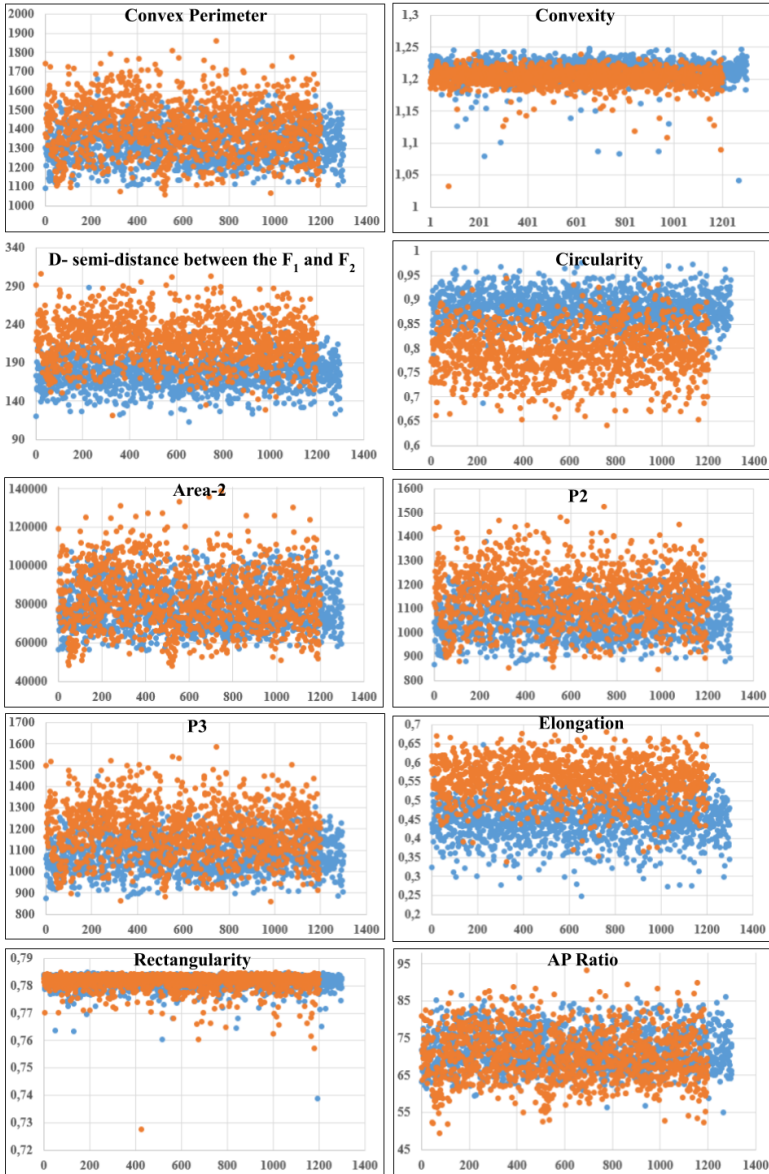
Figure 6: Distribution of features

Dataset-1 was created with the features in Table 1, Dataset-2 was created with the features determined within the scope of this study. Besides, the correlations (pearson) between the features and class value have been calculated to choose best separator features by determine the relation among the features. The correlations of the features are given in Table 4.

Table 3: The statical distribution of the features in this study

Feature	Min	Max	Mean	Std. Dev.
Convex Perimeter (CP)	1058,56	1858,593	1364,794	125,921
Convexity (Cx)	1,03247	1,248033	1,208089	0,016663
D	78,95048	306,1265	197,4336	32,40538
Circularity (c)	0,597742	0,975559	0,839062	0,06182
Area-2	47996,47	139003,8	81075,49	13706,89
Perimeter-2 (P2)	847,4746	1525,494	1103,484	107,9979
Perimeter-3 (P3)	858,902	1585,837	1133,599	116,8586
Elongation (El)	0,129485	0,681979	0,49879	0,075075
Rectangularity (R)	0,727577	0,785052	0,781318	0,003061
AP Ratio	49,29009	93,29467	70,9507	6,118016

Major Axis, Eccentricity, Roundness, Compactness, D, P2, P3, Aspect Ratio, Circularity, Elongation which are accepted as best seperator in Figure 6 and Koklu's study (Koklu et al., 2021) have been selected and created Dataset-3 with them.

Table 4: Correlations between the features and class values

A	P	MA	MiA	CA	ED	e	E
0,17	0,39	0,56	0,40	0,17	0,16	0,70	0,24
r	AR	C	D	CP	Cx	P2	P3
0,67	0,72	0,73	0,64	0,35	0,36	0,42	0,46
El	R	AP Ratio	c	A2	S		
0,72	0,002	0,12	0,73	0,17	0,12		

Classification

The performance of these Datasets is evaluated using classifiers such as k-nearest neighbor (k-NN), Gradient Boosting, Support Vector Machine (SVM) and Random Forest (RF) the help of Python programming. For all classifiers, 10% of the data was used as validation and test data. The training model has been tested with data not previously used in training. Therefore, test data is entirely different from training data. All models were validated through a 5-fold cross-validation process to evaluate the predictive ability as it allows the classifier to operate without bias and avoids the overfitting problem. The cross-validation was performed without data sharing between training and validation data to avoid overtraining. In order to measure the performances of each model, a confusion matrix which is defined in (Coskun & Yigit, 2018) and the ROC

curve, is created, and Accuracy (A), Recall (R), Precision (P), F-score (F), Balanced Accuracy, AUC (Area Under Curve), and Specificity (S) indicators are calculated to evaluate performance (Coskun et al., 2022).

k-NN

The "K" in KNN represents the number of nearest neighbors to consider when making a prediction (Kramer, 2013). For classification, KNN finds the K data points closest to the new data point in the training set and assigns the class label that occurs most frequently among those neighbors. For regression, it averages the target values of the K nearest neighbors to predict the target value for the new data point. KNN relies on a distance metric (e.g., Euclidean distance) to measure the similarity between data points. The most commonly used distance metrics are given in the Table 5.

Table 5: k-NN distance metric equations

Name	Equation
Euclidean	$\sqrt{\sum_{i=1}^{k}(x_i - y_i)^2}$
Manhattan	$\sum_{i=1}^{k}|x_i - y_i|$
Minkowski	$\left(\sum_{i=1}^{k}(|x_i - y_i|)^q\right)^{1/q}$

The choice of distance metric can significantly impact the algorithm's performance. The choice of the value of K is a critical hyperparameter in KNN. A small K can make the algorithm sensitive to noise. In contrast, a large K can make it less sensitive but potentially introduce bias (Kramer, 2013). KNN is considered a "lazy learner" because it does not build an explicit model during training. Instead, it memorizes the entire training Dataset and performs computations at prediction time. KNN can be computationally expensive, especially with large Datasets, as it requires computing distances to all training samples for each prediction. KNN is instance-based, using the entire training Dataset during prediction (Rhys, 2020). In this study the number of neighbors,

distance metric, and distance weight have been selected as 10, Euclidian, Squared inverse respectively.

Gradient Boosting

Gradient Boosting is a powerful ensemble learning algorithm widely used in machine learning for classification and regression tasks. It builds an ensemble of decision trees sequentially, where each tree corrects the errors made by the previous ones. Gradient Boosting is a boosting algorithm that combines the predictions of multiple weak learners (typically decision trees) to create a strong learner (Saupin, 2022). Unlike bagging methods like Random Forest, boosting methods focus on improving the model iteratively. Gradient Boosting trains decision trees sequentially. It starts with a single decision tree, and each subsequent tree is trained to correct the errors (residuals) of the previous trees. This leads to a reduction in the overall prediction error. The "Gradient" in Gradient Boosting refers to using gradient descent optimization to minimize the loss function. It optimizes the model's parameters by moving toward steepest descent in the loss function space. Gradient Boosting allows flexibility in choosing different loss functions depending on the problem, such as mean squared error for regression and deviance (logarithmic loss) for classification. The choice of the loss function influences the algorithm's behavior (Vandeput, 2021). Gradient Boosting introduces a learning rate hyperparameter that controls the contribution of each tree to the final prediction. Lower learning rates result in more robust models but require more trees for the same performance. Gradient Boosting can provide insights into feature importance by analysing how much each feature contributes to reducing the loss function. This can help in feature selection and understanding the Dataset. Gradient Boosting is a boosting algorithm based on loss function gradients. The gradient of the loss function for a single sample is called the residual. Briefly, it represents the capture error between the correct and predicted labels (Friedman, 2001). This error or residual measures the amount of misclassification; unlike AdaBoost, which uses weights instead of residuals, gradient boosting uses these residuals directly. Therefore, gradient boosting is considered another sequential ensemble method that aims to train weak learners on residuals (i.e., gradients) (Kunapuli, 2022).

SVM

SVM is a kernel-based learning approach that provides very fast and accurate results in subjects such as linear and non-linear classification, regression analysis, outlier detection, function and density estimation. It is

especially used in data mining in classification problems where the patterns between the variables of the data to be classified are unknown. Although it was initially used in two-class and linear classification problems, it later became available for non-linear or multi-class classification problems. Real-life classification problems are often non-linear problems consisting of many different classes. SVM aims to solve these problems more easily by making the nonlinear sample space linear in a higher plane (Burges, 1998). While doing this, it tries to find the linear equation that maximizes the distance between the closest elements of the classes. This is called margin maximization in the literature (Bennett & Demiriz, 1998). In other words, SVM aims to create the farthest upper (hyper) plane with a linear decision function between vectors belonging to two classes. Although many machine learning methods other than SVM work with this goal, Structural seeks solutions to minimize the possibility of misclassification through risk minimization. With these features, SVM is defined as a supervised learning method. In other words, the labels of which class the data belongs to are determined during the training phase. It is a machine learning function that tries to make predictions and generalize on new data by performing learning on training data. The positive aspects of DVM can be listed as follows (Osuna et al., 1997; Raghavendra & Deka, 2014);

- It does not require the assumption of prior knowledge about the distribution.
- It obtains high accuracy values.
- Can model complex decision boundaries.
- It can work with many independent variables.
- It Can work with both linear and non-linearly separable data.
- Compared to other classification methods, the problem of overfitting is less.

Random Forest

Random Forest (RF) is a popular ensemble learning technique in machine learning that combines the predictive power of multiple decision trees to achieve high accuracy and robustness in classification and regression tasks. This method introduces randomness through bootstrapping (random sampling of training data) and random feature selection at each node of the trees, mitigating overfitting and enhancing generalization (Ho, 1998). By aggregating the predictions of these individual trees through majority voting for classification or averaging for regression, Random Forest not only provides reliable and interpretable results but also excels in handling complex Datasets with diverse

applications spanning from image classification and fraud detection to recommendation systems and predictive maintenance (Sheppard, 2019). Random Forest is an ensemble method that combines the predictions of multiple decision trees to make more accurate and robust predictions. It belongs to the bagging family of ensemble methods.

At the core of Random Forest are decision trees. However, unlike a single decision tree, Random Forest uses a collection of decision trees to improve predictive accuracy and reduce overfitting.

The "random" in Random Forest comes from two sources of randomness (Maroco et al., 2011):

- Random Sampling: Each tree is trained on a random subset of the training data (with replacement), which is called bootstrapping or bagging. This introduces diversity among the trees.
- Random Subset of Features: At each node of a decision tree, a random subset of features is considered for splitting. This further enhances diversity and reduces the risk of overfitting.

For classification tasks, Random Forest combines the predictions of individual trees by using a majority vote. For regression tasks, it averages the predictions of individual trees. This ensemble approach often leads to more accurate and stable predictions. RF is accepted as one of the ensemble machine learning techniques with many classification trees on some randomly selected features from randomly selected samples with a bagging strategy and then using trees to vote for a given input vector to get a class label (Li et al., 2016). Therefore, the number of trees is usually the only setting parameter and has been adjusted to 50.

RESULTS AND DISCUSSION

For the classification of pumpkin seed features, confusion matrices for the models of KNN, GB, SVM and RF classifier methods with the highest accuracy result obtained by using all Datasets are presented in Figure 7. Both training and testing processes were performed on the same computer.

When the confusion matrices and performance metrics of the classifiers in Figure 8 are examined, it is seen that GB, SVM, KNN, RF have the best classification success respectively for all Datasets. Besides, the Dataset-2 which includes the features in this study and Dataset-3 which includes both the Koklu's (Koklu et al., 2021) and this study's features have better classification success.
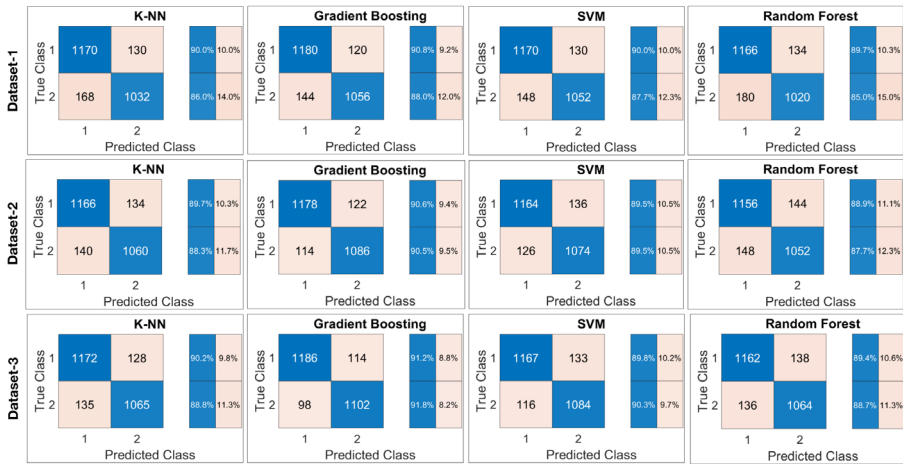
Figure 7: Confusion matrices of classifiers for all dataset

When the confusion matrices and performance metrics of the classifiers in Figure 8 are examined, it is seen that the accuracy of the Dataset-2 and Dataset-3 are higher than precision. This occurs when the model makes many positive predictions, including both true positives and false positives. If there are a large number of true negatives in the Dataset, the correct classifications of those true negatives can outweigh the false positives, resulting in a higher accuracy. But the precision of the Dataset-1 is higher than accuracy. This can happen when the model is very conservative in making positive predictions. It makes fewer positive predictions, but when it does, they are often correct. This results in a high precision but may lead to a lower accuracy because it misses many true positives. Considering the results of the best performing classification method (GB), it can be seen that the recall value for Dataset-2 and 3 is higher than the F-score value. For Dataset-1, this is the opposite. In this case, the following comments can be made for Dataset-1; The model has been trained is highly conservative and only predicts positive when it's very certain. As a result, it doesn't produce many false positives (low recall) but has a high precision because when it does predict positive, it's often correct. In such a situation, the precision component of the F-score dominates, and the F-score can be higher than recall because the high precision helps balance the equation. However, this doesn't mean it's always desirable to have an F-score higher than recall. Considering the results of the best performing classification method (GB), it can be seen that the specificity value for Dataset-2 and 3 is higher than the f-score and balanced accuracy values. For Dataset-1, this is the opposite. This case can be explained by; However, because the Dataset is imbalanced, the true negative rate (specificity) can be relatively low, even though it's still higher than random

chance. At the same time, the model achieves high precision and recall for the positive class, resulting in a higher F-score. The balanced accuracy, which considers both sensitivity and specificity, may also be higher because sensitivity is high due to the good performance on the positive class. In imbalanced Datasets, it's possible for models to achieve high F-scores and balanced accuracy while still having specificity that is relatively lower but better than random chance. This occurs when the model focuses on correctly classifying the positive class and is less concerned about the true negative rate. Within the scope of all these comments, it can be said that the model obtained using Dataset-1 focuses only on correctly classifying the positive class, and the models obtained using Datasets-2 and 3 focus on correctly separating both positive and negative classes.
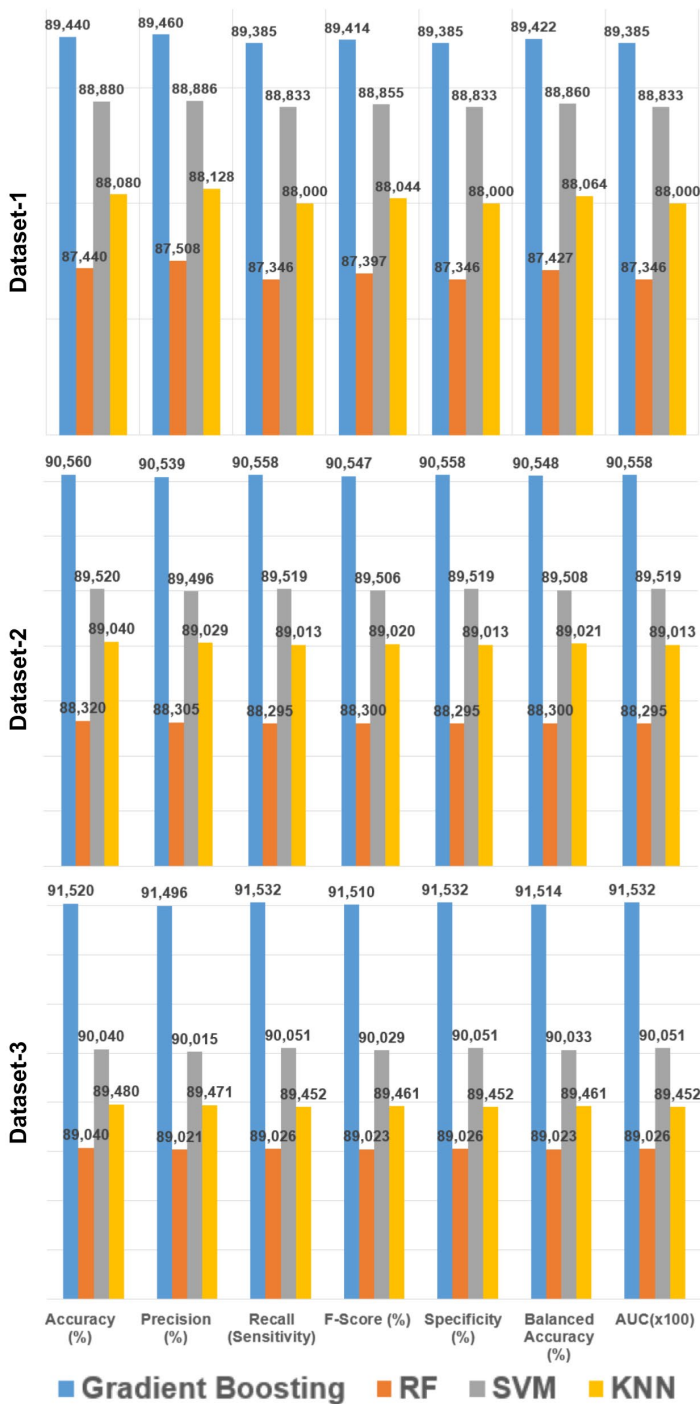
Figure 8: Performance metrics of all classifiers

The ROC curves belonging to the models with the highest accuracy values for the interpretation of the accuracy values are presented in Figure 9. When the ROC graphs are examined, it is seen that all models are very close to the upper left corner point (0,1); therefore, the ability of the models to diagnose classes fits quite well.
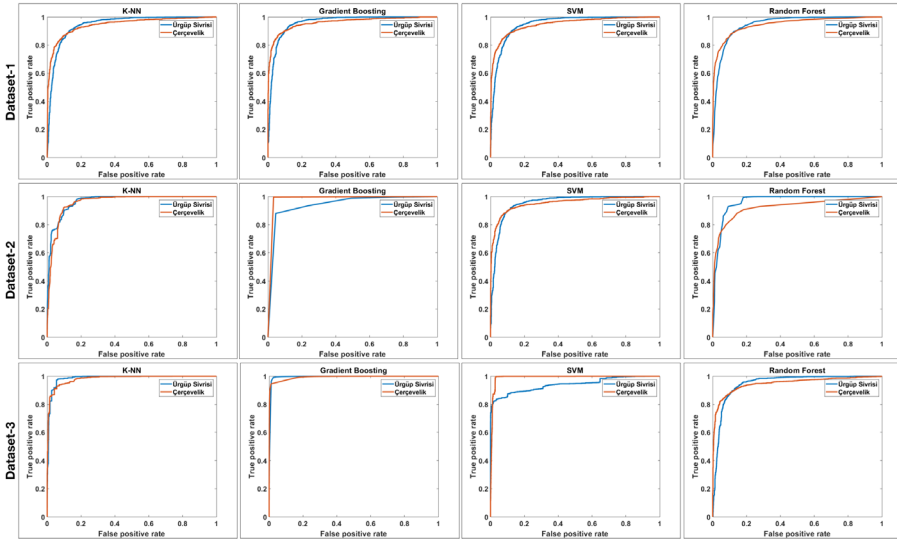

Figure 9: ROC curves of classifiers

CONCLUSION AND FUTURE WORKS

In this study, different features and machine learning methods were used to increase the classification success of Çeçevelik and Ürgüp Sivrisi pumpkin seeds used in Koklu (Koklu et al., 2021) studies. In this study, morphological features including shape and size features were selected for the feature. While determining the features on the training data, the best discriminant features were determined using the correlation method. In addition to the features determined in this study, 3 different data sets were created by determining the best discriminant features in the Koklu's study (Koklu et al., 2021). GB, KNN, SVM and RF methods were chosen for classification purposes. The best classification successes were obtained for data set-3. The best classification success was respectively GB, SVM, KNN and RF. In this context, in this study, both different features and different machine learning methods were tried to increase the classification success achieved in the Koklu's study. In order to increase the classification success, machine learning methods not used in this study can be tested by obtaining statistical features from the same data set in addition to the features used in this study.

REFERENCES

Bennett, K. P., & Demiriz, A. (1998). Semi-Supervised Support Vector Machines. *Advances in Neural Information Processing Systems*, *11*.

Burges, C. J. C. (1998). A tutorial on support vector machines for pattern recognition. Data Mining and Knowledge Discovery, 2(2), 121–167. https://doi.org/10.1023/A:1009715923555/METRICS

Coskun, H., & Yigit, T. (2018). Artificial Intelligence Applications on Classification of Heart Sounds. In Nature-Inspired Intelligent Techniques for Solving Biomedical Engineering Problems (pp. 146–183). IGI Global.

Coskun, H., Yiğit, T., Üncü, İ. S., Ersoy, M., & Topal, A. (2022). An Industrial Application Towards Classification and Optimization of Multi-Class Tile Surface Defects Based on Geometric and Wavelet Features. Traitement Du Signal, 39(6), 2011–2022. https://doi.org/10.18280/TS.390613

Friedman, J. H. (2001). Greedy Function Approximation: A Gradient Boosting Machine. The Annals of Statistics, 29(5), 1189–1232. https://www.jstor.org/stable/2699986

Gomes Ataide, E. J., Ponugoti, N., Illanes, A., Schenke, S., Kreissl, M., & Friebe, M. (2020). Thyroid Nodule Classification for Physician Decision Support Using Machine Learning-Evaluated Geometric and Morphological Features. Sensors 2020, Vol. 20, Page 6110, 20(21), 6110. https://doi.org/10.3390/S20216110

Ho, T. K. (1998). The random subspace method for constructing decision forests. IEEE Transactions on Pattern Analysis and Machine Intelligence, 20(8), 832–844.

Koklu, M., Sarigil, S., & Ozbek, O. (2021). The use of machine learning methods in classification of pumpkin seeds (Cucurbita pepo L.). Genetic Resources and Crop Evolution, 68(7), 2713–2726.

Kramer, Oliver. (2013). Dimensionality reduction with unsupervised nearest neighbors. Springer.

Kumar, M., Gupta, S., Gao, X. Z., & Singh, A. (2019). Plant Species Recognition Using Morphological Features and Adaptive Boosting Methodology. IEEE Access, 7, 163912–163918. https://doi.org/10.1109/ACCESS.2019.2952176

Kunapuli, G. (2022). Ensemble Methods for Machine Learning. Manning Publications.

Li, T., Zhou, M., Travieso-González, C. M., & Alonso-Hernández, J. B. (2016). ECG Classification Using Wavelet Packet Entropy and Random Forests. Entropy 2016, Vol. 18, Page 285, 18(8), 285.

Manik, F. Y., Herdiyeni, Y., & Herliyana, E. N. (2016). Leaf Morphological Feature Extraction of Digital Image Anthocephalus Cadamba. TELKOMNIKA (Telecommunication Computing Electronics and Control), 14(2), 630–637. https://doi.org/10.12928/TELKOMNIKA.V14I2.2675

Maroco, J., Silva, D., Rodrigues, A., Guerreiro, M., Santana, I., & De Mendonça, A. (2011). Data mining methods in the prediction of Dementia: A real-data comparison of the accuracy, sensitivity and specificity of linear discriminant analysis, logistic regression, neural networks, support vector machines, classification trees and random forests. BMC Research Notes, 4(1), 1–14.

MathMonks.com. (2023). Ellipse – Definition, Parts, Equation, and Diagrams. https://mathmonks.com/ellipse

Osuna, E., Freund, R., & Girosi, F. (1997). Improved training algorithm for support vector machines. Neural Networks for Signal Processing - Proceedings of the IEEE Workshop, 276–285. https://doi.org/10.1109/NNSP.1997.622408

Park, H. J., Park, B., & Lee, S. S. (2020). Radiomics and Deep Learning: Hepatic Applications. Korean Journal of Radiology, 21(4), 387–401.

Raghavendra, S., & Deka, P. C. (2014). Support Vector Machine Applications in The Field of Hydrology: A Review. Applied Soft Computing, 19, 372–386.

Rhys, H. I. (2020). Clustering based on density: DBSCAN and OPTICS - Machine Learning with R, the tidyverse, and mlr. In Machine Learning with R, the tidyverse and mlr.

S., E. J., K., D. B., P.A., K., & S., R. (2021). Muscle Fatigue Analysis In Isometric Contractions Using Geometric Features Of Surface Electromyography Signals. Biomedical Signal Processing and Control, 68, 102603.

Saupin, G. (2022). Practical Gradient Boosting A deep dive. AFNIL.

Sheppard, C. (2019). Tree-based machine learning algorithms: decision trees, random forests, and boosting. Clinton Sheppard.

Vandeput, N. (2021). Data Science For Supply Chain Forecasting.

Waranusast, R., Intayod, P., & Makhod, D. (2016). Egg Size Classification On Android Mobile Devices Using Image Processing And Machine Learning. Proceedings of the 2016 5th ICT International Student Project Conference, ICT-ISPC 2016, 170–173. https://doi.org/10.1109/ICT-ISPC.2016.7519263

ABSTRACT

In this study, classification was carried out using morphological features to recognize the types of pumpkin seeds (Koklu et. al., 2021). New morphological feature values were obtained using the open-access pumpkin seed feature data set. Three different data sets were used, using the features in this study and those in the previous study. Gradient boosting, support vector machine, k-nearest neighbors, and random forest machine learning techniques were used to increase classification success. As a result, models with higher classification metric values than previous study were created.

Keywords: classification, enhancing, morphological features, correlation.